Supersymmetry with custodial triplets

Mateo García Pepin

Supersymmetry with custodial triplets

Mateo García Pepin

Director de tesi:
Prof. Mariano Quirós Carcelén

Tutor de tesi:
Prof. Alex Pomarol Clotet

Memòria de recerca presentada per a l'obtenció del títol de Doctor en Física

Institut de Física d'Altes Energies
Departament de Física - Facultat de Ciències,
Universitat Autònoma de Barcelona

May 2016

Agradecimientos / Acknowledgments

Me gustaría agradecer a mi director de tesis, Mariano Quirós, todo su apoyo y dedicación.

Resumen / Abstract

Gracias a resultados experimentales pero también a argumentos teóricos, sabemos que el Modelo Estándar de la física de partículas es solo una descripción a bajas energías de una estructura más fundamental. Supersimetría, una simetría del espacio-tiempo que relaciona bosones y fermiones, proporciona algunos de los candidatos para completar el Modelo Estándar más favorecidos desde un punto de vista teórico. Sin embargo, la búsqueda sin resultado de partículas supersimétricas pone a estos modelos bajo cierta tensión, sobre todo porque muchas de las propiedades de supersimetría en su aplicación a la física de partículas están directamente relacionadas con su presencia a escalas de energía del orden de las que están siendo exploradas en LHC. Sin evidencias directas de supersimetría, ¿existe alguna medición indirecta que los físicos de partículas podrían usar para estudiar estos modelos? La partícula de Higgs descubierta en 2012 en LHC no es solo la ultima pieza del Modelo Estándar, también es una nueva ventana que podría ser útil en el estudio de física más allá del Modelo Estándar.

En la primera parte de esta tesis estudiamos las consecuencias del descubrimiento del bosón de Higgs para versiones mínimas (construidas con el menor numero posible de elementos) de supersimetría. Encontramos que la masa del Higgs es más pesada de lo que uno esperaría en las extensiones supersimétricas del Modelo Estándar más mínimas. Por lo tanto concluimos que puede que la búsqueda de "minimalidad" a la hora de formular teorías más allá del Modelo Estándar, no sea el camino más adecuado en este caso. Por eso construimos una realización un poco más "barroca" de supersimetría con la esperanza de que solucione el problema de la masa del Higgs, la teoría se llama "Modelo de Tripletes con Simetría Custodial". Este modelo presenta un sector de Higgs extendido y usa simetrías para resolver algunos de los problemas asociados a la introducción de nuevos grados de libertad en el potencial escalar de una teoría, al mismo tiempo, es capaz de proporcionar una masa para el Higgs en acuerdo con la medición experimental. Dedicamos la segunda parte de la tesis al estudio pormenorizado del Modelo de Tripletes con Simetría Custodial, de donde derivamos resultados muy interesantes con aplicaciones tanto en física de partículas como en cosmología.

We know from experimental results but also from theoretical arguments that the very successful Standard Model of particle physics is just a low energy description of a more fundamental structure. Supersymmetry, a space-time symmetry that relates bosons and fermions, provides some of the most theoretically favored candidates to complete the Standard Model. However, null results in the searches for supersymmetric particles put these models under stress, specially since many of the nice properties of supersymmetry at the particle physics level are directly tied with its presence at the energy scales that are now being probed at the LHC. With no direct evidence for supersymmetry, is there an indirect measurement that particle physicists could use to test these models? In 2012 the Higgs particle was discovered at LHC. Its discovery gives closure to the Standard Model but also opens up a new window that could be useful in the study of physics beyond the Standard Model.

In the first part of this thesis we study the consequences of the Higgs discovery for minimal versions of supersymmetry. We find that the measured mass of the Higgs particle is heavier than what is expected by the minimal realizations of a supersymmetric Standard Model. We thus consider that the search for minimality, i.e. building models with the least number of elements, in the formulation of beyond the Standard Model theories may not be such a good guiding principle in this case and construct a more baroque realization of supersymmetry, the Supersymmetric Custodial Triplet Model. This theory features an extended Higgs sector and uses symmetry as a tool to get rid of some of the problems associated with the introduction of new degrees of freedom to the scalar potential of a theory, at the same time, it is able to provide a Higgs that fits properly the experimental measurement of its mass. We devoted the second part of the thesis to an in depth study of the Supersymmetric Custodial Triplet Model, deriving very interesting results that can be useful both for particle physics, and cosmology.

List of published works

REFEREED ARTICLES

1. **Diphoton and Diboson Probes of Fermiophobic Higgs Bosons at the LHC**

   Antonio Delgado, Mateo Garcia-Pepin, Mariano Quiros, Jose Santiago, Roberto Vega-Morales

   Submitted to PRD for publication, arXiv:1603.0096 [hep-ph]

2. **Strong electroweak phase transition from Supersymmetric Custodial Triplets**

   Mateo Garcia-Pepin, Mariano Quiros

   Submitted to JHEP for publication, arXiv:1602.01351 [hep-ph]

3. **GMSB with Light Stops**

   Antonio Delgado, Mateo Garcia-Pepin, Mariano Quiros

   JHEP **1508** (2015) 159, arXiv:1505.07469 [hep-ph]

4. **Dark Matter from the Supersymmetric Custodial Triplet Model**

   Antonio Delgado, Mateo Garcia-Pepin, Bryan Ostdiek, Mariano Quiros

   Phys. Rev. D **92**, no. 1, 015011 (2015), arXiv:1504.02486 [hep-ph]

5. **Supersymmetric Custodial Higgs Triplets and the Breaking of Universality**

   Mateo Garcia-Pepin, Stefania Gori, Mariano Quiros, Roberto Vega, Roberto Vega-Morales, Tien-Tien Yu

   Phys. Rev. D **91**, no. 1, 015016 (2015) , arXiv:1409.5737 [hep-ph]

6. **Electroweak and supersymmetry breaking from the Higgs boson discovery**

   Antonio Delgado, Mateo Garcia-Pepin, Mariano Quiros

   Phys. Rev. D **90** (2014) no.1, 015016, arXiv:1312.3235 [hep-ph]

7. **Supersymmetric Custodial Triplets**

   Luis Cort, Mateo Garcia-Pepin, Mariano Quiros

   Phys. Rev. D **88** (2013) no.7, 075010 , arXiv:1308.4025 [hep-ph]

CONFERENCE PROCEEDINGS

1. **Gauge mediation with light stops**

   Antonio Delgado, Mateo Garcia-Pepin, Mariano Quiros

   Planck 2015, Ioannina (Greece)

   PoS PLANCK **2015** (2015) 109, arXiv:1511.03254 [hep-ph]

Contents

List of abbreviations

SM Standard Model

LHC Large Hadron Collider

QFT Quantum Field Theory

GR General Relativity

EFT Effective Field Theory

BSM Beyond the Standard Model

EWSB Electroweak Symmetry Breaking

EW Electroweak

DM Dark Matter

EWBG Electroweak Baryogenesis

SUSY Supersymmetry

MSSM Minimal Supersymmetric Standard Model

NMSSM Next to Minimal Supersymmetric Standard Model

SCTM Supersymmetric Custodial Triplet Model

SSB Spontaneous Symmetry Breaking

EOM Equation Of Minimum

VEV Vacuum Expectation Value

DOF Degree Of Freedom

LSP Lightest Supersymmetric Particle

NLSP Next to Lightest Supersymmetric Particle

SSSB Spontaneous Supersymmetry Breaking

GMSB Gauge Mediated Supersymmetry Breaking

MGM Minimal Gauge Mediation

RGE Renormalization Group Equation

EWPT Electroweak Phase Transition

VBF Vector Boson Fusion

VH Associated Higgs Production

DY Drell Yan production

"They sat thus for sometime while the light faded, Belle in another temporary vacuum of discontent, building for herself a world in which she moved romantically, finely and a little tragical [...]"

- William Faulkner, excerpt from *Sartoris*

Introduction

The Standard Model (SM) of particle physics found experimental completion on the 4$^{\text{th}}$ of July 2012, when the ATLAS and CMS experiments at the Large Hadron Collider (LHC) announced jointly the discovery of a new particle with a mass of 125 GeV and characteristics similar to that of the Higgs boson predicted by the SM [1, 2]. The beauty of the Standard Model relies not only on its capacity to explain with great accuracy a wide range of observed phenomena, it is also remarkable that it does so by means of a few symmetry rules and some particle content. By being able to explain a large set of complex dynamics within a single and simple structure, the SM is a great testament to the power of the reductionist approach. For centuries reductionism, i.e. trying to explain the largest amount of phenomena given the least amount of 'universal' rules, has proven to be very successful. For instance, it allowed Newton to understand that the force that pushes objects to the ground was also responsible for the movement of stars and planets, Maxwell to write a set of equations that explained electricity and magnetism as manifestations of the same force, and Einstein to unify the concepts of space and time.

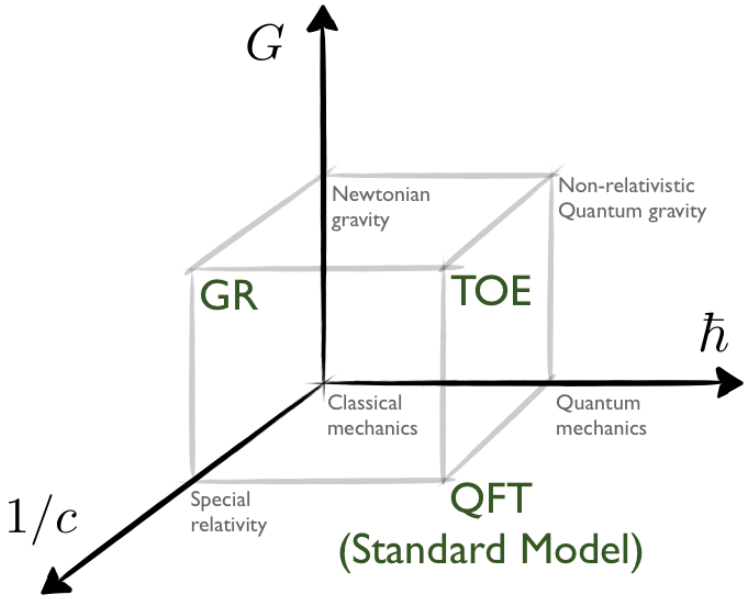

Figure 1: *Cube that schematically represents what are the features of the frameworks in which the SM (QFT) and ΛCDM (GR) are formulated. The axes are three fundamental constants that correspond to gravity (Newton's constant, G), quantum mechanics (Planck's constant, ħ) and special relativity (the inverse of the speed of light, 1/c). As a thought experiment one can vary them and modulate the importance of gravitational interactions, quantum mechanics and special relativity respectively. We can see from the cube that while GR is the relativistic classical field theory that describes gravitational interactions and fails to incorporate quantum mechanical nuances, QFT is the relativistic theory of quantum fields that is not able to include gravity. The theory of everything (TOE) will be the one able to explain phenomena in which velocities are relativistic and both gravity and quantum mechanics are taken into account.*

Quantum Field Theory (QFT), which describes the dynamics of relativistic quantum particles, and General Relativity (GR), our most sophisticated understanding of the force of gravity, also follow from considering the above strategy (see Figure 1). By using QFT and GR as frameworks, one is able to formulate the Standard Model and the Standard Model of Cosmology (ΛCDM)

which, together, can accurately predict the properties of matter from distances down to about $\sim 10^{-18}$ meters to the extreme conditions of the very early universe. In the spirit of reductionism, the logical next step would be to consider the SM and ΛCDM as part of the same structure, in other words, consider the SM as the microscopic description behind the physics at enormous scales of ΛCDM. The biggest issue that one faces when searching for a unified description of both models is that gravity runs into problems when quantized and GR can only be trusted as the low energy limit of a QFT with particles of spin-2 (gravitons). This is the infamous problem of quantum gravity; the absence of a framework that consistently incorporates GR and QFT (getting to the TOE tip of the cube in Figure 1) forbids us to write a model that would describe nature in a unified manner. However, only in very extreme conditions is a quantized theory of gravity necessary and for the most part we can try to describe the microscopic physics behind the properties of ΛCDM using the SM. The problem is that the SM falls short at describing a large set of observations which are well below the quantum gravity regime. This is an indication that, if we want to construct a unified picture, the SM needs to be completed by new physics Beyond the Standard Model (BSM).

On top of that, quantum field theories and in particular the SM have problems of their own when stabilizing scales related to elementary scalar masses. The Higgs boson is the excitation of the scalar field that is responsible for Electroweak Symmetry Breaking (EWSB), the mechanism that gives masses to SM fermions and massive gauge bosons. Under quantum corrections this field shows an extreme sensitivity to ultraviolet (UV) physics, i.e. physics at the highest possible energies. This sensitivity introduces such a degree of arbitrariness in the theory that the value of the electroweak (EW) scale ($\mathcal{Q}_{EW}$, the scale at which EWSB takes place) with respect to other dimensionful scales (for instance the Planck mass M_P, the scale at which gravity needs to be quantized) appears to be a 'lucky' accident ($\mathcal{Q}_{EW}/M_P \simeq 10^{-16}$) rather than something predicted from first principles. This is what is known as the hierarchy problem of the Standard Model. Actually, the hierarchy problem is not the only problem of this nature in fundamental physics; the cosmological constant problem (why the measured vacuum energy of the universe is so small?) is another big hierarchy for which our current understanding of the universe does not provide a satisfactory explanation. Although a 'lucky' accident is not logically excluded, these problems signal a 'theoretical discomfort' that may hint to bigger structures where these coincidences are explained in a more satisfying manner. The search for new physics beyond the SM based on these arguments is often dubbed as the naturalness strategy.

Supersymmetry (SUSY) is a space-time symmetry that relates fermions (matter) and bosons (radiation). In its presence dangerous quantum corrections to scalar masses cancel and there is a reason to explain $Q_{EW} \ll M_P$, therefore if supersymmetry is realized at a scale which is not much larger than $\mathcal{Q}_{EW}$ [1], it elegantly solves the hierarchy problem of the SM. Moreover, supersymmetric QFT's not only solve possible hierarchy problems but also unify the concepts of matter and radiation by grouping them as part of the same structure. As a sign of this SUSY has deep roots in String Theory, the best candidate that we have so far for a TOE.

However, for now supersymmetry has failed to pass experimental scrutiny and the world we are able to test looks non supersymmetric. SUSY (along with any other standard BSM proposal) does not appear as LHC pushes the scale that we probe to higher and higher values, hence, one is left with the question of what is the mechanism that stabilizes the EW scale after all. Also, the Higgs boson further increases the tension between SUSY and naturalness; with a mass of 125 GeV and couplings to other particles that are perfectly consistent with that of the SM, the

[1] If the masses of the supersymmetric copies of SM particles (superpartners) are not very heavy.

Higgs boson pushes the spectrum of superpartners towards even heavier masses than the current experimental limits [2]. In particular the Minimal Supersymmetric Standard Model (MSSM), the most economic formulation of a supersymmetric SM, is only able to fit the observed Higgs mass in extreme corners of its parameter space or with a very heavy spectrum of superpartners.

The absence of low energy signals and such an 'unnatural' Higgs mass have led some physicists to believe that maybe the answer to the hierarchy problem is not based on symmetries or new dynamics (bigger structures), but rather on environmental considerations. This would very roughly mean that the value of the EW scale is determined by probability and we just happen to live in a universe with observers (us) that are able to measure it. To embrace the latter as a solution (or answer) to the hierarchy problem is to take an alternative path to the naturalness strategy, which is very much related to the reductionist approach, that has brought physics so much success.

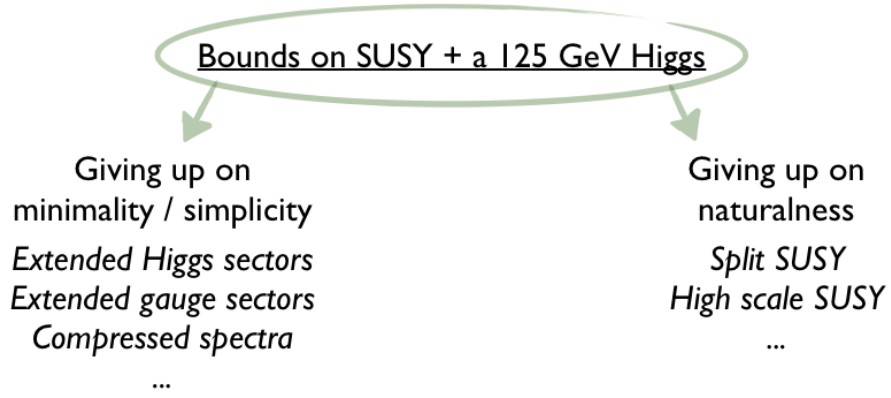

Figure 2: *Depiction of the crossroads in which SUSY phenomenology has entered after the first run of LHC. With limits on supersymmetric particles getting to the* ~ 1 *TeV mark and a Higgs mass that is 'heavy' and difficult to encompass with minimal versions of supersymmetry, one has to give up either on minimality/simplicity or on naturalness, the two driving principles for supersymmetric model building during the last few decades.*

Even if SUSY fails to solve the hierarchy problem of the SM, it still represents a step forward in the search for the unification of physical laws. In addition, its realistic particle physics implementations have very good phenomenological properties beyond solving the hierarchy problem. Thus, if we believe that SUSY is interesting enough and consider that it has to be realized in nature regardless of its position as a solution to the hierarchy problem, we are left with the situation depicted in Figure 2. A 125 GeV Higgs plus the absence of supersymmetric signals at LHC means that:

- Maybe the universe is indeed supersymmetric but at energy scales (distances) so large (so small) that LHC will not be able to probe it. In this case the EW scale is fixed by environmental considerations or non standard mechanisms that do not follow the usual naturalness strategy.

[2] If we consider natural a theory where the EW scale has no hierarchy problem, the heavier the superpartners are, the less natural the theory is.

- Maybe low-energy SUSY is indeed present but the version of supersymmetry that nature has chosen is not the simplest (more minimal) possibility and we need to consider models beyond the MSSM. This is not a very unreasonable option since the MSSM actually represents only a small fraction of the SUSY theory space.

The situation is such that making a decision is unavoidable. Either we give up on naturalness and focus on solving other problems, or we give up on minimality and try to come up with non minimal supersymmetric extensions of the SM that could ameliorate the tension between SUSY and naturalness.

The work presented in this thesis follows from making the choice to stick with naturalness and give up on minimality. We first analyze in detail the consequences of the Higgs discovery for minimal versions of SUSY theories and then, after concluding that the Higgs mass is difficult to fit naturally in the MSSM, we elaborate on the construction and properties of the Supersymmetric Custodial Triplet Model (SCTM). The SCTM is an extension of the MSSM which features a Higgs sector with three extra $SU(2)_L$ triplets of chiral superfields that will generate new tree level contributions to the Higgs mass. Thus allowing to accommodate the observed 125 GeV value without having to give up on naturalness.

Plan of the thesis

We will first set the grounds on Chapters 1 and 2, where we provide a brief overview of some of the topics needed to understand the rest of the thesis. In the former we introduce the Standard Model and some of its features, in particular the process by which the electroweak symmetry is spontaneously broken but also the custodial symmetry of the Higgs sector. After that, we motivate the need for BSM physics by listing some of the SM shortcomings, with special focus on the hierarchy problem. In Chapter 2 we introduce supersymmetry and the minimal supersymmetric generalization of the SM (the MSSM); we also comment on how low-energy supersymmetry solves the hierarchy problem.

The rest of the chapters are devoted to the presentation of the original research done by the author and collaborators (Luis Cort, Antonio Delgado, Stefania Gori, Bryan Ostdiek, Jose Santiago, Mariano Quirós, Roberto Vega, Roberto Vega-Morales and Tien-Tien Yu) on model building and the phenomenology of supersymmetric theories.

In Chapter 3, which is based on [3], we perform a thorough study of the consequences that the Higgs discovery has had on supersymmetric theories, in particular we focus on the MSSM an use the analysis to vindicate the naive depiction of Figure 2. As a consequence of this, we choose to stick with naturalness and try to come up with a model that could fit the experimentally measured Higgs mass without the need to go to extreme corners of the parameter space, or have very heavy superpartners. In our search for a model with such characteristics we find the SCTM, which we introduce in Chapter 4 only at tree level to analyze the interesting $SU(2)_L \otimes SU(2)_R \to SU(2)_V$ invariant structure. This chapter is based on [4]. In Chapter 5 we discuss how loop corrections modify the naive tree-level picture and propose a SUSY breaking mechanism in which the SCTM can be embedded. Once the UV completion is defined we can calculate realistic spectrums and the corresponding modifications to Higgs observables. We comment on the non standard phenomenology associated to these benchmark scenarios and end with a summary of the properties that the realistic realizations of the SCTM will show at the EW scale. This chapter is based on References [5] and [6].

The next Chapters are devoted to the study of features of the SCTM which are relevant for cosmology. In Chapter 6 we look at the neutralino Dark Matter (DM) properties of the model and find new ways of generating the correct relic abundance together with possible 'blind spots' in the direct detection cross sections. This chapter is based on [7]. Chapter 7 is based on [8]. In it we study the properties of the EW phase transition in the SCTM and analyze its viability for an Electroweak Baryogenesis (EWBG) scenario.

Finally, in Chapter 8 we study the collider consequences of the model which, as we will motivate along the rest of the work, are very important to probe its non standard features. This chapter is based on [9].

Disclaimer

By the time this thesis is being written some of the results presented are a few years old. The experimental input may (or may not) have changed with the release of LHC's early 13 TeV data. However, even if some bounds need to be updated, it is not going to be (yet) of great relevance for the overall picture that we present.

It is rare that results in theoretical particle physics can get outdated within the year, let this act as a testament of how exciting are these times in the field.

Part I: Particle physics in the LHC era

1

The Standard Model of particle physics

The Standard Model of particle physics, our current understanding of the tiniest scales to be probed at experiment, is a quantum field theory that describes three of the four fundamental forces, the Strong and Weak forces and the Electromagnetic force. It is formulated as a gauge theory, a type of field theory in which the Lagrangian is invariant under a continuous group of local transformations. We use gauge theories as a way of describing interactions between elementary particles.

In the first section of this chapter we construct the SM Lagrangian by determining its gauge group and the particle content, we then describe in detail the process by which the electroweak symmetry is broken and the gauge bosons become massive (Sec. 1.2). In Section 1.3 we look at the custodial symmetry of the Higgs sector that, as we will see, is of great relevance for the work that we present. Finally, we summarize the shortcomings of the MSSM with particular focus on the hierarchy problem (Sections 1.4 and 1.5 respectively). Note that this chapter is solely based on a series of books, reviews and articles and is by no means a thorough introduction suitable for the unexperienced. For more complete and pedagogical references we refer the reader to Refs. [10, 11].

1.1 Particle content and Lagrangian

The Standard Model gauge group is

$$\mathcal{G}_{\rm SM} \equiv SU(3)_C \otimes SU(2)_L \otimes U(1)_Y \,, \tag{1.1}$$

where $SU(3)_C$ describes the strong force of Quantum Chromodynamics (QCD) and $SU(2)_L \otimes U(1)_Y$ is the group of the Electroweak theory, which is responsible for the Weak and Electromagnetic forces. After EWSB the latter gets broken to the $U(1)_{QED}$ that describes Quantum Electrodynamics (QED), leaving at low energies $SU(3)_C \otimes U(1)_{QED}$ (see Sec. 1.2).

A direct consequence of imposing a gauge symmetry is the appearance in the spectrum of new massless spin-1 degrees of freedom (DOF's) that transform in the adjoint representation of the gauge group, these are called gauge bosons and they are the carriers of the force that is described by the gauge group. The particle content of the theory is completed after the matter fields and their transformation properties under the gauge symmetry are specified, for the Standard Model, these are listed in Table 1.1, where we also write the transformations under the space-time symmetries (Lorentz group).

Name	Fields	$SU(3)_C$	$SU(2)_L$	$U(1)_Y$	$SL(2,\mathbb{C})$	Spin
Gluons	G^A	**8**	**1**	0	$(\frac{1}{2},\frac{1}{2})$	1
W-bosons	W^a	**1**	**3**	0	$(\frac{1}{2},\frac{1}{2})$	1
B-boson	B	**1**	**1**	0	$(\frac{1}{2},\frac{1}{2})$	1
Quarks	q_L^i	**3**	**2**	$\frac{1}{6}$	$(\frac{1}{2},0)$	$\frac{1}{2}$
	u_R^i	**3**	**1**	$\frac{2}{3}$	$(0,\frac{1}{2})$	$\frac{1}{2}$
	d_R^i	**3**	**1**	$-\frac{1}{3}$	$(0,\frac{1}{2})$	$\frac{1}{2}$
Leptons	l_L^i	**1**	**2**	$-\frac{1}{2}$	$(\frac{1}{2},0)$	$\frac{1}{2}$
	e_R^i	**1**	**1**	-1	$(0,\frac{1}{2})$	$\frac{1}{2}$
Higgs	H	**1**	**2**	$\frac{1}{2}$	$(0,0)$	0

Table 1.1: *SM particle content. On top are described the Gauge bosons: G^A's ($A = 1,\dots,8$), W^a's ($a = 1,2,3$) and B, these last two will mix after EWSB to give rise to the massive $W^\pm$ and Z and the photon. Below we have the matter fields: quarks and leptons, the i index runs over the three families of fermions present in the SM. At the bottom of the table lies the Higgs, the field responsible for the breaking of the electroweak symmetry.*

Once the particle content and the gauge group are set we can write the most general Lagrangian that is compatible with both internal (gauge) and space-time symmetries,

$$\mathcal{L}_{\text{SM}} = \mathcal{L}_{\text{Gauge}} + \mathcal{L}_{\text{Fermions}} + \mathcal{L}_{\text{Higgs}}\,. \tag{1.2}$$

The gauge part of the Lagrangian features

$$\begin{aligned}\mathcal{L}_{\text{Gauge}} = &-\frac{1}{4}G^A_{\mu\nu}\left(G^{A\,\mu\nu} - \theta_3\frac{\alpha_3}{4\pi}\widetilde{G}^{A\,\mu\nu}\right) - \frac{1}{4}W^a_{\mu\nu}\left(W^{a\,\mu\nu} - \theta_2\frac{\alpha_2}{4\pi}\widetilde{W}^{a\,\mu\nu}\right)\\ &- \frac{1}{4}B_{\mu\nu}\left(B^{\mu\nu} - \theta_1\frac{\alpha_1}{4\pi}\widetilde{B}^{\mu\nu}\right),\end{aligned} \tag{1.3}$$

where $\alpha_i = g_i^2/(4\pi)$ and the field strength tensor $F^a_{\mu\nu} = \partial_\mu A^a_\nu - \partial_\nu A^a_\mu - g_j\epsilon^{abc}A^b_\mu A^c_\nu$, with its dual $\widetilde{F}_{\mu\nu} = \epsilon^{\mu\nu\rho\sigma}F_{\rho\sigma}/2$. The θ_i proportional terms are set to zero, in particular θ_3 is bounded to be really small, otherwise it will generate an amount of CP violation in the QCD sector that is excluded experimentally (Sec. 1.4).

The fermionic kinetic terms are,

$$\mathcal{L}_{\text{Fermions}} = \bar{\Psi}i\gamma^\mu D_\mu\Psi\,, \tag{1.4}$$

where the covariant derivative is defined as $D_\mu = \partial_\mu - ig'YB_\mu - gW^a_\mu T^a_R - g_sG^A_\mu t^a_R$. The fermions are grouped in $\Psi^T = (q^i_L \quad u^i_R \quad d^i_R \quad l^i_L \quad e^i_R)$ and the i index runs over the three fermion families of the Standard Model. The matrices t^A_R and T^a_R depend on the fermion representation; for the

fundamental representations of $SU(3)_C$ and $SU(2)_L$[1] they are given by the Gell-Mann matrices $\lambda^A/2$ and the Pauli matrices $\sigma^a/2$ respectively, while they are 0 for singlets.

And finally the Higgs part,

$$\begin{aligned}\mathcal{L}_{\text{Higgs}} = &\frac{1}{2}|D_\mu H|^2 + m^2|H|^2 + \frac{\lambda}{2}|H|^4 \\ &- \bar{q}_L^i h_{ij}^d d_R^j H - \bar{q}_L^i h_{ij}^u u_R^j \widetilde{H} - \bar{l}_L^i h_{ij}^e e_R^j H + h.c.\end{aligned} \tag{1.5}$$

The covariant derivative for the Higgs field is defined as $D_\mu = \partial_\mu - ig'/2B_\mu - gW_\mu^a\sigma^a$, $\widetilde{H} = i\sigma_2 H^*$ and h_{ij}^f are the Yukawa matrices. For simplicity we omit $SU(2)_L$ indices. Dirac masses for fermions are not possible in the SM without breaking the gauge symmetry, note that through the Yukawa terms, fermions get masses after EWSB once the Higgs field gets a vacuum expectation value.

A small note on higher dimensional operators

Above we are considering the SM as a $d = 4$ renormalizable field theory which does not feature any input coming from possible new physics at higher scales. A more subtle description of the SM is given in terms of Effective Field Theories (EFT's). The SM, as any field theory, can be though as an effective description of UV dynamics that generate higher dimensional operators. Therefore, the Lagrangian needs to be completed such that $\mathcal{L}_{\text{SM}} = \mathcal{L}^{d=4} + \mathcal{L}^{d>4}$, where

$$\mathcal{L}^{d>4} = \sum_{i,d} \frac{1}{\Lambda^{d-4}} \mathcal{O}_i^d \,. \tag{1.6}$$

These higher dimensional operators will always be suppressed by the scale at which they start to become relevant, which is normally considered the scale of new physics, and their effects can be used as a somewhat model independent probe of physics beyond the Standard Model, e.g. [12]. The use and study of EFT's is of great importance in all areas of theoretical physics, for instance, a description of the hierarchy problem of the SM in terms of an EFT will be given in Section 1.5. However, we will not go on much further than this on this topic; in this thesis we describe a specific model of new physics and there is no need to work in a model independent manner.

1.2 Electroweak symmetry breaking

The understanding of the process by which the electroweak symmetry is broken was an interdisciplinary [2] effort and, incontestably, one of the milestones of XX$^{\text{th}}$ century physics. It describes why the gauge structure of the SM follows

$$SU(3)_C \otimes SU(2)_L \otimes U(1)_Y \to SU(3)_C \otimes U(1)_{QED} \tag{1.7}$$

and gives rise to massive gauge bosons, moreover, it is directly related to the Higgs boson and therefore crucial for the studies carried out in this thesis. We will now try to describe it in detail.

[1] Which are **3** and **2**, since **n** is the fundamental representation of any $SU(N)$ group.

[2] The people who contributed to the formulation of EWSB drew concepts and ideas from condensed matter physics, showing how different natural phenomena that in principle look unrelated can have a very close theoretical link. As a way of 'returning the favor', insights coming from fundamental physics are now being used to develop new tools that describe the behavior of different materials [13].

As explained above, in the presence of gauge symmetries a set of massless spin-1 DOF's appears in the spectrum. Experimentally we do observe massless gauge bosons (the gluon and the photon) but also massive ones, the ones responsible for Weak interactions ($W^{\pm}$ and Z). This is already an indication that something is happening within the theory. Mass terms for gauge bosons explicitly break the gauge symmetry and one needs a way of giving them masses without spoiling the gauge structure of the theory. This can be done if instead of doing it explicitly we break the symmetry spontaneously, i.e. the Lagrangian has the symmetry but the parameters are such that the ground state of the Hamiltonian is not symmetric. After the process of breaking one may argue that some terms (for instance, mass terms for gauge bosons) in the Lagrangian exhibit an explicit breaking of the symmetry, however, this is not the case since the coefficients of the breaking terms are related by parameters that respect the symmetry. We will now present this point in more detail after a short comment.

The need to restore unitarity with a Higgs boson

Above we described briefly the somewhat top-down understanding of EWSB, another beautiful way of looking at this is by taking the bottom-up approach. It is tempting to think that the left hand side of (1.7) is useless if we end up having another symmetry structure that perfectly describes low energy physics. Therefore, let us take a Lagrangian that features massive gauge bosons and only respects the symmetry of the right hand side. If one tries to compute the scattering of massive gauge bosons (e.g. $W^+W^- \to W^+W^-$) what he finds is that the amplitude loses unitarity at some point and new degrees of freedom need to come in to restore it. This is precisely the role of the Higgs in this picture, it is though as the DOF that prevents the theory to break down more than the DOF that triggers EWSB. For a great pedagogical discussion see Section 2 of Ref. [14].

Spontaneous symmetry breaking

When we say that a theory is invariant or symmetric under a certain transformation we usually mean that the dynamics of the theory respect the symmetry and that there are observables which are invariant under those transformations too. However, it is possible that a symmetry is only respected at the level of the dynamics, with some observables breaking it. In this case one says that the theory is symmetric but the vacuum breaks the symmetry, this phenomenon is known as Spontaneous Symmetry Breaking (SSB) and it is precisely what happens in the Standard Model, where the electroweak symmetry is 'hidden' at low energies.

As a first example of SSB let us take a classical field theory which features a complex scalar field transforming non trivially under a global $U(1)$ symmetry ($\phi \to \mathrm{e}^{-iq\theta}\phi$)

$$\mathcal{L} = -\partial_\mu \phi^\dagger \partial^\mu \phi - m^2 \phi^\dagger \phi - \frac{1}{4}\lambda(\phi^\dagger\phi)^2 \,. \tag{1.8}$$

If $m^2 < 0$ the potential takes a mexican-hat shape (Fig. 1.1), therefore having a continuum of degenerate vacua given by

$$\phi = \sqrt{\frac{2}{\lambda}} m \, e^{-i\theta} \,. \tag{1.9}$$

Where θ is the phase that parametrizes the position in the flat direction.

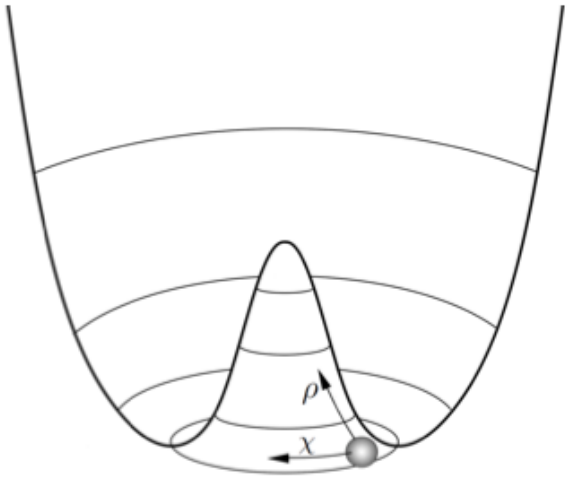

Figure 1.1: *Representation of a spontaneous symmetry breaking potential, 'the mexican hat'. The flat direction in field space gives rise to the massless mode, χ, while the radial direction has a U shaped potential and gives rise to the massive ρ.*

For simplicity we choose $\theta = 0$ and note that, when evaluated in the vacuum, the field ϕ will take a non zero value

$$\langle 0|\phi|0\rangle = \sqrt{2/\lambda}\, m \equiv v \neq 0\,. \tag{1.10}$$

This is what is called the Vacuum Expectation Value (VEV) and it sets the scale at which the spontaneous breaking of the symmetry happens. To see how the spectrum is affected let us study perturbations on top of one of these backgrounds. If

$$\phi(x) = \frac{1}{\sqrt{2}}(v + \rho(x))e^{-i\chi(x)/v}\,, \tag{1.11}$$

then the Lagrangian is

$$\mathcal{L} = -\frac{1}{2}\partial_\mu\rho\partial^\mu\rho - \frac{1}{2}\left(1+\frac{\rho}{v}\right)^2\partial_\mu\chi\partial^\mu\chi + m^2\rho^2 - \frac{\sqrt{\lambda}}{2}m\,\rho^3 - \frac{1}{16}\lambda\rho^4\,. \tag{1.12}$$

Which describes a massless excitation parametrized by the perturbation of the phase χ and a massive mode described by ρ. χ corresponds to the Nambu-Goldstone (NG) mode present whenever a symmetry is spontaneously broken, a direct consequence of the Goldstone theorem:

'The number of massless particles (Nambu-Goldstone bosons) is equal to the number of spontaneously broken generators of the symmetry'

Therefore with a $U(1)$, one broken generator, one massless mode in the spectrum. In the mexican hat picture χ and ρ correspond to moving in the angular (with zero energy cost, massless) and in the radial (where the value of the potential changes at every point, massive) directions. This extends naturally to the non-abelian case. Moreover, the effects of the quantization do not affect the main results, as the masslessnes of the NG mode holds at the quantum level.

SSB of local symmetries: The Higgs mechanism

The situation described above is not exactly what happens when one describes the spontaneous breaking of a gauge symmetry, which is local instead of global [3]. Let us see what happens to the $U(1)$ toy model if we promote the symmetry to a local one. The Lagrangian is then

$$\mathcal{L} = -(D_\mu\phi)^\dagger D^\mu\phi - m^2\phi^\dagger\phi - \frac{1}{4}\lambda(\phi^\dagger\phi)^2 - \frac{1}{4}F^{\mu\nu}F_{\mu\nu}\,, \tag{1.13}$$

where the derivative in the kinetic term has been promoted to a covariant one, D_μ, that introduces the interaction between the gauge and scalar fields. This potential is minimized for a non-zero VEV of the scalar field, that we can parametrize as v + perturbations

$$\phi(x) = \frac{1}{\sqrt{2}}(v + \rho(x))e^{i(\theta - \chi(x))}\,. \tag{1.14}$$

As in the global case we can set $\theta = 0$. The Lagrangian is now

$$\mathcal{L} = -\frac{1}{4}F^{\mu\nu}F_{\mu\nu} + \partial_\mu\rho(x)\partial^\mu\rho(x) + \frac{1}{4}\lambda v^2\rho(x)^2 + \frac{(v+\rho(x))^2}{v^2}\left(\partial^\mu\chi + vA^\mu\right)\left(\partial_\mu\chi + vA_\mu\right)\,. \tag{1.15}$$

This Lagrangian is explicitly gauge invariant, however we can now use a gauge transformation to set $\chi(x) = 0$, this is a concrete gauge called unitary gauge. Of course, if we now look at the Lagrangian

$$\mathcal{L} = -\frac{1}{4}F^{\mu\nu}F_{\mu\nu} + \partial_\mu\rho(x)\partial^\mu\rho(x) + \frac{1}{4}\lambda v^2\rho(x)^2 + (v+\rho(x))^2A^\mu A_\mu \tag{1.16}$$

we see that it is not gauge invariant anymore, this should not be a surprise since we have chosen a particular gauge. In addition we see that the gauge field has acquired a mass and that the NG mode has disappeared from the Lagrangian. This is the interesting difference with respect to the global case, the (apparent) Nambu-Goldstone boson is now non-physical since it can be removed by the appropriate choice of gauge. The number of degrees of freedom however remains unaltered compared to the global SSB case since now the gauge field has a mass and therefore an extra longitudinal polarization mode. The massive mode ρ remains there and cannot be removed by gauge transformations, this is the Higgs mode and the process by which the NG mode is 'eaten' by the vector boson is dubbed the Higgs mechanism.

This $U(1)$ toy model can easily be generalized to the $SU(2)_L \otimes U(1)_Y$ of the SM [4], for concreteness, we choose just to highlight some of the main features of the SM Higgs potential and SSB mechanism, without getting into too much detail.

The Higgs mechanism in the SM

We now come back to Eq. (1.5) and take a look at the scalar potential of the SM

$$V(H) = m^2|H|^2 + \frac{\lambda}{2}|H|^4\,, \tag{1.17}$$

[3] This topic is extremely subtle due to the fact that local symmetries are actually redundancies and cannot be broken. As we do not deal with these subtleties in this thesis we approach it by using the usual jargon of spontaneous breaking of gauge symmetries.

[4] The $SU(3)_C$ part of the symmetry remains unaltered after EWSB.

where the Higgs doublet has a structure determined by its quantum numbers,

$$H = \begin{pmatrix} G^+ \\ h^0 + iG^0 \end{pmatrix}. \tag{1.18}$$

To look for the VEV we take the neutral and real part of the potential $V(h^0)$ and search for its minima using the extremal condition $\partial V(h^0)/\partial h^0|_v = 0$ [5]. Provided that $m^2 < 0$, the values that satisfy the condition are

$$\langle 0|h^0|0\rangle = \frac{m}{\sqrt{\lambda}} \equiv v\,. \tag{1.19}$$

v is the electroweak VEV, the order parameter that will give masses to all particles in the SM. In the presence of the background $\langle h^0\rangle = v$, gauge bosons get masses (we say that they 'eat up' the goldstone modes and get longitudinal polarizations) through the kinetic terms in Eq. (1.5) and fermions through the Yukawa couplings, $m_f = h_f\, v$. The value of v is fixed by experiment so by measuring the masses of fermions we measure the entries of the Yukawa matrix. The Higgs particle is just a perturbation over the aforementioned background, we parametrize it in the following manner $h^0 = v + h/\sqrt{2}$ and from experiment we know that $v = 174$ GeV [6].

The Higgs potential of the SM depends only on two parameters m and λ, by the process of EWSB we are trading these two for v and m_h. Since we can determine the value of the physical Higgs mass by taking the second derivative of the potential, $m_h = V''(h^0)|_v/2$, we can infer the values of λ and m if we know the mass of the Higgs and the electroweak VEV, v. From $m_h = 125$ GeV and $v = 174$ GeV we get that $m = 88$ GeV and $\lambda \sim 0.26$. After the Higgs discovery and the determination of its mass, all SM parameters are known. This allows to extrapolate the theory to higher energies and, provided that there is no new physics below the scale that is being explored, make interesting predictions, for instance about the nature of the SM EW vacuum [15].

What happens with the SM gauge symmetry after EWSB?

After the Higgs field gets a VEV the vacuum state of the SM is not invariant under $SU(2)_L \otimes U(1)_Y$ because $T \cdot \langle H^T\rangle = T \cdot (0, v)^T \neq 0$, where T is any of the $SU(2)_L$ or $U(1)_Y$ generators. The gauge bosons corresponding to these broken generators are the ones who become massive, $W^\pm$ and Z. However, $(T_3 + Y)|0\rangle = Q_{QED}|0\rangle = 0$ is a symmetry of the vacuum and so the photon γ remains massless. This is why we say that $SU(2)_L \otimes U(1)_Y$ is broken to $U(1)_{QED}$ electromagnetism. Just for completeness, we write the gauge boson mass eigenstates after EWSB

$$W^\pm = \frac{1}{\sqrt{2}}(W_1 \mp iW_2)\,, \quad Z = c_{\theta_W} W_3 - s_{\theta_W} B \quad \text{and} \quad \gamma = s_{\theta_W} W_3 + c_{\theta_W} B\,. \tag{1.20}$$

where θ_W is the weak angle that rotates from (W_3, B) to (Z, γ), $s_{\theta_W} = \sin\theta_W = g'/\sqrt{g^2 + g'^2}$ and $c_{\theta_W} = \cos\theta_W = g//\sqrt{g^2 + g'^2}$.

[5] We want only neutral real scalar fields to acquire a VEV, other fields acquiring VEV's would generate dangerous breaking of symmetries for which we do not see any e.g. charge, CP, Lorentz symmetry, etc.

[6] There is another possible normalization where $h^0 = (v + h)/\sqrt{2}$ and $v = 246$ GeV, this one is used in the $U(1)$ example described above.

1.3 SM accidental symmetries and custodial symmetry

The actual structure of the Standard Model shows more internal symmetry than just the gauge group $\mathcal{G}_{\rm SM}$ and the CPT invariance of the Lagrangian. There are a few global symmetries that are not imposed and for which the SM Lagrangian shows an accidental (full or approximate) invariance. The presence of this accidental symmetries has interesting phenomenological consequences and it is taken as a guide when constructing models of new physics. We will focus here on the custodial symmetry of the Higgs sector, however, let us mention the rest as they are also of great importance in BSM model building. They are the $U(1)^5$ flavor symmetry, which is fully recovered when Yukawa couplings are set to zero, and the Lepton and Baryon number conservation, broken by neutrino oscillations and sphaleron transitions respectively, although these last two features are not present in the standard perturbative formulation of the SM.

The custodial symmetry of the Higgs sector

Let us now present in detail the custodial symmetry that protects the mass relation between the $W^\pm$ and Z fields

$$\rho \equiv \frac{M_W^2}{\cos\theta_W M_Z^2} = 1\,, \tag{1.21}$$

thanks to the following global symmetry breaking pattern

$$SU(2)_L \otimes SU(2)_R \to SU(2)_V\,. \tag{1.22}$$

To make this pattern manifest, we now rewrite the Higgs part of the Lagrangian, Eq. (1.5), in an $SU(2)_L \otimes SU(2)_R$ invariant manner. In order to do this, we first build an object for which we know the transformation rules under the global symmetry,

$$\bar{H} = (\widetilde{H},\, H) = \begin{pmatrix} H^{0*} & H^+ \\ -H^- & H^0 \end{pmatrix}\,. \tag{1.23}$$

$\bar{H}$ transforms as a $(\mathbf{2_L}, \bar{\mathbf{2}}_\mathbf{R})$ of $SU(2)_L \otimes SU(2)_R$ and we identify $Y = T_{3R}$ [7].

The complex conjugate representation is chosen for the $SU(2)_R$ ordering such that $\bar{H}$ gets a diagonal form after EWSB, this is why the $SU(2)_V$ is often called the diagonal subgroup, one could also write $(\mathbf{2_L}, \mathbf{2_R})$ and get the same result although maybe the symmetry breaking pattern would be less manifest. The $SU(2)_L$ is gauged, it corresponds to the usual $SU(2)_L$ group and acts on the components of H and $\widetilde{H}$, the $SU(2)_R$ part acts on $\bar{H}$, considering the $SU(2)_L$ doublets H and $\widetilde{H}$ as components of an $SU(2)_R$ structure [8]. This reasoning will also be applied in Chapter 4 to build 'bitriplets'.

The Higgs Lagrangian in terms of this 'bidoublet' $\bar{H}$ is

$$\mathcal{L}_{\rm Higgs} = \frac{1}{2}(D_\mu \bar{H})^\dagger (D^\mu \bar{H}) + m^2\,{\rm tr}\,[\bar{H}^\dagger \bar{H}] + \frac{\lambda}{2}\left({\rm tr}\,[\bar{H}^\dagger \bar{H}]\right)^2\,, \tag{1.24}$$

[7] It may seem that we used $Y = -T_{3R}$ but remember that when writing the complex conjugate of a triplet the generators change and $T_{3R}(\bar{\mathbf{n}}) = -T_3(\mathbf{n})$.

[8] See Appendix A.1 for further information.

where $h_{ij} \to 0$ and $g' \to 0$. We set these parameters to zero because $U(1)_Y$ and the Yukawa couplings are the two sources of explicit $SU(2)_L \otimes SU(2)_R$ breaking in the SM potential, in particular the top Yukawa will provide the main effect because of its relative size to the others [9].

After EWSB $\bar{H}$ gets a VEV and

$$\langle \bar{H} \rangle = \begin{pmatrix} v & 0 \\ 0 & v \end{pmatrix} , \tag{1.25}$$

thus, provided that the parameters of the $SU(2)_{L,R}$ transformations ($\mathcal{U}_{L,R} = \exp\{i\theta^a_{L,R}\sigma_a/2\}$) are equal ($\theta_L = \theta_R$), the symmetry is broken by the vacuum to $SU(2)_{L+R} \equiv SU(2)_V$. This is what we call the custodial symmetry [10].

The relation (1.21) is experimentally measured to a very good degree and large discrepancies to the $\rho = 1$ picture are not expected. At tree level, the SM features $\rho = 1$ automatically, however, it is not ensured in the presence of extended Higgs sectors that feature $SU(2)_L$ representations beyond the doublet if these acquire sizeable VEV's after EWSB. Imposing a symmetry breaking pattern such as that of Eq. (1.22) can be of great help when trying to build models with extended Higgs sectors as it will keep $\rho = 1$ at tree-level automatically (see Chap. 4).

The benefits of custodial symmetry do not stop at tree level, it also acts as a shield to dangerous loop contributions that could spoil the $\rho = 1$ relation, hence the name 'custodial'. Let us investigate this in more detail by considering radiative contributions to ρ,

$$\alpha T \equiv \Delta\rho = \frac{\Pi_{ZZ}(0)}{m_Z^2} - \frac{\Pi_{W^\pm W^\pm}(0)}{m_W^2} , \tag{1.26}$$

where $\Pi_{ii}(0)$ are contributions to the self energy of gauge bosons. αT is actually one of the Peskin-Takeuchi parameters [16], a set of observables that constrain the appearance of new physics in the electroweak sector by using measurements of different $\Pi_{ii}(0)$'s. Deviations from the relation (1.21) will be parametrized as $\rho = 1 + \alpha T$.

We now get rid of hypercharge impurities ($g' \to 0$) to continue with the argument, then

$$\alpha T = \frac{\Pi_{W^3W^3}(0) - \Pi_{W^\pm W^\pm}(0)}{m_W^2} . \tag{1.27}$$

Since it is made out of W boson self energies the T-parameter can be though of as being a spurious field that transforms in the $(\mathbf{3_L} \otimes \mathbf{3_L})$, with the following decomposition into irreducible representations: $\mathbf{1} \oplus \mathbf{3} \oplus \mathbf{5}$, and with αT sitting in the $\mathbf{5}$ irrep. If $\theta_L = \theta_R$, the custodial $SU(2)_{L+R}$ is a symmetry of the vacuum, thus forbidding anything but a singlet from getting a VEV, i.e. αT will be exactly zero and Eq. (1.21) will also hold at loop level. Since g' and the Yukawa couplings break explicitly $SU(2)_L \otimes SU(2)_R$, $SU(2)_V$ will not be an exact symmetry of the vacuum and αT will get non zero values. We can consider the T-parameter as the measure of the custodial breaking that a theory suffers. Models of new physics can introduce new contributions to custodial breaking beyond g' and h_t that will show up in αT, spoiling the $\rho = 1$ relation.

[9] Note that if $h^u = h^d$ one could write (u_R, d_R) as a $\mathbf{2}$ of $SU(2)_R$ and we would have an enhanced custodial symmetry, however, this is not the case and the Yukawa sector is a source of custodial breaking.

[10] Often 'custodial' refers to both the global $SU(2)_L \otimes SU(2)_R$ symmetry and the $SU(2)_V$ subgroup interchangeably. We will explicitly distinguish between them since the custodial symmetry is a symmetry of the gauge boson mass matrix and thus it is only well defined at the EW scale, while the global $SU(2)_L \otimes SU(2)_R$ can in principle be imposed at any scale. This point will be of great importance in the study of the SCTM as we will see in Chapter 5.

1.4 Open puzzles in fundamental physics

Let us now motivate extensions of the Standard Model by listing some of the puzzles in fundamental physics for which the SM has no explanation. These problems can be classified as being data driven or theoretical suggested.

Data driven

As successful as the SM is, it is not able to give an explanation to a number of experimental results.

- Neutrino masses: The observation of neutrino oscillations is an indication that neutrinos have a non zero mass. In the the renormalizable version of the SM no mass for neutrinos can be accommodated, however, if we consider higher dimensional operators, a $d = 5$ term that generates Majorana masses for the neutrinos via see-saw mechanism can be added to the Lagrangian. In order to generate the correct neutrino masses, the appearance of such a higher dimensional operator is probably tied to new physics at $\sim 10^{15}$ GeV.

- Dark Matter: Astrophysical (e.g. galaxy rotation curves) and cosmological (e.g. structure formation) observations reveal the presence of an extra contribution of matter to the energy budget of the universe that cannot be accounted for with SM particles. Thus far, the only evidence of this extra contribution is gravitational however, unless one changes radically the cosmological evolution determined by the very successful ΛCDM, it seems that the answer to the dark matter problem lies within particle physics beyond the Standard Model. In the form of a neutralino LSP, the SCTM can offer a viable DM candidate (see Chapter 6).

- Matter antimatter asymmetry: The baryon asymmetry of the universe (the imbalance between baryonic and antibaryonic matter) needs a microscopic mechanism that explains it. Both Leptogenesis and Electroweak Baryogenesis, the only mechanisms constructed up to now which are successful, cannot rely only on SM dynamics and one needs to go beyond. The SCTM offers an interesting avenue to construct successful EWBG models, we study it in Chapter 7

- Inflation: It is now well established (although not 100% experimentally confirmed) that the early universe went through a period of inflationary expansion after which structure was generated from initial quantum perturbations. If not, one would need satisfactory answers to the flatness and horizon problems that inflation solves elegantly. As elegant as the cosmological point of view is, it still lacks a microscopic picture that explains it. The SM, even if it looks like it could do the job in a very minimal way, fails to provide a good inflaton [11] candidate [17].

Theoretically suggested

Besides not being able to explain some experimental results, the SM gives reasons for 'unease'. These are not a clear indication that there 'must' be something else (and therefore not at the same level as the items described above), but rather a suggestion that the different features of

[11] The scalar field that drives inflation.

the SM that look ad-hoc are pointing towards a bigger structure, where arguments based on symmetries or new dynamics can give satisfactory answers.

- Fermionic structure: The top quark couples to the Higgs field with $\mathcal{O}(1)$ strength while the other fermions of the SM couple very weakly, on top of that, the Yukawa matrices for quarks seem to follow a hierarchical structure with no explanation whatsoever (Yukawa couplings are determined from experiment by measuring the masses of the different fermions in the SM). Where does this structure comes from? Also, leptons are parametrically lighter than quarks, why would that be?

- Gauge couplings: By extrapolating to higher energies the gauge couplings corresponding to the $\mathcal{G}_{\rm SM}$ structure of the SM, one finds an approximate unification at $\sim 10^{15}$ GeV that could be interpreted as a hint of a bigger group where $\mathcal{G}_{\rm SM} \subset \mathcal{G}_{\rm GUT}$. A unified group structure will also give an explanation as to why anomalies cancel in the SM.

- Strong CP-problem: The absence of CP-violation in QCD has been tested to great accuracy via measurements of the electric dipole moment of the neutron. Nevertheless, the gauge part of the SM Lagrangian (Eq. (1.3)) contains a term which can be a source of CP-violation unless it is tuned $\theta_3 \sim 0$. One is allowed to set this parameter as small as it needs to be, however, since in principle there is no reason for it to be zero (no symmetry protecting it, see Sec. 1.5) one is left with the question of what makes it so small. The Peccei-Quinn mechanism solves the strong CP-problem by means of a spontaneously broken symmetry, in addition it predicts an extra particle, the Axion, that can be a good DM candidate.

- Cosmological constant: The accelerated expansion of the universe can be accounted for by adding a vacuum energy term in the Lagrangian which is measured to be $\Lambda^4_{\rm CC} \sim 10^{-47}$ GeV^4 . However, in a similar manner to what happens with the Higgs mass (see Sec. 1.5), its natural value is $\Lambda^4_{\rm CC} \sim M_P^4 \sim 10^{76}$ GeV^4. This represents an enormous fine-tuning of about 129 orders of magnitude, even bigger than that of the Higgs mass, which has found no compelling solution yet. Only Weinberg was able to derive an upper bound (actually very close to the measured value) by considering anthropic arguments, i.e. the cosmological constant has to have the right value so we are able to measure it [18].

- Hierarchy problem of the SM: The hierarchy problem of the Higgs mass (or in a more general way, why is the EW scale much smaller than the Planck mass) is the only puzzle of the SM that points towards new physics at the TeV scale and it is central to the development of this thesis. We will further elaborate on it and naturalness arguments in general in the next Section (Sec. 1.5).

1.5 The hierarchy problem and naturalness

Let us first define the naturalness paradigm that we want our theory of the Weak interactions to fulfill:

'The EW scale scale should be insensitive to quantum effects from physics at much Higher scales'

The SM fails to confront this, elementary scalar masses such as the Higgs show an extreme sensitivity when coupled to heavy degrees of freedom. When computing radiative corrections to the Higgs mass generated by new heavy DOF's, a huge fine-tuning between Lagrangian parameters and counterterms is required in order to keep the mass of the Higgs light. By fine-tuning we mean the miraculous cancellation that makes $a - b = c$ hold while $a, b \gg c$. As explicitly showing this cancellation is subtle since it depends a lot on the choice of regulator and renormalization scheme, we rather present the problem in a Wilsonian approach by using effective field theory.

The SM as an EFT and quantum corrections to scalar and fermion masses

The SM as a renormalizable theory that is valid all the way up the UV does not have a hierarchy problem per se, it is only when we consider that the Higgs is coupled to new physics above the EW scale that it appears. However, with no direct signs of BSM physics that couple to the Higgs sector, is it reasonable to consider the SM as an EFT? There is overwhelming experimental evidence for BSM already at the particle physics level (see Sec. 1.4). Moreover, even if we think that every problem of the SM is solved by dynamics that do not couple to the Higgs and therefore do not generate dangerous loop contributions, we will always end up having to deal with gravity, i.e. graviton loops, at M_P [12]. This is why it is very reasonable to consider the SM as an EFT.

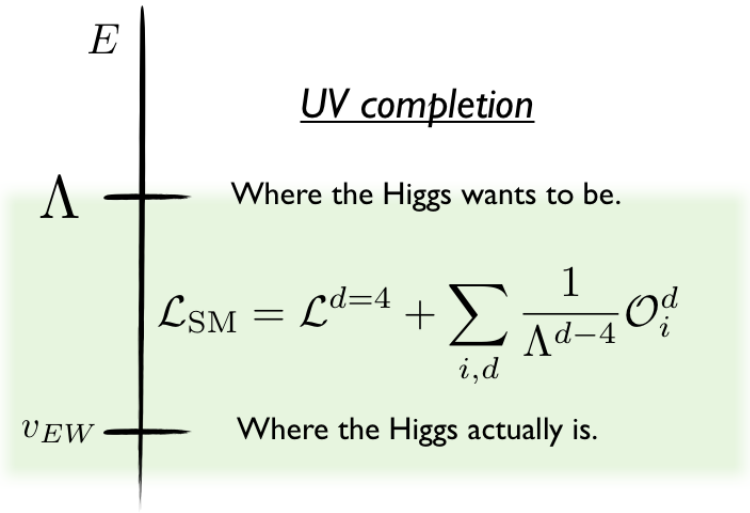

Figure 1.2: *Depiction of how the SM looks like when regarded as an EFT. The shaded region is the range of validity of the EFT, the full Lagrangian is the $d = 4$ renormalizable Lagrangian + higher dimensional operators generated by new dynamics beyond Λ.*

Once we consider the SM as an effective theory we generate a physical cutoff Λ that represents the scale at which the EFT breaks down and new dynamics need to enter to explain the observed phenomena, see Fig. 1.2. This allows to compute corrections to the masses of different particles and get an explicit dependence on the scale of new physics without having to specify a concrete

[12] This is true provided that our current understanding of the Planck mass as a UV cutoff for the low energy field theory description holds. It may happen that M_P is not as related to field theory as we think, then, in the absence of new physics below M_P and considering that the field theoretical description breaks down above, the Higgs mass will not suffer a hierarchy problem [19].

UV completion. We do so by using a regulator that introduces the cutoff in a sharp manner so that the dependence on it is explicit. We first consider corrections to fermion masses. Take for instance one of the SM fermions and consider the diagram depicted in the left panel of Figure 1.3, which is generated by the kinetic term for fermions in the SM Lagrangian, Eq. (1.4). A gauge boson generates a loop and therefore a correction to the mass of the fermion,

$$\delta m_f \sim m_f \log\left(\frac{\Lambda}{m_f}\right). \tag{1.28}$$

Note how the correction to the fermion mass is proportional to itself. This is the key point, if the mass is zero at tree level no mass is generated radiatively. In this case we say that the mass is protected by a symmetry, the chiral symmetry that is recovered when fermion masses are set to zero,

$$\psi \to \gamma_5 \psi\,, \quad \bar{\psi} \to -\bar{\psi}\gamma_5\,. \tag{1.29}$$

Something similar happens for vector bosons whose masses are protected by the gauge symmetry.

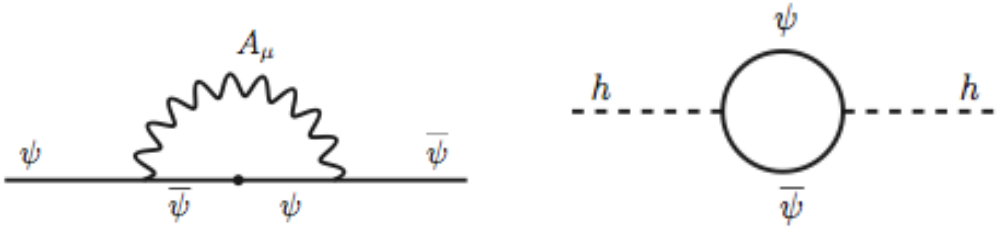

Figure 1.3: *Left: Generic correction the mass of a SM fermion generated by gauge bosons. Right: Correction to the SM Higgs generated by one of the SM fermions.*

Now we consider the correction to the mass of the Higgs which is shown in the right panel of Fig. 1.3 and is generated by a Yukawa type term $y\,\bar{\psi}\psi h$ as those of (1.5),

$$\delta m_h^2 \sim y^2 \Lambda^2\,. \tag{1.30}$$

Here the correction is not proportional to the mass and even if we set it to zero at tree level a mass of the order of the cutoff is generated through loops. No symmetry arises if we set the mass of the Higgs to zero so no symmetry protects it from becoming as heavy as Λ (see Figure 1.2). This is in agreement with the naturalness criterion proposed by 't Hooft [20]:

'At any energy scale, a physical parameter a is allowed to be very small only if the replacement $a = 0$ would increase the symmetry of the system'

Which is followed in the SM by fermion and gauge boson masses while it does not by the Higgs mass, i.e. the Higgs mass is unnatural.

With this in mind, it is important to stress that the hierarchy problem does not break the consistency of the SM as the absence of a Higgs would (see Sec. 1.2). The correct Higgs mass can be fitted after the renormalization procedure by adding counterterms to the Lagrangian such that the large loop contributions cancel. However, how large are the cancellations needed between

different Lagrangian parameters to keep $m_h \sim \mathcal{Q}_{EW}$? For instance, if we take the cutoff of the effective theory to be $\Lambda = M_P$, the cancellations must be of the order of one part in 10^{32}. Just to put things in perspective, the degree of accuracy needed for these to happen is similar to that of trying to balance a pencil on its tip where the tip is one millimeter wide and the length is roughly the diameter of the solar system [13]!

Of course, such degree of fine-tuning is unsettling. In fact it is so unsettling that it has been the main motivation for constructing BSM theories during the last decades and it is the reason why one expects new physics to appear in the (now in his second run) LHC. Every other SM problem could be solved by new physics at a scale out of the current experimental reach, however, common solutions to the hierarchy problem predict new physics at or just above ($\sim$ 1 TeV) the EW scale.

Standard and new solutions to the hierarchy problem

To stabilize the EW scale one can:

- Lower the cutoff of the effective SM so that the hierarchy between Λ and m_h is mild enough (see Figure 1.2). This is the case of theories which feature extra dimensions or consider the Higgs as a composite particle, both can be related through the AdS/CFT correspondence and are usually classified as strongly coupled proposals for solving the hierarchy problem. In particular the composite Higgs idea is a variation of the strong symmetry breaking paradigm that interpolates between Technicolor theories and the Higgs model. Inspired by the chiral symmetry breaking of QCD, one can obtain a scalar boson naturally lighter than the other resonances belonging to the strong sector if it emerges as the pseudo Nambu-Goldstone boson of an enlarged global symmetry breaking pattern [14, 22] [14]. At low energies the composite Higgs will almost look as an elementary one so the theory will be able to satisfy electroweak precision tests. Concerning the hierarchy problem the situation is really similar as to what it happens in QCD with the pion, corrections to its mass are saturated at the scale where the pion decays ($f_\pi \sim 130$ MeV). The same thing will happen here, a scale ($f > v$) at which corrections to the Higgs mass saturate is set, depending on how much difference between scales we have (roughly $\xi = v/f$), the amount of tuning needed can be considered natural or not.

- Introduce a new symmetry such that large radiative contributions cancel out, the paradigm of that being supersymmetry. One advantage of SUSY with respect to other proposals is that it robustly solves the hierarchy problem without UV sensitivity, once present, scalar masses will be protected against dangerous loop corrections up to M_P. While compositeness solves the hierarchy $f/\mathcal{Q}_{\rm EW}$, it does not give an answer to what might happen between f and M_P. We will further discuss supersymmetric theories and the solution they provide to the hierarchy problem in Chapter 2 (Sec. 2.5).

During recent years and due to the absence of BSM signals at colliders, solutions who do not follow the common strategies have been explored. One recently proposed possibility is that the

[13] This analogy is taken from [21], a very interesting reference where these topics are discussed.

[14] Note that 'pseudo' comes from the fact that this enlarged global symmetry will be explicitly broken by couplings between the strong and the elementary sector. Due to this, radiative corrections will generate a non vanishing mass for the normally massless Nambu-Goldstone bosons.

EW scale (the Higgs mass) is fixed dynamically in the early universe [23], also, motivated by the success of the anthropic arguments that Weinberg used to derive the bound on the cosmological constant, some effort has been thrown into explaining the smallness of the EW scale and the different hierarchies between fundamental constants through the notion of the multiverse and the landscape of vacua in string theory (for a review see Ref. [24]). Another interesting class of solutions is that of neutral naturalness, where the top partners associated to the introduction of new physics are color 'neutral' (not charged under $SU(3)_C$) and their collider bounds are greatly reduced. The best known realization of the latter is the twin Higgs model [25].

2

Supersymmetry and the MSSM

In this chapter we introduce the paradigm of supersymmetry, whose nature beyond that of a mathematical entity is yet to be confirmed. In the first section of the chapter (Sec. 2.1) we present the concept of SUSY and its most interesting theoretical features. Then, in Sections 2.2 and 2.3 we briefly detail $N = 1$ supersymmetric field theories in $d = 4$ dimensions in order to build realistic supersymmetric generalizations of the SM. We introduce the MSSM in Section 2.4, paying particular attention to the way in which EWSB is achieved and to the features of its Higgs sector. We also discuss the solution to the hierarchy problem that SUSY provides (Sec. 2.5) and some extra phenomenological consequences of building supersymmetric extensions of the SM (Sec. 2.6). As with the previous chapter, we do not pretend to make an in depth dissertation about supersymmetry as there is plenty of literature discussing these topics in a more pedagogical manner [26–29].

2.1 What is supersymmetry?

Supersymmetry maps particles and fields of integer spin (bosons) into particles and fields of half integer spin (fermions) and viceversa

$$Q\,|\text{boson}\rangle = |\text{fermion}\rangle \quad \text{and} \quad \bar{Q}\,|\text{fermion}\rangle = |\text{boson}\rangle\,. \tag{2.1}$$

Since it changes the spin of the particle (hence, its space-time properties) it is a space-time symmetry. When introducing SUSY, the usual space-time Poincaré invariance of the theory is extended with fermionic generators that together with the bosonic ones form the Superpoincaré algebra. The bosonic generators are the usual ones

$$M^{\mu\nu} \to \textit{Lorentz group} \quad \text{and} \quad P^{\mu} \to \textit{translations}\,, \tag{2.2}$$

where within the Lorentz group we have: boosts ($k^i = M^{i\,0}$) and rotations ($J_i = \epsilon_{imn}\, M^{mn}$). The fermionic generators are

$$Q^A_\alpha\,,\ \bar{Q}^{A}_{\dot{\alpha}} \tag{2.3}$$

Where α are two component weyl spinor indices and A is an index that runs over the number of fermionic generators, i.e. the number of supersymmetries. The commutation relations with other generators are the following

$$[Q, P^{\mu}] = 0\,, \quad [Q, G] = 0 \quad \text{and} \quad [Q, M^{\mu\nu}] \neq 0\,. \tag{2.4}$$

Q commutes with translations and quantum numbers given by internal symmetries such as gauge or global symmetries [1], it does not with Lorentz generators. What this means is that in a theory where SUSY is exactly realized, particles with different spin will be classified into (super)multiplets with common mass and quantum numbers.

Formal motivations for supersymmetry

From a purely theoretical point of view there are a few arguments which should be able to convince ourselves that the study of SUSY theories is an avenue worth being pursued.

- Up to now, the path of understanding physical laws has always pointed towards unification. The formulation of the Standard Model, which describes in a unified way all known non-gravitational interactions, is the greatest accomplishment of this strategy. By relating bosons and fermions supersymmetry provides a unified description of radiation (particles which are force carriers) and matter. It is therefore reasonable to think that SUSY looks like a really natural framework where to formulate a theory that is able to describe all known interactions in a unified way.
- Through the Haag-Lopuszanski-Sohnius extension [30] of the Coleman-Mandula theorem [31] (which does not include fermionic generators in the Poincaré algebra) we know that the most general continuous symmetry group allowed by the S-matrix is

  $$\textit{Superpoincaré} \otimes \textit{Internal symmetries}$$

  Which is precisely what a SUSY quantum field theory features. Maybe nature has realized all possible kinds of allowed symmetries?
- Finally, space-time supersymmetry is a prediction of String Theory, the best candidate for a theory of everything we have so far.

While all three arguments point towards SUSY as probably being realized in nature, they do not tell us anything about the scale at which this should happen, we might just happen to live in a universe that features supersymmetry but at such small distances that we will never be able to tell it.

2.2 $N = 1$ supersymmetric field theories

Although one can have several supersymmetries [2] for almost all phenomenological purposes one only deals with theories which realize only one, $N = 1$. The MSSM is constructed as the most economic $N = 1$ extension of the SM so in order to describe it in detail, let us first briefly introduce the formulation of $N = 1$ supersymmetric field theories.

[1] Actually, some particular internal symmetries (e.g. R-symmetries, which are relevant for the study of SUSY breaking) do not commute with Q.

[2] Note that there are limits on the maximum number possible which come from the maximum spin that is allowed for local interacting theories. The reason is that any supermultiplet contains particles with spin as large as $(1/4)N$, therefore to describe gauge theories with maximal spin-1 we can have $N = 4$ at most, whereas we can have $N = 8$ for theories that incorporate gravity and have maximal spin-2 (supergravities).

The superfield formalism

In SUSY theories one does not deal with single particle states but with supermultiplets of particle states with common mass and quantum numbers but different spin. It is for this reason that a Lagrangian written in terms of single particle states will not feature manifest supersymmetry. In order to make supersymmetry manifest, one needs to construct a framework where supermultiplets are mathematical entities whose transformation properties under all symmetries are well defined. In the $N = 1$ case this framework is the superfield formalism that we now introduce.

The first step is to enlarge the usual space-time coordinates x^μ to include anti-commuting Grassman coordinates $(\theta_\alpha, \bar{\theta}_{\dot{\alpha}})$ which are associated with the fermion generators $(Q_\alpha, \bar{Q}_{\dot{\alpha}})$, this enlargement is a direct consequence of extending the Poincaré symmetry. We call this the superspace

$$(x^\mu, \theta_\alpha, \bar{\theta}_{\dot{\alpha}}) \,, \tag{2.5}$$

and it is just a trick to make the properties of supersymmetry more transparent. A field in the superspace is dubbed a superfield and it is a function of the variables in (2.5), $Y = Y(x, \theta, \bar{\theta})$. Since θ_α and $\bar{\theta}_{\dot{\alpha}}$ anticommute, any product of more than two θ's or two $\bar{\theta}$'s will vanish. Hence, the most general superfield has the following form

$$\begin{aligned} Y(x^\mu, \theta, \bar{\theta}) = f(x) \,+\, \theta\,\psi(x) \,+\, \bar{\theta}\,\bar{\chi}(x) \,+\, \theta\theta\, m(x) \,+\, \bar{\theta}\bar{\theta}\, n(x) + \\ +\, \theta\sigma^\mu\bar{\theta}\, v_\mu(x) \,+\, \theta\theta\,\bar{\theta}\,\rho(x) \,+\, \theta\theta\,\bar{\theta}\bar{\theta}\, d(x) \,. \end{aligned} \tag{2.6}$$

Note that each of the terms is a Poincaré transforming field, this shows that a superfield is just a collection (a multiplet) of ordinary fields.

The construction of actions invariant under supersymmetry will provide further constrains on the form of the superfields. Supersymmetric invariant actions are constructed by integrating in superspace a suitable defined superfield, this is because

$$\int d^4x\, d^2\theta\, d^2\bar{\theta}\, Y(x, \theta, \bar{\theta}) \tag{2.7}$$

is a supersymmetric invariant quantity when Y is a superfield. We can thus construct products of superfields $\mathcal{Y} = \prod_i Y_i$ [3] which should give rise upon integration in superspace to a Lagrangian density that is real, dimension four and that transforms as a scalar density under Poincaré transformations,

$$\mathcal{S} = \int d^4x\, d^2\theta\, d^2\bar{\theta}\; \mathcal{Y}(x, \theta, \bar{\theta}) = \int d^4x\, \mathcal{L}(\phi(x), \psi(x), A_\mu(x), \dots) \,. \tag{2.8}$$

Actually this last point is automatic, if the action is constructed in this way we can guarantee that the Lagrangian in the right hand side of the equation is Poincaré and supersymmetric invariant. We just have to make sure that $\mathcal{Y}$ is constructed in such a way that the realness and dimensionality are correct and that the given internal symmetries are also respected.

The superfield $\mathcal{Y}$ is in general a product of superfields that cannot be the basic object to construct invariant actions, i.e. it is not an irreducible representation of the supersymmetry algebra. By imposing supersymmetric invariant constrains we can restrict the form of $\mathcal{Y}$ while making sure that the resulting object is still a superfield and hence a representation of the SUSY

[3] A product of superfields is a superfield.

algebra. Two of these constrains are very important to construct realistic particle models and will result in the definition of chiral and vector superfields, these are the objects where the matter (chiral) and radiation (vector) of the SM are embedeed.

A chiral (anti-chiral) superfield Φ is a superfield such that

$$\bar{D}_{\dot{\alpha}}\Phi = 0 \quad (D_\alpha \Psi = 0)\,, \tag{2.9}$$

where $\bar{D}_{\dot{\alpha}} = \bar{\partial}_{\dot{\alpha}} + i\,\theta^\beta \sigma^\mu_{\beta\dot{\alpha}}\partial_\mu$ ($D_\alpha = \partial_\alpha + i\,\sigma^\mu_{\alpha\dot{\beta}}\bar{\theta}^{\dot{\beta}}\partial_\mu$). Note that if Φ is chiral $\bar{\Phi}$ is anti-chiral and thus chiral superfields are not real. Once the constrain is applied to (2.6) the form of a chiral superfield is

$$\begin{aligned}\Phi(x,\theta,\bar{\theta}) = \phi(x) + \sqrt{2}\theta\psi(x) + i\,\theta\sigma^\mu\bar{\theta}\partial_\mu\phi(x) - \theta\theta F(x) - \frac{i}{\sqrt{2}}\theta\theta\partial_\mu\psi(x)\sigma^\mu\bar{\theta} \\ - \frac{1}{4}\theta\theta\,\bar{\theta}\bar{\theta}\,\Box\phi(x)\,.\end{aligned} \tag{2.10}$$

ϕ is the scalar part (squarks, sleptons or Higgs), ψ is the fermion (quark, leptons or higgsino) and F is an non-dynamical auxiliary field that is needed to match the number of degrees of freedom of bosons and fermions on-shell [4]. Actually, the number of DOF's coincides precisely with those of an $N = 1$ chiral supermultiplet that is built on states rather than on fields, hence a chiral superfield is an irreducible representation of the SUSY algebra.

In order to get vector fields we impose a reality condition

$$V = \bar{V}\,, \tag{2.11}$$

after applying the constrain to (2.6) and gauge fixing to the Wess-Zumino gauge [5] we get

$$V_{WZ}(x,\theta,\bar{\theta}) = \theta\sigma^\mu\bar{\theta}\,V_\mu(x) + i\,\theta\theta\,\bar{\theta}\,\bar{\lambda}(x) + i\,\bar{\theta}\bar{\theta}\,\theta\,\lambda(x) + \frac{1}{2}\,\theta\theta\,\bar{\theta}\bar{\theta}D(x)\,. \tag{2.12}$$

V_μ corresponds to gauge particles (γ, $W^\pm$, Z, gluon), λ, $\bar{\lambda}$ to the gauginos and D plays the same role as the F field in the chiral superfield. It can also be shown that the DOF's match those of a vector supermultiplet thus making the vector superfield an irreducible representation of the SUSY algebra.

$N = 1$ Lagrangians

Once we know the objects where we will accommodate the DOF's we can construct a SUSY invariant Lagrangian to determine the interactions of the theory. The most general $N = 1$ renormalizable (thus, with canonical Kahler potential) Lagrangian is

$$\mathcal{L} = \mathcal{L}_{\text{SYM}} + \mathcal{L}_{\text{matter}} + \mathcal{L}_{\text{FI}}\,. \tag{2.13}$$

The pure gauge sector for any Yang-Mills group with coupling constant g is

$$\begin{aligned}\mathcal{L}_{\text{SYM}} &= \frac{1}{32\pi}\text{Im}\left(\tau\int d^2\theta\,\text{tr}\,[W^\alpha W_\alpha]\right) \\ &= \text{tr}\left[-\frac{1}{4}F_{\mu\nu}F^{\mu\nu} - i\lambda\sigma^\mu D_\mu\bar{\lambda} + \frac{1}{2}D^2\right] + \theta_{YM}\frac{\alpha}{16\pi}\,\text{tr}\left[F_{\mu\nu}\widetilde{F}^{\mu\nu}\right]\,,\end{aligned} \tag{2.14}$$

[4] In a supermultiplet $n^f_{\text{DOF}} = n^b_{\text{DOF}}$.

[5] From now on and during the rest of this discussion we will assume to be in the Wess-Zumino gauge.

where W^α is the supersymmetric generalization of the field strength, i.e. the gauge invariant object that should enter the action, τ is the complexified gauge coupling $\tau = \theta_{YM}/2\pi + 4\pi i/g^2$ and α and θ_{YM} where previously defined below Eq. (1.3).

The matter Lagrangian describes the interactions between the chiral superfields Φ (also $\chi_{\rm SF}$), and with the vector superfields V (also $V_{\rm SF}$) corresponding to the gauge group described in $\mathcal{L}_{\rm SYM}$,

$$\begin{aligned}\mathcal{L}_{\rm matter} &= \int d^2\theta\, d^2\bar\theta\, \bar\Phi\, e^{2gV}\Phi + \int d^2\theta\, W(\Phi) + \int d^2\bar\theta\, \overline{W}(\bar\Phi) \\ &= \overline{D_\mu\phi} D^\mu\phi - i\psi\sigma^\mu D_\mu\bar\psi + \bar F F + i\sqrt{2}\, g\, \bar\phi\lambda\psi - i\sqrt{2}\, g\, \bar\psi\bar\lambda\phi + g\,\bar\phi D\phi \\ &\quad - \frac{\partial W}{\partial\phi^i}F^i - \frac{\partial\overline{W}}{\partial\bar\phi_i}F_i - \frac{1}{2}\frac{\partial^2 W}{\partial\phi^i\partial\phi^j}\psi^i\psi^j - \frac{1}{2}\frac{\partial^2\overline{W}}{\partial\bar\phi_i\partial\bar\phi_j}\bar\psi_i\bar\psi_j\,.\end{aligned} \tag{2.15}$$

W is the superpotential, an holomorphic function of $\chi_{\rm SF}$'s (and not their complex conjugates), thus the superpotential is a $\chi_{\rm SF}$ itself and it is ensured that the last two integrals in the first line of the equation are supersymmetric invariant. Also, the superpotential does not contain derivatives since $D_\alpha\Phi$ is not a $\chi_{\rm SF}$ and in order for the theory to be renormalizable it has to be at most cubic in the fields [6]. Once the gauge structure is set, the superpotential is the only thing left to be defined when constructing an $N = 1$ renormalizable theory.

Finally, we need to also introduce the Fayet-Iliopulos term,

$$\mathcal{L}_{\rm FI} = 2g\sum_A \xi_A \int d^2\theta\, d^2\bar\theta\, V^A = g\sum_A \xi_A\, D^A\,, \tag{2.16}$$

that is present for any abelian $U(1)$ factors that the gauge group contains and where ξ_A are real constants [7]. This term is neglected in most phenomenological studies of the MSSM, its presence either leads to SUSY or gauge symmetry breaking, hence generating phenomenological problems. To have $\xi = 0$ is also motivated by UV considerations since it is a term that is not allowed in supergravity theories.

The total Lagrangian can be written on-shell by integrating out the auxiliary fields D and F using their equations of motion

$$\begin{aligned}\mathcal{L} &= \mathrm{tr}\left[-\frac{1}{4}F_{\mu\nu}F^{\mu\nu} - i\lambda\sigma^\mu D_\mu\bar\lambda\right] + \theta_{YM}\frac{\alpha}{16\pi}\,\mathrm{tr}\left[F_{\mu\nu}\widetilde{F}^{\mu\nu}\right] + \overline{D_\mu\phi}D^\mu\phi - i\psi\sigma^\mu D_\mu\bar\psi \\ &\quad + i\sqrt{2}\, g\,\bar\phi\lambda\psi - i\sqrt{2}\, g\,\bar\psi\bar\lambda\phi - \frac{1}{2}\frac{\partial^2 W}{\partial\phi^i\partial\phi^j}\psi^i\psi^j - \frac{1}{2}\frac{\partial^2\overline{W}}{\partial\bar\phi_i\partial\bar\phi_j}\bar\psi_i\bar\psi_j - V(\phi,\bar\phi)\,,\end{aligned} \tag{2.17}$$

where the scalar potential is

$$V(\phi,\bar\phi) = \bar F^i F_i + \frac{1}{2}D^a D_a = \frac{\partial W}{\partial\phi^i}\frac{\partial\overline{W}}{\partial\bar\phi_i} + \frac{g^2}{2}\sum_a |\bar\phi_i (T^a)^i_j\phi^j + \xi^a|^2\,, \tag{2.18}$$

and where $\xi^a = 0$ for non abelian group factors (when $a \neq A$). If the total gauge group is a direct product of groups (as it is with $\mathcal{G}_{\rm SM}$), then the scalar potential

$$V(\phi,\bar\phi) = \bar F^i F_i + \frac{1}{2}\sum_a D^a D_a = \frac{\partial W}{\partial\phi^i}\frac{\partial\overline{W}}{\partial\bar\phi_i} + \frac{1}{2}\sum_a g_a^2\, |\bar\phi_i (T^a)^i_j\phi^j + \xi|^2\,, \tag{2.19}$$

[6] For the $\int d^2\theta\, W$ type terms in Eq. (2.15) to be of dimension 4, the superpotential is bounded to have at most dimension 3 since the mass dimension of a $\chi_{\rm SF}$ is 1. If we want the theory to be renormalizable the superpotential can have only linear, quadratic and cubic terms in the $\chi_{\rm SF}$'s.

[7] $A = 1, 2, \ldots, n$ where n is the number of abelian factors.

where again, ξ is only present for $U(1)$ factors and is normally set to zero in most phenomenological studies (this work included).

2.3 Supersymmetry breaking

If present in nature at all, SUSY must be broken since we see no superpartners which are degenerate with their corresponding SM particles. Just as the electroweak symmetry is (see Section 1.2), we expect the breaking of supersymmetry to be spontaneous, i.e. with a Lagrangian that preserves supersymmetry and a vacuum state that does not. In that way SUSY will be hidden at low energies in accordance with the absence of SUSY signals at experiment, so with spontaneously broken SUSY one expects the picture to be similar as to what is depicted in Figure 2.1.

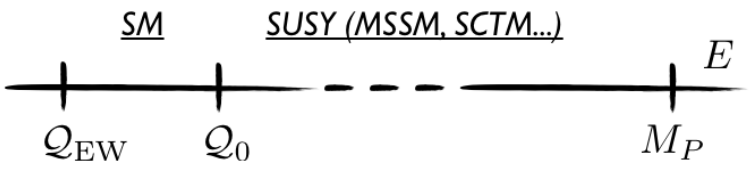

Figure 2.1: *If superpartners lie around some scale $\mathcal{Q}_0$, above that scale ($E > \mathcal{Q}_0$) the theory would behave in a supersymmetric way while below, $E < \mathcal{Q}_0$, not.*

Spontaneous supersymmetry breaking

We will now present a few basics on spontaneous SUSY breaking (SSSB) and mention the main shortcoming of SSSB models when applied to realistic situations, thus motivating the soft supersymmetry breaking paradigm.

If supersymmetry is spontaneously broken it means that the vacuum is not invariant under supersymmetry transformations, therefore in the $N = 1$ case

$$Q_\alpha|0\rangle \neq 0 \quad \text{and} \quad \bar{Q}_{\dot{\alpha}}|0\rangle \neq 0\,. \tag{2.20}$$

Using the supersymmetry algebra ($\{Q_\alpha, \bar{Q}_{\dot{\alpha}}\} = -2\sigma^\mu_{\alpha\dot{\alpha}} P_\mu$) we can relate the SUSY generators with the Hamiltonian of the theory since $H = P_0$. If the equation above holds (if supersymmetry is broken in the vacuum state) then

$$\langle 0|H|0\rangle = \frac{1}{4}\left(|Q_1|0\rangle|^2 + |\bar{Q}_1|0\rangle|^2 + |Q_2|0\rangle|^2 + |\bar{Q}_2|0\rangle|^2\right) > 0\,, \tag{2.21}$$

and so the vacuum has positive energy. We can neglect spacetime dependent effects and possible fermion condensates and consider that $\langle 0|H|0\rangle = \langle 0|V|0\rangle$, where V is the scalar potential of the theory, Eq. (2.19). V only depends on the scalar components of the superfields and features two contributions: (i) the F-terms, which are fixed by the Yukawa couplings and fermion masses of the superpotential [8] and (ii), the D-terms, determined by the gauge structure.

[8] The derivative considers only the scalar part of the superpotential W, in practice it is just a matter of taking scalar fields instead of chiral superfields.

The set of supersymmetric vacua is described by the following equations,

$$F_i(\phi) = 0 \quad \text{and} \quad D^a(\phi, \bar{\phi}) = 0\,. \tag{2.22}$$

If there is any field configuration that solves both equations simultaneously then the vacuum is supersymmetric. If there is no field configuration that solves (2.22) then the F-terms and/or the D-terms acquire VEV's and $\langle 0|V|0\rangle > 0$, thus breaking SUSY. Whether SSSB is triggered by F-terms or D-terms acquiring a VEV classifies the models as being of the O'Raifeartaigh type or the Fayet-Iliopoulos type respectively.

Although appealing, SSSB runs into difficulties when constructing models that aim at producing realistic particle physics scenarios. This is due mainly because of the following sum rule

$$\mathrm{Str}[m^2] = \sum_j (-1)^{2j}(2j+1)\,\mathrm{tr}[m_j^2]\,, \tag{2.23}$$

that relates the masses of bosons and fermions in any spontaneously broken supersymmetric theory. In order for the sum rule to hold, some of the superpartners need to be lighter than their actual SM partners, in clear contrast with experiment. It is for this reason that SSSB cannot be triggered by DOF's that couple to the MSSM fields directly, we instead need to postulate a new 'hidden' sector whose dynamics are decoupled from the (MSSM-like) 'observable' sector. The hidden sector will break SUSY spontaneously and then the breaking will be transmitted to the observable sector by some messenger fields that are sensitive to the dynamics in both sectors.

Soft SUSY breaking and mediation mechanisms

After SSSB in the hidden sector, the imprint left by the messengers of SUSY breaking will be in the form of explicit breaking terms in the Lagrangian. An explicit breaking of supersymmetry is dangerous in the sense that it can spoil the nice properties that SUSY introduces, not only at low energies but all the way up the UV. In order to keep the UV behavior of SUSY safe, not all explicit breaking operators are allowed, only those whose dimension is $d < 4$ do not produce a dangerous breaking of supersymmetry. This is because their coefficients have positive mass dimension, i.e. they are relevant terms in the Lagrangian that vanish in the UV, where SUSY will still hold as a symmetry. The key point here is that any SSSB mechanism can be parametrized by terms of this kind as it is precisely what a spontaneous breaking does, it hides the symmetry in the IR while in the UV it is fully recovered. Consequently, if we expect SUSY breaking to happen in some hidden sector and then, through its transmission, leave and imprint in the form of explicit breaking terms in the Lagrangian, we are sure that these breaking terms will be of the type described above. Hence, after SSSB the Lagrangian will be

$$\mathcal{L}_{\mathrm{SUSY}} + \mathcal{L}_{\mathrm{soft}}\,, \tag{2.24}$$

where $\mathcal{L}_{\mathrm{SUSY}}$ is defined in Eq. (2.17) and $\mathcal{L}_{\mathrm{soft}}$ for an $N = 1$ theory is

$$\mathcal{L}_{\mathrm{soft}} = -\left(\frac{1}{2}M_a\lambda^a\lambda^a + \frac{1}{6}a^{ijk}\phi_i\phi_j\phi_k + \frac{1}{2}b^{ij}\phi_i\phi_j + t^i\phi_i\right) + h.c. - (m^2)^i_j\bar{\phi}^j\phi_i\,. \tag{2.25}$$

The equation above includes: Scalar squared mass terms for the scalar components of the χ_{SF}'s (Higgses, sleptons and squarks), $(m^2)^i_j$ and b^{ij}, masses for the fermionic components of V_{SF}'s

(gaugino masses for each gauge group), M_a, trilinear terms for scalars (a^{ijk}) and tadpole couplings (t^i) which will only be present if there is a singlet in the theory [9].

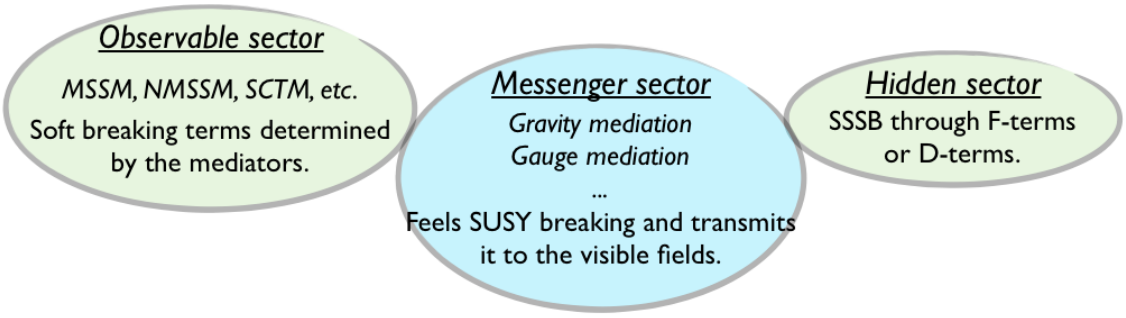

Figure 2.2: *Depiction of what is presumed to be the structure of SUSY breaking in most phenomenological scenarios.*

The way in which the breaking is transmitted to the observable sector (what the messenger sector is) is critical to determine the texture of the soft breaking terms. The messenger fields will couple in such a way that they will feel the breaking once the F or D-terms of the hidden sector get a VEV, after that, direct couplings or loops involving messengers will generate the soft terms for the visible fields. Actually, to generate a spectrum of superpartners, it is sufficient to just propose a set of messenger fields and assume that they couple to a superfield whose F or D-term gets a VEV that breaks SUSY. There is no need to specify the mechanism by which this superfield has acquired the VEV. This is the power of the soft breaking paradigm, it is a tool to study a supersymmetric model without having to specify every single piece of it, specially since coming up with SSSB mechanisms free of problems of their own is a challenging task.

Before presenting the two main ways in which SSSB can be mediated to the observable sector, let us remark that there are a few exceptions which do not follow precisely the soft breaking paradigm and still produce phenomenologically viable situations. For instance, SUSY breaking is neither transmitted by gravitons nor extra messenger fields when the breaking is triggered by the presence of large extra dimensions [32, 33], also, terms beyond those appearing in (2.25) are generated.

Gravity mediation

Gravity couples universally to everything that has a mass, therefore, gravitons are perfectly valid messengers of supersymmetry breaking if there is some hidden sector that is a singlet under $\mathcal{G}_{\rm SM}$ and breaks SUSY. If we parametrize the breaking by a spurion $\chi_{\rm SF}$, X, the most general form of the Lagrangian that describes the gravitational interactions between X and the visible sector

[9] There exist a few other soft terms that we choose not to include, these are either not present in minimal pictures or set to zero by the mediation mechanism and will not be relevant in this work.

fields is

$$\mathcal{L} = \int d^2\theta\, d^2\bar{\theta} \left(a\, \frac{\bar{X}X}{M_P^2} \bar{Y}^i Y_i + b\, \frac{\bar{X}X}{M_P^2} Y_i Y_j + c\, \frac{\bar{X}}{M_P} Y_i Y_j + h.c. \right) + \int d^2\theta \left(d\, \frac{X}{M_P} W_a^\alpha W_\alpha^a + e\, \frac{X}{M_P} Y_i Y_j Y_k + h.c. \right) . \tag{2.26}$$

Where for the MSSM, Y are the $\chi_{\rm SF}$'s of Table 2.1 and every term is written in a $\mathcal{G}_{\rm SM}$ invariant manner. After SSSB, $\langle F_X \rangle \neq 0$ and we recover the Lagrangian (2.25). Specifically, the scalar squared mass terms will be generated by the first and second terms in the upper line, $(m^2)^i_j$ and b^{ij} respectively, in the second line, the first term will be responsible for the gaugino masses M_a and the second term will generate the trilinear terms a^{ijk}. The third term in the first line does not generate a soft breaking term but an effective superpotential mass [10].

As we see from the structure of (2.26) gravity mediation generates universal soft terms up to order one coefficients, therefore, they share a common mass scale

$$m_{\rm soft} \sim \frac{\langle F_X \rangle}{M_P} . \tag{2.27}$$

If we want $m_{\rm soft} \sim 1$ TeV, then SUSY will be broken around $\sqrt{\langle F_X \rangle} \sim 10^{11}$ GeV. This is why gravity mediation is considered to be a high-scale SUSY breaking mechanism, the scale at which the soft terms are generated is orders of magnitude above the EW scale. We explore scenarios with universal soft parameters (typical of gravity mediation) for the MSSM in Section 3.2.

The gravitino mass

Because it is a space-time symmetry, to include gravity supersymmetry needs to be promoted from global to local and thus become what is dubbed supergravity. Once this is done, a new spin-3/2 massless 'gauge' field appears in the spectrum, the gravitino [11]. After SSSB, the goldstino (the goldstone mode of a fermionic symmetry) also appears and through what is called the super-Higgs mechanism (in analogy to the bosonic Higgs mechanism of gauge theories) the gravitino will absorb the latter as its longitudinal helicity $\pm 1/2$ components and become massive. The mass of the gravitino is then given by $m_{3/2} = \langle F_X \rangle / \sqrt{3} M_P$. In particular for gravity mediated scenarios, the mass of the gravitino is $m_{3/2} \sim 100$ GeV and a neutralino LSP is normally expected.

Gauge mediation

In this scenario it is through gauge interactions that SUSY breaking is transmitted. A set of messenger fields that do not couple directly to the observable sector but transform non trivially under $\mathcal{G}_{\rm SM}$ is responsible for the mediation once SUSY is broken. In the minimal version of gauge mediation (MGM) the interaction between the spurion X and the messengers is given by the superpotential $W = \lambda X \bar{\Phi} \Phi$. After F_X gets a VEV, gauginos will get masses at one loop by direct couplings with the messenger fields, then, scalar sparticles will get a contribution to their squared masses at two loops via the now softly broken $V_{\rm SF}$'s (i.e. gaugino masses). a^{ijk}'s and

[10] Actually, through this term supergravity may be able to solve the μ-problem of the MSSM that is explained below Eq. (2.33), [34].

[11] As SUSY is a fermionc symmetry, the generators of the SUSY algebra Q and $\bar{Q}$ are of spinorial nature.

b^{ij}'s are heavily suppressed in this scenario as they will only get contributions at higher loop orders, they can be considered zero. As we will discuss below, the latter is a source of tension for gauge mediation since ensuring correct EW breaking with the right value of the Higgs mass gets complicated when $b^{ij} \sim a^{ijk} \sim 0$. The typical values for the soft masses in MGM are given in Section 3.2 (Eqs. (3.20) and (3.21)), they are all of the same order of magnitude, which can be considered to be

$$m_{\text{soft}} \sim \frac{g^2}{16\pi^2}\frac{\langle F_X\rangle}{M}\,, \tag{2.28}$$

where M is the messenger mass.

The great advantage of gauge mediation with respect to gravity mediated scenarios is that it automatically solves the flavor problem of softly broken supersymmetric theories: In principle, a general set of soft terms can spoil the flavor structure of the theory and be responsible for dangerous flavor changing neutral currents (FCNC's) unless a special texture is introduced ad-hoc. Gravitational interactions are flavor blind and give no explanation whatsoever for a flavor texture at the field theory level, only considering particular string compactifications can this problem be addressed in gravity mediated situations. Meanwhile, gauge interactions are flavor diagonal and gauge mediation is free from any flavor problem. The latter holds provided that gauge mediation is the only source of SUSY breaking, the flavor structure can always be spoiled by gravitational interactions and we need to ensure that the terms in (2.26) are sufficiently suppressed [12]. With this in mind we can derive bounds for the SUSY breaking scale and the messenger mass. If we require that gravity mediated contributions do not account for more than 1/1000 of the soft squared masses then $M \lesssim 10^{-3/2}(\alpha/4\pi)M_P \sim 10^{15}$ GeV, so asking for $m_{\text{soft}} \sim 1$ TeV gives the following upper bound on the SUSY breaking scale $\sqrt{\langle F_X\rangle} \lesssim 10^{10}$ GeV. We also want that the RGE running does not spoil the flavor structure so even lighter messenger masses (the scale at which the soft terms are generated) are favored and one really expects $\sqrt{\langle F_X\rangle} < 10^{10}$ GeV (hence, low-scale SUSY breaking). Since $m_{3/2} = \langle F_X\rangle/\sqrt{3}M_P$ the gravitino will always be the LSP in gauge mediation [13].

In summary, gauge mediated supersymmetry breaking (GMSB) is a very predictive mechanism that automatically solves the flavor problem, however, minimal GMSB models fail at ensuring correct EW breaking. In particular minimal GMSB does not generate a b-term (m_3^2 in the MSSM) that is able to solve the Eqs. (2.33). One needs to go beyond MGM or expect m_3^2 to be generated by new and unknown dynamics. Actually, even considering extensions of MGM, it is really difficult to accommodate EW breaking since any new contributions to m_3^2 will most likely affect also the value of μ and there will be a mismatch of a few orders of magnitude ($m_3^2/\mu^2 \sim 10^2$) between parameters that should be similar. This is what is called the μ/B_μ problem of gauge mediation [36]. On top of that, since $a^{ijk} \sim 0$ in MGM models, the Higgs mass measurement is a source of serious tension if one wants to get a light spectrum of superpartners (see Chapter 3). We explore gauge mediated scenarios in depth in Sections 3.2 (MGM for the MSSM) and 5.3 (where we construct a non standard realization for the SCTM).

[12] One cannot get rid of gravitational contributions to the soft terms, gravity mediation will always be there as a source of SUSY breaking, however, since the terms in (2.26) are suppressed by M_P, if the scale at which SUSY is broken $\langle F_X\rangle$ is low enough, the contribution of gravity to $\mathcal{L}_{\text{soft}}$ will be negligible.

[13] Only recently a mechanism that features gauge mediation without a gravitino LSP has been proposed [35], it uses extra dimensions to make the gravitino superheavy and opens up the possibility of having neutralino LSP in a gauge mediated context.

2.4 The MSSM.

With the particle content listed in Table 2.1 we can write the following renormalizable superpotential for the MSSM

$$W = \mu\, H_1 \cdot H_2 + y_u^{ij}\, Q_i \cdot H_2 \bar{u}_j + y_d^{ij}\, Q_i \cdot H_1 \bar{d}_j + y_e^{ij}\, L_i \cdot H_1 \bar{e}_j \,. \tag{2.29}$$

A note on 'R-parity' and dark matter

Eq. (2.29) is not the most general superpotential that is holomorphic in the $\chi_{\rm SF}$'s and in agreement with the symmetries of the theory, it should also include terms that violate either baryon number B or total lepton number L. The existence of such terms is forbidden by the experimental searches for B and L-violating processes (remember that B and L number conservation are accidental symmetries of the SM Lagrangian). In the search of a way to forbid such B and L violating terms one could consider them to be exact symmetries of the MSSM Lagrangian, still, B and L are known to be violated by non perturbative effects so it is difficult to think that they are fundamental symmetries of nature. By means of imposing and extra discrete symmetry to the MSSM Lagrangian one is able to forbid the unwanted terms while allowing Eq. (2.29) to be constructed. This extra symmetry is called 'R-parity'; SM particles have charges $P_R = +1$ while superpartners $P_R = -1$, hence, only an even number of superpartners is allowed at every vertex and the lightest supersymmetric particle (LSP) must be stable. Therefore, if R-parity is assumed, supersymmetry can provide a good dark matter candidate.

Scalar potential and EW breaking in the MSSM

A full study of the MSSM Lagrangian will be too lengthy and out of the scope of this thesis, we therefore restrict ourselves to the presentation of the part that is most interesting for our studies, the scalar potential. The latter is the piece that will trigger EWSB and will determine the Higgs physics of the theory. The scalar potential of an $N = 1$ SUSY theory is

$$V = V_F + V_D + V_{\rm soft} \,, \tag{2.30}$$

where for the MSSM $V_F + V_D$ is simply (2.19) for the superpotential (2.29) and $\mathcal{G}_{\rm SM}$, and the scalar part of the soft terms (2.25) is determined by the SUSY breaking mechanism. More specifically

$$\begin{aligned} V_F &= \mu^2 \left(|H_2^0|^2 + |H_2^+|^2\right) + \mu^2 \left(|H_1^0|^2 + |H_1^-|^2\right) \,, \\ V_D &= \frac{1}{4}(g^2 + g'^2) \left(|H_2^0|^2 - |H_1^0|^2 + |H_2^+|^2 - |H_1^-|^2\right)^2 + \frac{1}{2} g^2 |H_2^+ H_1^{0\,*} + H_u^0 H_1^{-\,*}|^2 \,, \\ V_{\rm soft} &= m_{H_2}^2 \left(|H_2^0|^2 + |H_2^+|^2\right) + m_{H_1}^2 \left(|H_1^0|^2 + |H_1^-|^2\right) + \left\{m_3^2 \left(H_2^+ H_1^- - H_2^0 H_1^0\right) + h.c.\right\} \,, \end{aligned} \tag{2.31}$$

where we are considering all parameters real. We now demand that the minimum of the potential breaks the electroweak symmetry down to Electromagnetism. We thus rotate away all possible VEV's for charged and imaginary components of the scalar fields and keep only the neutral and real part,

$$V = m_2^2 \, |H_2^0|^2 + m_2^2 \, |H_1^0|^2 - m_3^2 \left(H_1^0 H_2^0 + h.c.\right) + \frac{1}{4}(g^2 + g'^2) \left(|H_2^0|^2 - |H_1^0|^2\right)^2 \,, \tag{2.32}$$

where we consider that $\phi_R = \phi$ and $m_{1,2}^2 = m_{H_{1,2}}^2 + \mu^2$.

Name	$V_{\rm SF}$	Spin 1/2	Spin 1	$SU(3)_C$	$SU(2)_L$	$U(1)_Y$
gluino, gluons	G^A	$\widetilde{G}^A$	G^A	**8**	**1**	0
wino, W-boson	W^a	$\widetilde{W}^{\pm}$, $\widetilde{W}^0$	$W^{\pm}$, W^0	**1**	**3**	0
bino, B-boson	B	$\widetilde{B}^0$	B^0	**1**	**1**	0
	$\chi_{\rm SF}$	Spin 0	Spin 1/2			
squarks, quarks	Q^i	$(\tilde{u}_L \;\; \tilde{d}_L)$	$(u_L \;\; d_L)$	**3**	**2**	$\frac{1}{6}$
	$\bar{u}^i$	$\tilde{u}^*_R$	$u^\dagger_R$	$\bar{\mathbf{3}}$	**1**	$-\frac{2}{3}$
	$\bar{d}^i$	$\tilde{d}^*_R$	$d^\dagger_R$	$\bar{\mathbf{3}}$	**1**	$\frac{1}{3}$
sleptons, leptons	L^i	$(\tilde{\nu} \;\; \tilde{e}_L)$	$(\nu \;\; e_L)$	**1**	**2**	$-\frac{1}{2}$
	$\bar{e}^i$	$\tilde{e}^*_R$	$e^\dagger_R$	**1**	**1**	1
Higgs, higgsinos	H_2	$(H_2^+ \;\; H_2^0)$	$(\tilde{H}_2^+ \;\; \tilde{H}_2^0)$	**1**	**2**	$\frac{1}{2}$
	H_1	$(H_1^0 \;\; H_1^-)$	$(\tilde{H}_1^0 \;\; \tilde{H}_1^-)$	**1**	**2**	$-\frac{1}{2}$

Table 2.1: *MSSM particle content. V_{SF} and χ_{SF} stand for vector and chiral superfields respectively. We explicitly show the $SU(2)_L$ structure for doublets and the i index runs over the three families of fermions (although it is omitted in the component fields). Superpartners of the SM particles are specified with a tilde.*

Now, applying the minimization conditions $|\partial V/\partial H_1^0|_{v_1} = 0$ and $|\partial V/\partial H_2^0|_{v_2} = 0$ and after some algebra we get a set of equations that, by taking μ, m_3 and $m_{H_{1,2}}$ as input parameters, should return the Z boson mass and $\tan\beta$,

$$\begin{aligned} \sin 2\beta &= \frac{2m_3^2}{m_1^2 + m_2^2}\,, \\ m_Z^2 &= \frac{|m_{H_1}^2 - m_{H_2}^2|}{\sqrt{1-\sin^2 2\beta}} - m_{H_2}^2 - m_{H_1}^2 - 2\mu^2\,. \end{aligned} \tag{2.33}$$

The Z boson mass is defined as $m_Z = (g'^2 + g^2)(v_1^2 + v_2^2)/2$. From the equations above we can see what is called the 'μ-problem' of the MSSM. Without tuned cancellations, one expects the parameters appearing in the equations to be $\mathcal{O}(m_Z)$, this is feasible for m_3 and $m_{H_{1,2}}$ which are SUSY breaking parameters, it will be a task of the SUSY breaking mechanism to keep them close enough to m_Z. However, μ is a supersymmetric invariant parameter of the superpotential with no reason to be $\mathcal{O}(m_Z)$, it can in principle take much bigger values as one expects the cutoff of the MSSM to be well above the EW scale.

The Higgs sector and its decoupling limit

After ensuring that the scalar potential of the MSSM produces correct EW breaking we can calculate the scalar spectrum. Since we have introduced an extra complex doublet the number

of scalar DOF's of the Higgs sector is doubled in the MSSM, it features, besides the massless Goldstone modes which will be eaten by the gauge bosons, 4 massive states, the light and heavy neutral CP-even Higgses (h and H), a pseudoscalar (A) and a charged scalar $H^{\pm}$.

$$\begin{aligned} m_A^2 &= \frac{2m_3^2}{\sin(2\beta)} = 2\mu^2 + m_{H_1}^2 + m_{H_2}^2 \\ m_{h,H}^2 &= \frac{1}{2}\left(m_A^2 + m_Z^2 \mp \sqrt{(m_A^2 - m_Z^2)^2 + 4m_Z^2 m_A^2 \sin^2(2\beta)}\right) \\ m_{H^\pm}^2 &= m_A^2 + m_W^2 \end{aligned} \tag{2.34}$$

By taking the limit $m_A \to \infty$ one recovers the SM Higgs sector, only one massive CP-even mode. Every state but h becomes super heavy in that limit and therefore we can identify h as the SM-like state.

Although the decoupling limit is here taken in the mass basis, it can also be thought of at the $SU(2)_L$ doublet level: From the H_1 and H_2 MSSM basis one can rotate to a basis where we have a light SM-like doublet H and a superheavy one $\mathcal{H}$. This procedure is used in Chapter 3 where we further elaborate on the Higgs mass, loop corrections and the consequences of the 2012 discovery for supersymmetric theories.

2.5 The importance of the scale

Supersymmetry provides a solution to the hierarchy problem. It is actually the symmetry that will be recovered in full glory if the scalar mass is zero, thus making the Higgs mass in agreement with 't Hooft's criterion for the naturalness of Lagrangian parameters. SUSY prevents the scalar masses to become ultra heavy by introducing new degrees of freedom (the superpartners) which will generate diagrams (Fig. 2.3) that will cancel the very large corrections that enter the Higgs mass at loop order (remember that loops of bosons and fermions have a relative minus sign).

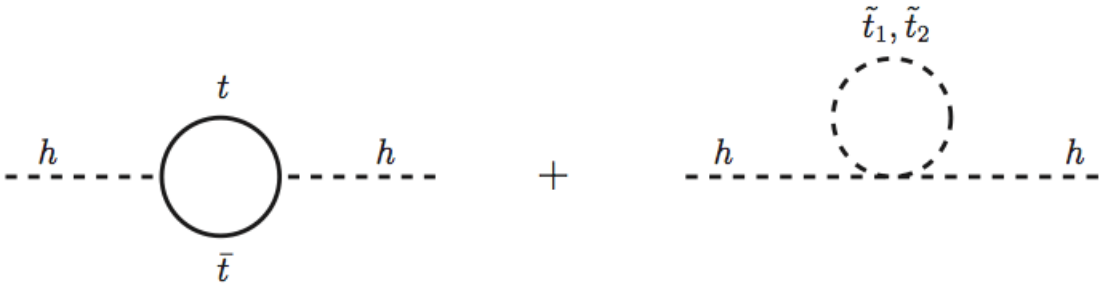

Figure 2.3: *Contributions to the Higgs mass given by the top/stop sector.*

The solution to the hierarchy problem is however very dependent on the scale at which supersymmetry is realized, i.e. the mass of the superpartners $\mathcal{Q}_0$, so in order to cancel dangerous loop contributions to the Higgs mass without much fine-tuning, all superpartners need to remain as light as possible. Some contributions will present a more severe tuning than others, for instance, the contribution coming from a loop of top quarks will be larger than any other since it will be proportional to h_t^2 (see Eq. (1.30)) which is larger than the other Yukawas. This requires the

stops (the scalar superpartners of top quarks) to be as light as possible, while other superpartners can be somewhat heavier as they have to cancel smaller contributions. We can thus identify the stop mass as the fine-tuning measure in the model, i.e. the lighter the stops are, the more natural the model is [14]. Let us make this point as clear as possible by taking the one loop correction to the MSSM Higgs mass given by the top/stop system (Fig. 2.3),

$$\delta m_h \sim \frac{3h_t^4 v^2}{4\pi^2} \log\left(\frac{m_{\tilde{t}}^2}{m_t^2}\right). \tag{2.35}$$

From the above we can see that if the stops are very heavy the logarithm gets very large and the contribution given by radiative corrections can exceed that of the tree level piece.

A Higgs mass which is mainly achieved through radiative corrections is a reason for unease if one follows Veltman's naturalness criterion [37]:

'Radiative effects should not exceed tree-level effects in size'

It is thus needed that stops are as light as possible in order to make the logarithm small. Other particles will generate a situation similar to Eq. (2.35) but their couplings to the Higgs will be smaller than h_t and therefore the logarithm can be larger while generating a contribution of the same order. Another way of looking at this is by considering $\mathcal{Q}_0$ (stop masses) as the cutoff of the SM. As we discussed in Section 1.5, effective field theory ties the cutoff to the scale of new physics so in order to keep the Higgs mass stabilized one should keep it as low as possible.

As we just showed, the naturalness of the theory is directly tied to the masses of the superpartners, which are given by the supersymmetry breaking mechanism rather than the EW breaking procedure by which the SM DOF's get masses. It will be a challenge of the SUSY breaking mechanism to generate a spectrum of superpartners that is light enough, this is why studying SUSY breaking mechanisms and its mediation to the observable sector is such an important task.

A note on the little hierarchy problem

The Standard Model is consistent with all present experimental data including the recent measurements of the Higgs mass and its couplings to gauge bosons and fermions. By the same token experiments are also putting bounds on possible BSM physics whose aim is to solve the SM hierarchy problem, i.e. to understand the big hierarchy $\mathcal{Q}_{EW}/M_P \simeq 10^{-16}$, or equivalently the stability of the electroweak vacuum. The fact that there is already a small hierarchy between experimental bounds and the EW scale ($\mathcal{Q}_{EW}/\mathcal{Q}_{Exp} \simeq 10^{-2}$) is becoming a problem, specially since the the non observation of additional particles pushes the cutoff to higher and higher scales [15]. This is what is dubbed the little hierarchy problem (Fig. 2.4) and it is shared by any natural explanation of the EW scale, e.g. supersymmetry, compositeness or extra dimensions.

[14] Fortunately, the RGE running will make the 3$^{\text{rd}}$ generation fermion superpartners lighter than the 1$^{\text{st}}$ and 2$^{\text{nd}}$, this is because the former couple directly to Yukawa couplings that are parametrically larger than the ones of the 1$^{\text{st}}$ and 2$^{\text{nd}}$ generation, so the RGE running will tend to lower their masses in a more severe way. Depending on how much running the correlations will be strong or negligible.

[15] LHC will only give a final word on the scale of new physics at the end of its current (second) run. Actually, as this thesis is being written, an intriguing excess at 750 GeV in the $\gamma\gamma$ invariant mass spectrum has been reported both by the ATLAS and CMS collaborations. A plethora of BSM realizations for the excess have been proposed, some of them within supersymmetry [38] or even in the non supersymmetric GM model [39].

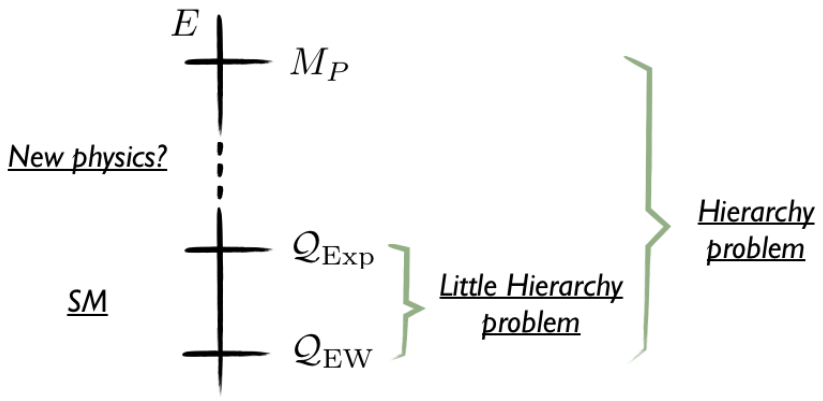

Figure 2.4: *If we treat $\mathcal{Q}_{\rm Exp}$ as the SM cutoff, experimental searches at the LHC are already an indication that, at least in the simpler realizations of BSM theories, the EW scale is already a bit tuned. This problem is worsened in the minimal MSSM, where LHC bounds are not the only indication for heavy stops (Chapter 3).*

2.6 Further phenomenological advantages of SUSY

The phenomenological advantages of supersymmetry are beyond only solving the hierarchy problem. One can construct theories where supersymmetry is present at an intermediate or high scale, thus not fully solving the hierarchy problem, that still provide a great deal of interesting solutions to tackle some of the SM problems [16]. The discussion about phenomenology is however very model dependent and here we shall just list a few features which are common to a wide class of supersymmetric theories.

- It predicts that EWSB happens through an elementary scalar, in good agreement with observation. On top of that, SUSY can also give a dynamical explanation as to why the SM potential features a tachyonic mass, i.e. why the SM potential breaks the EW symmetry [41] (see Chapter 3).
- The MSSM and some of its extensions improve considerably the unification of gauge coupling constants and provide a better behaved IR limit for Grand Unified Theories (GUT's).
- If R parity is assumed, the LSP is stable and if it is neutral it can be a dark matter candidate that freezes out to the correct relic density. We explore the cosmological consequences of R-parity in the SCTM in Chapter 6.
- It is the natural low energy limit of string theories which aim at describing the phenomenology of particle physics and cosmology [42].

[16] For instance, Split SUSY theories [40].

3

The MSSM after the Higgs discovery

After the 7 and 8 TeV runs the Large Hadron Collider (LHC) has firmly established the existence of a scalar boson with a mass $m_h \simeq 125$ GeV. In particular the strengths measured in the WW, ZZ, $\gamma\gamma$, $b\bar{b}$ and $\tau\tau$ decay channels by the ATLAS and CMS collaborations are consistent with the Standard Model (SM) Higgs with a mass $m_h = 126 \pm 0.4$ (stat) ± 0.4 (syst) GeV [1] and $m_h = 125.3 \pm 0.4$ (stat) ± 0.5 (syst) GeV [2], respectively. The Higgs discovery is of the utmost importance as it is the first direct experimental confirmation of the mechanism of EWSB. It is therefore interesting to explore the consequences of the present Higgs mass data on a possible underlying supersymmetric theory, in particular on the way supersymmetry triggers EWSB at low energy, on the scale at which supersymmetric partners first appear ($\mathcal{Q}_0$) and also on the scale $\mathcal{M}$ at which supersymmetry breaking is transmitted from the hidden to the observable sector. We do this by adopting the following attitude: We assume that supersymmetry is solving the big hierarchy problem from $\mathcal{Q}_0/M_P$ but perhaps not necessarily the little hierarchy problem from $\mathcal{Q}_{EW}/\mathcal{Q}_0$ and see what LHC8 data is telling about the parameters of the supersymmetric theory. Thus, by determining $\mathcal{Q}_0$ we will learn about where supersymmetry (the MSSM) stands after the Higgs discovery as a solution to the hierarchy problem.

The following analysis just reflects the present experimental situation concerning the Higgs discovery and the non observation (yet) of any supersymmetric particle. In the future, it might happen that supersymmetric signals are found or that they are not. In both cases the analysis presented in this chapter should be correspondingly constrained. In case where supersymmetric signals are found, they would give information about our energy scale $\mathcal{Q}_0$ which in turn will give indirect information about the scale at which supersymmetry breaking is transmitted $\mathcal{M}$. In the other case, in which supersymmetric signals not be found at the end of the LHC13-14 run, the data will put a lower bound on the scale $\mathcal{Q}_0$ by which also the scale $\mathcal{M}$ will be correspondingly constrained, suggesting that perhaps we will need a higher energy collider to uncover BSM physics as the HE-LHC (at 33 TeV) & VHE-LHC (at 100 TeV) [43].

We start Section 3.1 giving naive estimates of $\mathcal{Q}_0$ by looking at the one-loop Higgs mass formula, which we then vindicate using a proper run-and-match procedure that will take care of very large logarithms. Comments on the nature of EWSB at low energy (does EWSB proceed via radiative breaking or not?) are also made. In Section 3.2 we discuss the scale $\mathcal{M}$, getting first results from a bottom up perspective that will be then confirmed by top down examples. Finally, in Section 3.3 we make a small summary of the results concerning $\mathcal{Q}_0$ to motivate our interest in building extensions of the MSSM.

3.1 EWSB in SUSY with a 125 GeV Higgs

Before doing a proper analysis we can learn a lot by simply looking at the MSSM analytical one-loop expression for the Higgs mass [44]

$$m_h^2 = m_Z^2 \cos^2 2\beta + \frac{3m_t^4}{4\pi^2 v^2}\left[\log\left(\frac{\mathcal{Q}_0^2}{m_t^2}\right) + \frac{x_t^2}{\mathcal{Q}_0^2}\left(1 - \frac{x_t^2}{12\mathcal{Q}_0^2}\right)\right], \tag{3.1}$$

where $x_t = (A_t - \mu/\tan\beta)$ and we consider that $\mathcal{Q}_0 = \sqrt{m_{\tilde{t}_1} m_{\tilde{t}_2}}$. This formula has three contributions: (i), the tree-level contribution, that is maximized when $\tan\beta$ is large, (ii), a logarithm that gets larger has the stops get heavier and finally, (iii), a threshold correction that depends on the mixing in the stop sector and that gets larger whenever this mixing is maximized. It is clear by looking at this formula that making $m_h = 125$ GeV is not automatic. If we want to keep stop masses light (in order to solve the hierarchy problem) we are forced to go to a corner in the parameter space where $\tan\beta$ and x_t are as large as possible and we can generally say that:

'The MSSM runs into difficulties when combining a light spectrum of superpartners (light stops) with a 126 *GeV Higgs'*

Roughly, what this means is that either we give up on SUSY as a solution to the hierachy problem [1] [45, 46], or we give up on minimality (or simplicity) and build models beyond the MSSM that could more naturally accommodate the measured Higgs mass. This is depicted in the Figure 2 of the introduction.

Using the analytical Higgs mass is useful to get a qualitative understanding of the situation, however, it is not enough if we want to make quantitative statements. The logarithm present in (3.1) gets dangerously large for heavy stop masses and one needs to take care of it by performing a resummation to get trustable results. Thus, it is more convenient to use a run-and-match procedure. Since we know from experiment that $\mathcal{Q}_0$ is reasonably above the EW scale, we can assume that the SM is an EFT that emerges at $\mathcal{Q}_0$ from an underlying MSSM to extract the relevant information on the mechanism by which the MSSM triggers EWSB.

The matching and the scale $\mathcal{Q}_0$

Consistently with present experimental data we assume that below the scale $\mathcal{Q}_0$ we just have the SM spectrum and the matching conditions are the ones to enforce EWSB at the EW scale $\mathcal{Q}_{EW} = m_h$. The quadratic terms in the MSSM potential can be written as

$$V_2 = m_1^2|H_1|^2 + m_2^2|H_2|^2 + m_3^2(H_1 \cdot H_2 + h.c.) \tag{3.2}$$

with $H_1 \cdot H_2 \equiv H_1^a \varepsilon_{ab} H_2^b$ ($\varepsilon_{12} = -1$) and we are defining $m_1^2 = m_{H_1}^2 + \mu^2$ and $m_2^2 = m_{H_2}^2 + \mu^2$, where m_{H_i} is the soft breaking mass for H_i and μ is the supersymmetric Higgsino mass. They can also be written in matrix form

$$V_2 = (H_1^\dagger, \widetilde{H}_2^\dagger) \begin{pmatrix} m_1^2 & m_3^2 \\ m_3^2 & m_2^2 \end{pmatrix} \begin{pmatrix} H_1 \\ \widetilde{H}_2 \end{pmatrix} \tag{3.3}$$

[1] Or at least to the little hierarchy problem, SUSY can fail to explain the hierarchy between the EW scale and $\mathcal{Q}_0$ but still stabilize the hierarchy $\mathcal{Q}_0 \ll M_P$.

where $\widetilde{H}_2 \equiv \varepsilon H_2^*$. The diagonalization of the mass matrix

$$\mathcal{M}_0^2 = \begin{pmatrix} m_1^2 & m_3^2 \\ m_3^2 & m_2^2 \end{pmatrix} \tag{3.4}$$

then yields the mass eigenvalues

$$m_\mp^2 = \frac{m_1^2 + m_2^2}{2} \mp \sqrt{\left(\frac{m_1^2 - m_2^2}{2}\right)^2 + m_3^4}\,. \tag{3.5}$$

We wish to match the MSSM with the SM at the (common) scale $\mathcal{Q}_0 \equiv m_0$ of supersymmetric masses. In particular we will rotate the MSSM Higgs sector $(H_1, \widetilde{H}_2)$ into the basis $(H, \mathcal{H})$ where H is the SM Higgs doublet and $\mathcal{H}$ its heavy orthogonal combination. We then identify the mass squared of the (light) SM Higgs H with the tachyonic mass $m_-^2 = -m^2(\mathcal{Q}_0)$ and consequently the mass squared of its (heavy) orthogonal combination $\mathcal{H}$ with $m_+^2 \equiv m_{\mathcal{H}}^2 = m_1^2 + m_2^2 + m^2$. This can be done by the fixing

$$m_3^4 = (m_1^2 + m^2)(m_2^2 + m^2) \tag{3.6}$$

leading to the mixing angle β given by [2]

$$\tan^2\beta = \frac{m_1^2 + m^2}{m_2^2 + m^2}\,, \quad \text{i.e.} \quad m^2 = \frac{m_1^2 - m_2^2\tan^2\beta}{\tan^2\beta - 1}\,, \tag{3.7}$$

where all quantities are evaluated at the matching scale $\mathcal{Q} = \mathcal{Q}_0$, which rotates the Higgs basis $(H_1, \widetilde{H}_2)$ into the mass eigenstates $(H, \mathcal{H})$ as

$$\begin{aligned} H &= \cos\beta H_1 - \sin\beta\widetilde{H}_2 \\ \mathcal{H} &= \sin\beta H_1 + \cos\beta\widetilde{H}_2\,. \end{aligned} \tag{3.8}$$

The potential for the SM Higgs then reads as

$$V_{\rm SM} = -m^2(\mathcal{Q}_0)|H|^2 + \frac{\lambda(\mathcal{Q}_0)}{2}|H|^4 + \cdots \tag{3.9}$$

In order to make a precise calculation of the Higgs mass we have to first match the SM quartic coupling λ and the supersymmetric parameters at the scale $\mathcal{Q}_0$. We will improve over the tree-level ($\ell = 0$) matching by considering the one-loop ($\ell = 1$) and leading two-loop ($\ell = 2$) threshold effects as given by [47]

$$\lambda(\mathcal{Q}_0) = \sum_{\ell\geq 0}\Delta^{(\ell)}\lambda\,, \tag{3.10}$$

where

$$\begin{aligned} \Delta^{(0)}\lambda &= \frac{1}{4}(g^2 + g'^2)c_{2\beta}^2\,, \\ 16\pi^2\Delta^{(1)}\lambda &= 6y_t^4 s_\beta^4 X_t^2\left(1 - \frac{X_t^2}{12}\right) - \frac{1}{2}y_b^4 s_\beta^4(\mu/\mathcal{Q}_0)^2 + \frac{3}{4}y_t^2 s_\beta^2(g^2 + g'^2)X_t^2 c_{2\beta} \\ &\quad + \left(\frac{1}{6}c_{2\beta}^2 - \frac{3}{4}\right)g^4 - \frac{1}{2}g^2 g'^2 - \frac{1}{4}g'^4 - \frac{1}{16}(g^2 + g'^2)^2 s_{4\beta}^2\,, \\ (16\pi^2)^2\Delta^{(2)}\lambda &= 16y_t^4 s_\beta^4 g_3^2\left(-2X_t + \frac{1}{3}X_t^3 - \frac{1}{12}X_t^4\right) + \mathcal{O}(h_t^6 s_\beta^4,\, g^4,\, g^2 g'^2,\, g'^4)\,, \end{aligned} \tag{3.11}$$

[2] Note that here the β angle is defined at $\mathcal{Q}_0$ and not at the EW scale after EWSB as it is usually presented, thus it is defined in terms of masses instead of VEV's.

and we are using the notation $X_t = (A_t(\mathcal{Q}_0) - \mu(\mathcal{Q}_0)/\tan\beta)/\mathcal{Q}_0$, $s_\beta \equiv \sin\beta$ and so on. For the numerical calculation we are also taking into account the $\mathcal{O}(y_t^6 s_\beta^4, \dots)$ two-loop threshold corrections whose explicit expression can be found in Ref. [47]. We are neglecting the corrections proportional to y_τ^4 as we are not envisaging values of the parameter $\tan\beta$ such that y_τ is relevant [3].

The couplings y_t and y_b are the top and bottom Yukawa couplings in the MSSM. They are related to the corresponding SM couplings h_t and h_b by [47]

$$h_t = y_t s_\beta \left(1 - \frac{1}{6\pi^2} g_3^2 \mathcal{Q}_0^2 X_t I(m_{\tilde{t}_1}, m_{\tilde{t}_2}, \mathcal{Q}_0) + \mathcal{O}(y_b^2, g^2, g'^2)\right),$$
$$h_b = y_b c_\beta \left(1 - \frac{1}{6\pi^2} g_3^2 \mathcal{Q}_0^2 X_b I(m_{\tilde{b}_1}, m_{\tilde{b}_2}, \mathcal{Q}_0) + \frac{1}{16\pi^2} y_t^2 t_\beta \mathcal{Q}_0^2 X_t I(m_{\tilde{t}_1}, m_{\tilde{t}_2}, \mathcal{Q}_0) + \dots\right), \quad (3.12)$$

where $X_b = (A_t(\mathcal{Q}_0) - \mu(\mathcal{Q}_0)\tan\beta)/\mathcal{Q}_0$, we are assuming a nearly degenerate spectrum at $\mathcal{Q}_0$, and only the leading one-loop QCD and top Yukawa coupling corrections are kept. The function $I(x, y, z)$ can be found in Ref. [47].

The parameters of the potential (3.9) have to be run with the SM renormalization group equations (RGE) down to the scale $\mathcal{Q}_{EW} = m_h$, where minimizing the SM potential should lead to $m^2(m_h) = \frac{1}{2}m_h^2$, $m_h^2 = 2\lambda(m_h)v^2$. For a similar analysis see Refs. [48] and especially [49, 50] where the relation between the mass of the Higgs and the scale of supersymmetry breaking was first analyzed. Here in agreement with the used threshold corrections we are using the two-loop RGE as given in [51].

Finally going from the running Higgs mass m_h to the pole Higgs mass M_h requires the calculation of the Higgs boson self energy $\Pi(p^2)$ as $M_h^2 = m_h^2 + \Delta\Pi$ where $\Delta\Pi = \Pi(p^2 = M_h^2) - \Pi(p^2 = 0)$. Here we keep only the leading correction to $\Delta\Pi$ coming from the top quark loop exchange given by [52]

$$\Delta\Pi_{tt} = \frac{3h_t^2 M_t^2}{4\pi^2}\left[2 - Z(M_t^2/M_H^2)\right], \; Z(x) = 2\sqrt{4x-1}\arctan\left(1/\sqrt{4x-1}\right), \; x > 1/4 \quad (3.13)$$

For the actual values of $M_t \simeq \overline{m}(m_t) + 10$ GeV [53] (the pole top quark mass) and M_h, the correction in (3.13) is of the order of the experimental error in the Higgs mass. Any uncertainty coming from neglected higher order corrections will therefore be much smaller than those from the experimental errors in α_3, M_t and M_h, which can be estimated to ± 2 GeV at 2σ [47].

Notice that, for fixed values of the supersymmetric parameters $\tan\beta$ and X_t, $\mathcal{Q}_0$ is a function of the Higgs mass m_h. This prediction comes from the intersection of the function $\lambda(\mathcal{Q})$, which is determined mainly by the value of the Higgs mass (with some dependence on the actual values of $h_t(m_h)$ and $\alpha_3(m_h)$), with the value $\lambda(\mathcal{Q}_0)$ given by Eq. (4.2). So given that the Higgs mass is fixed to $m_h = 126$ GeV, we can predict $\mathcal{Q}_0 = \mathcal{Q}_0(\tan\beta, X_t)$ as it is shown in the left panel plot of Fig. 3.1. We have used as an input the running top mass in the $\overline{\text{MS}}$ scheme evaluated at the top mass $\overline{m}_t(m_t) = 163.5$ GeV. We can see that for small values of $\tan\beta$ the values of $\mathcal{Q}_0$ are large and insensitive to the values of the mixing X_t. This is due to the fact that the threshold effect is proportional to $h_t^2(\mathcal{Q}_0)$ and the Standard Model RGE leads to small values of $h_t(\mathcal{Q}_0)$ for large values of the scale $\mathcal{Q}_0$. On the other hand for large values of $\tan\beta$ the values of $\mathcal{Q}_0$ are smaller and consequently the RGE running is small and $\mathcal{Q}_0$ becomes sensitive to the mixing X_t. In particular values of $\mathcal{Q}_0$ in the TeV region require large values of $\tan\beta$ ($\tan\beta \gtrsim 5$) and large values of X_t ($X_t \gtrsim 1.8$).

[3] The yukawas in the MSSM are m_u/v_2 and m_d/v_1 for up-type and down-type particles respectively.

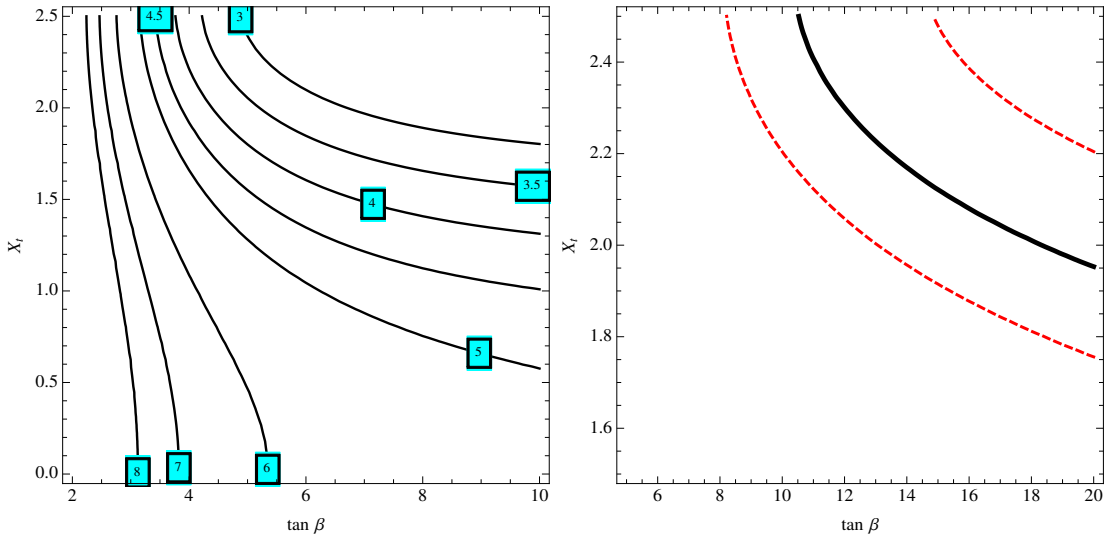

Figure 3.1: *Left panel: Contour lines of* $\log_{10}[\mathcal{Q}_0/GeV]$ *(for the values specified in the plot) in the plane* $(\tan\beta, X_t)$*. Right panel: Contour line of* $m_2^2(\mathcal{Q}_0) = 0$*, as given by Eq. (3.14), in the plane* $(\tan\beta, X_t)$*. The inner region corresponds to radiative electroweak breaking.*

As for the error in $\overline{m}_t(m_t)$ it is safe to consider the experimental range of the running top mass to be given by $\Delta\overline{m}_t = \pm 2$ GeV at 2σ [53, 54]. In order to see the relevance of the error in $\overline{m}_t(m_t)$ we plot, in the left panel of Fig. 3.2, $\mathcal{Q}_0$ as a function of $\tan\beta$ for various values of X_t, and in the right panel of Fig. 3.2, $\mathcal{Q}_0$ as a function of X_t for different values of $\tan\beta$. In fact the

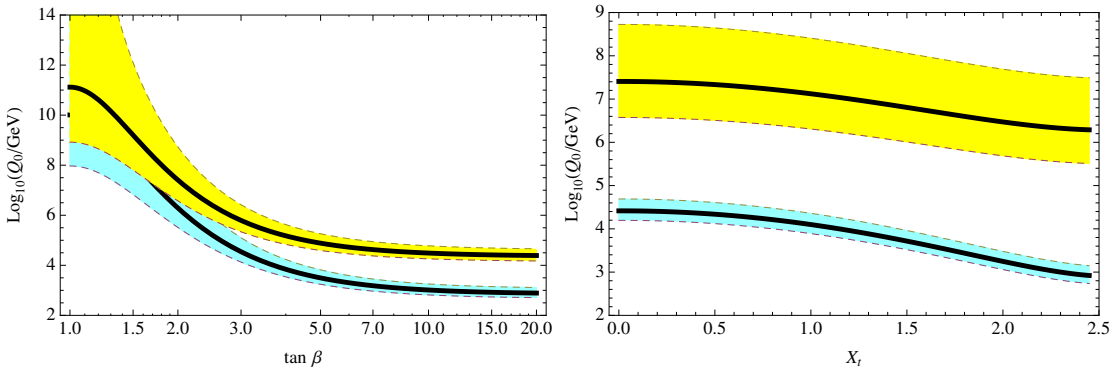

Figure 3.2: *Left panel: Plot of* $\mathcal{Q}_0$ *as a function of* $\tan\beta$ *for* $X_t = 0$ *(upper band) and* $X_t = \sqrt{6}$ *(lower band). The width of bands corresponds to the experimental error* $\Delta\overline{m}_t = \pm 2$ *GeV. Right panel: Plot of* $\mathcal{Q}_0$ *as a function of* X_t *for* $\tan\beta = 2$ *(upper band) and* 15 *(lower band).*

upper border of each band corresponds to $\Delta\overline{m}_t = -2$ GeV and the lower border to $\Delta\overline{m}_t = +2$ GeV. We can see from both panels of Fig. 3.2 that the error in the determination of $\mathcal{Q}_0$, $\Delta\mathcal{Q}_0$ arising from the error in $\overline{m}_t(m_t)$ is large (small) for small (large) values of $\tan\beta$. The reason for this behavior is that the error $\overline{m}_t(m_t)$ is amplified by the RGE running and it is consequently large (small) for large (small) running, which means small (large) values of $\tan\beta$. In the same way, as we can see from the right panel of Fig. 3.2, the error $\Delta\mathcal{Q}_0$ is uncorrelated with X_t as it

has little influence on the RGE running. This translates into a big overlapping in the left panel of Fig. 3.2 for small values of $\tan\beta$ and different values of X_t. In fact notice that for the limiting case $\tan\beta = 1$ and $X_t = 0$ we have that $\lambda(\mathcal{Q}_0) \lesssim 0$ and the Standard Model potential is unstable. This corresponds, for the central value of the quark top mass, to $\mathcal{Q}_0 \sim 10^{11}$ GeV. However for the lowest allowed value of the top quark mass the instability scale can go to Planckian values in agreement with various calculations in the literature [15,55]. In this case it has been shown that the Veltman condition [37] (or absence of quadratic divergences) can also be satisfied [56]. Note that this conclusions are not qualitatively different from what was guessed using Eq. (3.1).

The nature of electroweak breaking

Eq. (3.7) actually implies the existence of the electroweak minimum in the SM effective theory and indeed it is reminiscent of the minimum equation in the MSSM [4]. In fact Eq. (3.7) can be traded by the SM minimum equation. It can be written as

$$m_2^2(\mathcal{Q}_0) = \frac{m_{\mathcal{H}}^2(\mathcal{Q}_0) - m^2(\mathcal{Q}_0)\tan^2\beta}{\tan^2\beta + 1} \tag{3.14}$$

where we identify $m_{\mathcal{H}}^2(\mathcal{Q}_0) \equiv \mathcal{Q}_0^2$ and the value obtained for $m_2^2(\mathcal{Q}_0)$ characterizes the type of electroweak breaking, e.g. radiative versus non-radiative symmetry breaking [5], provided that after the SM RGE running we get $m^2(\mathcal{Q}_{EW}) = m_h^2/2$. For instance in the limit $\tan\beta \to \infty$ (or more precisely for $\tan^2\beta \gg m_{\mathcal{H}}^2(\mathcal{Q}_0)/m^2(\mathcal{Q}_0)$) we get the conditions for radiative breaking, $m_2^2(\mathcal{Q}_0) \simeq -m^2(\mathcal{Q}_0) < 0$, while for small values of $\tan\beta$ we get the conditions for non-radiative breaking $m_2^2(\mathcal{Q}_0) \simeq m_{\mathcal{H}}^2(\mathcal{Q}_0)/(\tan^2\beta+1) > 0$. In particular we show in the right panel of Fig. 3.1 the contour plot corresponding to $m_2^2(\mathcal{Q}_0) = 0$ for the central value of $\overline{m}_t(m_t)$ (thick solid line) and for the 2σ values corresponding to $\pm\Delta\overline{m}_t(m_t)$ (thin solid lines). The inner area corresponds to the region where there is radiative electroweak symmetry breaking $m_2^2(\mathcal{Q}_0) < 0$ while in the outer region the breaking is not radiative and $m_2^2(\mathcal{Q}_0) > 0$. Of course the values of $m_2^2(\mathcal{Q}_0)$ should depend to a large extent on the values of $\tan\beta$ and X_t.

In Fig. 3.3 we plot the absolute value of m_2, $|m_2(\mathcal{Q}_0)|$, as a function of $\tan\beta$ for different values of X_t (left panel) and as a function of X_t for different values of $\tan\beta$ (right panel). Notice that points where electroweak breaking becomes radiative are characterized by the fact that $|m_2| = 0$ and for larger values of $\tan\beta$ (left panel of Fig. 3.3) or larger values of X_t (right panel of Fig. 3.3), m_2^2 becomes negative and thus $|m_2|$ takes on positive values. Again we can see that, as for the results in Fig. 3.2, the effects of the error $\Delta\overline{m}_t(m_t)$ are amplified for small values of $\tan\beta$ while they stay small for large values of $\tan\beta$. We can also see that radiative breaking only occurs for large values of $\tan\beta$, $\tan\beta \gtrsim 8$, and/or large values of the mixing $X_t \gtrsim 1.8$ in the range $\tan\beta \lesssim 20$.

[4] Were neglecting the Standard Model RGE running both equations would be equivalent upon identification of $m_H^2 \leftrightarrow m_Z^2$.

[5] Although EW breaking is in all cases driven by the MSSM RGE running from $\mathcal{M}$ to $\mathcal{Q}_0$, we will be conventionally dubbing radiative breaking the case where $m_2^2(\mathcal{Q}_0) \leq 0$ so that the EW breaking proceeds by a tachyonic mass as in the SM.

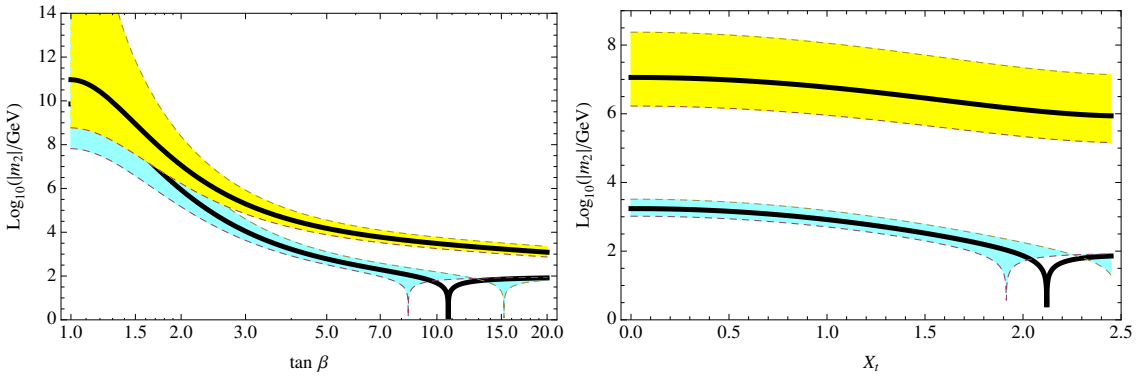

Figure 3.3: *Left panel: Plot of* $|m_2(\mathcal{Q}_0)|$ *as a function of* $\tan\beta$ *for* $X_t = 0$ *(upper band) and* $X_t = \sqrt{6}$ *(lower band). The width of bands corresponds to the experimental error* $\Delta\overline{m}_t = \pm 2$ *GeV. Right panel: Plot of* $|m_2(\mathcal{Q}_0)|$ *as a function of* X_t *for* $\tan\beta = 2$ *(upper band) and* 15 *(lower band).*

3.2 The messenger scale $\mathcal{M}$

Above we have computed, using the measured value of the Higgs mass, the value of the scale $\mathcal{Q}_0$ at which the MSSM matches with the Standard Model and the value of the parameter $m_2^2(\mathcal{Q}_0)$ which guarantees a correct electroweak Standard Model breaking at the scale $\mathcal{Q}_{EW} = m_h$. We are here making the conservative assumption (alas, consistent with present experimental data) that only the SM states survive below the matching scale $\mathcal{Q}_0$. For large values of $\mathcal{Q}_0$ this amounts to assume a high-scale MSSM beyond $\mathcal{Q}_0$, in contradistinction with other possibilities, as those dubbed as split (or mini-split) supersymmetry. Using these tools we will now get information on the scale at which supersymmetry breaking is transmitted to the observable sector, the messenger scale $\mathcal{M}$.

As we have seen both $\mathcal{Q}_0$ and $m_2^2(\mathcal{Q}_0)$ are (for fixed values of the Standard Model parameters) functions of the MSSM parameters $\tan\beta$ and X_t defined at the scale $\mathcal{Q}_0$: $\mathcal{Q}_0 \equiv f_0(\tan\beta, X_t)$ and $m_2^2(\mathcal{Q}_0) \equiv f_2(\tan\beta, X_t)$. Now from the EWSB condition (3.7) one can also compute $m_1^2(\mathcal{Q}_0) \equiv f_1(\tan\beta, X_t)$ as

$$m_1^2(\mathcal{Q}_0) = m_2^2(\mathcal{Q}_0)\tan^2\beta + m^2(\mathcal{Q}_0)(\tan^2\beta - 1) \tag{3.15}$$

so that both squared mass parameters m_1^2 and m_2^2 are fixed at the scale $\mathcal{Q}_0$ for fixed values of $\tan\beta$ and X_t. We will now define the scale at which supersymmetry breaking is transmitted $\mathcal{M}$ as the scale at which

$$m_1^2(\mathcal{M}) = m_2^2(\mathcal{M})\ . \tag{3.16}$$

where we are running the MSSM parameters from the scale $\mathcal{Q} = \mathcal{Q}_0$ to the scale $\mathcal{Q} = \mathcal{M}$ by using the two-loop RGE [57]. Notice that this condition is rather generic in most models of supersymmetry breaking, as models based on gravity mediation or minimal gauge mediation, as well as in string constructions [45, 58, 59]. In models where the former assumption on the Higgs bosons mass at $\mathcal{M}$ is not fulfilled the condition of Eq. (3.16) should be accordingly modified.

As we are assuming that the effective theory below $\mathcal{Q}_0$ is just the Standard Model we are implicitly assuming that, at the matching scale the heavy Higgs $\mathcal{H}$ decouples, so that $m_{\mathcal{H}}(\mathcal{Q}_0) = \mathcal{Q}_0$. On the other hand the scale at which supersymmetry breaking is transmitted, given by (3.16),

does have little dependence on the spreading on boundary conditions imposed for the rest of the supersymmetric spectrum. Actually any moderate splitting among the different superparners will have little impact in the value of $\mathcal{M}$, as its dependence is logarithmic, and the corresponding results fall inside the bands defined by the experimental errors in M_t and $\alpha_3(M_Z)$. Thus we will next consider two generic situations.

Bottom-up approach

The most precise (and ideal) way by which the Standard Model will emerge as the low energy effective theory below the matching scale $\mathcal{Q}_0$ is when all supersymmetric particles are (approximately) degenerate at the decoupling scale [6]. So we will here assume for all sfermions ($\widetilde{f}$), Higgsinos (with mass μ) and gauginos a degenerate mass at the matching scale $\mathcal{Q}_0$

$$m_{\widetilde{f}}(\mathcal{Q}_0) = M_i(\mathcal{Q}_0) = \mu(\mathcal{Q}_0) = \mathcal{Q}_0 \quad (i = 1, 2, 3) \tag{3.17}$$

We will leave $X_t(\mathcal{Q}_0)$ (and consequently the mixing $A_t(\mathcal{Q}_0)$) and $\tan\beta(\mathcal{Q}_0)$ as free parameters in the plots.

Note that by imposing the matching scheme in Eq. (3.17) the merging between the SM and the MSSM happens at the scale $\mathcal{Q}_0$ and the running from the low scale $\mathcal{Q}_0$ to the high scale $\mathcal{M}$ can be done straightforwardly using the two-loop MSSM RGE and the boundary conditions (3.17). This is shown in the left panel (right panel) of Fig. 3.4 where we plot contour lines of

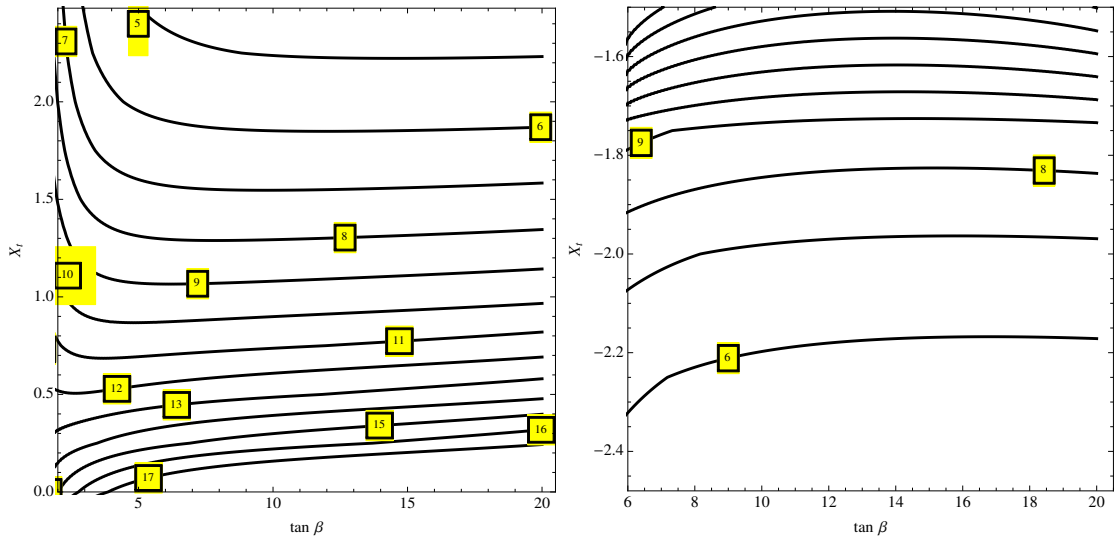

Figure 3.4: *Contour lines of constant* $\log_{10}[\mathcal{M}/\mathrm{GeV}]$ *in the* $(\tan\beta, X_t)$ *plane for* $X_t \geq 0$ *(left panel) and* $X_t < 0$ *(right panel).*

constant $\log_{10}(\mathcal{M}/\mathrm{GeV})$ in the $(\tan\beta, X_t)$ plane for the central value of the top quark mass and positive (negative) values of the parameter X_t.

[6] Of course in practice there should be some spreading of supersymmetric masses over the scale $\mathcal{Q}_0$, a (more realistic) situation which will be studied in the next section.

We can see from the left panel of Fig. 3.4 that having supersymmetry breaking transmission at high scale requires both large values of $\tan\beta$ and small and positive values of the mixing X_t. For example for values of $\mathcal{M}$ of the order of the unification scale $\mathcal{M} \simeq 10^{16}$ GeV one requires $\tan\beta \gtrsim 3$ and $X_t \lesssim 0.3$. Moreover for large values of $\tan\beta$ the value of $\mathcal{M}$ depends almost uniquely on the mixing X_t. For example even for $\tan\beta \simeq 20$ the scale at which supersymmetry is broken can go down to values as low as $\mathcal{M} \sim 10^5 - 10^6$ GeV for values of the mixing $X_t \simeq 2$. On the other hand for low values of $\tan\beta$ and large values of X_t there is small dependence on the mixing. As we can see from the left panel of Fig. 3.4 for values $X_t \simeq 0$ we can get values of $\mathcal{M}$ as large as M_P. For negative values of X_t the value of $\mathcal{M}$ grows quickly to trans Planckian values and rapidly disappears as there is no solution to the Eq. (3.16). A solution appears again for values $X_t \simeq -1.5$ for which we have again values of $\mathcal{M} \simeq M_P$, and again the values of $\mathcal{M}$ decrease when we increase the absolute value of X_t as we have shown in the right panel of Fig. 3.4.

Of course, as it was the case of the matching scale $\mathcal{Q}_0$, the scale at which supersymmetry is transmitted $\mathcal{M}$ is affected by the experimental error in the determination of the top quark mass $\Delta\overline{m}_t$. This effect is shown numerically in Fig. 3.5. We plot in the left panel of Fig. 3.5

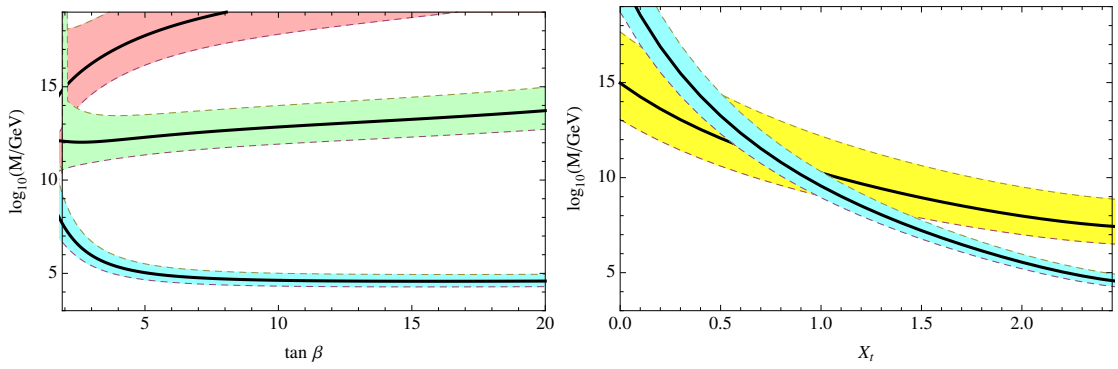

Figure 3.5: *Left panel: Plot of* $\log_{10}[\mathcal{M}/GeV]$ *as a function of* $\tan\beta$ *for* X_t *=0 (upper band),* X_t *=0.5 (central band) and* $X_t = \sqrt{6}$ *(lower band). The width of bands corresponds to the experimental error* $\Delta\overline{m}_t = \pm 2$ *GeV. Right panel: Plot of* $\mathcal{M}$ *as a function of* X_t *for* $\tan\beta = 2$ *(wider band) and* 15 *(narrower band).*

$\log_{10}(\mathcal{M}/\text{GeV})$ as a function of $\tan\beta$ for different values of the mixing X_t =0, 0.5, and $\sqrt{6}$ for the values of the $\overline{\text{MS}}$ top quark mass $\overline{m}_t(m_t) = 163.5 \pm 2$ GeV. This effect is mainly inherited from the uncertainty in the determination of the matching scale $\mathcal{Q}_0$, which explains why the effect is larger for $\tan\beta = 1$. Similarly the plot of $\log_{10}(\mathcal{M}/\text{GeV})$ as a function of X_t for fixed values of $\tan\beta$ =2 and 15, is shown in the right panel of Fig. 3.5 where we can also see that the uncertainty in the determination of $\mathcal{M}$ decreases with increasing values of $\tan\beta$.

Top-down approach

In the previous section we have assumed that all supersymmetric particles exactly decouple at the matching scale $\mathcal{Q}_0$, by which we were assuming a degenerate spectrum at this scale. Of course this is not the generic case in (realistic) models of supersymmetry breaking which provide some pattern of masses at the scale $\mathcal{M}$. These masses run, with the MSSM RGE, from the scale $\mathcal{M}$ to $\mathcal{Q}_0$ and thus they decouple at the scale $\sim \mathcal{Q}_0$ with different thresholds.

In this section we will consider different supersymmetric spectra, for which the scale at which supersymmetry breaking is transmitted and the matching scale with the Standard Model satisfy the general values which have been obtained in the previous section: in particular they are consistent with electroweak symmetry breaking with a Higgs mass of 126 GeV. We will not commit ourselves to any particular mechanism of supersymmetry breaking but instead will consider generic pattern of supersymmetric spectra at the scale where supersymmetry breaking is transmitted, which can arise from different mechanisms. In particular we will consider two classes of models, which are simply particular examples while many others can be easily found and studied:

- Models with universal soft parameters, typical of gravity mediated-like models, although not necessarily arising from gravity mediation.
- Gauge mediated models, where the values of supersymmetric parameters satisfy, at the scale $\mathcal{M}$, typical ratios provided by gauge mediation.

Universal soft parameters

We now consider some universal soft breaking parameters at the scale $\mathcal{M}$. In particular we will assume the rather general pattern

$$m_{\widetilde{Q}_3}(\mathcal{M}) = m_{\widetilde{U}_3^c}(\mathcal{M}) = m_{\widetilde{D}_3^c}(\mathcal{M}) \equiv m_0, \quad M_i(\mathcal{M}) \equiv m_{1/2}, \quad m_1(\mathcal{M}) = m_2(\mathcal{M}) \tag{3.18}$$

by which all third generation squarks [7] are degenerate at the scale $\mathcal{M}$, as well as the three gauginos and the two MSSM Higgs doublets. We have then considered the common masses m_0 and $m_{1/2}$ as free parameters only subject to the constraint of getting a correct electroweak symmetry breaking.

We have considered in Fig. 3.6 two generic models which correspond to $\tan\beta = 10$, and

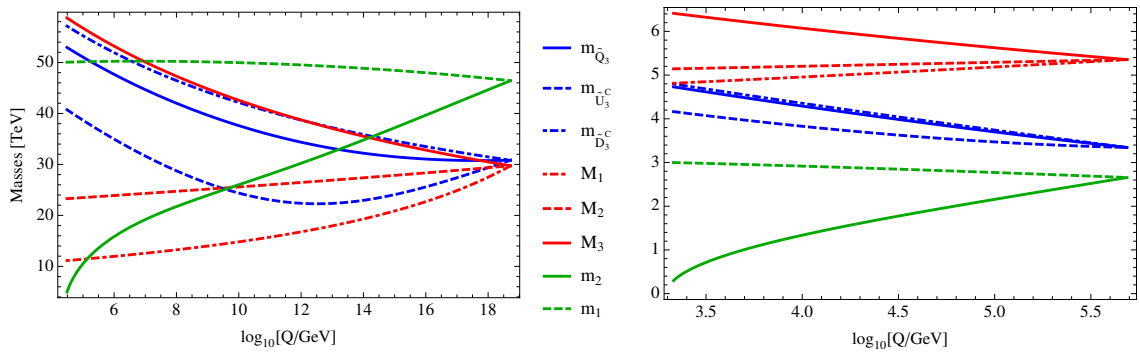

Figure 3.6: *RGE running between $\mathcal{M}$ and $\mathcal{Q}_0$ of the supersymmetric spectrum for the case* $\tan\beta = 10$, $X_t = 0$ *(left panel) and* $X_t = 2$ *(right panel) with universal boundary conditions.*

$X_t = 0$ (left panel) and $X_t = 2$ (right panel). As for the case of $X_t = 0$ a quick glance at the left panel of Fig. 3.1 shows that the matching scale is $\mathcal{Q}_0 \sim 100$ TeV while from Fig. 3.4 the scale where supersymmetry breaks is $\mathcal{M} \sim 2 \times 10^{18}$ GeV. Also from the right panel of Fig. 3.1 ($X_t = 0$

[7] Third generation sleptons as well as first and second generation sfermions do not play any role in the RGE and thus their values decouple from the present problem.

does not appear in the plot as it is well below the area where radiative breaking exists) we see that the breaking is not radiative in the sense that $m_2^2(\mathcal{Q}_0) > 0$ and indeed from Fig. 3.3 we can see that, according with the correct electroweak symmetry breaking, $m_2(\mathcal{Q}_0) \simeq 3$ TeV. As we can see from the left panel of Fig. 3.6 the values for the common squark and gaugino masses which fit these conditions are: $m_0 \simeq m_{1/2} \simeq 30$ TeV. Also the value of $X_t = 0$ at the matching scale $\mathcal{Q}_0$ translates into the mixing $A_t(\mathcal{M}) \simeq 1.7\, m_0$. Notice that, as the value of $\mathcal{M}$ is around the Planck scale, this scenario could arise in models where supersymmetry breaking is transmitted by gravitational interactions.

If we now increase the value of X_t, as in the right panel of Fig. 3.6, in which $X_t = 2$, then looking again at Fig. 3.1 we see that the matching scale is $\mathcal{Q}_0 \sim 1$ TeV and the electroweak breaking is (almost) radiative as $m_2(\mathcal{Q}_0) \sim 100$ GeV. Likewise, from Fig. 3.4, the scale at which supersymmetry is broken is $\mathcal{M} \sim 5 \times 10^5$ GeV. Here we can see a general phenomenon by which the scale where supersymmetry breaking is transmitted (i.e. the scale of unification of m_1 and m_2) strongly goes down when the mixing increases if we fix the correct conditions for electroweak breaking. The reason is the contribution of the mixing to the RGE as

$$\beta_{m_2^2} = \frac{3h_t^2}{4\pi^2} A_t^2 + \cdots . \tag{3.19}$$

To prevent electroweak breaking at high scale ($\mathcal{Q} \gg \mathcal{Q}_0$) we then let the scale $\mathcal{M}$ go down. For the same reason we need gauginos heavier than squarks as the former ones contribute with negative sign to $\beta_{m_2^2}$. As we can see in the right panel of Fig. 3.6 this condition translates into $m_0 \simeq 3.3$ TeV and $m_{1/2} \simeq 5.3$ TeV while at the matching scale $\mathcal{Q}_0$ all the supersymmetric spectrum is in the interval $3 - 6$ TeV.

Gauge mediated models

In this section we will apply the previous results to the particular case in which supersymmetry breaking is transmitted to the observable sector by gauge interactions (GMSB). We will assume in particular the minimal GMSB model whose main features we now summarize.

Supersymmetry is broken, in a hidden sector, by a spurion chiral superfield $X = F\theta^2$ which is coupled to a set of pairs, $\Phi_i + \overline{\Phi}_i$, of messenger fields, in vector like $\mathbf{r} + \bar{\mathbf{r}}$ representations of the gauge group with the superpotential $W = \sum_i \Phi_i \{\lambda_i X + M_i\} \overline{\Phi}_i$.

Gauginos acquire a Majorana mass, by one loop diagrams, given by [29]

$$M_a(\mathcal{M}) = \frac{\alpha_a(\mathcal{M})}{4\pi} \Lambda_G, \qquad \Lambda_G \simeq \sum_i n_i \frac{\lambda_i F}{M_i} = N \frac{F}{M} \tag{3.20}$$

where n_i is the Dynkin index for the pair $\Phi_i + \overline{\Phi}_i$ [8], and $N = \sum_i n_i$. For the last equality of Eq. (3.20) we are assuming universal messenger masses as $M_i \equiv \lambda_i M$ (for $\forall i$). Likewise supersymmetric scalars (squarks and sleptons) acquire soft breaking squared masses through two loop diagrams as

$$m_{\tilde{f}}^2(\mathcal{M}) = 2 \sum_a C_a^{\tilde{f}} \frac{\alpha_a^2(\mathcal{M})}{16\pi^2} \Lambda_S^2, \quad \Lambda_S^2 = \sum_i n_i \frac{(\lambda_i F)^2}{M_i^2} = N \frac{F^2}{M^2} \tag{3.21}$$

[8] We are using a normalization where $n_{SU(\mathbf{N})} = 1$ for the $\mathbf{N} + \overline{\mathbf{N}}$ representation of $SU(\mathbf{N})$, $n_{U(1)} = 6Y^2/5$, and α_1 is the $U(1)$ gauge coupling which satisfies the unification condition $\alpha_a(M_{GUT}) = \alpha_{GUT}$.

where $C_a^{\widetilde{f}}$ is the quadratic Casimir of the representation to which $\widetilde{f}$ belongs in the group G_a [9], and again for the last equality of Eq. (3.21) we are assuming universal messenger masses. In fact for the case of universal messenger masses the ratio $\Lambda_G^2/\Lambda_S^2 = N$ is given by the number of messengers, however in more general cases (which can arise e.g. for several X fields overlapping with the Goldstino field) one can treat Λ_G and Λ_S as free parameters. The soft breaking parameter A_t is not generated at one loop so we will fix it as $A_t(\mathcal{M}) = 0$ and will let it to develop at the scale $\mathcal{Q}_0$ by the MSSM RGE running, which is equivalent to a two loop effect.

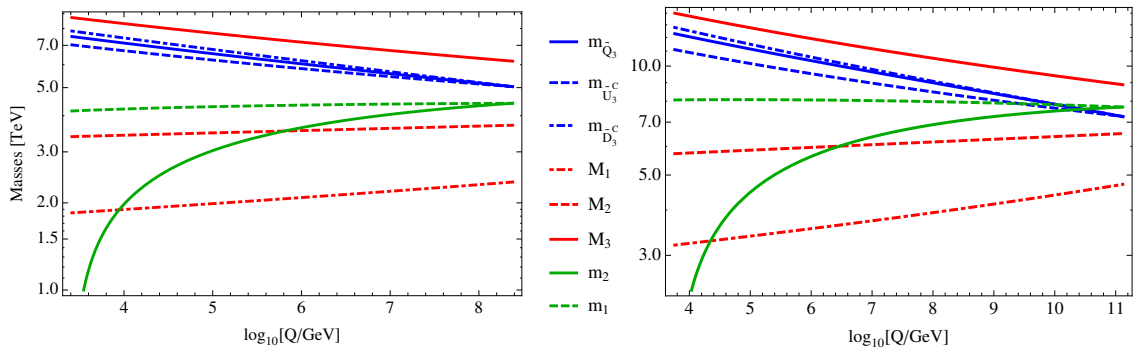

Figure 3.7: *RGE running between $\mathcal{M}$ and $\mathcal{Q}_0$ of the supersymmetric spectrum for the case $A_t(\mathcal{M}) = 0$ and $\tan\beta = 15$ (left panel) and $\tan\beta = 8$ (right panel) with gauge mediated boundary conditions.*

In Fig. 3.7 we are presenting two typical cases where GMSB is consistent with the conditions imposed by electroweak breaking for a 126 GeV Higgs mass. The case $\tan\beta = 15$ is presented in the left panel and $\tan\beta = 8$ in the right panel. In both cases we have fixed $\Lambda_G = 2\Lambda_S$ which corresponds to four messengers, $N = 4$, in minimal GMSB models. Both cases are, as we will see, consistent with perturbative unification.

For the case $\tan\beta = 15$ in the left panel of Fig. 3.7 we get $\Lambda_G \simeq 1.4 \times 10^6$ GeV, $\mathcal{M} \simeq 3 \times 10^8$ GeV, and the scale of supersymmetry breaking $\sqrt{F} \simeq 10^7$ GeV while the expansion parameter $F/\mathcal{M}^2 \simeq 10^{-3}$ is small, and the gravitino mass is $m_{3/2} \simeq 20$ keV. Notice that $m_{H_i}^2(\mathcal{M}) < m_{\widetilde{Q}}^2(\mathcal{M})$ although $m_i^2(\mathcal{M}) > m_{\widetilde{Q}}^2(\mathcal{M})$ because of the contribution of μ^2 in m_i^2. This case is perfectly consistent with perturbative unification and the messengers change the value of the gauge couplings at the unification scale by $\delta\alpha_{GUT}^{-1} \simeq -11$. Even if $A_t(\mathcal{M}) = 0$ a nonzero (and negative) value is generated at the scale $\mathcal{Q}_0$ such that $X_t \simeq -1.8$.

For the case shown in the right panel of Fig. 3.7 that corresponds to $\tan\beta = 8$ we get the following values of the parameters: $\Lambda_G \simeq 2 \times 10^6$ GeV, $\mathcal{M} \simeq 10^{11}$ GeV, $\sqrt{F} \simeq 3 \times 10^8$ GeV with the expansion parameter $F/\mathcal{M}^2 \simeq 4 \times 10^{-6}$ and $m_{3/2} \simeq 20$ MeV. This case is also consistent with perturbative unification with a value of the gauge couplings at the unification scale and the messengers change the value of the gauge couplings at the unification scale by $\delta\alpha_{GUT}^{-1} \simeq -8$. Similarly a nonzero negative value of X_t is generated as $X_t \simeq -1.6$.

[9] We are using a normalization where for $SU(3)$ triplets, $C_3 = 4/3$, for $SU(2)_L$ doublets, $C_2 = 3/4$, and $C_1 = 3Y^2/5$. In all cases $C_a = 0$ for gauge singlets.

3.3 Discussion: $\mathcal{Q}_0$ and the reasons to go beyond the MSSM

It is now widely accepted that the simplest versions of supersymmetry with the simplest assumptions about the supersymmetric spectrum are under stress. As it is summarized in the left panel of Figure 3.1, to accommodate the Higgs mass and if we want to retain the minimal framework, we are forced in a position of either tolerating large stop loops (heavy stops) or attempting to induce large threshold corrections which have tuning problems of their own, since the large trilinear couplings A_t which feed the mixing parameter X_t are not a prediction in most models of supersymmetry breaking. Therefore, the tension between the MSSM and naturalness goes beyond stops not showing up in experiment. Even if we come up with a model that is able to evade experimental searches for superpartners [10], we are left with the problem of how to adjust the Higgs mass in a natural way.

In summary, if we decide to stick with naturalness as a driving principle in the search for BSM physics, we have to do some model building in order to properly fit the Higgs mass. To raise the Higgs mass without superheavy stops or maximal mixing we have a couple of possibilities:

- Enhance the tree-level contribution to the Higgs mass. Since the size of the tree level contribution is set by the Higgs quartics, this suggests new contributions to the quartic couplings which can be given by either F or D-terms. New F-term contributions imply additional DOFs coupled to the Higgs (singlet extended MSSM, NMSSM; triplet extended MSSM, TMSSM [62, 63]; etc.), while new D-term contributions imply new gauge groups broken at a low scale [64].

- Enhance the loop-level contribution to the Higgs mass with additional matter. We know that chiral multiplets with large couplings to the Higgs enhance the radiative contribution to the physical Higgs mass; it is easy to imagine a situation where new loops add to the dominant top sector contribution.

The former are in some sense the most 'natural', since they do not require radiative corrections to exceed tree-level contributions and can be made in agreement with Veltman's naturalness criterion (Sec. 2.5). In particular, the SCTM adds three extra $SU(2)_L$ triplets of $\chi_{\rm SF}$'s to the MSSM and thus raises the Higgs mass through F-term contributions in a natural way.

[10] There are a few possibilities which can alleviate the bounds on stops. Some of them just require a smart choice for the spectrum (compressed scenarios [60]) while others do require some model building (Dirac gauginos [61]).

Part II: Supersymmetric custodial triplets

4

The Supersymmetric Custodial Triplet Model

The MSSM extensions which can increase the Higgs mass by a tree-level F-term are limited to fields in the superpotential which can couple at the renormalizable level to the MSSM Higgs sector $H_{1,2}$. They are an $SU(2)_L$ singlet S and/or triplets with hypercharge $Y = (0, \pm 1)$, $\Sigma_{0,\pm 1}$. Any of the above extra Higgses would add (depending on the value of $\tan\beta$) an extra tree-level contribution to the Higgs mass.

The singlet extension of the MSSM dubbed the NMSSM (the next to minimal supersymmetric Standard Model) is the extended Higgs sector that has been studied the most. It has been shown that it can raise the Higgs mass and solve some drawbacks of the MSSM such as the μ-problem, however as it is noted in Refs. [65, 66], it also suffers from problems of its own. Extra doublets would not feed the tree level Higgs mass and so the next possible choice is the $SU(2)_L$ triplet. Adding triplets to the Higgs sector raises the Higgs mass and gives rise to interesting phenomenology that is worth studying. The problem with triplet representations is that introducing only Σ_0 or $\Sigma_{\pm 1}$ has a general problem, the neutral component of the triplets will acquire a vacuum expectation value v_Δ which will spoil the $\rho = 1$ relationship unless v_Δ is small enough. This requires a large soft mass for the triplet that introduces a tuning problem, for instance, in calculable models such as gauge mediated supersymmetry breaking it is difficult to get heavy triplets while keeping the rest of the spectrum light. The way out is using the whole set $\Sigma_{0,\,\pm 1}$ and providing the theory with a global $SU(2)_L \otimes SU(2)_R$ symmetry, spontaneously broken to the custodial $SU(2)_V$ symmetry after electroweak breaking. This kind of models were first introduced in the context of non supersymmetric theories by Georgi and Machacek in Ref. [67] and further studied in Refs. [68–70]. As the hierarchy problem is worsened with respect to the Standard Model (extended Higgs sector means more scalar masses to stabilize) it is worth considering the supersymmetric generalization.

In this chapter, we introduce the Supersymmetric Custodial Triplet Model and study some of its main features. As a prologue, in Section 4.1 we begin by briefly discussing the GM model and its relation to custodial symmetry. We then present the particle content and the scalar potential of the SCTM in Section 4.2 and also discuss the interesting tree level structure of the scalar spectrum (Sections 4.3 and 4.4), the fermion sector (Sec. 4.5), the restoration of unitarity in the model (Sec. 4.6) and the impact on Higgs observables that the addition of the triplets might have (Sec. 4.7). We end by arguing in Section 4.8 that the tree level picture cannot be the end of the story as loop corrections will break custodial symmetry, hence modifying the naive picture presented in this chapter.

4.1 Triplets and custodial symmetry: The GM model

Let us first describe the non supersymmetric cousin of the SCTM, the GM model. As the SCTM does, it uses custodial symmetry to protect the ρ parameter from dangerous contributions, thus allowing for sizeable triplet VEV's. In the GM model, two $SU(2)_L$ scalar triplets are added to the SM in such a way that the Higgs potential preserves a global $SU(2)_L \otimes SU(2)_R$ symmetry which is then broken to the vector custodial subgroup $SU(2)_V$ after EWSB, thus predicting $\rho = 1$ at tree-level.

More specifically, on top of the SM Higgs doublet, it introduces one real scalar triplet with hypercharge $Y = 0$, $\phi = (\phi^+, \phi^0, \phi^-)^T$, and one complex scalar triplet with $Y = 1$, $\chi = (\chi^{++}, \chi^+, \chi^0)^T$. The doublet and triplets are then organized in terms of representations of $SU(2)_R$ in order to have objects for which the transformation rules under $SU(2)_L \otimes SU(2)_R$ are defined, just as in Section 1.3. The bidoublet is the same as what is defined in Eq. (1.23) while the $(\mathbf{3_L}, \bar{\mathbf{3}}_\mathbf{R})$ transforming bitriplet

$$\bar{\Delta}_{\rm GM} = (\tilde{\chi},\, \phi,\, \chi) = \begin{pmatrix} \chi^{0*} & \phi^+ & \chi^{++} \\ \chi^- & \phi^0 & \chi^+ \\ \chi^{--} & \phi^- & \chi^0 \end{pmatrix} . \tag{4.1}$$

If EWSB proceeds such that $v_H \equiv \langle H^0 \rangle$, $v_\phi \equiv \langle \phi^0 \rangle = v_\chi \equiv \langle \chi^0 \rangle$, i.e. the triplet VEV's are aligned and $\theta_L = \theta_R$, then $SU(2)_L \otimes SU(2)_R$ will be broken to the custodial subgroup $SU(2)_V$, which ensures that the ρ parameter is equal to one at tree-level as in the SM. This can be explicitly seen by taking the gauge boson masses and computing the deviation from $\rho = 1$ when the triplet VEV's have a generic configuration,

$$\rho - 1 \equiv \Delta\rho = \frac{2(v_\phi^2 - v_\chi^2)}{v_H^2 + 4v_\chi^2}. \tag{4.2}$$

Thus, having custodial symmetry, which requires $v_\phi = v_\chi$, ensures that $\rho = 1$ at tree-level and protects it from radiative corrections.

Main drawbacks of the GM model

In the GM model the ρ problem of theories with triplets is solved in and elegant way by using a global symmetry that is already accidentally present in the SM. However, the nice tree level structure that it provides does not hold under quantum scrutiny. Besides worsening the hierarchy problem of the SM by adding more scalars, the GM model suffers from some consistency problems when radiative corrections are taken into account.

As in the SM, the Yukawa and hypercharge interactions lead to an explicit breaking of the $SU(2)_L \otimes SU(2)_R$ symmetry by radiative corrections. Thus, even if the Higgs sector of the theory is $SU(2)_L \otimes SU(2)_R$ invariant at one particular scale, in general it will be driven by the RGE evolution of the couplings and mass parameters to a point which violates this global symmetry. In the GM model this implies that, if the scale at which $SU(2)_L \otimes SU(2)_R$ holds (which we call $\mathcal{Q}_{\rm cus}$) is far above the electroweak scale, RGE evolution will typically lead to large deviations from $\rho = 1$ at the EW scale, in conflict with experiments. Thus in the GM model one is forced to impose the scale $\mathcal{Q}_{\rm cus}$, which is a priori unrelated to v, to be close to the electroweak scale. The particular choice of the scale $\mathcal{Q}_{\rm cus}$ will also greatly affect the phenomenology of the model [69, 70]. Let us

also emphasize that there should be new dynamics at the scale $\mathcal{Q}_{\rm cus}$ where the $SU(2)_L \otimes SU(2)_R$ symmetry is imposed. Otherwise, this $SU(2)_L \otimes SU(2)_R$ symmetric point is simply an arbitrary point in the RGE evolution which 'accidentally emerges' via running from some $SU(2)_L \otimes SU(2)_R$ violating point at higher energies, a scenario that is certainly unappealing. In other words, to avoid relying on this accidental emergence of the global $SU(2)_L \otimes SU(2)_R$, the scale $\mathcal{Q}_{\rm cus}$ should also be taken as the cutoff of the theory. In the GM model this implies a cutoff at or around the electroweak scale, i.e. the introduction of new dynamics or degrees of freedom beyond those found in the GM model (e.g. a strongly coupled sector as originally proposed [67]). These problems can be seen as an indication that the GM model should be embedded in a larger theory which would presumably resolve these issues.

We will show during this work how the supersymmetric generalization of the GM model (the SCTM) can not only stabilize the scalar masses but also provide a way of circumventing the issues listed above. It will give a natural scale at which the $SU(2)_L \otimes SU(2)_R$ symmetry holds, the scale at which supersymmetry breaking is transmitted to the observable sector $\mathcal{Q}_{\rm cus} \equiv \mathcal{M}$ (Chapter 5), and also a reason to why having $v \ll \mathcal{M}$ does not generate $\rho \neq 1$ in all cases (Appendix A.1).

4.2 Introduction to the SCTM: Tree level definitions

Field content and $SU(2)_L \otimes SU(2)_R$ representations

The model features a Higgs sector manifestly invariant under $SU(2)_L \otimes SU(2)_R$. The MSSM Higgs sector H_1 and H_2 with respective hypercharges $Y = (-1/2,\, 1/2)$

$$H_1 = \begin{pmatrix} H_1^0 \\ H_1^- \end{pmatrix}, \quad H_2 = \begin{pmatrix} H_2^+ \\ H_2^0 \end{pmatrix} \tag{4.3}$$

is complemented with $SU(2)_L$ triplets, Σ_{-1}, Σ_0 and Σ_1 with hypercharges $Y = (-1,\, 0,\, 1)$

$$\Sigma_{-1} = \begin{pmatrix} \frac{\chi^-}{\sqrt{2}} & \chi^0 \\ \chi^{--} & -\frac{\chi^-}{\sqrt{2}} \end{pmatrix}, \quad \Sigma_0 = \begin{pmatrix} \frac{\phi^0}{\sqrt{2}} & \phi^+ \\ \phi^- & -\frac{\phi^0}{\sqrt{2}} \end{pmatrix}, \quad \Sigma_1 = \begin{pmatrix} \frac{\psi^+}{\sqrt{2}} & \psi^{++} \\ \psi^0 & -\frac{\psi^+}{\sqrt{2}} \end{pmatrix}, \tag{4.4}$$

where $Q = T_{3L} + Y$. The two doublets and the three triplets are organized under $SU(2)_L \otimes SU(2)_R$ as $\bar{H} = (\mathbf{2_L}, \mathbf{\bar{2}_R})$, and $\bar{\Delta} = (\mathbf{3_L}, \mathbf{\bar{3}_R})$ where

$$\bar{H} = \begin{pmatrix} H_1 \\ H_2 \end{pmatrix}, \quad \bar{\Delta} = \begin{pmatrix} -\frac{\Sigma_0}{\sqrt{2}} & -\Sigma_{-1} \\ -\Sigma_1 & \frac{\Sigma_0}{\sqrt{2}} \end{pmatrix} \tag{4.5}$$

and $T_{3R} = Y$. The invariant products for doublets $A \cdot B \equiv A^a \epsilon_{ab} B^b$ and anti-doublets $\bar{A} \cdot \bar{B} \equiv \bar{A}_a \epsilon^{ab} \bar{B}_c$ are defined by $\epsilon_{21} = \epsilon^{12} = 1$.

Scalar potential

The $SU(2)_L \otimes SU(2)_R$ invariant superpotential is then defined as

$$W_0 = \lambda \bar{H} \cdot \bar{\Delta} \bar{H} + \frac{\lambda_3}{3} \,\mathrm{tr}\, \bar{\Delta}^3 + \frac{\mu}{2} \bar{H} \cdot \bar{H} + \frac{\mu_\Delta}{2} \,\mathrm{tr}\, \bar{\Delta}^2 , \tag{4.6}$$

and the soft terms are also written in a $SU(2)_L \otimes SU(2)_R$ invariant manner

$$V_{\text{soft}} = m_H^2 |\bar{H}|^2 + m_\Delta^2 \text{ tr } |\bar{\Delta}|^2 + \frac{1}{2} m_3^2 \bar{H} \cdot \bar{H} + \left\{ \frac{1}{2} B_\Delta \text{ tr } \bar{\Delta}^2 + A_\lambda \bar{H} \cdot \bar{\Delta} \bar{H} + \frac{1}{3} A_{\lambda_3} \text{ tr } \bar{\Delta}^3 + h.c. \right\} . \tag{4.7}$$

Then the total potential is

$$V = V_F + V_D + V_{\text{soft}} \tag{4.8}$$

and can be easily computed. We have chosen not to write the superpotential yukawa terms and their soft trilinear counterparts to make the $SU(2)_L \otimes SU(2)_R$ invariance manifest. The total expression in component fields can be found in Appendix A.2.

The neutral components of all fields can be parametrized as

$$X = v_X + \frac{X_R + i X_I}{\sqrt{2}}, \quad X = H_1^0, H_2^0, \phi^0, \chi^0, \psi^0 \,, \tag{4.9}$$

where we define by v_1, v_2, v_ϕ, v_χ and v_ψ the VEV's for the fields H_{1R}^0, H_{2R}^0, ϕ_R^0, χ_R^0 and ψ_R^0 respectively. When the field VEV's are related by $v_1 = v_2 \equiv v_H$, $v_\phi = v_\chi = v_\psi \equiv v_\Delta$, the $SU(2)_L \otimes SU(2)_R$ symmetry is broken to the custodial (diagonal) subgroup $SU(2)_V$ (see Appendix A.1) and the (tree-level) parameter $\rho = 1$ [1]. The value of v_H (v_Δ) can be determined by the experimental measurements of the W mass if v_Δ (v_H) is given,

$$v^2 = 2 v_H^2 + 8 v_\Delta^2 \,, \tag{4.10}$$

where $v = 174$ GeV. It is more convenient to use v_Δ as a free parameter and then fix v_H, as v_Δ is the parameter that controls the decoupling of the scalar triplet sector (Section 4.4). The tadpole conditions [2]

$$\left.\frac{\partial V}{\partial H_{1\,R}^0}\right|_0 = \left.\frac{\partial V}{\partial H_{2\,R}^0}\right|_0 = \left.\frac{\partial V}{\partial \phi_R^0}\right|_0 = \left.\frac{\partial V}{\partial \chi_R^0}\right|_0 = \left.\frac{\partial V}{\partial \psi_R^0}\right|_0 = 0 \tag{4.11}$$

at the custodial VEV allow to eliminate the parameters m_H^2 and m_Δ^2 in the potential as a function of the other parameters

$$\begin{aligned} m_H^2 &= m_3^2 + 3 v_\Delta [\lambda(\lambda_3 v_\Delta - \mu_\Delta) - A_\lambda] + 6 \lambda \mu v_\Delta - 3 \lambda^2 (v_H^2 + 3 v_\Delta^2) \,, \\ m_\Delta^2 &= \frac{v_H^2 (2\lambda\mu - 6\lambda^2 v_\Delta - A_\lambda) - v_\Delta B_\Delta + (2\lambda_3 v_\Delta - \mu_\Delta)[\lambda v_H^2 - (\lambda_3 v_\Delta - \mu_\Delta) v_\Delta]}{v_\Delta} \,. \end{aligned} \tag{4.12}$$

[1] The nature of the ρ parameter discussed in this chapter and Appendix A.1 is that of a vacuum determined from an $SU(2)_L \otimes SU(2)_R$ invariant potential. In Chapter 5 we discuss quantum corrections to ρ, these do not come from the explicit computation of diagrams but rather from an RGE improved situation where the potential is not $SU(2) \otimes SU(2)_R$ invariant anymore. To avoid clutter we choose not so signal this in our notation and expect that context will help the reader to distinguish between both situations, the full tree-level and the RGE improved.

[2] For the sake of clarity, in the next chapters and when working with the scalar potential and minimization conditions we will consider the real part of the neutral fields without specifying so.

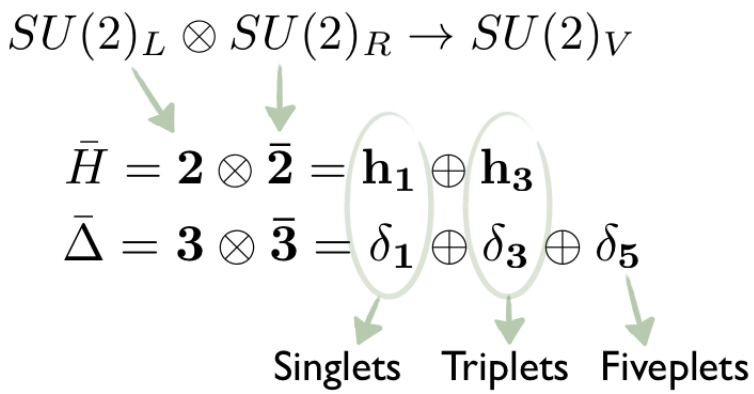

Figure 4.1: *A schematic figure of the scalar spectrum and its tranformation properties under $SU(2)_V$, the mixing angle between the $SU(2)_L$ doublet and triplet sectors will determine how much of doublet or triplet component will have each mass eigenstate. From now on, we will refer to the former and their orthogonal as being doublet-like and triplet-like states respectively.*

$SU(2)_V$ representations

Before discussing the mass spectrum we will change the states $\bar{H}$ and $\bar{\Delta}$, which are representations of the Lagrangian group $SU(2)_L \otimes SU(2)_R$ symmetry, into representations of the custodial vacuum $SU(2)_V$ symmetry. To this end we will decompose the representations as $\bar{H} = h_1 \oplus h_3$ and $\bar{\Delta} = \delta_1 \oplus \delta_3 \oplus \delta_5$ where the subscripts indicate the dimensionality of the $SU(2)_V$ representations. For the doublet part

$$\begin{aligned} h_1^0 &= \frac{1}{\sqrt{2}}(H_1^0 + H_2^0)\,, \\ h_3^+ &= H_2^+, \quad h_3^0 = \frac{1}{\sqrt{2}}(H_1^0 - H_2^0)\,, \quad h_3^- = H_1^-\,, \end{aligned} \tag{4.13}$$

while the triplet decomposes as

$$\begin{aligned} \delta_1^0 &= \frac{\phi^0 + \chi^0 + \psi^0}{\sqrt{3}}\,, \\ \delta_3^+ &= \frac{\psi^+ - \phi^+}{\sqrt{2}},\ \delta_3^0 = \frac{\chi^0 - \psi^0}{\sqrt{2}},\ \delta_3^- = \frac{\phi^- - \chi^-}{\sqrt{2}}\,, \\ \delta_5^{++} &= \psi^{++},\ \delta_5^+ = \frac{\phi^+ + \psi^+}{\sqrt{2}},\ \delta_5^0 = \frac{-2\phi^0 + \psi^0 + \chi^0}{\sqrt{6}},\ \delta_5^- = \frac{\phi^- + \chi^-}{\sqrt{2}},\ \delta_5^{--} = \chi^{--}\,. \end{aligned} \tag{4.14}$$

Notice that the field components of $h_{1,3}$ and $\delta_{1,3,5}$ are complex. After electroweak breaking they decompose into real representations of $SU(2)_V$ with a common mass for all components, including the massless Goldstone triplet.

We then decompose the neutral components of fields in (4.13) and (4.14) as

$$\begin{aligned} h_1^0 &= \sqrt{2}v_H + \frac{h_{1R}^0 + ih_{1I}^0}{\sqrt{2}}, \quad \delta_1^0 = \sqrt{3}v_\Delta + \frac{\delta_{1R}^0 + i\delta_{1I}^0}{\sqrt{2}}\,, \\ h_3^0 &= \frac{h_{3R}^0 + ih_{3I}^0}{\sqrt{2}}, \quad \delta_3^0 = \frac{\delta_{3R}^0 + i\delta_{3I}^0}{\sqrt{2}}\,, \\ \delta_5^0 &= \frac{\delta_{5R}^0 + i\delta_{5I}^0}{\sqrt{2}}\,. \end{aligned} \tag{4.15}$$

Note that as expected, only $SU(2)_V$ singlets acquire vacuum expectation values if custodial symmetry is present.

4.3 The Higgs sector

We will describe in this section the spectrum of the scalar and pseudoscalar sectors. After EW breaking in the custodial minimum and because of the residual custodial invariance of the Higgs sector the mass eigenstates transform as representations of the custodial group $SU(2)_V$ (i.e. singlets, triplets and fiveplets). Therefore a change to the $SU(2)_V$ basis will greatly simplify the mass matrix, making it possible to compute analytical expressions for the mass eigenvalues and mixing angles. By an abuse of language we will sometimes refer to a scalar (pseudoscalar) multiplet as one whose neutral component is a scalar (pseudoscalar).

$SU(2)_V$ scalar singlets

'Features the Higgs boson and its orthogonal triplet-like state'

There are in the spectrum two real neutral scalar $(h_{1R}^0, \delta_{1R}^0)$ singlets mixed by the mass matrix $\mathcal{M}_S^2$

$$(h_{1R}^0, \delta_{1R}^0)\mathcal{M}_S^2 \begin{pmatrix} h_{1R}^0 \\ \delta_{1R}^0 \end{pmatrix} \tag{4.16}$$

where

$$\begin{aligned} (\mathcal{M}_S^2)_{11} &= 6\lambda^2 v_H^2\,, \\ (\mathcal{M}_S^2)_{22} &= \frac{v_H^2\left[\lambda(2\mu - \mu_\Delta) - A_\lambda\right] + v_\Delta^2\left[-A_3 + \lambda_3(4\lambda_3 v_\Delta - 3\mu_\Delta)\right]}{v_\Delta}\,, \\ (\mathcal{M}_S^2)_{12} &= (\mathcal{M}_S^2)_{21} = \sqrt{6}v_H\left[A_\lambda + \lambda(6\lambda v_\Delta - 2\lambda_3 v_\Delta - 2\mu + \mu_\Delta)\right]\,. \end{aligned} \tag{4.17}$$

The eigenvectors can be written in term of the rotation with angle α_S as

$$\begin{pmatrix} S_1 \\ S_2 \end{pmatrix} = \begin{pmatrix} \cos\alpha_S & -\sin\alpha_S \\ \sin\alpha_S & \cos\alpha_S \end{pmatrix} \begin{pmatrix} h_{1R}^0 \\ \delta_{1R}^0 \end{pmatrix} \tag{4.18}$$

where the mixing angle α_S is given by

$$\sin 2\alpha_S = \frac{2(\mathcal{M}_S^2)_{12}}{\sqrt{\mathrm{tr}^{\,2}(\mathcal{M}_S^2) - 4\det(\mathcal{M}_S^2)}}, \quad \cos 2\alpha_S = \frac{(\mathcal{M}_S^2)_{22} - (\mathcal{M}_S^2)_{11}}{\sqrt{\mathrm{tr}^{\,2}(\mathcal{M}_S^2) - 4\det(\mathcal{M}_S^2)}} \tag{4.19}$$

and we are assuming that $m^2_{S_1} < m^2_{S_2}$.

As we can see from Fig. 4.3 one expects $v_\Delta < v_H$ and therefore it will be useful to provide the series expansion of the different masses and mixing angles in powers of v_Δ. We will just present series expansions in powers of v_Δ to have an analytical feeling of the results although the numerical analysis will be done with the complete expressions. In particular for the above masses

$$\begin{aligned} m^2_{h_{\rm MSSM}} \equiv m^2_{S_1} &= 6\lambda^2 v_H^2 + \mathcal{O}(v_\Delta)\,, \\ m^2_{S_2} &= \frac{\lambda(2\mu - \mu_\Delta) - A_\lambda}{v_\Delta} + \mathcal{O}(v_\Delta)\,, \\ \sin\alpha_S &= -\sqrt{6}\frac{v_\Delta}{v_H} + \mathcal{O}(v_\Delta^2)\,. \end{aligned} \tag{4.20}$$

We can see from above that the scalar singlet S_1 plays the role of the light CP-even MSSM Higgs h when the triplet scalar sector is decoupled (in the limit where $v_\Delta \to 0$) [3].

$SU(2)_V$ pseudoscalar singlets

'Features the MSSM pseudoscalar and its orthogonal triplet-like state'

There are two pseudoscalar singlets $(h^0_{1I}, \delta^0_{1I})$ mixed by the mass matrix $\mathcal{M}^2_P$

$$(h^0_{1I}, \delta^0_{1I})\mathcal{M}^2_P \begin{pmatrix} h^0_{1I} \\ \delta^0_{1I} \end{pmatrix} \tag{4.21}$$

where

$$\begin{aligned} (\mathcal{M}^2_P)_{11} &= 2\left(m_3^2 - 3v_\Delta\left[A_\lambda + \lambda(-\lambda_3 v_\Delta + \mu_\Delta)\right]\right)\,, \\ (\mathcal{M}^2_P)_{22} &= -\frac{v_H^2(A_\lambda - 2\lambda\mu) + v_\Delta(-3A_3 v_\Delta + 2B_\Delta - 4\lambda\lambda_3 v_H^2) + (\lambda v_H^2 - \lambda_3 v_\Delta^2)\mu_\Delta}{v_\Delta}\,, \\ (\mathcal{M}^2_P)_{12} &= (\mathcal{M}^2_P)_{21} = \sqrt{6}v_H\left[\lambda(-2\lambda_3 v_\Delta + \mu_\Delta) - A_\lambda\right]\,. \end{aligned} \tag{4.22}$$

The eigenvectors can be written in term of the rotation with angle α_P as

$$\begin{pmatrix} P_1 \\ P_2 \end{pmatrix} = \begin{pmatrix} \cos\alpha_P & -\sin\alpha_P \\ \sin\alpha_P & \cos\alpha_P \end{pmatrix} \begin{pmatrix} h^0_{1I} \\ \delta^0_{1I} \end{pmatrix} \tag{4.23}$$

where the mixing angle α_P is defined as in Eq. (4.19) and we are assuming that $m^2_{P_1} < m^2_{P_2}$. The expansion of the mass eigenvalues and the mixing angle in powers of v_Δ yields

$$\begin{aligned} m^2_{A_{\rm MSSM}} \equiv m^2_{P_1} &= 2m_3^2 + \mathcal{O}(v_\Delta)\,, \\ m^2_{P_2} &= \frac{v_H^2\left[\lambda(2\mu - \mu_\Delta) - A_\lambda\right]}{v_\Delta} - 2B_\Delta + 4\lambda\lambda_3 v_H^2 + \mathcal{O}(v_\Delta)\,, \\ \sin\alpha_P &= \frac{2(\lambda\mu_\Delta - A_\lambda)}{\lambda(2\mu - \mu_\Delta) - A_\lambda}\frac{v_\Delta}{v_H} + \mathcal{O}(v_\Delta^2)\,. \end{aligned} \tag{4.24}$$

Notice also from Eq. (4.24) that the pseudoscalar P_1 plays the role (in the limit $v_\Delta \to 0$) of the massive MSSM pseudoscalar.

[3] As the custodial ordering holds at tree level, during this chapter we will use S_1 to refer to the light doublet-like CP-even Higgs, i.e. the Higgs boson.

$SU(2)_V$ scalar triplets

'Features the MSSM heavy and charged higgses and their orthogonal triplet-like states'

There are two scalar triplets (T_H, T_Δ) defined as

$$T_H = \begin{pmatrix} \frac{1}{\sqrt{2}}(h_3^+ + h_3^{-*}) \\ h_{3R}^0 \\ \frac{1}{\sqrt{2}}(h_3^- + h_3^{+*}) \end{pmatrix}, \quad T_\Delta = \begin{pmatrix} \frac{1}{\sqrt{2}}(\delta_3^+ + \delta_3^{-*}) \\ \delta_{3R}^0 \\ \frac{1}{\sqrt{2}}(\delta_3^- + \delta_3^{+*}) \end{pmatrix} \tag{4.25}$$

which are mixed by the squared mass matrix $\mathcal{M}^2$ as

$$(T_H, T_\Delta)\mathcal{M}^2 \begin{pmatrix} T_H \\ T_\Delta \end{pmatrix} \tag{4.26}$$

where

$$\begin{aligned} \mathcal{M}_{11}^2 &= G^2 v_H^2 + 2\lambda(-4\lambda v_\Delta^2 + \lambda v_H^2 + 4\mu v_\Delta) + 2m_3^2 - 2v_\Delta[A_\lambda + \lambda(\mu_\Delta - \lambda_3 v_\Delta)]\,, \\ \mathcal{M}_{22}^2 &= \frac{4G^2 v_\Delta^3 - 2\lambda v_H^2(\lambda v_\Delta - \mu) - v_\Delta[2B_\Delta - 3\lambda\lambda_3 v_H^2 + 2v_\Delta(A_3 + \lambda_3^2 v_\Delta)] - (\lambda v_H^2 - 2\lambda_3 v_\Delta^2)\mu_\Delta}{v_\Delta}\,, \\ \mathcal{M}_{12}^2 &= \mathcal{M}_{21}^2 = 2v_H\left[-A_\lambda + v_\Delta(G^2 - 4\lambda^2 - \lambda\lambda_3) + \lambda\mu_\Delta\right]\,. \end{aligned} \tag{4.27}$$

In (4.27) $G^2 = g^2$ for the charged components and $G^2 = g^2 + g'^2$ for the neutral components. This just reflects the fact that the hypercharge coupling g' breaks the custodial $SU(2)_V$ symmetry and thus spoils the triplet structure of T_H and T_Δ and therefore of the two triplet mass eigenstates. The triplets eigenvectors are given by [4]

$$\begin{pmatrix} T_1 \\ T_2 \end{pmatrix} = \begin{pmatrix} \cos\alpha_T & -\sin\alpha_T \\ \sin\alpha_T & \cos\alpha_T \end{pmatrix} \begin{pmatrix} T_H \\ T_\Delta \end{pmatrix} \tag{4.28}$$

where again the mixing angle α_T is defined as in Eq. (4.19) and we are assuming that $m_{T_1}^2 < m_{T_2}^2$. The expansion of the mass eigenvalues and the mixing angle in powers of v_Δ yields

$$\begin{aligned} m_{H^\pm_{\rm MSSM}}^2 \equiv m_{T_1}^2 &= G^2 v_H^2 + 2m_3^2 + 2\lambda^2 v_H^2 + \mathcal{O}(v_\Delta)\,, \\ m_{T_2}^2 &= \frac{v_H^2}{v_\Delta}\left[\lambda(2\mu - \mu_\Delta) - A_\lambda\right] - 2B_\Delta - 2\lambda^2 v_H^2 + 3\lambda\lambda_3 v_H^2 + \mathcal{O}(v_\Delta)\,, \\ \sin\alpha_T &= \frac{2(\lambda\mu_\Delta - A_\lambda)}{\lambda(2\mu - \mu_\Delta) - A_\lambda}\frac{v_\Delta}{v_H} + \mathcal{O}(v_\Delta^2)\,. \end{aligned} \tag{4.29}$$

As it happens with other MSSM-like states, T_1 does not get super heavy when $v_\Delta \to 0$. This triplet, which features neutral and charged components, will correspond to the MSSM charged and heavy Higgs, which in the MSSM custodial limit will be degenerate in mass.

[4] The presence of the $\mathcal{O}(g'^2)$ terms can be easily accounted for by just keeping in mind the different definition of G^2 for the mass eigenstates and mixing angles of the neutral and charged components of the triplets. This breaking will be tiny.

$SU(2)_V$ pseudoscalar triplets

'Features the Goldstone triplet and its massive orthogonal triplet-like triplet'

There are two pseudoscalar triplets, the massless triplet $G = \left(G^+, G^0, G^-\right)^T$ describing the massless Goldstone bosons with components

$$\begin{aligned} G^0 &= \cos\theta\, h_{3I}^0 + \sin\theta\, \delta_{3I}^0\,, \\ G^\mp &= \cos\theta\, \frac{h_3^{\pm *} - h_3^\mp}{\sqrt{2}} + \sin\theta\, \frac{\delta_3^{\pm *} - \delta_3^\mp}{\sqrt{2}} \end{aligned} \tag{4.30}$$

and the massive triplet $A = \left(A^+, A^0, A^-\right)^T$

$$\begin{aligned} A^0 &= -\sin\theta\, h_{3I}^0 + \cos\theta\, \delta_{3I}^0\,, \\ A^\mp &= -\sin\theta\, \frac{h_3^{\pm *} - h_3^\mp}{\sqrt{2}} + \cos\theta\, \frac{\delta_3^{\pm *} - \delta_3^\mp}{\sqrt{2}}\,, \end{aligned} \tag{4.31}$$

where the mixing angle is defined as

$$\sin\theta = \frac{2\sqrt{2}v_\Delta}{v}, \quad \cos\theta = \frac{\sqrt{2}v_H}{v}\ . \tag{4.32}$$

The mass of the triplet A is given by

$$m_A^2 = \frac{v_H^2 + 4v_\Delta^2}{v_\Delta}\left(\lambda\left[2\mu - \mu_\Delta - (2\lambda + \lambda_3)v_\Delta\right] - A_\lambda\right)\,. \tag{4.33}$$

The expansion of the mass eigenvalues and the mixing angle in powers of v_Δ yields

$$m_A^2 = \frac{v_H^2}{v_\Delta}\left[\lambda(2\mu - \mu_\Delta) - A_\lambda\right] + \lambda(\lambda_3 - 2\lambda)v_H^2 + \mathcal{O}(v_\Delta)\,. \tag{4.34}$$

$SU(2)_V$ fiveplets

The complex fiveplet in $\bar{\Delta}$ splits into two fiveplets: A scalar fiveplet F_S which contains the neutral scalar δ_{5R}^0, and a pseudoscalar fiveplet F_P which contains the neutral pseudoscalar δ_{5I}^0. They are defined as

$$F_S = \begin{pmatrix} \frac{1}{\sqrt{2}}(\delta_5^{++} + \delta_5^{--*}) \\ \frac{1}{\sqrt{2}}(\delta_5^{+} + \delta_5^{-*}) \\ \delta_{5R}^0 \\ \frac{1}{\sqrt{2}}(\delta_5^{-} + \delta_5^{+*}) \\ \frac{1}{\sqrt{2}}(\delta_5^{--} + \delta_5^{++*}) \end{pmatrix}, \quad F_P = \begin{pmatrix} \frac{1}{\sqrt{2}}(\delta_5^{--*} - \delta_5^{++}) \\ \frac{1}{\sqrt{2}}(\delta_5^{-*} - \delta_5^{+}) \\ \delta_{5I}^0 \\ \frac{1}{\sqrt{2}}(\delta_5^{+*} - \delta_5^{-}) \\ \frac{1}{\sqrt{2}}(\delta_5^{++*} - \delta_5^{--}) \end{pmatrix} \tag{4.35}$$

with masses squared

$$\begin{aligned} m_{F_S}^2 &= \frac{v_H^2(2\lambda\mu - 6\lambda^2 v_\Delta^2 - A_\lambda) + v_\Delta[3\lambda\lambda_3 v_H^2 + 2v_\Delta(A_3 - \lambda_3^2 v_\Delta)] - (\lambda v_H^2 - 6\lambda_3 v_\Delta^2)\mu_\Delta}{v_\Delta}\,, \\ m_{F_P}^2 &= \frac{v_H^2(2\lambda\mu - 6\lambda^2 v_\Delta^2 + \lambda\lambda_3 v_\Delta - A_\lambda) - 2v_\Delta B_\Delta - (\lambda v_H^2 - 4\lambda_3 v_\Delta^2)\mu_\Delta}{v_\Delta}\ . \end{aligned} \tag{4.36}$$

The power expansion in v_Δ of $m^2_{F_S}$ and $m^2_{F_P}$ reads as

$$m^2_{F_S} = \frac{v_H^2}{v_\Delta}\left[\lambda(2\mu - \mu_\Delta) - A_\lambda\right] - 3\lambda(2\lambda - \lambda_3)v_H^2 + \mathcal{O}(v_\Delta)\,,$$
$$m^2_{F_P} = \frac{v_H^2}{v_\Delta}\left[\lambda(2\mu - \mu_\Delta) - A_\lambda\right] - 2B_\Delta - \lambda(6\lambda - \lambda_3)v_H^2 + \mathcal{O}(v_\Delta)\,. \tag{4.37}$$

4.4 Parameter dependece and decoupling considerations

In order to investigate the parameter dependence of the model we choose a set of benchmark parameters

$$A_\lambda = A_{\lambda_3} = 0,\ \mu = \mu_\Delta = 250\ \text{GeV},\ m_3 = 500\ \text{GeV},\ B_\Delta = -m_3^2,\ \lambda_3 = -0.35\ . \tag{4.38}$$

As for the value of λ we will trade it for the mass $m_{S_1} \simeq 125$ GeV. Since the relevant values of λ are moderately small we will consistently neglect the radiative corrections to the mass eigenvalue arising from the λ coupling and those from the bottom quark Yukawa coupling (since $\tan\beta = 1$), and will only keep those coming from the top Yukawa coupling. Moreover as we are neglecting trilinear soft supersymmetry breaking terms in Eq. (4.38) we will do so for the trilinear coupling A_t in the stop sector which we will neglect. On the other hand this choice is the most conservative one as, in the absence of threshold corrections from the stop sector, the only tree level contribution to the Higgs mass comes from the coupling λ which (along with the leading radiative corrections) has to cope with the experimental value of the Higgs mass. Therefore by including the leading ($\propto h_t^2$) one-loop corrections and the subleading two-loop QCD corrections ($\propto h_t^2\alpha_3$) [44] one obtains for $m_{\tilde{t}} \simeq 650\,\text{GeV}$ that radiative corrections amount to a contribution $\simeq (72\,\text{GeV})^2$ to the squared Higgs mass which leaves a tree-level squared mass contribution $\simeq (104\,\text{GeV})^2$. The corresponding value of λ is plotted in Fig. 4.2 as a function of v_Δ.

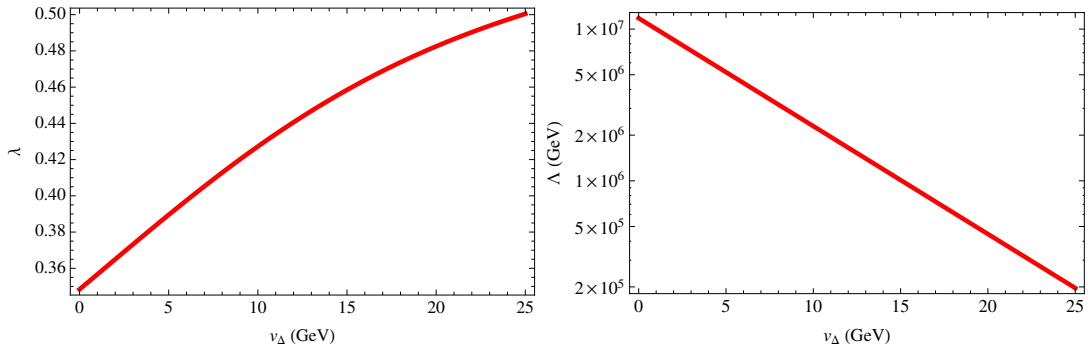

Figure 4.2: *Left: Plot of λ as a function of v_Δ for the values of supersymmetric parameters in Eq. (4.38), $\lambda_3 = -0.35$ and $m_{S_1} \simeq 126$ GeV. Right: Plot of the scale at which the couplings reach Landau poles as a function of v_Δ for the (initial) values of $\lambda(m_t)$ as given in the left panel.*

Conditions for correct EW breaking

Conditions (4.12) guarantee the existence of a non-trivial extremal but by no means enforce electroweak breaking. A set of sufficient conditions for the existence of a non-trivial minimum can be imposed by the condition $\det H|_0 < 0$ (where $H|_0$ is the Hessian matrix, or matrix of second derivatives, at the origin) which implies that the origin is a saddle point. This condition translates into a set of constraints in the space of supersymmetric parameters. To leading order in v_Δ these conditions can be written as

$$\begin{aligned} \lambda(2\mu - \mu_\Delta) - A_\lambda &> 0 \\ 3v_H^2\lambda^2 - 2m_3^2 &< 0 \end{aligned} \tag{4.39}$$

which hold for small values of v_Δ. Of course when v_Δ grows conditions (4.39) are not a good approximation. In order to illustrate this fact we show in Fig. 4.3 the plot of $\det H|_0/v^{10}$, where $v^2 = 2v_H^2 + 8v_\Delta^2$, in the (λ, v_Δ) plane for $\lambda_3 = -0.35$ (left panel) and in the (λ_3, v_Δ) plane for $\lambda = 0.45$ (right panel). In both plots the region on the left (right) of the thick solid line fulfills (does not fulfill) the EW breaking condition. In the plots of Fig. 4.3 we can see that, for fixed values of the supersymmetric parameters, there is an upper bound on the value of v_Δ such that beyond the bound electroweak symmetry breaking does not hold. As we will see in the next sections the chosen values of supersymmetric parameters are consistent with a SM-like Higgs with a mass ~ 125 GeV.

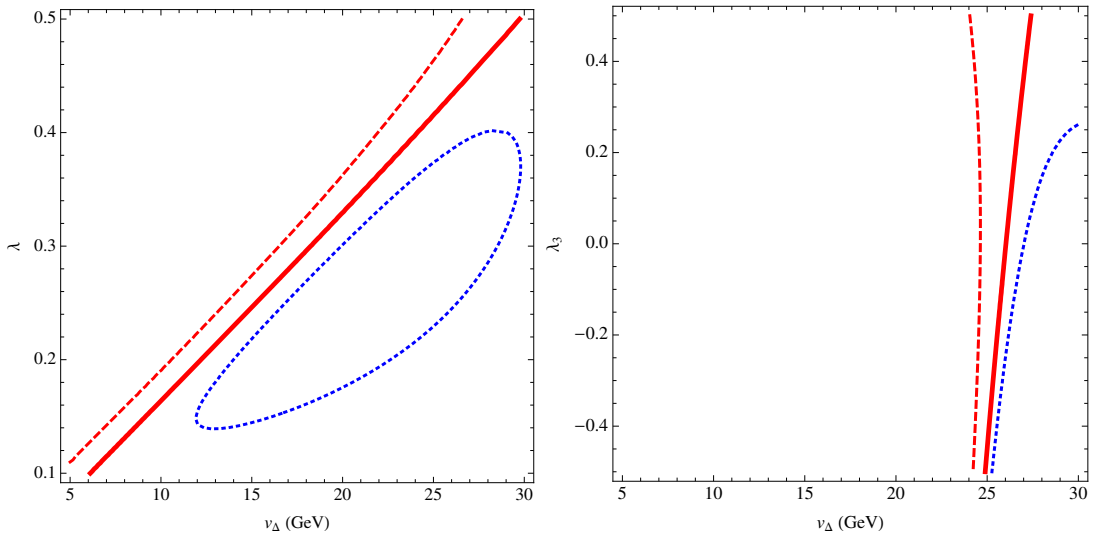

Figure 4.3: *Left: For the values of supersymmetric parameters given in Eq. (4.38), contour lines of* $\det H|_0/v^{10}$ *=-10 (dashed line), 0 (solid line) and 5 (dotted line) in the* (λ, v_Δ) *plane for* $\lambda_3 = -0.35$. *Right: Contour lines of* $\det H|_0/v^{10}$ *=-10 (dashed line), 0 (solid line) and 5 (dotted line) in the* (λ_3, v_Δ) *plane for* $\lambda = 0.45$.

Landau poles

A very general feature of this model is that it requires an ultraviolet (UV) completion as the dimensionless couplings reach Landau poles for scales below the Planck scale as an effect of the renormalization group running. In the right panel of Fig. 4.2 we plot the value of the Landau pole for the couplings as a function of v_Δ for the custodial values of the parameters at m_t given in Eq. (4.38). The origin of the existence of the Landau pole is three-fold:

- The very existence of three $SU(2)_L$ triplets makes the weak coupling g to become non-perturbative at one-loop at a scale $\sim 10^{13}$ GeV.
- Since the top sector obtains its mass at tree-level only from the $SU(2)_L$ doublet VEV v_H, large values of v_Δ necessitate large top Yukawa couplings at the electroweak scale in order to reproduce the observed top mass. One can see this by writing the top Yukawa coupling in terms of v_Δ as

$$y_t = \frac{m_t}{v_H} = \frac{m_t}{\sqrt{(v^2 - 8v_\Delta^2)/2}}, \tag{4.40}$$

  which leads to the absolute constraint $v > 2\sqrt{2}v_\Delta \Rightarrow v_\Delta \lesssim 62$ GeV. Furthermore, if we demand $y_t \lesssim 4\pi$ at the scale $\mathcal{M}$, then it is typically difficult to get values for v_Δ much larger than ~ 30 GeV if we want to have a UV completion around $\mathcal{O}(100\,\text{TeV})$, because y_t increases when run up to higher energies.
- The starting value of $\lambda(m_t)$ has to cope with the experimental value of the Higgs mass $m_h = 125$ GeV after considering the top-stop sector radiative corrections to the Higgs mass. We have conservatively assumed zero mixing in the stop sector $A_t \simeq 0$ so that for other values of the mixing (as e.g. for maximal mixing $A_t \simeq \sqrt{6}m_Q$) the initial value $\lambda(m_t)$ can be decreased and thus the location of the Landau pole moved away.

As a consequence of this behaviour we conclude that the considered model requires low-scale supersymmetry breaking (see Chapter 5).

General considerations on decoupling regions

The masses of the eigenstates studied earlier are provided in Fig. 4.4 for the choice of supersymmetric parameters given in Eq. (4.38). We are using the same color code for the mass eigenstates which are mixed, through a mixing angle, from the original interaction states: in all cases the eigenstates which decouple in the $v_\Delta \to 0$ limit (triplet-like) are presented in solid lines and their companions in dashed lines. As we can see from Fig. 4.4, S_1 (the SM-like Higgs) is the lightest scalar and the second to lightest scalar is F_S which is supermassive for $v_\Delta \to 0$ but becomes as massive as S_1 for $v_\Delta \simeq 25$ GeV. We could think that this is in conflict with present experimental data for the present choice of supersymmetric parameters. However, as we will see in the following section, this state will be weakly coupled to gauge bosons, as its couplings are suppressed by $\sin\theta$, and it is not coupled at all to fermions (see Chapters 5 and 8). The third to lightest scalar is S_2 which is supermassive in the limit $v_\Delta \to 0$ and whose mass becomes $\simeq 300$ GeV for $v_\Delta \simeq 25$ GeV. Unlike F_S this state is coupled to both gauge bosons and fermions but, as it is the orthogonal combination to the SM-like Higgs S_1, it is weakly coupled and should not be easily detected at

LHC. Finally the heaviest scalars, T_1 and T_2 are superheavy. Similarly the lightest pseudoscalar is A, the orthogonal combination to the Goldstone bosons, whose mass grows when $v_\Delta \to 0$. In the region $v_\Delta \sim 25$ GeV its mass is $m_A \simeq 250$ GeV. It does not couple to gauge bosons and its coupling to fermions is suppressed by $\sin\theta$. Notice that rates with couplings proportional to $\sin\theta$ are suppressed by $\sin^2\theta \lesssim 0.16$ for $v_\Delta \lesssim 25$ GeV.

From the previous results in this section it is clear that there are three decoupling limits in the Higgs sector:

- The limit $m_\Delta \to \infty$ (i.e. $v_\Delta \to 0$) in which case all states arising from the triplet $\bar{\Delta}$ are very heavy and decouple from the Higgs sector in the doublet $\bar{H}$. In this limit the heavy states are the scalar S_2 and pseudoscalar P_2 singlets, the scalar T_2 and pseudoscalar A triplets and the scalar F_S and pseudoscalar F_P fiveplets. Similarly the light states are (apart from the massless Goldstone triplet G) the scalar S_1 and pseudoscalar P_1 singlets and the scalar triplet T_1. As $v_\Delta < v_H$ we expect this limit to provide an approximate classification of the states.

- The limit $m_H \to \infty$ (i.e. $m_3^2 \to \infty$) in which case the previous light states split into heavy and light states. Heavy states, with masses controlled by the supersymmetry breaking parameter m_H^2, i.e. by m_3^2, are the pseudoscalar singlet P_1 and the scalar triplet T_1. In particular P_1 plays the role of the massive MSSM pseudoscalar, and the scalar triplet T_1 that of massive neutral and charged Higgses in the MSSM with decoupled triplets. Finally the only light scalar (not controlled by the supersymmetry breaking scale) is the scalar singlet S_1 which plays the role of the MSSM light SM-like Higgs.

- There is also the limit $|B_\Delta| \to \infty$ and $m_3^2 \to \infty$ in which we recover the scalar spectrum found in the GM model. B_Δ is the triplet sector equivalent of m_3^2 so this limit is like taking the decoupling limit of the MSSM thus getting rid of all scalars and pseudoscalars which are controlled by the supersymmetry breaking parameters.

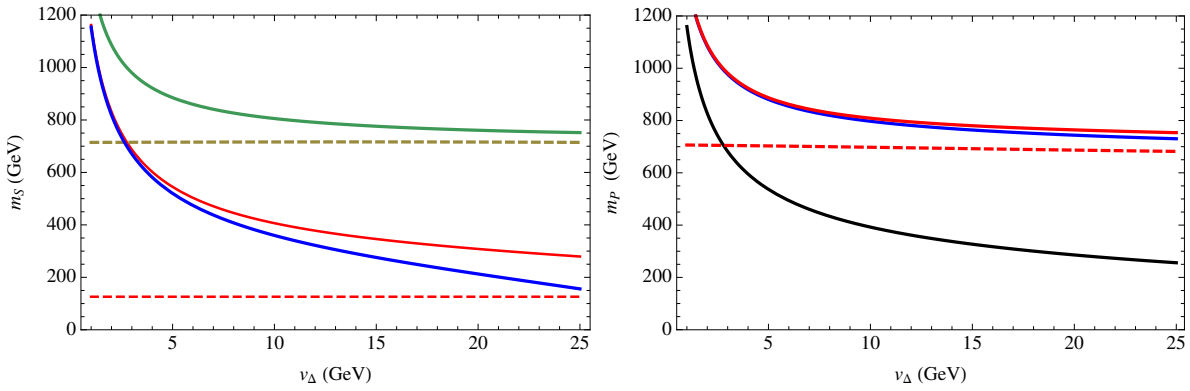

Figure 4.4: *Left: Masses (in GeV) of scalar multiplets as a function of v_Δ. From bottom-up the different lines correspond to the mass eigenstates: S_1, F_S, S_2, T_1, T_2. Right: The same for the pseudoscalar multiplets. From bottom-up the different lines correspond to the mass eigenstates: A, P_1, F_P, P_2.*

4.5 The fermion sector

In this section we will present the mass matrices for fermions in the Higgs doublet-triplet mixed sectors. These matrices also present ordering under custodial symmetry since the change to the custodial basis holds at the superfield level, however, the eigenvalues cannot be analitically computed due to the presence of gauginos, which spoil the $SU(2)_V$ structure.

Neutralinos

In the basis $(\tilde{B}, \tilde{W}_3, \tilde{H}_1^0, \tilde{H}_2^0, \tilde{\phi}^0, \tilde{\chi}^0, \tilde{\psi}^0)$ the neutralino Majorana mass matrix is given by

$$\mathcal{M}_{1/2}^0 = \begin{pmatrix} M_1 & 0 & -\frac{g' v_H}{\sqrt{2}} & \frac{g' v_H}{\sqrt{2}} & 0 & -\sqrt{2} g' v_\Delta & \sqrt{2} g' v_\Delta \\ 0 & M_2 & \frac{g v_H}{\sqrt{2}} & -\frac{g v_H}{\sqrt{2}} & 0 & \sqrt{2} g v_\Delta & -\sqrt{2} g v_\Delta \\ -\frac{g' v_H}{\sqrt{2}} & \frac{g v_H}{\sqrt{2}} & 2\lambda v_\Delta & \lambda v_\Delta - \mu & \lambda v_H & 0 & 2\lambda v_H \\ \frac{g' v_H}{\sqrt{2}} & -\frac{g v_H}{\sqrt{2}} & \lambda v_\Delta - \mu & 2\lambda v_\Delta & \lambda v_H & 2\lambda v_H & 0 \\ 0 & 0 & \lambda v_H & \lambda v_H & \mu_\Delta & -\lambda_3 v_\Delta & -\lambda_3 v_\Delta \\ -\sqrt{2} g' v_\Delta & \sqrt{2} g v_\Delta & 0 & 2\lambda v_H & -\lambda_3 v_\Delta & 0 & -\lambda_3 v_\Delta + \mu_\Delta \\ \sqrt{2} g' v_\Delta & -\sqrt{2} g v_\Delta & 2\lambda v_H & 0 & -\lambda_3 v_\Delta & -\lambda_3 v_\Delta + \mu_\Delta & 0 \end{pmatrix} \tag{4.41}$$

In Fig. 4.5 we make contour plots in the plane (v_Δ, M_2) of the lightest neutralino mass eigenvalue (left panel) and the heaviest neutralino mass eigenvalue (right panel), both in GeV, for the values of parameters in Eq. (4.38) and $M_1 = 200$ GeV.

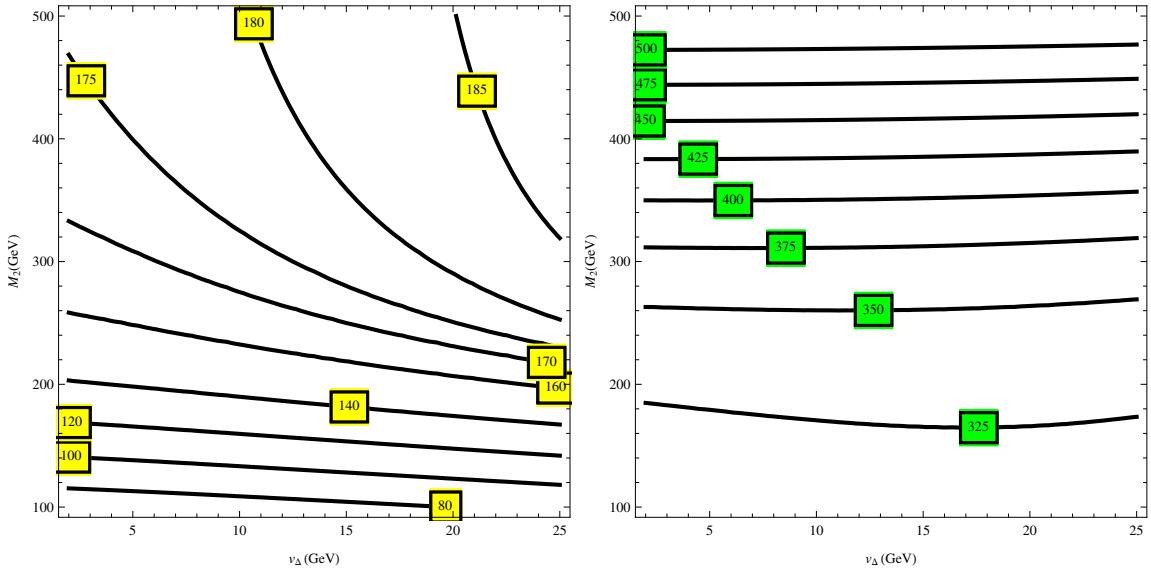

Figure 4.5: *Contour plots in the plane (v_Δ, M_2) of the lightest (left panel) and heaviest (right panel) neutralino masses for the values of the supersymmetric parameters in Eq. (4.38) and $M_1 = 200$ GeV. All masses are in GeV*

Charginos

The mass Lagrangian for charginos with $Q_f = \pm 1$ in the basis $\Psi^+ = (\widetilde{W}^+, \widetilde{H}_2^+, \widetilde{\phi}^+, \widetilde{\psi}^+)^T$ and $\Psi^- = (\widetilde{W}^-, \widetilde{H}_1^-, \widetilde{\phi}^-, \widetilde{\chi}^-)^T$ is given by

$$\mathcal{L}_{1/2}^{\pm} = -\frac{1}{2} \begin{pmatrix} \Psi^{+T} & \Psi^{-T} \end{pmatrix} \begin{pmatrix} 0 & \mathcal{M}_{1/2}^{\pm T} \\ \mathcal{M}_{1/2}^{\pm} & 0 \end{pmatrix} \begin{pmatrix} \Psi^{+} \\ \Psi^{-} \end{pmatrix} + h.c. \tag{4.42}$$

where

$$\mathcal{M}_{1/2}^{\pm} = \begin{pmatrix} M_2 & g v_H & \sqrt{2} g v_\Delta & -\sqrt{2} g v_\Delta \\ g v_H & \lambda v_\Delta + \mu & -\sqrt{2}\lambda v_H & \sqrt{2}\lambda v_H \\ -\sqrt{2} g v_\Delta & \sqrt{2}\lambda v_H & \mu_\Delta & \lambda_3 v_\Delta \\ \sqrt{2} g v_\Delta & -\sqrt{2}\lambda v_\Delta & \lambda_3 v_\Delta & \mu_\Delta \end{pmatrix} \tag{4.43}$$

In Fig. 4.6 we make contour plots in the plane (v_Δ, M_2) of the simply charged lightest chargino mass eigenvalue (left panel) and the heaviest chargino mass eigenvalue (right panel) for the values of parameters in Eq. (4.38).

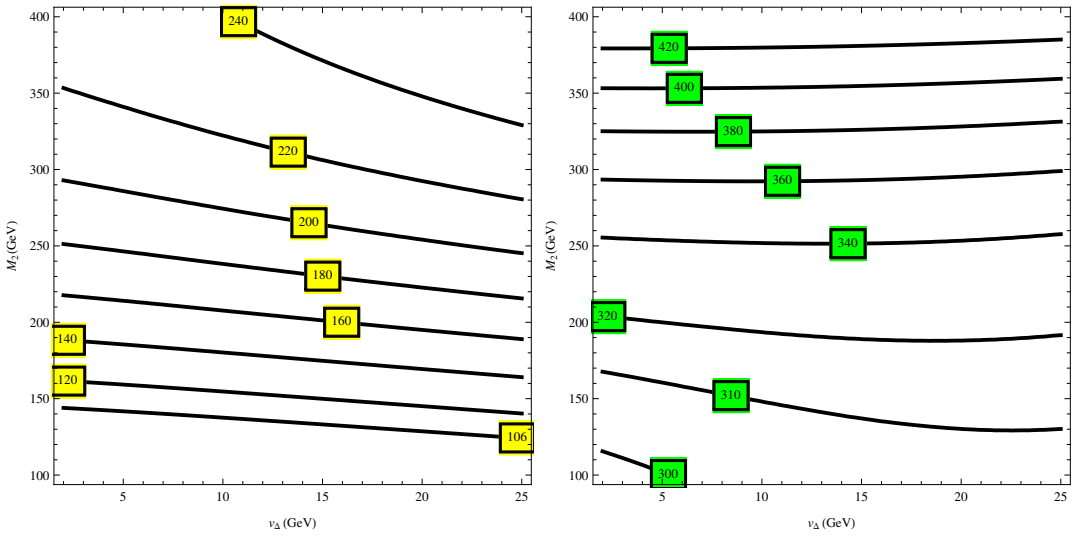

Figure 4.6: *Contour plots in the plane (v_Δ, M_2) of the lightest (left panel) and heaviest (right panel) chargino masses for the values of the supersymmetric parameters in Eq. (4.38). All masses are in GeV.*

Finally for the doubly charged fermions $(\widetilde{\psi}^{++}, \widetilde{\chi}^{--})$ the Dirac mass is given by

$$\mathcal{M}_{1/2}^{\pm\pm} = \mu_\Delta - \lambda_3 v_\Delta \tag{4.44}$$

which using the chosen set of parameters in Eq. (4.38) is $\mathcal{M}_{1/2}^{\pm\pm} \simeq \mu_\Delta = 250$ GeV.

4.6 Comments about unitarity restoration in the model

Perturbative unitarity translates into bounds on scattering amplitudes involving longitudinally polarized gauge bosons [71]. In particular the condition to achieve perturbative unitarity is that tree-level scattering amplitudes $V_L V_L \to V_L V_L$, where V_L denotes the longitudinal polarization of the gauge boson V, mediated by the Higgs sector reproduce at high energy ($s \to \infty$) the SM behavior. These amplitudes involve the trilinear couplings $g_{\mathcal{H}VV}$ where $\mathcal{H}$ goes over the set of mass eigenstates described in Section 4.3. The relevant couplings can be found in Appendix A.3.

In order to exhibit how unitarity works in this model we will choose two particular amplitudes: the elastic scatterings $Z_L W_L^+ \to Z_L W_L^+$ and $W_L^+ W_L^+ \to W_L^+ W_L^+$.

The scattering $Z_L W_L^+ \to Z_L W_L^+$

In this reaction the SM Higgs h contributes in the t-channel and therefore in the limit $s \to \infty$ the amplitude is proportional to t with the coupling

$$g_{hWW}^{SM} \cdot g_{hZZ}^{SM} = g^2 m_W^2 / \cos^2 \theta_W \,. \tag{4.45}$$

In the supersymmetric custodial triplets model (SCTM) there are neutral scalars $\mathcal{H}_i^0 = S_1, S_2, F_S^0$ which contribute in the t-channel and provide an amplitude proportional to t in the limit where $s \to \infty$. On the other hand F_S^+ is exchanged in the s and u-channels and provide amplitudes proportional to $s + u \simeq -t$. Therefore the total amplitude is proportional to t with a coupling equal to

$$\sum_{\mathcal{H}_i^0 = S_1, S_2, F_S^0} g_{\mathcal{H}_i^0 W^+ W^-} \cdot g_{\mathcal{H}_i^0 ZZ} - g^2_{F_S^+ W^- Z} \,. \tag{4.46}$$

Now we can see that using Eqs. (A.33) the coupling in Eq. (4.46) reproduces the SM coupling of Eq. (4.45).

The scattering $W_L^+ W_L^+ \to W_L^+ W_L^+$

In this reaction the SM Higgs h contributes in the t and u channels so that in the limit where $s \to \infty$ the amplitude is proportional to $t + u$ with a coupling

$$(g_{hWW}^{SM})^2 = g^2 m_W^2 \,. \tag{4.47}$$

Similarly to the previous amplitude, in the SCTM the neutral scalars $\mathcal{H}_i^0$ contribute to the t and u channels with an amplitude, in the limit $s \to \infty$, proportional to $t + u \simeq -s$. Moreover the doubly charged scalar F_S^{++} is exchanged in the s channel with an amplitude proportional to s. Adding up the four terms one gets an amplitude which, in the asymptotic limit, is proportional to the coupling

$$\sum_{\mathcal{H}_i^0 = S_1, S_2, F_S^0} g^2_{\mathcal{H}_i^0 W^+ W^-} - g^2_{F_S^{++} W^- W^-} \tag{4.48}$$

which, using the actual values of the couplings in (A.33), reproduces the SM result, Eq. (4.47).

4.7 A study of the light Higgs behavior

In this section we will study the light CP-even Higgs rates to a pair of gauge bosons VV ($V = W, Z, \gamma$) and SM fermions ff ($f = t, b, \tau$). We will first consider tree-level processes. The ratios $r_{\mathcal{H}XX}$ are the quantities

$$r_{\mathcal{H}XX} = \frac{g_{\mathcal{H}XX}}{g^{\rm SM}_{hXX}} \quad \mathcal{H} = S_1, S_2 \quad \text{with} \quad X = V(W,Z), f(t,b,\tau) \tag{4.49}$$

where $g_{\mathcal{H}XX}$ and g^{SM}_{hXX} are the couplings between the Higgs $\mathcal{H}$ and the field X in the SCTM and in the SM, respectively.

Tree-level rates

The angles α_S and θ play a fundamental role in the interactions of the Higgs with the SM fields, as shown in Eq. (A.33) and Table 4.1.

r_{S_1VV}	r_{S_1ff}
$\cos\alpha_S \cos\theta - \sqrt{\frac{8}{3}} \sin\alpha_S \sin\theta$	$\frac{\cos\alpha_S}{\cos\theta}$

Table 4.1: *Ratios (4.49) for the different channels.*

We plot in Fig. 4.7 the ratios of the SM-like Higgs S_1 couplings to gauge bosons r_{S_1VV} (left panel, solid line) and fermions r_{S_1ff} (left panel, dashed line). As we can see from the left panel of the couplings of the Higgs (S_1) to VV and ff are in very good agreement with the 68% CL intervals on r_{hVV} and r_{hff} (when profiling over the other parameter) as measured for instance by the ATLAS Collaboration [72]: $r_{hVV} = [1.05, 1.21]$ and $r_{hff} = [0.73, 1.07]$.

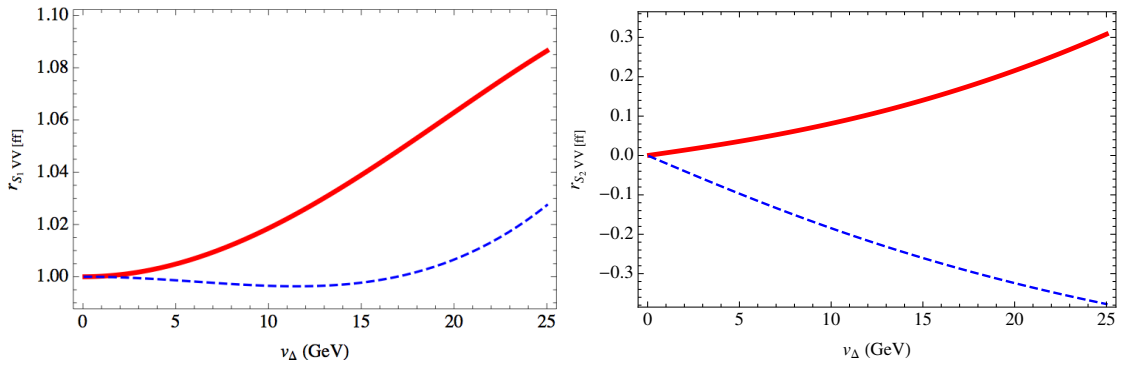

Figure 4.7: *Left: Plots of the ratios r_{S_1VV} (upper solid line) and r_{S_1ff} (lower dashed line) as functions of v_Δ. Right: Plots of the ratios r_{S_2VV} (upper solid line) and r_{S_2ff} (lower dashed line) as functions of v_Δ.*

Other CP-even neutral states

The triplet-like singlet counterpart of the Higgs S_2 and other $CP-$even neutral states couple to SM particles as listed in Table 4.2. While the couplings of the singlets (S_1 and S_2) are controlled

r_{S_2VV}	r_{S_2ff}
$\sin\alpha_S\cos\theta+\sqrt{\frac{8}{3}}\cos\alpha_S\sin\theta$	$\frac{\sin\alpha_S}{\cos\theta}$

$r_{T_i^0VV}$	$r_{T_1^0uu}$	$r_{T_1^0dd}$	$r_{T_2^0uu}$	$r_{T_2^0dd}$	$r_{F_S^0WW}$	$r_{F_S^0ZZ}$	$r_{F_S^0ff}$
0	$-\frac{\cos\alpha_T}{\cos\theta}$	$\frac{\cos\alpha_T}{\cos\theta}$	$-\frac{\sin\alpha_T}{\cos\theta}$	$\frac{\sin\alpha_T}{\cos\theta}$	$\frac{\sin\theta}{\sqrt{3}}$	$-\frac{2\sin\theta}{\sqrt{3}}$	0

Table 4.2: *Ratios (4.49) for the different channels. Notation is $u=t$, $d=b,\tau$.*

by the angles α_S and θ, the couplings of the CP-even scalars contained in the triplets T_i ($i=1,2$) and fiveplets F_S^0 are controlled by the angles α_T and θ. We plot results for the couplings of S_2 to gauge bosons r_{S_2VV} (right panel, solid line) and fermions r_{S_2ff} (right panel, dashed line) in the right plot of Figure 4.7. As we can see, in the given range of v_Δ the signal strengths for the orthogonal eigenstate S_2 is very suppressed. For instance for the gluon fusion Higgs production decaying into VV or ff the signal strength is $\propto r^2_{S_2VV(ff)}\lesssim 0.1$. Similarly the pseudoscalar A can decay to fermions with a signal strength $\propto r^2_{Aff}\lesssim 0.1$. This is a direct consequence of their triplet-like nature.

The diphoton rate

In this model the extra charged states will contribute to the $S_1\to\gamma\gamma$ decay rate when they propagate in the loop. This rate is dominated in the Standard Model by the propagation of W gauge bosons and top quarks in the loop. The extra contribution from a bosonic or fermionic Q-charge sector can be determined from the QED effective potential [73, 74]

$$\mathcal{L}_{\gamma\gamma}=F^2_{\mu\nu}\frac{\alpha}{16\pi}2\sum_{J,Q}b_J^Q\log\det\mathcal{M}_J^Q(X_R),\quad J=0,\,1/2\,;\quad X=H_1^0,H_2^0,\phi^0,\psi^0,\chi^0 \tag{4.50}$$

where $b_{1/2}^{Q_f}=\frac{4}{3}N_cQ_f^2$ for a Q_f-charge Dirac fermion, $b_0^{Q_S}=\frac{1}{3}N_cQ_S^2$ for a complex Q_S-charge spin-0 boson (N_c being the number of colors of the corresponding field) and where we have subtracted from the determinant in (4.50) possible zero-modes (e.g. charged Goldstone bosons). By expanding $\mathcal{L}_{\gamma\gamma}$ to linear order in the fields X_R and projecting them into S_1 we get for the ratio $r_{S_1\gamma\gamma}$ the general expression

$$\begin{aligned}&\left[A_1(\tau_W)+\frac{4}{3}A_{1/2}(\tau_t)\right]r_{S_1\gamma\gamma}\\&=\left(\cos\alpha_S\cos\theta-\sqrt{\frac{8}{3}}\sin\alpha_S\sin\theta\right)A_1(\tau_W)+\frac{4}{3}\frac{\cos\alpha_S}{\cos\theta}A_{1/2}(\tau_t)\\&+v_H\left\{\frac{\cos\alpha_S}{\cos\theta}\left(\frac{\partial f}{\partial H_{1R}^0}+\frac{\partial f}{\partial H_{2R}^0}\right)-\sqrt{\frac{2}{3}}\frac{\sin\alpha_S}{\cos\theta}\left(\frac{\partial f}{\partial\psi_R^0}+\frac{\partial f}{\partial\chi_R^0}+\frac{\partial f}{\partial\phi_R^0}\right)\right\}\Bigg|_{v_X},\end{aligned} \tag{4.51}$$

where $A_1(\tau_W) \simeq -8.3$ and $A_{1/2}(\tau_t) \simeq 1.4$ and

$$\begin{aligned} f(X_R) &= \sum_{Q,J} b_J^Q \log\det \mathcal{M}_J^Q(X_R) \\ &= \frac{4}{3}\log\det \mathcal{M}_{1/2}^{\pm} + \frac{16}{3}\log\det \mathcal{M}_{1/2}^{\pm\pm} + \frac{1}{6}\log\det \left|\mathcal{M}_0^{\pm}\right|^2 + \frac{2}{3}\log\det \left|M_0^{\pm\pm}\right|^2 . \end{aligned} \tag{4.52}$$

Where we have replaced the minimum conditions (4.12) in the mass matrices $\mathcal{M}_J^Q$ in (4.52) but *not* the field VEV's so that they depend on the background fields $H_{1R}^0, H_{2R}^0, \phi_R^0, \psi_R^0, \chi_R^0$. In particular it is easy to deduce the contribution from the SM particles $(t, W^{\pm})$ in the second line of Eq. (4.52) from the general expression in the third line of (4.51) by using the background dependent masses

$$m_t = h_t H_{2R}^0, \quad m_W^2 = \frac{1}{2}g^2\left[(H_{1R}^0)^2 + (H_{1R}^0)^2 + 4(\phi_R^0)^2 + 2(\psi_R^0)^2 + 2(\chi_R^0)^2\right] . \tag{4.53}$$

As we have, both in the fermionic and the bosonic sectors, doubly charged fields they are expected to dominate the $\gamma\gamma$ production since it is proportional to Q^2. Actually we define the excess in $\gamma\gamma$ with respect to the Standard Model production as

$$r_{S_1\gamma\gamma} = 1 + \Delta r_{S_1\gamma\gamma} \tag{4.54}$$

where $\Delta r_{S_1\gamma\gamma}$ is the excess in $r_{S_1\gamma\gamma}$, with respect to the Standard Model contribution, coming from the modified coupling of the Standard Model fields and from the extra charged particles. This excess is plotted in the left panel of Fig. 4.8 where the solid line corresponds to the extra contribution from W and t coming from the modified coupling of these particles to the Higgs S_1, the dashed line is the contribution from the doubly charged scalar $F_S^{\pm\pm}$ which becomes lighter with increasing values of v_Δ (see Fig. 4.4) and the dotted line the contribution from the doubly charged charginos, where we have taken $M_2 = 150$ GeV. The full value of $r_{S_1\gamma\gamma}$ is plotted in the right panel of Fig. 4.8 for $M_2 = 150$ GeV (solid line) and $M_2 = 300$ GeV (dashed line).

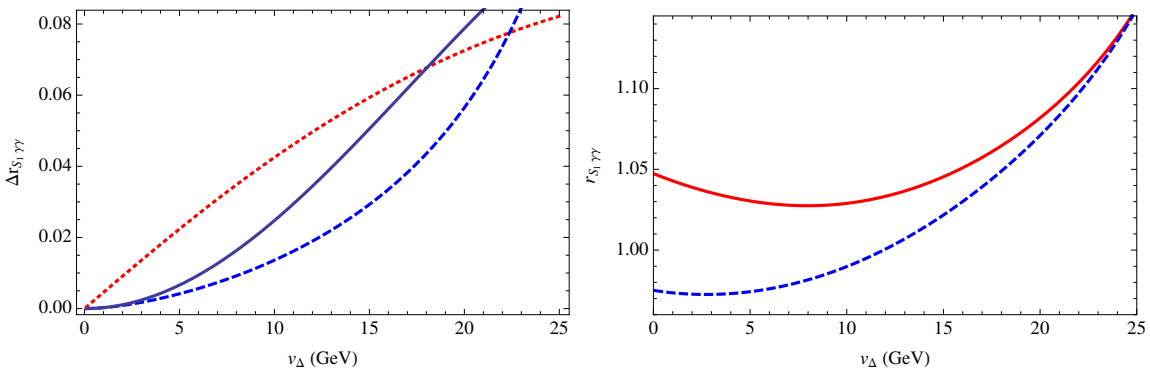

Figure 4.8: *Left: Contribution to $\Delta r_{S_1\gamma\gamma}$ from W and t (solid line), from the doubly charged scalar $F_S^{\pm\pm}$ (dashed line) and from the doubly charged chargino (dotted line) for $M_2 = 150$ GeV. Right: Solid (dashed) line is the plot of $r_{S_1\gamma\gamma}$ for $M_2 = 150$ GeV (300 GeV).*

Higgs signal strengths

From the values of r_{S_1XX} determined in the previous section one can compute the predicted signal strength $\mathcal{R}_{S_1XX}$ of the decay channel $S_1 \to XX$, with $X = V, f, \gamma$:

$$\mathcal{R}_{S_1XX} = \frac{\sigma(pp \to S_1)BR(S_1 \to XX)}{[\sigma(pp \to h)BR(h \to XX)]_{SM}} \,. \tag{4.55}$$

In particular for the gluon-fusion (gF), the associated production with heavy quarks (S_1tt), the associated production with vector bosons (VS_1) and the vector boson fusion (VBF) production processes, one can write $\mathcal{R}^{(gF)}_{S_1XX} = \mathcal{R}^{(S_1tt)}_{S_1XX} = r^2_{S_1ff} r^2_{S_1XX}/\mathcal{D}$ and $\mathcal{R}^{(VBF)}_{S_1XX} = \mathcal{R}^{(VS_1)}_{S_1XX} = r^2_{S_1VV} r^2_{S_1XX}/\mathcal{D}$ where $\mathcal{D} \simeq 0.74\, r^2_{S_1ff} + 0.26\, r^2_{S_1VV}$.

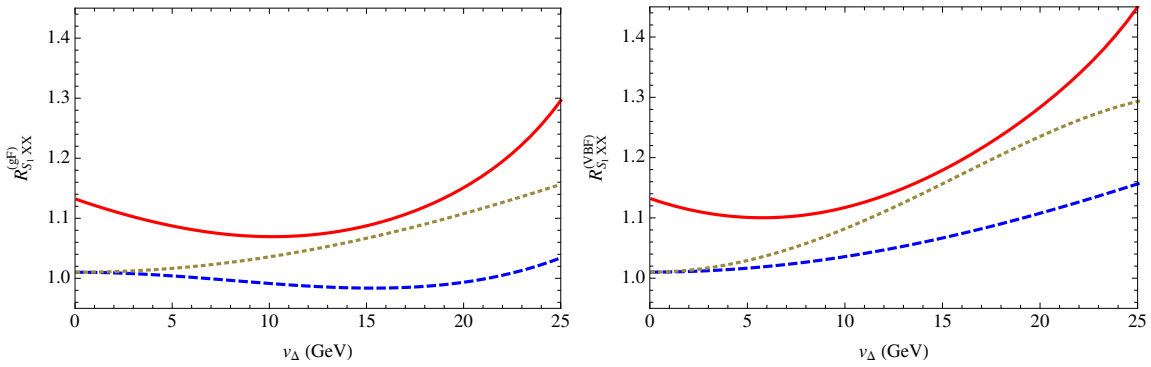

Figure 4.9: *Left: Plot of the gluon fusion Higgs strengths, normalized to the corresponding Standard Model values, for the $\gamma\gamma$ channel (solid line), bb and $\tau\tau$ channels (dashed line) and WW and ZZ channels (dotted line) as a function of v_Δ. Right: The same for weak vector boson fusion Higgs strengths.*

In Fig. 4.9 we plot $\mathcal{R}^{(gF)}_{S_1XX}$ (left panel) and $\mathcal{R}^{(VBF)}_{S_1XX}$ (right panel) for $X = \gamma$ (solid lines), $X = b, \tau$ (dashed lines) and $X = W, Z$ (dotted lines). The supersymmetric parameters are fixed in Eq. (4.38) and $M_2 = 150$ GeV. We can see that large values of v_Δ trigger deviations with the Standard Model expectations although no strong statement can be made at this moment from experimental results. We can just quote the ATLAS best fits for global signal strengths in individual channels [72]: $\mathcal{R}_{h\tau\tau} = 0.8 \pm 0.7$, $\mathcal{R}_{hWW} = 1.0 \pm 0.3$ and $\mathcal{R}_{hZZ} = 1.5 \pm 0.4$ and $\mathcal{R}_{h\gamma\gamma} = 1.6 \pm 0.3$.

4.8 Discussion: Towards the realistic SCTM

We have presented in this chapter a supersymmetric model which feeds new F-term contributions to the tree level part of the Higgs mass. As a consequence of adding extra $\chi_{\rm SF}$'s to the particle content of the MSSM, a set of new states which are not present in the minimal picture does show up, these are ordered under a residual $SU(2)_V$ symmetry that the vacuum has if the VEV's acquired by the neutral components of the scalar triplets are aligned ($v_\psi = v_\chi = v_\phi \equiv v_\Delta$). At the same time this symmetry also protects the relation $\rho = 1$. It is shown in Figure 4.4 how the new scalar states can be light if v_Δ is sizable; these can contribute non negligibly to Higgs

observables (Sec. 4.7), moreover, a sizable v_Δ will be responsible for a great deal of the SCTM interesting features as we will explore in the following chapters.

Thanks to the $SU(2)_V$ invariant structure, the model shows a great deal of calculability, however, during this chapter we have considered that the Higgs sector respects a global $SU(2)_L \otimes SU(2)_R$ invariance which is then broken to the diagonal (custodial) symmetry subgroup $SU(2)_V$. As the Yukawa and hypercharge couplings explicitly violate the custodial symmetry, radiative corrections, mainly those of the top quark Yukawa coupling, will spoil the $SU(2)_L \otimes SU(2)_R$ structure and therefore the custodial invariance of the vacuum. Since the model at tree-level has proven to have interesting properties that we do not want to spoil, if we want the custodial vacuum to be considered as a good approximation, we should study the effect of these custodially breaking quantum corrections and see whether we can have realistic realizations of the SCTM with remnants of the $SU(2)_V$ invariance.

5

The SCTM at the quantum level

In order to perform a realistic study of the SCTM the first thing that should be determined is at which scale the full $SU(2)_L \otimes SU(2)_R$ invariance holds, $\mathcal{Q}_{\rm cus}$. We point out that, as this theory is supersymmetric, a natural choice for $\mathcal{Q}_{\rm cus}$ is the messenger scale $\mathcal{M}$, the scale at which supersymmetry breaking is transmitted from the hidden to the observable sector. Thus, unlike in the GM model, this allows $\mathcal{Q}_{\rm cus}$ to now be associated with a physical scale which, once known, can be used to predict the value of ρ at the electroweak scale through RGE evolution. Conversely, a measurement of ρ now gives a constraint on the scale of SUSY breaking. If we where to fix $\mathcal{Q}_{\rm cus}$ to be below the messenger scale $\mathcal{M}$ we would reintroduce the accidental emergence problem of the global $SU(2)_L \otimes SU(2)_R$ described in Section 4.1. Also, requiring $\mathcal{M}$ to be above the messenger scale will need of assumptions about the SUSY breaking mechanism which we will not consider here. We conclude then that the best choice is $\mathcal{Q}_{\rm cus} \equiv \mathcal{M}$ and study different situations generated by this assumption (Fig. 5.1).

We first show how to parametrize the custodial breaking of the vacuum in Section 5.1, then in Section 5.2 we study a general case without specifying the mechanism of supersymmetry breaking but that will be useful to shed light on the nature of custodial breaking. We also study a precise case of low-scale supersymmetry breaking where the SCTM is embedded into a gauge mediation mechanism, thus providing a realistic UV complete scenario of the SCTM at the EW scale (Sec. 5.3). We end up by summarizing the properties of the custodially broken SCTM at the EW scale (Sec. 5.4) and compare them to the results of the tree level situation of Chapter 4.

5.1 Custodially breaking SCTM

Due to the presence of $SU(2)_L \otimes SU(2)_R$ breaking by $U(1)_Y$ and Yukawa interactions, the RGE running will split the $SU(2)_L \otimes SU(2)_R$ invariant operators into $SU(2)_L$ ones, therefore, the custodial potential of Chapter 4 needs to be rewritten [1]

$$\begin{aligned} W = &-\lambda_a H_1 \cdot \Sigma_1 H_1 + \lambda_b H_2 \cdot \Sigma_{-1} H_2 + \sqrt{2}\lambda_c H_1 \cdot \Sigma_0 H_2 + \sqrt{2}\lambda_3 \,\mathrm{tr}\,\Sigma_1 \Sigma_0 \Sigma_{-1} \\ &- \mu H_1 \cdot H_2 + \frac{\mu_a}{2}\,\mathrm{tr}\,\Sigma_0^2 + \mu_b \,\mathrm{tr}\,\Sigma_1 \Sigma_{-1} + y_t\, Q \cdot H_2\, \bar{t} + y_b\, Q \cdot H_1\, \bar{b} + y_\tau\, L \cdot H_1\, \bar{e}\,. \end{aligned} \tag{5.1}$$

[1] We implicitly assume global lepton number conservation so that the supersymmetric $SU(2)_L \otimes SU(2)_R$ violating operator $\Sigma_1 LL$ is forbidden but in principle it can be included as part of a model to generate neutrino masses [75,76]. It is actually a natural choice to not introduce this operator since we expect the superpotential to be generated in a custodial manner at the messenger scale $\mathcal{M}$, however, assuming lepton number conservation ensures that also the trilinear term in the soft part of the potential is kept to zero.

The scalar potential will be as in Eq. (4.8), where

$$V_F = \sum_X \left| \frac{\partial W^0}{\partial X} \right|^2 \quad \text{with} \quad X = H_1^0, H_2^0, \psi^0, \phi^0, \chi^0, \tag{5.2}$$

which are the neutral components of the $SU(2)_L$ doublets and triplets. Also, the neutral components of the D-terms are given by

$$V_D = \frac{g^2 + g'^2}{8}(|H_1^0|^2 - |H_2^0|^2 + 2|\chi^0|^2 - 2|\psi^0|^2)^2 \tag{5.3}$$

and vanish in the custodial limit. g and g' are the $SU(2)$ and $U(1)_Y$ couplings respectively. Finally, the soft SUSY breaking terms are given by [2]

$$\begin{aligned} V_{\text{soft}} = {} & m_{H_1}^2 H_1^\dagger H_1 + m_{H_2}^2 H_2^\dagger H_2 + m_{\Sigma_0}^2 \Sigma_0^\dagger \Sigma_0 + m_{\Sigma_1}^2 \Sigma_1^\dagger \Sigma_1 + m_{\Sigma_{-1}}^2 \Sigma_{-1}^\dagger \Sigma_{-1} - m_3^2\, H_1 \cdot H_2 \\ & + \left\{ \frac{B_a}{2} \mathrm{tr}\, \Sigma_0^2 + B_b\, \mathrm{tr}\, \Sigma_1 \Sigma_{-1} - A_a\, H_1 \cdot \Sigma_1 H_1 + A_b H_2 \cdot \Sigma_{-2} H_2 + \sqrt{2} A_c\, H_1 \cdot \Sigma_0 H_2 \right. \\ & \left. + \sqrt{2} A_3\, \mathrm{tr}\, \Sigma_1 \Sigma_0 \Sigma_{-1} + a_t\, \widetilde{Q} \cdot H_2 \tilde{t}_R^* + a_b\, \widetilde{Q} \cdot H_1 \tilde{b}_R^* + a_\tau\, \widetilde{L} \cdot H_1 \tilde{\tau}_R^* + h.c. \right\}. \end{aligned} \tag{5.4}$$

Note that we are introducing the $SU(2)_L \otimes SU(2)_R$ explicit breaking related to the Yukawa sector as we are not considering the custodial case anymore. The full $SU(2)_L \otimes SU(2)_R$ invariance of the Higgs sector is recovered whenever

$$\begin{aligned} \lambda_a = \lambda_b = \lambda_c \equiv \lambda, \quad \mu_a = \mu_b \equiv \mu_\Delta\,, \\ m_{H_1} = m_{H_2} \equiv m_H, \quad m_{\Sigma_0} = m_{\Sigma_1} = m_{\Sigma_{-1}} \equiv m_\Delta\,, \\ A_a = A_b = A_c \equiv A_\lambda, \quad B_a = B_b \equiv B_\Delta. \end{aligned} \tag{5.5}$$

After solving the equations of minimum (EOM's) for the scalar potential corresponding to the five neutral field directions $(H_1^0, H_2^0, \psi^0, \phi^0, \chi^0)$ we can parametrize the minimum by two VEV's (v_H, v_Δ) and three angles $(\beta, \theta_1, \theta_0)$,

$$\begin{aligned} v_1 &= \sqrt{2} \cos\beta\, v_H, \quad v_2 = \sqrt{2} \sin\beta\, v_H, \\ v_\psi &= 2 \cos\theta_1 \cos\theta_0\, v_\Delta, \quad v_\chi = 2 \sin\theta_1 \cos\theta_0\, v_\Delta \\ v_\phi &= \sqrt{2} \sin\theta_0\, v_\Delta \end{aligned} \tag{5.6}$$

With this parametrization, custodial symmetry is controlled by the three Euler angles $(\beta, \theta_0, \theta_1)$ where

$$\tan\beta = \frac{v_2}{v_1}\,, \quad \tan\theta_1 = \frac{v_\chi}{v_\psi} \quad \text{and} \quad \tan\theta_0 = \frac{\sqrt{2} v_\phi}{\sqrt{v_\psi^2 + v_\chi^2}}\,, \tag{5.7}$$

in the custodial limit $\tan\beta = \tan\theta_0 = \tan\theta_1 = 1$. Notice that $v^2 = v_1^2 + v_2^2 + 2(2v_\phi^2 + v_\psi^2 + v_\chi^2) = 2v_H^2 + 8v_\Delta^2$ (where $v = 174$ GeV) for any value of $\tan\beta$ and $\tan\theta_{1,0}$ so one can trade the parameter

[2] We do not consider possible Dirac gaugino mass terms of the form $m_D \widetilde{\Sigma}_0^a \widetilde{W}^a$ which would violate the global $SU(2)_L \otimes SU(2)_R$. These terms could appear from D-term supersymmetry breaking corresponding to a hidden $U(1)'$ whose chiral density breaks supersymmetry as $W'_\alpha = \theta_\alpha D$ and the effective operator $(1/M) \int d^2\theta W'_\alpha W_a^\alpha \Sigma_0^a$ yields a Dirac gaugino mass. We just assume that the UV completion of the SCTM can explain its absence.

v_H by v_Δ [3]. In fact from the configuration in Eq. (5.6) the breaking of custodial symmetry (and the value of the T parameter) is measured by $(\tan^2\theta_0 - 1)$ as

$$\rho - 1 \equiv \Delta\rho \equiv \alpha T = \frac{2v_\phi^2 - (v_\psi^2 + v_\chi^2)}{\frac{1}{2}(v_1^2 + v_2^2) + 2(v_\psi^2 + v_\chi^2)} = -4\frac{\cos 2\theta_0\, v_\Delta^2}{v_H^2 + 8\cos^2\theta_0 v_\Delta^2}\,. \tag{5.8}$$

Note that, besides the custodial vacuum, also $2v_\phi^2 = v_\chi^2 + v_\psi^2$ can be responsible for $\rho = 1$.

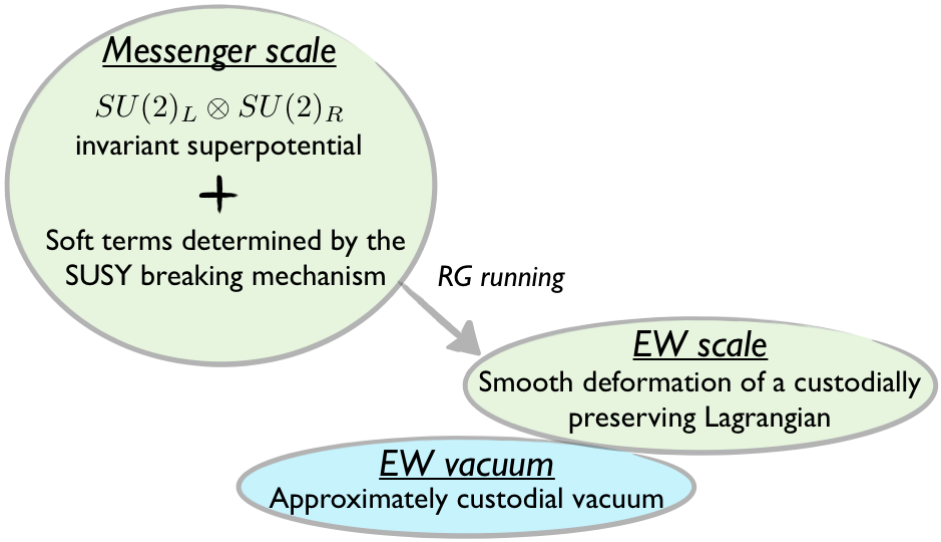

Figure 5.1: *Depiction of what we will consider as a realistic situation in the SCTM: Up to (small) breaking effects caused by the SUSY breaking mechanism (Section 5.3), a (nearly) full $SU(2)_L \otimes SU(2)_R$ invariant situation is generated by UV dynamics at the scale at which supersymmetry breaking is transmitted to the observable sector (the messenger scale, $\mathcal{M}$). Then, due to the explicit breaking of g' and y_t, the RG running of parameters down to the EW scale will deform this situation into a non $SU(2)_L \otimes SU(2)_R$ invariant one and the vacuum will not fully respect the remnant $SU(2)_V$ symmetry anymore. However, as we will consider $\mathcal{O}(100)$ TeV messenger masses, the deformation caused by the running will be small enough and we expect the $SU(2)_V$ breaking to be mild, i.e. most of the general features of the tree level (custodial) situation will hold.*

5.2 A study with universal soft terms

In this section we examine the electroweak vacuum of a theory that features $SU(2)_L \otimes SU(2)_R$ invariance at the messenger scale $\mathcal{M}$ which is then explicitly broken by the RGE running, in order to derive constrains on how heavy the messenger masses $\mathcal{M}$ are and how large can v_Δ be, i.e. how much of a contribution is given by the triplet sector to EWSB. We will find that $\rho \approx 1$ can be accommodated even without custodial symmetry at the electroweak scale and with sizeable contributions from the Higgs triplets to EWSB.

[3] The vacuum parametrization of Eq. (5.6) preserves the modulus (the EW VEV) and therefore the relation (4.10) is valid for both custodial and non custodial situations.

We begin by specifying that the messenger sector, which transmits supersymmetry breaking to the observable sector, exhibits the $SU(2)_L \otimes SU(2)_R$ invariance and then proceeds through effective operators as

$$\int d^2\theta\, d^2\bar{\theta}\, \frac{X^\dagger X}{\mathcal{M}^2} Y^\dagger Y, \quad Y = H, \Delta, Q, L, U^c, D^c, E^c, \tag{5.9}$$

where $X = \theta^2 F$ is the spurion superfield responsible for supersymmetry breaking.

Procedure

For our analysis, given the boundary conditions at the scale $\mathcal{M}$, we will consider $\mathcal{M}$ and v_Δ as free parameters. For each different (v_Δ, $\mathcal{M}$) point we will run the RGE's down to the EW scale and after that solve the EOM's to characterize the vacuum with the non custodial parameters given after the running (see Figure 5.1), with the value of v_H determined by (4.10) [4]. As m_3^2 and $B_{a,b}$ have their RGE's decoupled from the rest of the parameters, we can consistently fix two parameters m_3^2 and $B_+ \equiv B_a + B_b$ from their respective EOM's. The other three EOM's (including the one for $B_- \equiv B_a - B_b$), which vanish identically in the custodial limit, self-consistently determine the values of the custodial breaking angles ($\tan\beta, \tan\theta_0, \tan\theta_1$), which are therefore a prediction of the EOM's for given values of v_Δ and $\mathcal{M}$. This procedure is explained in detail in Appendix B.2 while the full set of RGE's is given in Appendix B.1.

Note that the EOM's are just criticality conditions as they do not tell us whether we are really exploring a minimum of the potential, and much less if this minimum is the absolute one. The minimum condition will be provided by the absence of tachyonic states in the scalar spectrum. Moreover, each minimum that we will find is likely the deepest one since it consists on a smooth deformation of an $SU(2)_V$ preserving minimum where the D-terms vanish, therefore with minimized energy (see App. A.1).

Benchmark values

For illustrative purposes and considering the $SU(2)_L \otimes SU(2)_R$ invariant boundary conditions (5.5) we will choose an example scenario by fixing the following parameters at the high scale $\mathcal{M}$,

$$\begin{aligned} &\lambda_3 = -0.35,\ \mu = \mu_\Delta = 250\,\text{GeV}, \\ &A_\lambda = A_3 = A_t = A_b \equiv A_0 = 0, \\ &m_H = m_\Delta = 1000\,\text{GeV},\ M_1 = M_2 = M_3 \equiv m_{1/2}, \\ &m_Q = m_{U^c} = m_{D^c} \equiv m_0 = 500\,\text{GeV}. \end{aligned} \tag{5.10}$$

Our results will be shown for different values of $m_{1/2}$: (1, 1.1, 1.2, 1.3) TeV [5]. The parameter λ is fixed by the condition that the Higgs field dominantly responsible for EWSB (h) has a mass of ~ 125 GeV.

[4] In contrast to the MSSM study performed in Chapter 3, this model features light stop masses and one can consider $v \sim m_{\text{stops}} \equiv \mathcal{Q}_0$ to a good approximation. Hence, we neglect any threshold and running effects generated between v and $\mathcal{Q}_0$.

[5] Since the values for the squark masses and for the gluino mass M_3 increase as we run to lower scales, we find that our benchmark point leads to a spectrum that satisfies current direct search constraints from the LHC searches.

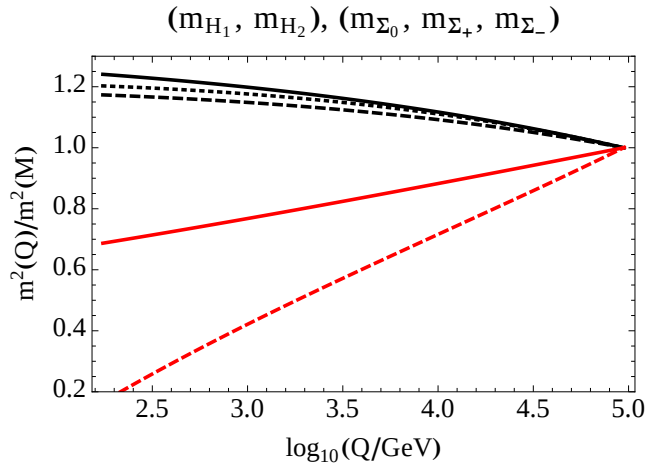

Figure 5.2: *Running of* $(m^2_{H_1}, m^2_{H_2})$ *(red lines from top to bottom) and* $(m^2_{\Sigma_0}, m^2_{\Sigma_+}, m^2_{\Sigma_-})$ *(black lines from bottom to top), normalized to their values at the scale* $\mathcal{M} = 10^5$ *GeV for* $m_{1/2} = 1.2$ *TeV and* $v_\Delta = 20$ *GeV.*

ρ parameter vs. custodially breaking vacuum

We show in Figure 5.2 the results of the RGE running parameters $(m^2_{H_1}, m^2_{H_2})$ (red lines from top to bottom) and $(m^2_{\Sigma_0}, m^2_{\Sigma_+}, m^2_{\Sigma_-})$ (black lines from bottom to top), normalized to their values at the scale $\mathcal{M}$ (chosen to be 10^5 GeV), as functions of the renormalization group scale $\mathcal{Q}$ ($< \mathcal{M}$) and for $v_\Delta = 20$ GeV, $m_{1/2} = 1.2$ TeV. The dispersion in $(m^2_{H_1}, m^2_{H_2})$, which is responsible for generating $\tan\beta \neq 1$ at $\mathcal{Q}_{EW}$, is much larger than the dispersion in the sector $(m^2_{\Sigma_0}, m^2_{\Sigma_+}, m^2_{\Sigma_-})$ that is responsible for the departure of $\tan\theta_0$ and $\tan\theta_1$ from their custodial values. This is because the largest contribution to the doublet splitting comes from the custodial breaking by the top and bottom Yukawa sectors to which the doublet couples at tree-level. The splitting in the triplet sector is instead mainly driven by the hypercharge interactions since triplets do not couple to the top and bottom sectors at tree-level. Thus the splitting in the triplet mass parameters due to the top and bottom Yukawa interactions is a higher order effect, giving in general $|\tan\theta_0 - 1|, |\tan\theta_1 - 1| < |\tan\beta - 1|$.

These features can be seen by examining Eq. (5.8) and the right panel of Figure (5.3). In the left panel we show the regions allowed at the 95% C.L. by the experimental value of the T parameter ($\Delta\rho = \alpha T$), corresponding to the fit value $T = 0.07 \pm 0.08$ [77]. We show results for various values of the common gaugino mass $m_{1/2} = 1$ (black lines), 1.1 (blue lines), 1.2 (red lines) and 1.3 (orange lines) TeV, at the scale $\mathcal{M}$. The allowed region is inside the corresponding solid lines with the dashed lines indicating the $T = 0$ contour. One could interpret the funnel regions that appear for large v_Δ values as a fine-tuning of the scale $\mathcal{M}$. However, in the absence of a precise theory of supersymmetry breaking one could also interpret these regions as a precise prediction of the scale $\mathcal{M}$ which should be provided by the underlying supersymmetry breaking sector. We also show the low $SU(2)_L \otimes SU(2)_R$ scale $\mathcal{M}$ region only for illustrative purposes to demonstrate that, as in the GM model, the parameter space for v_Δ opens up considerably as $\mathcal{M} \to v$. A proper treatment of this region should also include threshold corrections in the renormalization group running. Furthermore, one must ensure that the physical particle masses

are below $\mathcal{M}$ which is a consistency condition since, as discussed above, $\mathcal{M}$ serves as the cutoff for the theory.

We see at this point that the extra freedom (A.27) of the SCTM with respect to the non-supersymmetric GM model, comes into play allowing for $T = 0$ contours (dashed lines) throughout the parameter space. In fact, generically the three VEV's v_ϕ, v_ψ, v_χ are not equal along the $T = 0$ contours. The new direction allows for $\mathcal{Q}_{\rm cus}$ scales well above ~ 100 TeV and sizable triplet VEV's to be comfortably within the allowed region. These $T = 0$ contours will shift slightly after including the sub-dominant one-loop corrections using the RGE improved Lagrangian, however, as loop corrections to the ρ parameter are related to the custodial breaking and therefore proportional to $\tan\alpha_i - 1$ (with $\alpha_i = \beta, \theta_0, \theta_1$), we expect the shift to be small.

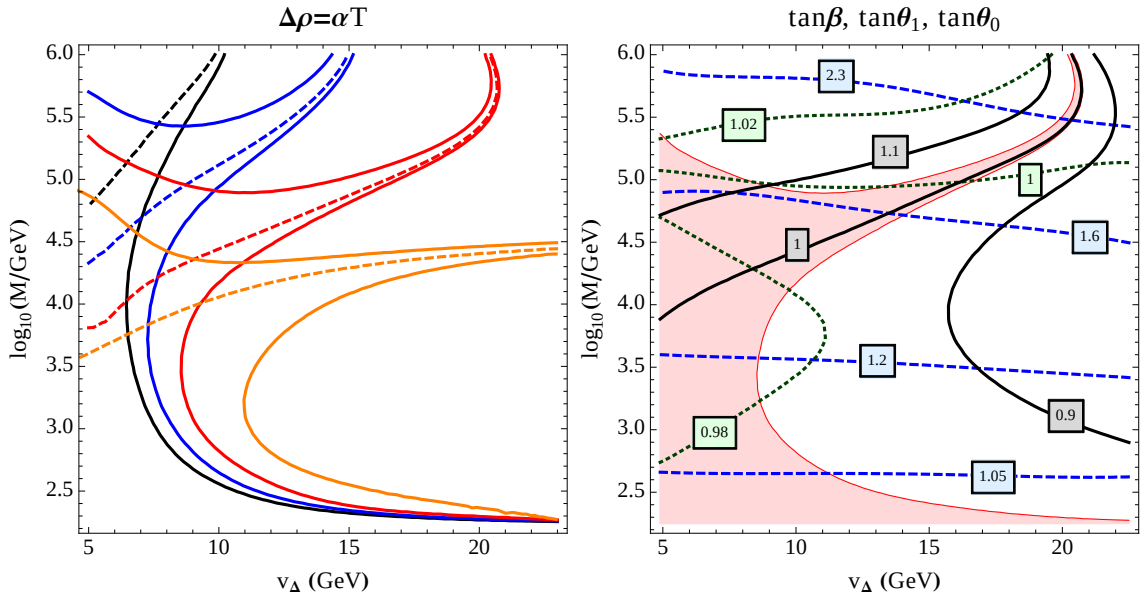

Figure 5.3: *Left: Regions allowed by the T parameter as a function of $\mathcal{M}$ and v_Δ. The region between the solid lines corresponds to the allowed 95% CL interval, having fixed the parameters as in Eq. (5.10) and for $m_{1/2}(\mathcal{M})$ =1 (solid black lines), 1.1 (solid blue lines), 1.2 (solid red lines) and 1.3 (solid orange lines) TeV. The corresponding dashed lines are for $T = 0$. Right: Contours of $\tan\beta$ (blue dashed), $\tan\theta_0$ (black solid), and $\tan\theta_1$ (dark green dotted) for $m_{1/2} = 1.2$ TeV. Shaded pink region is allowed at 95 % CL by the T parameter.*

In the right panel of Figure 5.3 we show contours of $\tan\beta$ (blue dashed), $\tan\theta_0$ (black solid), and $\tan\theta_1$ (dark green dotted). The shaded region is the one allowed by the T parameter at the 95% CL for $m_{1/2} = 1.2$ TeV. As expected from Eq. (5.8), in the region allowed by the ρ parameter deviations from $\tan\theta_0 = 1$ are very small. Furthermore, as anticipated from the results of the running in Fig. 5.2, the violation of custodial symmetry is much larger in $\tan\beta$, which can have values as large as $\tan\beta \gtrsim 2$ than for the parameters $\tan\theta_0$ and $\tan\theta_1$ which depart from their custodial values only by a few percent. We note the presence of a 'crossover' point where the triplet VEV's are aligned, $\tan\theta_0 = \tan\theta_1 = 1$, as found in the GM model. This limit is not equivalent to the GM model since the scale $\mathcal{M}$ is still much greater than the electroweak scale and after the RGE running it will lead to a significantly different scalar spectrum from the one found in the GM model.

After checking these results, let us emphasize that even a realistic (RGE improved) version of the SCTM is free of the generic issues found in supersymmetric models with only one Higgs triplet, which in general acquires a VEV that must be tuned to be very small (∼3 GeV at 95% CL from Ref. [77] for our normalization choice, $v = 174$ GeV) in order to satisfy electroweak precision data (see for example Refs. [63, 78]). In contrast, in the SCTM one can obtain triplet VEV's as large as ~ 25 GeV. Although 25 GeV does not appear large, the actual contribution to EWSB is much larger. As we can see from Fig. 5.4, for $v_\Delta = 25$ GeV triplets give a $\sim 15\%$ contribution which is significantly larger than the $\mathcal{O}(0.1\%)$ allowed by the ρ parameter in conventional triplet extended SUSY models.

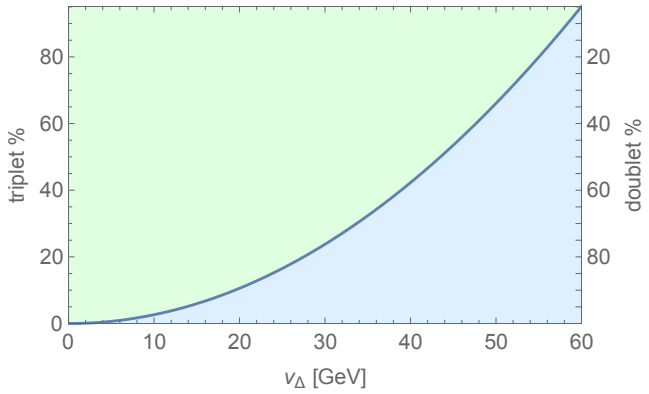

Figure 5.4: *% of contribution to EWSB given by triplets (light blue) and doublets (light green) derived from the relation (4.10), which at the same time is related to the definition of the doublet-triplet mixing angle (4.32). Values of $v_\Delta > 25$ GeV are disfavored for a number of reasons: ρ parameter constraints (Fig. 5.3), issues with Landau poles (Fig. 4.2), etc. Due to this, the actual contribution to EWSB coming from the triplet sector is roughly bounded to be at most ~ 15 %.*

The Higgs boson Mass

Apart from electroweak data, the model needs to be contrasted with LHC data and in particular with measurements of the Higgs properties. We focus on a subset of observables which reflect the essential features of the model. Most of them will show a great similarity with the custodially invariant picture, however, the mild custodial breaking induced by the RGE running will generate properties that are unique of the quantum picture. We begin by analyzing the experimentally measured Higgs mass and conclude that the value of ~ 125 GeV can be obtained for messenger scales $\gtrsim 100$ TeV and triplet VEV's as large as $v_\Delta \sim 25$ GeV inside the allowed T-parameter region.

The tree-level mass squared of the Higgs-like state (h [6]) deviates from its custodial value $m_h^2 = 6\lambda^2 v_H^2 + \mathcal{O}(v_\Delta^2)$. This mass is computed numerically, however in the decoupling limit (large values of m_H^2 and m_Σ^2), and neglecting $\mathcal{O}(v_\Delta^2)$ corrections one can write the analytical

[6] In the custodial theory this state was called S_1 as it is the lightest custodial singlet. We are changing the notation here as custodial symmetry is broken and therefore it no longer provides a good classification.

approximation

$$m_h^2/v^2 \simeq \frac{1}{2}(g_1^2+g_2^2)\cos^2 2\beta + \lambda_c^2 \sin^2 2\beta + 4\lambda_a^2 \cos^4\beta + 4\lambda_b^2 \sin^4\beta \tag{5.11}$$

which reduces to $6\lambda^2 v_H^2$ for $v_\Delta = 0$ and in the custodial limit $\tan\beta = 1$, $\lambda_a = \lambda_b = \lambda_c \equiv \lambda$. Since strictly speaking we are not working in the decoupling limit and/or in the $v_\Delta \to 0$ limit we will compute the tree-level mass of the Higgs-like state numerically. For that we will compute the squared mass matrix of the CP-even neutral Higgs sector

$$(\mathcal{M}_S^2)_{ij} = \frac{1}{2}\frac{\partial^2 V}{\partial\varphi_i \partial\varphi_j}\,, \tag{5.12}$$

with $\varphi_i = (H_1^0, H_2^0, \psi^0, \phi^0, \chi^0)$ and where the minimum conditions are applied. The SM-like Higgs h is easily identified as the only state whose mass is not controlled by supersymmetry breaking parameters and yields the pure SM Higgs in the strict decoupling limit (see Section 4.4 of Chapter 4).

Let U be the orthogonal matrix diagonalizing the squared mass matrix (5.12) such that $U_{ij}\varphi_j = \mathcal{H}_i$ where we are calling the mass eigenstates as $\mathcal{H}_i$ $(i = 1,\dots 5)$ and we identify the lightest eigenstate (the SM-like Higgs) as $h \equiv \mathcal{H}_1$. Conversely the interaction states are projected onto the mass eigenstates as $\varphi_j = U_{ji}\mathcal{H}_i$ so that the projection of the state φ_i onto h is given by the matrix element U_{j1}. In particular the superpotential top Yukawa coupling projects into the SM Yukawa coupling as

$$y_t Q_L U^C H_2 = y_t U_L U^C U_{21}\, h + \cdots \equiv h_t^{SM} U_L U^C\, h + \dots \tag{5.13}$$

where

$$y_t = \frac{m_t}{\sin\beta\sqrt{v^2 - 8v_\Delta^2}}, \quad h_t^{SM} = U_{21} y_t\,. \tag{5.14}$$

Finally v_h can be obtained consistently from

$$\begin{aligned} v_h =& U_{1j}\langle\varphi_j\rangle = \left(\sqrt{2}U_{11}\cos\beta + \sqrt{2}U_{12}\sin\beta\right) v_H \\ &+ \left(2U_{13}\cos\theta_1\cos\theta_0 + \sqrt{2}U_{14}\sin\theta_0 + 2U_{15}\sin\theta_1\cos\theta_0\right) v_\Delta \end{aligned} \tag{5.15}$$

where the values of β, θ_1 and θ_0 are provided by the solutions to the minimum equations (App. B.2).

Radiative corrections are widely dominated by the top/stop sector as the top Yukawa coupling is enhanced by a value of $v_\Delta > 0$, which makes the denominator in (5.14) smaller than in the MSSM. Now the leading radiative corrections from the top/stop sector are given by

$$\Delta m_h^2 = \frac{3}{4\pi^2}\left(h_t^{SM}\right)^4 v_h^2 \left[\log\frac{\mathcal{Q}_0^2}{m_t^2} + X_t\right] \quad \text{with} \quad X_t = \widetilde{A}_t^2\left(1 - \frac{\widetilde{A}_t^2}{12}\right), \tag{5.16}$$

and where $\widetilde{A}_t = (A_t - \mu/\tan\beta)/\mathcal{Q}_0$ and $\mathcal{Q}_0 = \sqrt{m_{\tilde{t}_1} m_{\tilde{t}_2}}$ [7]. The prefactor in Eq. (5.16) can be written as

$$\left(h_t^{SM}\right)^4 v_h^2 = \frac{U_{21}^2\, m_t^4}{\sin^2\beta(v^2 - 8v_\Delta^2)}\,, \tag{5.17}$$

[7] $\tilde{t}_1$ and $\tilde{t}_2$ are the physical stop masses which are calculated by diagonalizing the stop mass matrix, Eq. (5.19). Also note that A_t and μ are given at the weak scale after the RGE running, in particular the trilinear A_t is related to the RGE parameter a_t by $A_t = a_t/y_t$.

from where the enhancement with respect to the MSSM correction when $v_\Delta > 0$ is manifest as $U_{21}/\sin\beta \sim \mathcal{O}(1)$. Thus the SCTM allows in general for larger tree-level and one-loop contributions to the Higgs mass than those that can be found in the MSSM [8]. Taking as an example $\lambda = 0.5$, $v_\Delta \sim 25$ GeV, and $\mathcal{M} \sim 100$ TeV gives a tree-level contribution to the Higgs mass ~ 100 GeV which is larger than m_Z, the absolute upper bound on the tree-level contribution allowed in the MSSM, Eq. (3.1).

By giving fixed boundary values for the soft-breaking terms and fixing the value of m_h to its experimental value, we can obtain the value of the parameter λ (the custodial value of parameters $\lambda_{a,b,c}$) as a function of $(\mathcal{M}, v_\Delta)$. To determine which are the competing effects leading to the 125 GeV Higgs mass we show in the left panel of Fig. 5.5 contour lines of λ (defined at the high scale $\mathcal{M}$) reproducing the observed Higgs mass (including the stop loop corrections) in the $(v_\Delta, \mathcal{M})$ plane for the benchmark point (5.10) and fixing $m_{1/2} = 1.2$ TeV. The Higgs mass is achieved both at tree-level through λ and radiatively through enhanced stop corrections at large v_Δ, or large RGE effects for high scales of $\mathcal{M}$. In particular, smaller values of λ are required at large $\mathcal{M}$. This might be at first surprising since λ (or more precisely $\lambda_{a,b,c}$) runs to smaller values as we go down from $\mathcal{M}$ to $\mathcal{Q}_{EW}$, implying small tree-level contributions from the triplet sector. However, as we increase $\mathcal{M}$ beyond $\gtrsim 10^4$ GeV, the increasing values of $\tan\beta$ from $\tan\beta = 1$ (see right panel Fig. 5.3) lead to the 'turning on' of the tree-level MSSM contribution, allowing for smaller values of λ to be consistent with the observed Higgs mass. Fig. 5.5 also ensures that the correct Higgs mass can be reproduced with perturbative values of λ.

Stops in the SCTM

We also examine whether light top squarks ($\lesssim 1$ TeV) together with small trilinear terms can be accommodated in the SCTM while still reproducing the observed Higgs mass, in contrast to the MSSM which requires large A-terms to avoid multi-TeV top squarks. In order to do this we have to diagonalize the stop mass matrix to get the physical stop masses. These are given by

$$\mathcal{L}_{\text{stop}} = -\begin{pmatrix}\tilde{t}_L^* & \tilde{t}_R^*\end{pmatrix}\mathcal{M}_{\tilde{t}}\begin{pmatrix}\tilde{t}_L \\ \tilde{t}_R\end{pmatrix}, \tag{5.18}$$

with

$$\mathcal{M}_{\tilde{t}} = \begin{pmatrix} m_{\tilde{Q}}^2 + m_t^2 & m_t\left(A_t - \frac{\mu}{\tan\beta}\right) \\ m_t\left(A_t - \frac{\mu}{\tan\beta}\right) & m_{\tilde{t}}^2 + m_t^2 \end{pmatrix}, \tag{5.19}$$

where the values of $m_{\tilde{Q}}$ and $m_{\tilde{t}}$ are given at the weak scale by the RGE's (Appendix B.1). In the right panel of Fig. 5.5 we show the allowed values for the physical lightest stop mass which reproduces a Higgs mass of 125.5 ± 1.0 GeV, for the example parameter point, $\lambda = 0.45$, $\mathcal{M} = 65$ TeV, $m_{1/2} = 1.2$ TeV, $v_\Delta = 10$ GeV and all other parameters fixed to the values in (5.10), except we now allow the soft and trilinear mass parameters to be in the ranges $m_0 \in [500, 1000]$ GeV and $A_0 \in [-250, 500]$ GeV. In the region allowed by the ρ parameter (shaded pink) we see top squarks as light as ~ 950 GeV which can produce the correct Higgs mass for modest values of the trilinear couplings at the electroweak scale $X_t \equiv A_t - \mu/\tan\beta \sim -750$ GeV. These numbers should be compared to the MSSM prediction where for trilinear terms ~ 1 TeV and $\tan\beta \sim 20$, the top squarks should be heavier than ~ 6 TeV (Chapter 3 and [3, 47, 79, 80]), showing that the SCTM indeed helps to alleviate the MSSM fine-tuning problem (see also [81]).

[8] Actually, in the custodial limit where $\tan\beta = 1$ there is no tree-level contribution from the doublet (or MSSM) sector to the Higgs mass (5.11), thus the SCTM makes most of the tree level Higgs mass with F-term contributions coming from the triplet sector.

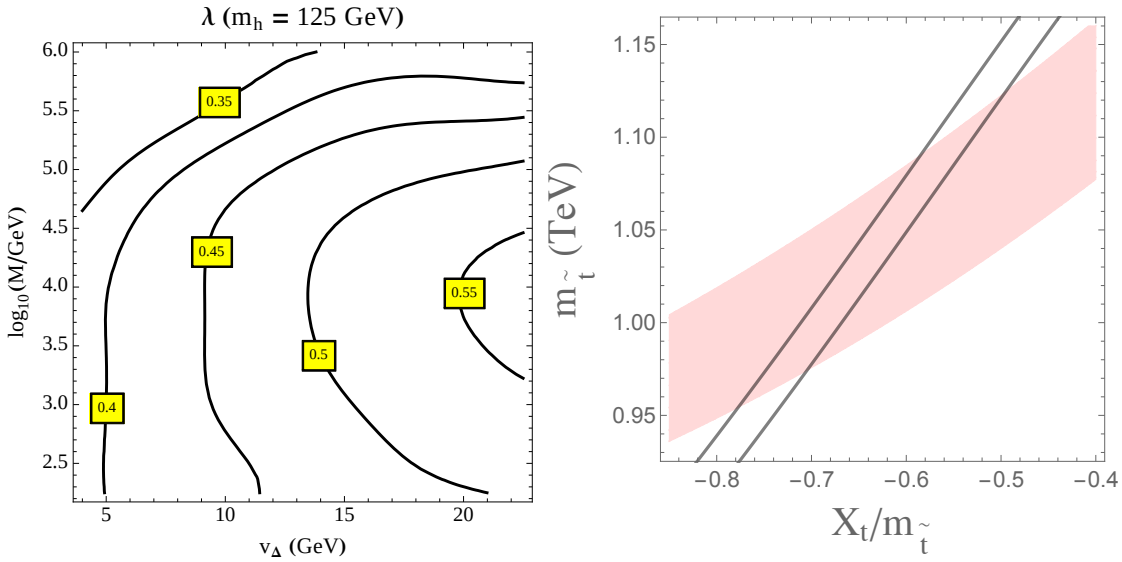

Figure 5.5: *Left: Contours of λ, defined at the high scale $\mathcal{M}$, reproducing the observed value of the Higgs mass $\sim$ 125 GeV for the $SU(2)_L \otimes SU(2)_R$ symmetric parameters in Eq. (5.10) and $m_{1/2} = 1.2$ TeV. Right: The solid black lines represent the region producing a Higgs mass of 125.5 ± 1.0 GeV in the $X_t/m_{\tilde{t}} - m_{\tilde{t}}$ plane, where $m_{\tilde{t}}$ is the physical mass of the lightest stop and $X_t \equiv A_t - \mu/\tan\beta$. The shaded pink band is the region allowed by constraints on the ρ parameter. We have fixed the parameters $\lambda = 0.45$, $\mathcal{M} = 65$ TeV, $m_{1/2} = 1.2$ TeV, $v_\Delta = 10$ GeV while the rest are given in (5.10), except we now allow $m_0 \in [500, 1000]$ GeV and $A_0 \in [-250, 500]$. We do not explicitly show the region favored by the MSSM since it arises only at much heavier stop masses ($m_{\tilde{t}} \gtrsim 6$ TeV [3, 47, 79, 80]).*

Smoking guns

The next observables we consider, and potential smoking guns of the model at the LHC, are the normalized couplings of the Higgs to gauge bosons and bottom quarks: r_{hWW}, r_{hZZ}, and r_{hbb}, where r_{hXX} is defined in Eq. (4.49). Of course the rotation matrix U plays a major role in the interaction of the Higgs h with the SM fields and the normalized couplings are given by

$$\begin{aligned}
r_{hWW} &= U_{11}\cos\beta\cos\theta + U_{12}\sin\beta\cos\theta \\
&\quad + \sqrt{2}U_{13}\cos\theta_1\cos\theta_0\sin\theta + 2U_{14}\sin\theta_0\sin\theta + \sqrt{2}U_{15}\sin\theta_1\cos\theta_0\sin\theta \\
r_{hZZ} &= U_{11}\cos\beta\cos\theta + U_{12}\sin\beta\cos\theta \\
&\quad + 2\sqrt{2}U_{13}\cos\theta_1\cos\theta_0\sin\theta + 2\sqrt{2}U_{15}\sin\theta_1\cos\theta_0\sin\theta \\
r_{huu} &= U_{12}\sin\beta\cos\theta \\
r_{hdd} &= U_{11}\cos\beta\cos\theta
\end{aligned} \tag{5.20}$$

where θ is defined in (4.32).

In the left panel of Figure 5.6, we show results for r_{hWW} (dark green dotted), r_{hZZ} (blue dashed), and r_{hbb} (black solid) in the $(v_\Delta, \mathcal{M})$ plane. Again we superimpose the region allowed by electroweak precision constraints (pink shaded region). In the SCTM the Higgs can have couplings to W and Z bosons larger than the ones predicted by the SM (see also Refs. [82, 83]), but

still well within current experimental bounds [84,85]. In particular, at large values of v_Δ, the two couplings can deviate from the SM prediction by as much as $(5-10)\%$ for our chosen parameter point. Such a deviation could possibly be measured at a high luminosity LHC [86–89]. This is in contrast to models with only additional Higgs doublets and singlets, which can only reduce the Higgs couplings to gauge bosons. It has also interesting implications for trying to extract the total width of the 125 GeV Higgs boson without making the theoretical assumption $r_{hWW}, r_{hZZ} \leq 1$ (see e.g. [90, 91]). We also see in Fig. 5.6 that, for this parameter point, the Higgs coupling to bottom quarks is only mildly modified with respect to the SM.

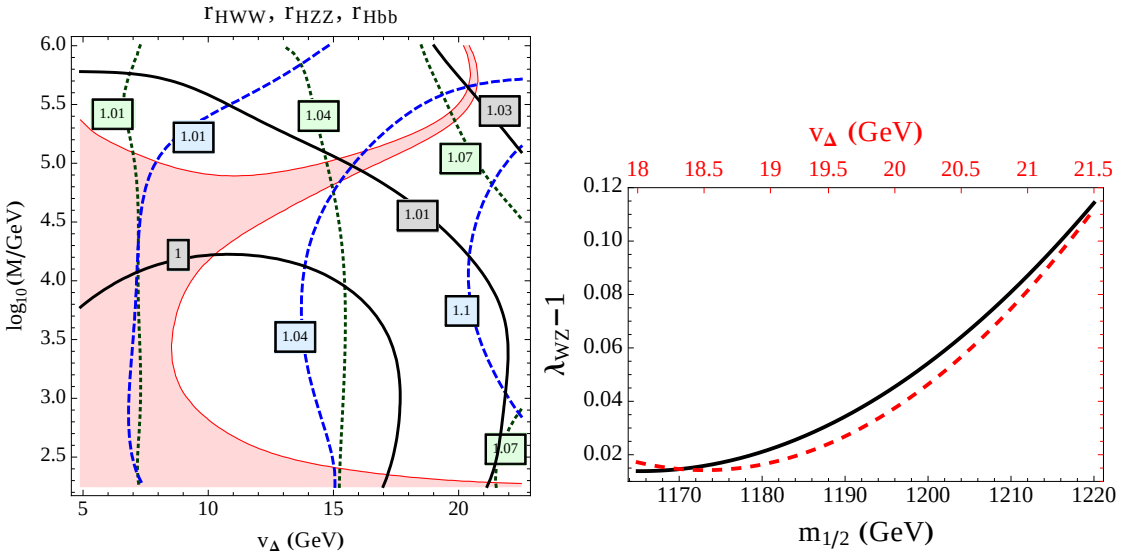

Figure 5.6: *Left: Contours of r_{hWW} (dark green dotted), r_{hZZ} (blue dashed), and r_{hbb} (black solid) in the $(v_\Delta, \mathcal{M})$ plane for the values of the parameters given in (5.10) and $m_{1/2} = 1.2$ TeV. Right: Deviation from the universal condition $\lambda_{WZ} = 1$ along the $2v_\phi^2 = v_\chi^2 + v_\psi^2$ direction (or $\tan\theta_0 = 1$, which provides $\Delta\rho = 0$) as a function of $m_{1/2}$ (black solid line) and v_Δ (red dashed line) for parameter values given in (5.10) and $\mathcal{M} = 850$ TeV.*

The breaking of 'universality'

We also examine the ratio of the normalized couplings $r_{hWW}/r_{hZZ} \equiv \lambda_{WZ}$ [84, 85] since it is a direct measure of the violation of custodial symmetry induced by the RGE running. In the SM and in the MSSM, custodial symmetry implies $\lambda_{WZ} = 1$, but in the SCTM it is possible to have deviations from this universal relation. In the right panel of Fig. 5.6, we show the quantity $\lambda_{WZ} - 1$ as a function of the gaugino mass $m_{1/2}$ and v_Δ along the $2v_\phi^2 = v_\chi^2 + v_\psi^2$ (i.e. $\tan\theta_0 = 1$ yielding $\Delta\rho = 0$) direction for parameter values given in Eq. (5.10) and $\mathcal{M} = 850$ TeV. Since in the SCTM the ratio λ_{WZ} is a function of all three vacuum angles $(\beta, \theta_0, \theta_1)$ it will be in general different from one, even in the direction $2v_\phi^2 = v_\chi^2 + v_\psi^2$, on which $\Delta\rho = 0$. At large values of v_Δ deviations from universality as large as $\sim (10-15)\%$ are achievable. This is well within present experimental constraints and potentially observable at a HL-LHC [86–89].

Other observables

Of course there are many additional Higgs observables that could be used to test the SCTM. Generically, the particle spectrum has several charged particles which can contribute to the $h\gamma\gamma$ decay width. These particles will also modify the $h \to 4\ell$ and $h \to 2\ell\gamma$ decays, which could be used to probe the underlying CP properties of the model [92–98].

Furthermore, the model will be tested by the direct searches for the additional scalars and fermions arising in the spectrum. Particularly interesting signatures are the decays of the doubly charged Higgs scalars to $W^{\pm}W^{\pm}$ [99–101] and the decay of the singly charged scalars to $W^{\pm}Z$, a decay found only in models with larger than doublet representations [69]. Additionally, in the SCTM the doubly charged Higgsino will decay to same sign W boson pairs plus missing energy. In particular, a doubly charged fermion with a mass near that of the doubly charged scalar would be a strong hint of the SCTM. We will further explore these possibilities in the next section where the spectrum of the model is computed in a few benchmark cases within a specific gauge mediation mechanism.

5.3 Gauge mediated supersymmetry breaking in the SCTM

In this section we explore the possibility of having a gauge mediated mechanism to break SUSY in the SCTM. The interest of this study is twofold: (i), it will provide a UV completion to the SCTM in the form of low-scale supersymmetry breaking (as required by ρ parameter constrains) and (ii), it will also be interesting from a gauge mediation perspective as GMSB models run into difficulties if they want to encompass the Higgs mass with a light superparticle spectrum. Let us now motivate this as if we where trying to build a model for low-scale supersymmetry breaking and see how the SCTM arises as a natural possibility.

Gauge mediation vs. the Higgs mass

Gauge mediated supersymmetry breaking is an elegant mechanism to transmit supersymmetry breaking from the hidden to the observable sector which solves the supersymmetric flavor problem (see Section 2.3). The supersymmetric flavor problem is just the realization that, depending on the mediation mechanism, the supersymmetric theory can introduce flavor violating interactions that could spoil its phenomenological viability. The problem is automatically solved by GMSB models, as the gauge interactions are flavor diagonal, provided that the scale of messengers is low enough so that the gravitational contributions to SUSY breaking can be neglected.

A main feature of GMSB in the MSSM is that the predicted value of the stop mixing parameter A_t is very small at the messenger scale $\mathcal{M}$ since it comes from two-loop diagrams. As a consequence, minimal models of GMSB require superheavy (> 5 TeV) stops to reproduce the experimental value of the Higgs mass (see Chapter 3 and Refs. [47, 79]), this fact reintroduces a little hierarchy problem with stops very far away from the LHC reach. Two options appear to tackle this problem in GMSB theories. One option is increasing the value of the radiative contributions to the Higgs mass, either by generating large values of the mixing parameter A_t, or by enlarging the MSSM with heavy vector-like fermions strongly coupled to the Higgs sector [102]. In particular, generating large values of A_t can be done by introducing direct messenger-MSSM superpotential couplings [103–112]. These models, dubbed extended GMSB, do not necessarily

lead to minimal flavor violation (MFV) and the flavor constraints require a special texture. The second option, without enlarging the SM gauge group, is increasing the value of the Higgs mass by means of a tree-level F-term from an extended MSSM Higgs sector.

As we already know from previous chapters, the MSSM extensions which can increase the Higgs mass by a tree-level F-term are the following: The singlet S and/or triplets with hypercharge $Y = (0, \pm 1)$, $\Sigma_{0,\pm 1}$. We can exclude the presence of the singlet, as it does not get any mass from GMSB unless we enlarge the gauge group such that S transforms as a non-trivial representation of the enlarged gauge group, or we consider an extended GMSB model with direct superpotential messenger-MSSM couplings [113], which could result again in flavor constraints. The only surviving possibility is then adding the triplets $\Sigma_{0,\pm 1}$, however introducing only Σ_0 or $\Sigma_{\pm 1}$ will spoil the $\rho = 1$ relationship unless v_Δ is small enough, which requires a large soft mass for the triplet. Since in GMSB the contribution to each mass is tied by the the gauge structure of the theory, it will be impossible for gauge mediation to generate large $SU(2)_L$ triplet masses while keeping the rest of the spectrum light. Therefore, trying to solve the $\rho = 1$ problem in this way would recreate a strong naturalness (little hierarchy) problem. The way out is tied to the SCTM, using the whole set $\Sigma_{0,\pm 1}$ and providing the theory with a global $SU(2)_L \otimes SU(2)_R$ symmetry spontaneously broken to the custodial $SU(2)_V$ after EW breaking.

We know that custodial symmetry is spoiled by radiative corrections proportional to the hypercharge and top Yukawa couplings and that the RGE running departs from the custodial symmetry conditions. As concluded in the last section (see Fig. 5.8), one can allow for some departure from the $\rho = 1$ custodial solution but not too much. This can be fulfilled in a GMSB mechanism provided that the messenger scale $\mathcal{M}$ is low enough, which is a natural condition in GMSB models, moreover, GMSB provides custodial boundary values to the Higgs sector, except for the contribution of the hypercharge coupling that will break explicitly custodial invariance. As we will see, this explicit breaking will not change the main features nor the phenomenology of the model. The model is then able to fit the ~ 125 GeV measurement without the need of super-heavy stops and generates large triplet VEV's that can participate in the EW breaking up to a $\sim 15\%$ order, as a byproduct, it will give rise to interesting phenomenology.

We are now going to define a non-minimal gauge mediated mechanism which will provide a soft spectrum for the SCTM consistent with all electroweak and LHC data, thus alleviating the tension between the Higgs mass, light stops and the supersymmetric flavor problem. Typical benchmark scenarios for this model are proposed and a study on their phenomenology is performed.

Gauge mediation in the SCTM

In the minimal realization of gauge mediation (MGM) the messenger fields transform under $\mathbf{r}$ and $\bar{\mathbf{r}}$ representations of $SU(5)$ and feel the breaking of supersymmetry through the superpotential, $W = \lambda^{ij} X \Phi_i \bar{\Phi}_j$, where X is an spurion field that parametrizes the breaking of supersymmetry in the secluded sector. As MGM provides a very rigid framework to encompass low energy phenomenology, we will consider a particular model of general gauge mediation (GGM) [114] where there is more flexibility to accommodate the supersymmetric mass spectrum of the SCTM. We will consider a model where messengers transform only under one of the SM gauge groups $SU(3) \otimes SU(2)_L \otimes U(1)_Y$ and will choose (non-exotic) representations which are contained in $SU(5)$. In particular, to transmit supersymmetry breaking to the observable sector, we choose

the messenger representations [9]

$$\Phi_8 = (\mathbf{8},\mathbf{1})_0, \quad \Phi_3 = (\mathbf{1},\mathbf{3})_0 \quad \text{and} \quad \left[\Phi_1 = (\mathbf{1},\mathbf{1})_1,\, \bar{\Phi}_1 = (\mathbf{1},\mathbf{1})_{-1}\right] . \tag{5.21}$$

According with GGM we will explore the more general case where the messengers have independent mass terms instead of getting all their mass from the spurion superfield. For simplicity, we also consider that the scalar component of X does not acquire a VEV [10], thus $\langle X\rangle = \theta^2 F$.

$$W = \left(\tilde{\lambda}_8^{ij} X + \mathcal{M}_8^{ij}\right)\Phi_{8i}\Phi_{8j} + \left(\tilde{\lambda}_3^{ij} X + \mathcal{M}_3^{ij}\right)\Phi_{3i}\Phi_{3j} + \left(\tilde{\lambda}_1^{ij} X + \mathcal{M}_1^{ij}\right)\bar{\Phi}_{1i}\Phi_{1j} . \tag{5.22}$$

We now impose an $O(n_8)\otimes O(n_3)\otimes O(n_1)$ global symmetry in the superpotential, where n_8, n_3 and n_1 are the of number of copies of each messenger respectively [11]. Due to this symmetry, the dot product is the only invariant that can be built, thus ensuring the diagonal form of $\tilde{\lambda}_A^{ij}$ ($\equiv \delta^{ij}\tilde{\lambda}_A$) and $\mathcal{M}_A^{ij}$ ($\equiv \delta^{ij}\mathcal{M}_A$) in the mass basis. Via messenger parity, this symmetry prevents dangerous one-loop contributions to the masses of sleptons [36, 116]. Moreover for simplicity we will consider a common messenger scale so that we will assume $\mathcal{M}_A \equiv \mathcal{M}$ ($A = 8, 3, 1$).

Within this setup and with $\Lambda_8 \equiv \tilde{\lambda}_8\Lambda$, $\Lambda_3 \equiv \tilde{\lambda}_3\Lambda$ and $\Lambda_1 \equiv \tilde{\lambda}_1\Lambda$ ($\Lambda \equiv F/\mathcal{M}$) the gaugino masses at the messenger scale are;

$$\begin{aligned} M_3 &= \frac{\alpha_3(\mathcal{M})}{4\pi} 3\, n_8\, g(\Lambda_8/\mathcal{M})\,\Lambda_8 , \\ M_2 &= \frac{\alpha_2(\mathcal{M})}{4\pi} 2\, n_3\, g(\Lambda_3/\mathcal{M})\,\Lambda_3 , \\ M_1 &= \frac{\alpha_1(\mathcal{M})}{4\pi} \frac{6}{5} n_1\, g(\Lambda_1/\mathcal{M})\,\Lambda_1 , \end{aligned} \tag{5.23}$$

where we are using $SU(5)$ normalization for the $U(1)$. For sfermions,

$$\begin{aligned} m_{\tilde{f}}^2 = 2\Bigg\{ & C_3^f \left(\frac{\alpha_3(\mathcal{M})}{4\pi}\right)^2 3\, n_8\, f(\Lambda_8/\mathcal{M})\,\Lambda_8^2 + C_2^f \left(\frac{\alpha_2(\mathcal{M})}{4\pi}\right)^2 2\, n_3\, f(\Lambda_3/\mathcal{M})\,\Lambda_3^2 \\ & + C_1^f \left(\frac{\alpha_1(\mathcal{M})}{4\pi}\right)^2 \frac{1}{2}\left(\frac{6}{5}\right)^2 n_1\, f(\Lambda_1/\mathcal{M})\,\Lambda_1^2 \Bigg\} . \end{aligned} \tag{5.24}$$

Where C_a^f is the quadratic Casimir of the sfermion $\tilde{f}$ [12]. The functions $g(x)$ and $f(x)$ come from two loop exact results and were first computed in Refs. [117, 118]

$$\begin{aligned} g(x) &= \frac{1}{x^2}\left\{(1+x)\log(1+x)\right\} + (x \to -x) , \\ f(x) &= \frac{1+x}{x^2}\left\{\log(1+x) - 2\mathrm{Li}_2\left(\frac{x}{1+x}\right) + \frac{1}{2}\mathrm{Li}_2\left(\frac{2x}{1+x}\right)\right\} + (x \to -x) . \end{aligned} \tag{5.25}$$

They become relevant for small values of $\mathcal{M}$, as it is our case.

As showed in Eqs. (5.23) and (5.24) an unusual messenger sector will modify the boundary conditions at the messenger scale with respect to the minimal scenario. For instance, assuming

[9] Φ_8 and Φ_3 where already used as messengers in [115].

[10] In fact we are assuming that $\langle X\rangle \ll \mathcal{M}_A$, $A = 8, 3, 1$.

[11] In the case of n_1, it is the number of pairs $(\Phi_1, \tilde{\Phi}_1)$ due to anomaly cancelation.

[12] It is equal to $\frac{N^2-1}{2N}$ for the fundamental $\mathbf{N}$ representation of $SU(N)$ and, in our notation $C_1^f = Y_f^2$, where Y_f is the SM hypercharge of $\tilde{f}$.

$g(x_i) \simeq 1$ we can write, at one loop, an RGE invariant gaugino mass relation which will be different from the minimal case $M_1(\mathcal{M})/\alpha_1(\mathcal{M}) = M_2(\mathcal{M})/\alpha_2(\mathcal{M}) = M_3(\mathcal{M})/\alpha_3(\mathcal{M})$. In particular

$$\frac{M_1(\mathcal{M})}{\alpha_1(\mathcal{M})} : \frac{M_2(\mathcal{M})}{\alpha_2(\mathcal{M})} : \frac{M_3(\mathcal{M})}{\alpha_3(\mathcal{M})} = \frac{6}{5} n_1 \tilde{\lambda}_1 : 2 n_3 \tilde{\lambda}_3 : 3 n_8 \tilde{\lambda}_8 \,. \tag{5.26}$$

This shows that, besides $\mathcal{M}$ and $\sqrt{F}$, the boundary conditions depend on the two sets of parameters: (n_8, n_3, n_1) and $(\tilde{\lambda}_8, \tilde{\lambda}_3, \tilde{\lambda}_1)$. As a result of this, once the superpotential parameters, $\mathcal{M}$ and $\sqrt{F}$ are fixed, the low energy features of the theory will be determined by our choice of n_A and $\tilde{\lambda}_A$.

Procedure

In a similar spirit to the one taken in the previous section (Fig. 5.1) we explore the model at the EW scale by means of the EOM's. Five neutral scalar fields will generate five minimization conditions that will fix five parameters. Since we are working on a top down approach, where we will run down from the messenger scale $\mathcal{M}$ to the EW scale, we will need to keep consistency between the boundary conditions and the EOM's. As the parameters m_3^2 and $B_{a,b}$ have their RGE's decoupled from the rest, we can consistently fix two of them, e.g. m_3^2 and B_a at the EW scale. The value of B_b at the weak scale will be consistently fixed in agreement with its EOM by choosing at the messenger scale $\mathcal{M}$ a custodial parameter B_Δ satisfying the boundary condition $B_a(\mathcal{M}) = B_b(\mathcal{M}) \equiv B_\Delta$ [13]. The other three EOM's self consistently determine the values of the custodial breaking angles $(\tan\beta, \tan\theta_0, \tan\theta_1)$ which are then a prediction of the EOM's for a given value of v_Δ.

Benchmark scenarios

Due to the strongest color contribution, if gluinos are heavier than stops they will raise the stop masses through the RGE running, making their boundary condition at the messenger scale unimportant. In a gauge mediated context we can generally say that, the heavier the gluino, the heavier the stop. Therefore we will fix the gluino mass at the electroweak scale as low as possible consistently with the most stringent bounds released by the LHC data [120], i.e. $M_3 = 1.5$ TeV at the low scale. For a fixed value of $\mathcal{M}$ (after considering the RGE running effects) this will fix the supersymmetry breaking parameter F.

We will choose a low value of $\mathcal{M}$ so that the custodial breaking by the RGE running is minimized. In fact loop corrections to the ρ parameter, that are related to the custodial breaking, are parametrized by $\tan\alpha_i - 1$, with $\alpha_i = \beta, \theta_0, \theta_1$. As explained in the previous section, because of the strong effect of the top quark Yukawa coupling, the running differentiates the two soft doublet masses from each other much more than the three triplet ones among themselves. This results in a much bigger vacuum misalignment in the doublet sector that is dictated by the amount of running (i.e. by the size of the messenger scale $\mathcal{M}$) and with little dependence on v_Δ. We are therefore left with a situation at the EW scale where $\tan\beta \neq 1$ and $(\tan\theta_0, \tan\theta_1 \sim 1)$ (right

[13] We expect the same physics responsible for generating the effective behaviour that we describe in this paper to produce the correct values of m_3^2 and B_Δ at the messenger scale $\mathcal{M}$. However, without proper identification of the UV dynamics, one faces a μ-B_μ like problem in the triplet sector as well. Both problems could be solved from a bottom up perspective by introducing direct $SU(2)_L \otimes SU(2)_R$ invariant superpotential couplings between the messengers and the Higgs fields (doublets and triplets) as it is done in more minimal scenarios [119].

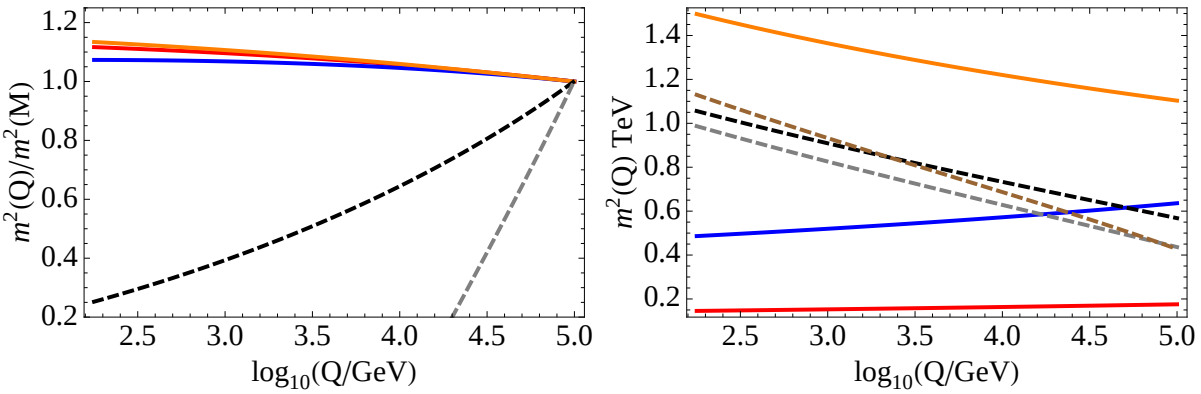

Figure 5.7: *Left: Running of* $(m^2_{H_1}, m^2_{H_2})$ *(dashed lines) and* $(m^2_{\Sigma_0}, m^2_{\Sigma_1}, m^2_{\Sigma_{-1}})$ *(solid lines), normalized to their values at the messenger scale for benchmark scenario #1. Right: Running of gaugino (solid:* M_3 *orange,* M_2 *blue and* M_1 *red) and squark (dashed:* $m_{\tilde{Q}}$ *black,* $m_{\tilde{t}}$ *gray and* $m_{\tilde{b}}$ *brown) mass parameters for benchmark scenario #1.*

panel of Fig. 5.8) and so the loop contributions to the ρ parameter coming from the doublet (MSSM) sector will be dominant. As small values of $\mathcal{M}$ will minimize the resulting value of $\tan\beta - 1$, we will fix the messenger scale to $\mathcal{M} = 100$ TeV. In particular, as we will see in the next section, this will translate into $\tan\beta = 1.38$ for the benchmark scenario #1 and $\tan\beta = 1.32$ for the benchmark scenario #2.

As a consequence of the low value of the messenger scale, the gravitino ($\tilde{G}$) is the LSP, as usual in gauge mediation [14]. Although the chosen value of $\mathcal{M}$ is also in agreement with cosmological bounds on the gravitino mass [121], the gravitino will not provide the observed relic density by itself, another component will have to enter to fill the DM relic density up to the current observed value. Also, the next to lightest supersymmetric particle (NLSP) will play an important role in the phenomenology of the model. In particular we will see that, in each of the benchmark scenarios studied below, because of the low values of $\sqrt{F}$ the decay $NLSP \to \tilde{G} + ...$ will be prompt, i.e. it will decay inside the detector but with no displaced vertex, and the experimental signature will be an imbalance in the final state momenta and a pair of photons or charged leptons.

Benchmark scenario #1: a Bino-like NLSP

For this scenario we will choose the number of messengers and their couplings with the hidden sector as

$$n_1 = 1,\ n_3 = 2,\ n_8 = 6 \quad \text{and} \quad \tilde{\lambda}_1 = 0.9,\ \tilde{\lambda}_3 = 0.5,\ \tilde{\lambda}_8 = 0.1\,. \tag{5.27}$$

Note in particular the hierarchy that we establish between $\tilde{\lambda}_8$ and $\tilde{\lambda}_1$. We do this to have stops as light as possible along with sleptons above their experimental bounds. In minimal versions of gauge mediation the contributions given by different gauge groups cannot be disentangled and it is difficult to accommodate light stops without too light sleptons.

As in the general example presented in the previous section the $SU(2)_L \otimes SU(2)_R$ invariant λ of the superpotential will be fixed at the messenger scale such that the correct Higgs mass is

[14] For the neutralino to be the LSP in this scenario, one would need to apply to the SCTM a mechanism similar as that of Ref. [35].

reproduced [15],

$$\lambda(M) = 0.68 \tag{5.28}$$

We also fix the superpotential parameter $\lambda_3 = 0.35$, although it will have little effect on the low energy spectrum. The boundary conditions at the messenger scale of μ (and μ_Δ) are adjusted to make sure that the vacuum is close enough to the direction $\tan\theta_0 = 1$, and ρ falls within the allowed T parameter band. In this case we choose both parameters μ and μ_Δ equal at the messenger scale

$$\mu(\mathcal{M}) = \mu_\Delta(\mathcal{M}) = 1.3 \text{ TeV}\,. \tag{5.29}$$

Of course, the values that will actually fix the Higgs mass are at the EW scale. λ and μ_Δ are superpotential parameters that we assume to be generated in an $SU(2)_L \otimes SU(2)_R$ invariant fashion. We show how the running will split these supersymmetric parameters and their EW scale values in Fig. 5.8.

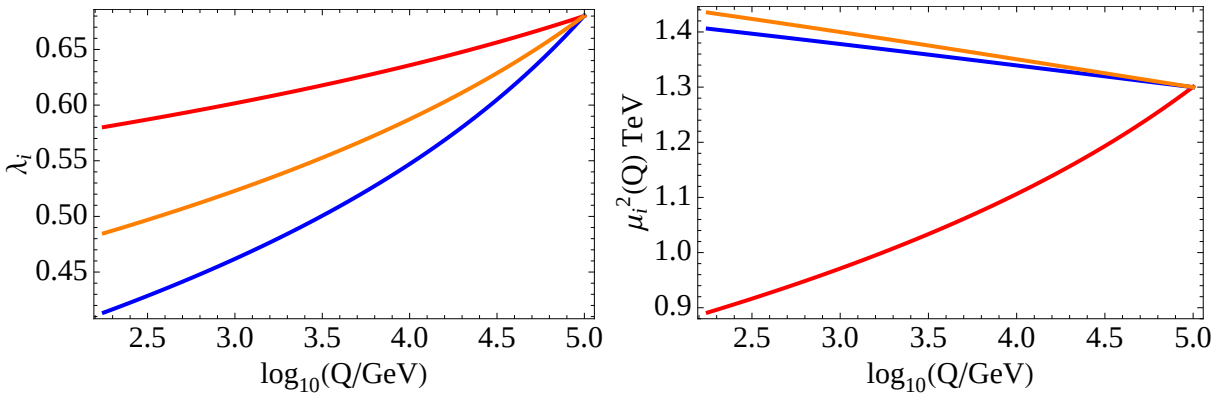

Figure 5.8: *Left: For benchmark scenario #1, running of λ_a (red), λ_c (orange) and λ_b (blue). Right: For benchmark scenario #1, running of μ (red), μ_a (blue) and μ_b (orange).*

In this scenario the NLSP is a bino-like neutralino that will mainly decay to the gravitino through the following process $\chi_1^0 \to \gamma\tilde{G}$. If we know its mass and the supersymmetry breaking scale $\sqrt{F}$, we can calculate the average distance travelled in the LAB frame by an NLSP produced with energy E before it decays [29],

$$L_{\chi_1^0}^{NLSP} = \frac{1}{\kappa_\gamma}\left(\frac{100\,\text{GeV}}{m_{\chi_1^0}}\right)^5\left(\frac{\sqrt{F}}{100\,\text{TeV}}\right)^4\sqrt{\frac{E^2}{m^2}-1}\cdot 10^{-2}\,\text{cm}, \tag{5.30}$$

with $\kappa_\gamma = |N_{11}\cos\theta_W + N_{12}\sin\theta_W|^2$, N_{11} and N_{12} being the projections of χ_1^0 to the Bino and Wino respectively (in our case $N_{11} \simeq 1$ and $N_{12} \simeq 0$). In this scenario $\sqrt{F} = 94$ TeV and $m_{\chi_1^0} = 143$ GeV, this translates in an average distance of flight well below the detector precision (~ 0.1 cm) even if the particle is boosted because it is produced with very high energy.

[15] To fit the 125 GeV value we include the dominant loop contributions to the Higgs mass [44].

Benchmark scenario #2: $\tilde{\tau}_R$ as the NLSP

Now we present an example of a spectrum where the NLSP is $\tilde{\tau}_R$. We also choose $\mathcal{M} = 100$ TeV and a similar hierarchy between $\tilde{\lambda}$'s, the main difference with #1 will come in the larger number of messengers,

$$n_1 = 10,\, n_3 = 6,\, n_8 = 5 \quad \text{and} \quad \tilde{\lambda}_1 = 0.9,\, \tilde{\lambda}_3 = 0.5,\, \tilde{\lambda}_8 = 0.2\,. \tag{5.31}$$

Custodial values in the superpotential are also asjusted at the messenger scale to get the correct Higgs mass and $\rho = 1$ at the electroweak scale,

$$\lambda(\mathcal{M}) = 0.78,\, \lambda_3(\mathcal{M}) = 0.35 \quad \text{and} \quad \mu(\mathcal{M}) = \mu_\Delta(\mathcal{M}) = 1.5 \ \text{TeV}. \tag{5.32}$$

The $\tilde{\tau}$ will decay into the gravitino through $\tilde{\tau} \to \tau \tilde{G}$ and we can get its average flight distance from (5.30) with $\kappa_\gamma = 1$. In this case $\sqrt{F} = 73$ TeV and $m_{\tilde{\tau}} = 343$ GeV and one finds that $L^{NLSP}_{\#\,2} < L^{NLSP}_{\#\,1}$.

Phenomenology of the Gauge Mediated SCTM

Figs. 5.9 and 5.10 show the spectrum in the two previous benchmark scenarios with light stops (in both cases below 1 TeV) [16], the correct Higgs mass and a non negligible contribution of the triplet sector to EWSB. In particular, in both examples $v_\Delta = 20$ GeV (v_H is set by the relation (4.10)), which corresponds to about a 10% of the W and Z masses given by the triplets.

In both scenarios the gravitino cosmology is very simple as $m_{3/2} \sim \mathcal{O}(\text{few})$ eV and the gravitinos are stable particles which do not overclose the Universe, $\Omega_{3/2}h^2 \simeq 10^{-3}$. We now look at phenomenological features and possible smoking gun signatures for the present model and in particular for the two benchmark scenarios.

Neutralinos and Charginos

We first analyze the fermionic sector of the theory. The addition of three triplet chiral superfields will enhance the number of neutralinos and charginos. Three extra neutralinos, two new charginos and a doubly charged chargino will be present in the spectrum. The fermion spectrum comes from the neutralino and chargino mass matrices, which are derived from the mass Lagrangian

$$\mathcal{L}_{1/2} = -\frac{\partial^2 W}{\partial\phi_i\phi_j}\psi_i\psi_j - \sqrt{2}g^a(\phi T^a\psi)\lambda^a + \mathcal{L}_{\text{soft}-\text{fermions}}\,, \tag{5.33}$$

where ϕ are the Higgs scalars, ψ their fermionic superpartners (higgsinos and tripletinos) and λ^a the gauginos corresponding to each gauge group, g^a. For neutralinos we have then

$$\mathcal{L}^0_{1/2} = -\frac{1}{2}\psi^0_i\mathcal{M}^{0\,ij}_{1/2}\,\psi^0_j + h.c.\,, \tag{5.34}$$

where $\psi^0_i = \left(\widetilde{B}^0, \widetilde{W}^3, \widetilde{H}^0_1, \widetilde{H}^0_2, \widetilde{\phi}^0, \widetilde{\chi}^0, \widetilde{\psi}^0\right)$. For charginos the mass Lagragian is as in Eq. (4.42) but with a mass matrix different from Eq. (4.43) since the parameters are not $SU(2)_L \otimes SU(2)_R$ invariant anymore. Finally, the doubly charged chargino mass matrix is given by

$$\mathcal{L}^\pm_{1/2} = -\frac{1}{2}\begin{pmatrix} \psi^{++} & \chi^{--} \end{pmatrix}\begin{pmatrix} 0 & \mathcal{M}^{\pm T}_{1/2} \\ \mathcal{M}^\pm_{1/2} & 0 \end{pmatrix}\begin{pmatrix} \psi^{++} \\ \chi^{--} \end{pmatrix} + h.c. \tag{5.35}$$

[16] The physical stop masses are derived as in the previous section by means of Eqs. (5.18) and (5.19).

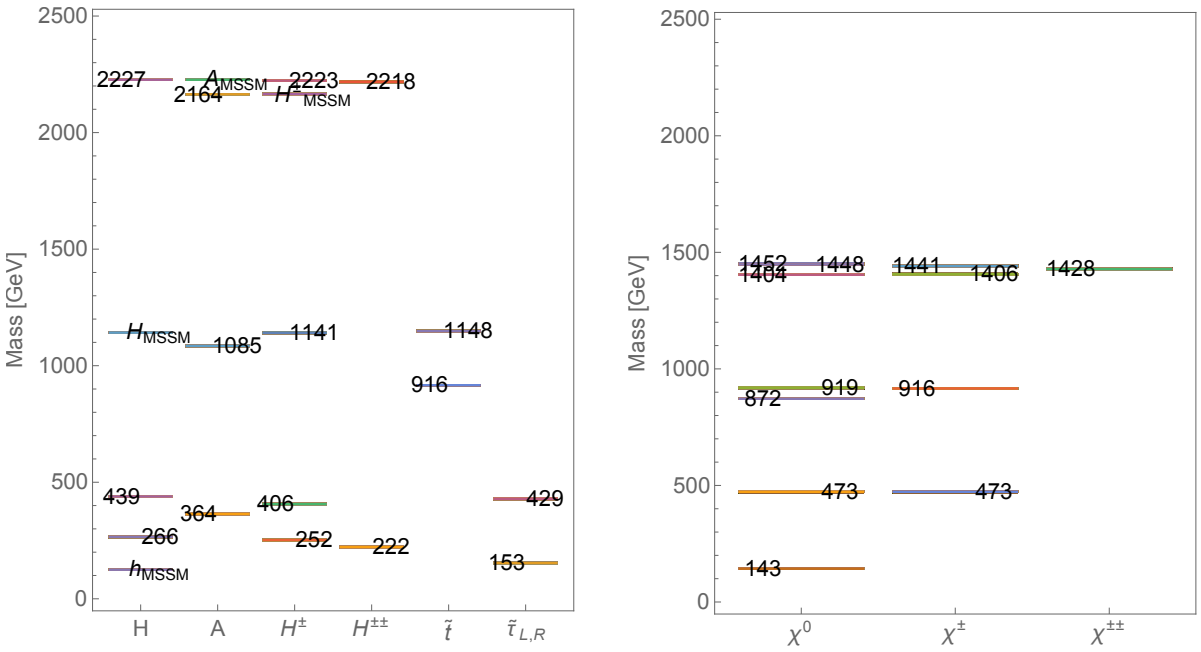

Figure 5.9: *Left: Scalar spectrum for scenario #1. MSSM-like scalars are quoted as so. Right: Fermion spectrum for scenario #1.*

Figs. 5.9 and 5.10 show the different mass values for scenarios #1 and #2, respectively. As we can see there is a clear hierarchy between states which in part will be determined by the relation (5.26). In Fig. 5.9 this relation is,

$$\frac{M_1}{\alpha_1} : \frac{M_2}{\alpha_2} : \frac{M_3}{\alpha_3} = 1.08 : 2 : 1.8 \quad \text{[scenario \#1]}. \tag{5.36}$$

The lightest fermion is the NLSP, a Bino-like neutralino. The next neutralino and first chargino correspond to a Wino-like multiplet, since M_2 at the low scale is around $450 - 500$ GeV (right panel of Fig. 5.8). In this scenario $\tilde{\chi}_2^0$ and the lightest chargino $\tilde{\chi}_1^{\pm}$ are (quasi) degenerate in mass. The ATLAS supersymmetric searches [122] on $\tilde{\chi}_2^0\tilde{\chi}_1^{\pm}$ production followed by W and Z decays, combined with three-lepton searches, exclude a mass region for degenerate $\tilde{\chi}_2^0$ and $\tilde{\chi}_1^{\pm}$ between 100 GeV and 410 GeV. These bounds are satisfied since the mass of $\tilde{\chi}_2^0$ and $\tilde{\chi}_1^{\pm}$ is ~ 473 GeV. The heavier states are doublet-like Higgsinos and tripletinos.

In scenario #2 the gaugino mass relation is

$$\frac{M_1}{\alpha_1} : \frac{M_2}{\alpha_2} : \frac{M_3}{\alpha_3} = 10.8 : 6 : 3 \quad \text{[scenario \#2]}\,, \tag{5.37}$$

this different hierachy is explicit in Fig. 5.10, with a fermion spectrum heavier than in the previous case, also satisfying all present experimental bounds.

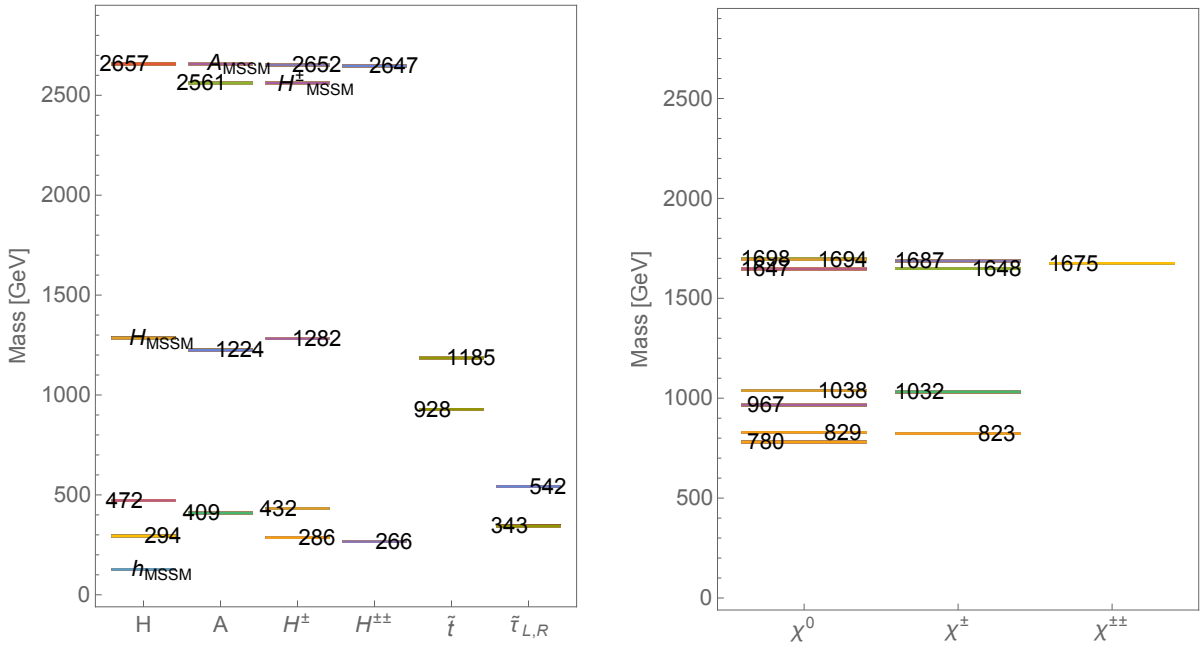

Figure 5.10: *Left: Scalar spectrum for scenario #2. MSSM-like scalars are quoted as so. Right: Fermion spectrum for scenario #2.).*

Sleptons

ATLAS and CMS searches place strong bounds on slepton masses [122,123] [17]. These will change depending on whether $\tilde{\tau}_R$ is the NLSP or not. If $\tilde{\tau}_R$ is the NLSP, LHC searches give $m_{\tilde{\tau}_R} \gtrsim 250$ GeV and $m_{\tilde{\tau}_L} \gtrsim 300$ GeV. Bounds are relaxed if we have a neutralino NLSP to which the $\tilde{\tau}_R$ decays. In this case, from the exclusion regions in the $(m_{\tilde{\chi}_1^0}, m_{\tilde{\tau}_R})$ plane from decays $\tilde{\tau}_R \to \tau\tilde{\chi}_1^0$, it turns out that for $m_{\tilde{\chi}_1^0} \gtrsim 100$ GeV there is no LHC constraint on $m_{\tilde{\tau}_R}$, so that only the LEP bound $m_{\tilde{\tau}_R} \gtrsim 100$ GeV survives. The latter case applies to our benchmark scenario #1 where $m_{\tilde{\chi}_1^0} > 100$ GeV. In the benchmark scenario #2 we explore the former case and we can see from the mass spectrum that $m_{\tilde{\tau}_R}$ and $m_{\tilde{\tau}_L}$ are above their experimental lower bounds.

Higgs scalars

There are a total of five neutral *CP*-even, 4 *CP*-odd, 5 singly charged, and two doubly charged massive Higgs scalar fields in this model. We will calculate the scalar spectrum by diagonalizing

[17] We consider the physical masses of $\tilde{\tau}_{L,R}$ to be the RGE parameters $m_{\tilde{\tau}_L}$ and $m_{\tilde{\tau}_R}$, neglecting any possible mixing between them. This is a good approximation since $y_\tau \ll y_t$.

the corresponding mass matrices, e.g. for real neutral scalars Eq. (5.12), but also

$$(\mathcal{M}^2_{\text{Ps}})_{ij} = \frac{1}{2}\frac{\partial^2 V}{\partial\varphi_i^I \partial\varphi_j^I}\,, \quad (\mathcal{M}^2_{\text{Ch}})_{ij} = \frac{\partial^2 V}{\partial\varphi_i^\pm \partial\varphi_j^{\pm *}} \quad \text{and} \quad (\mathcal{M}^2_{\text{D.Ch}})_{ij} = \frac{\partial^2 V}{\partial\varphi_i^{\pm\pm} \partial\varphi_j^{\pm\pm *}}\,, \tag{5.38}$$

where,

$$\begin{aligned} \varphi_i^I &= (H_1^{0\,I}, H_2^{0\,I}, \psi^{0\,I}, \phi^{0\,I}, \chi^{0\,I})\,, \\ \varphi_i^\pm &= (H_1^-, \chi^-, \phi^-, H_2^+, \psi^+, \phi^+)\,, \\ \text{and} \quad \varphi_i^{\pm\pm} &= (\chi^{--}, \psi^{++})\,. \end{aligned} \tag{5.39}$$

With the help of a smooth limit to the MSSM scalar sector when $v_\Delta \to 0$, we can identify the MSSM-like states as those which remain light in that limit (see Section 4.4). Due to the small mixing angles between doublets and triplets, the MSSM-like scalars will have a larger doublet component whereas the rest will be mainly composed of triplets.

Note that the doublet sector is in its decoupling regime and in both cases (Figs. 5.9 and 5.10) there are some light triplet-like scalars, specifically a neutral (H), a charged ($H^\pm$) and a doubly charged ($H^{\pm\pm}$) one. From Chapter 4 we know that, in the custodial case, scalars align themselves under degenerate $SU(2)_V$ multiplets and in particular these light triplet-like scalars correspond to F_S, the $SU(2)_V$ fiveplet that for large enough v_Δ is the lightest triplet-like multiplet, just above the Higgs-like custodial singlet (see Fig. 4.4 in Sec. 4.4). Of course, since $SU(2)_V$ does not hold anymore, the multiplet is not degenerate in mass, thus the mass splitting between H, $H^\pm$ and $H^{\pm\pm}$ that we see in Figs. 5.9 and 5.10.

Probing these new triplet-sector states is challenging since the new $SU(2)_L$ triplets do not couple to matter at tree level. For the neutral ones, searches for fermiophobic Higgses constrain their masses to be roughly above 194 GeV [124]. Moreover, the main production process for these states is vector boson fusion and the coupling between a Higgs like scalar and two vector bosons is proportional to its VEV, which for the triplet like states will be v_Δ, around an order of magnitude smaller than v. Due to this, the production cross section will then be smaller than the production of doublet-like scalars and the bound on triplet-like neutral states can be significantly relaxed. In Chapter 8 we perform an analysis that enables us to derive bounds which are independent of the triplet VEV, hence, much more robust. Although fermiophobic neutral scalars do appear in this model, they are not an exclusive feature of triplet Higgs sectors and cannot be considered as a smoking gun of the model. Nevertheless the model features a few characteristic signatures:

- The first one is the appearance of light charged scalars with the coupling $H^\pm W^\mp Z$ and decay channel $H^\pm \to W^\pm Z$, which is forbidden for charged Higgses coming from doublet representations. This possibility has been explored in [125]. Through the search of $H^\pm \to W^\pm Z$, and in the context of the non-supersymmetric GM model, ATLAS is able to put bounds on the mass of the triplet-like $H^\pm$. Here we can do a similar consideration to the one we did in searches of fermiophobic neutral scalars. The width of $H^\pm$ is proportional to the squared of $\sin\theta = 2\sqrt{2}v_\Delta/v$, a factor which parametrizes the amount of mass given by triplets to the W and the Z. The experimental bounds grow stronger as $\sin\theta \to 1$ and disappear for $\sin\theta < 0.5$. In our model v_Δ is small compared to v so $\sin\theta$ is at most 0.35 and the bounds do not apply. The triplet-like nature that is responsible for this suppression in the couplings is explicitly shown in Figure 5.11.

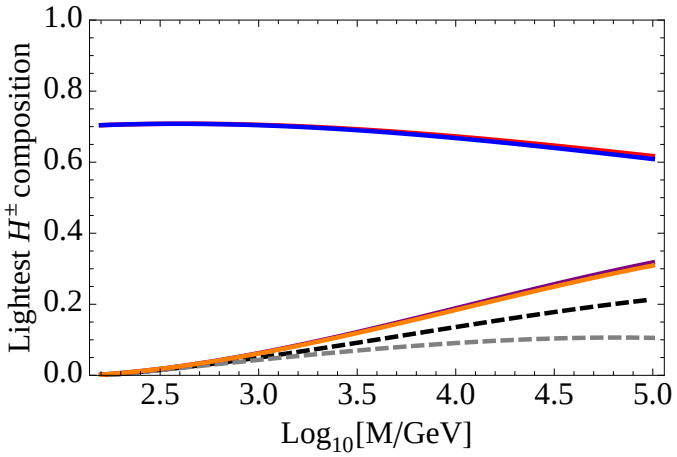

Figure 5.11: *Plot that shows the composition of the lightest $H^{\pm}$ state for points computed with different values of the messenger mass scale, $\mathcal{M}$. Thick lines correspond to components coming from the triplet sector and dashed ones are components of the doublet sector. The lightest $H^{\pm}$ will be dominantly triplet like even including the custodial breaking caused by the running, this means that its couplings to gauge bosons will be weighted by the factor $\sim v_{\Delta}/v$. The other possible smoking gun of the model, the doubly charged state $H^{\pm\pm}$ will be totally triplet as there is no doubly charged component coming from the doublet sector.*

- The second one is a light doubly charged scalar. Since it does not couple to matter at tree level its only decay mode is $H^{\pm\pm} \to W^{\pm}W^{\pm}$. In [101] this possibility is studied and bounds on doubly charged scalars are given by looking at possible $H^{\pm\pm} \to W^{\pm}W^{\pm}$ processes. The authors find that with the current LHC data $m_{H^{\pm\pm}} \gtrsim 96$ GeV, a bound obviously satisfied by our benchmark scenarios.

Finally, there is also a light pseudoscalar in the spectrum. These are mostly constrained by flavor measurements and electroweak precision observables in the two Higgs doublet model [126] and require $m_A \gtrsim 300$ GeV. However, these bounds rely on the fact that the pseudoscalar has to decay primarily on $b\bar{b}$ and $\tau\bar{\tau}$ which happens only when $\tan\beta \gg 1$. For our model $\tan\beta \sim 1$ at every point of the parameter space so the experimental constraints are relaxed.

Higgs couplings

We now calculate the normalized couplings of the Higgs to vector bosons and fermions, Eq. (5.20), in the two benchmark scenarios to find that they agree with what was originally predicted in the more general universal models (Fig. 5.6). We also look at the loop induced coupling $r_{\gamma\gamma}$ that will contribute to the $h \to \gamma\gamma$ rate [18]. We end up by computing the predicted signal strength μ_{hXX}

[18]The formula for $r_{h\gamma\gamma}$ is similar to what is given in Eq. (4.51), however, in the non custodial situation the projections from gauge eigenstates to the Higgs mass eigenstate cannot be computed analytically and we have,

$$\left[A_1(\tau_W) + \frac{4}{3}A_{1/2}(\tau_t)\right] r_{\mathcal{H}\gamma\gamma} = A_1(\tau_W) r_{\mathcal{H}WW} + \frac{4}{3}A_{1/2}(\tau_t) r_{\mathcal{H}uu} \tag{5.40}$$
$$+ \frac{v}{\sqrt{2}}\left\{U_{11}\frac{\partial f}{\partial H_1^0} + U_{12}\frac{\partial f}{\partial H_2^0} + U_{13}\frac{\partial f}{\partial \psi^0} + U_{14}\frac{\partial f}{\partial \phi^0} + U_{15}\frac{\partial f}{\partial \chi^0}\right\}.$$

of the decay channel $h \to XX$, with $X = V, f, \gamma$. Results for the two benchmark scenarios are presented in Tab. 5.3.

Scenario #1	WW	ZZ	$b\bar{b}$	$t\bar{t}$	$\gamma\gamma$
r_{hXX}	1.05	1.04	1.01	1.01	1.22
$\mu_{hXX}^{(gF)}, \mu_{hXX}^{(htt)}$	1.07	1.05	1	0.99	1.45
$\mu_{hXX}^{(WF)}, \mu_{hXX}^{(Wh)}$	1.16	1.14	1.08	1.07	1.58
$\mu_{hXX}^{(ZF)}, \mu_{hXX}^{(Zh)}$	1.14	1.11	1.06	1.05	1.54
Scenario #2	WW	ZZ	$b\bar{b}$	$t\bar{t}$	$\gamma\gamma$
r_{hXX}	1.05	1.04	1.01	1.01	1.18
$\mu_{hXX}^{(gF)}, \mu_{hXX}^{(htt)}$	1.07	1.06	0.99	0.95	1.35
$\mu_{hXX}^{(WF)}, \mu_{hXX}^{(Wh)}$	1.16	1.15	1.08	1.05	1.46
$\mu_{hXX}^{(ZF)}, \mu_{hXX}^{(Zh)}$	1.15	1.14	1.07	1.03	1.45

Table 5.1: *Top: Higgs couplings and signal strengths for scenario #1. Bottom: Higgs couplings and signal strengths for scenario #2.*

From Tab. 5.3 we see that the benchmark points are in agreement with the ATLAS current measurements [127] within the present uncertainties. The Higgs is a doublet-like state and therefore its couplings to vector bosons and fermions will not be greatly modified since the rest of the doublet-like spectrum is heavy enough. However, because custodial invariance is broken at the electroweak scale by the RGE running, it turns out that there is a corresponding breaking of universality as the parameter $\lambda_{WZ} = r_{WW}/r_{ZZ}$ departs from one. In particular as we can see from Tab. 5.3, $\lambda_{WZ} - 1 \simeq 1\%$ for the benchmark scenario #1 and $\lambda_{WZ} - 1 \simeq 3\%$ for the benchmark scenario #2. As emphasized in Section 5.2 this breaking is one of the possible smoking guns of our model (left panel of Fig. 5.6).

As the precision in the measurements of the Higgs properties increases, Higgs couplings can offer one of the most promising avenues to probe this model, in particular through the $r_{h\gamma\gamma}$ coupling which is loop induced and can have large modifications. New charged triplet-like light scalar states like $H^{\pm}$ or $H^{\pm\pm}$ are present and will modify the coupling by circulating along the loop. The lighter these particles are, the greater their effect will be in $r_{h\gamma\gamma}$ and since the masses of triplet-like states scale with v_Δ, $h \to \gamma\gamma$ will soon put bounds on v_Δ. In order to illustrate this point we show in Fig. 5.12 a scenario with the same values of the parameters as the benchmark scenario #1, but with $v_\Delta = 10$ GeV. In this case the scalar spectrum is heavier and the contributions to $r_{h\gamma\gamma}$ are smaller [19].

5.4 Discussion: General features of the SCTM

During this chapter we explored how we expect a 'realistic' realization of the SCTM to work (Fig. 5.1), we scanned the departure from custodial invariance and explored what are the consequences for phenomenology in this consistent picture.

[19] The presence of light charginos could also modify $r_{h\gamma\gamma}$. Note however that in the cases under study $\mu_{a,b}$ is large and no beyond the MSSM light charginos appear in the spectrum.

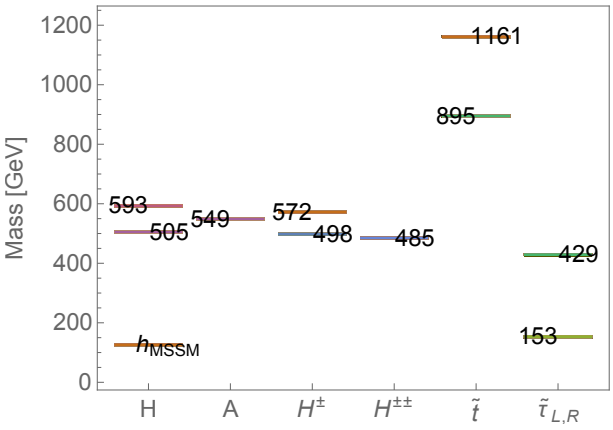

	WW	ZZ	$b\bar{b}$	$t\bar{t}$	$\gamma\gamma$
r_{hXX}	1.02	1.02	1	1	1.05
$\mu_{hXX}^{(gF)}, \mu_{hXX}^{(htt)}$	1.03	1.03	0.98	0.98	1.1
$\mu_{hXX}^{(WF)}, \mu_{hXX}^{(Wh)}$	1.07	1.08	1.03	1.03	1.15
$\mu_{hXX}^{(ZF)}, \mu_{hXX}^{(Zh)}$	1.08	1.08	1.03	1.03	1.15

Figure 5.12: *Left: Scalar spectrum of the benchmark scenario #1 with $v_\Delta = 10$ GeV. λ, μ and μ_Δ are again adjusted at the messenger scale so the correct Higgs mass is reproduced and $\rho = 1$. Other scalar states are above* 1.3 *TeV. Right: Higgs couplings and signal strengths with $v_\Delta = 10$ GeV.*

We started by arguing that in the SCTM, the scale at which $SU(2)_L \otimes SU(2)_R$ holds is most naturally identified with the messenger scale $\mathcal{M}$, at which supersymmetry breaking is transmitted to the observable sector. This leads to a connection between the experimentally measured value of ρ and the supersymmetry breaking scale. With this identification, it is shown how once the $SU(2)_L \otimes SU(2)_R$ boundary conditions are specified at the scale $\mathcal{M}$, then for a given triplet VEV v_Δ, the tree-level value of ρ can be predicted through renormalization group evolution (Appendix B.2). By utilizing an extra VEV direction (Appendix A.1), which itself is a consequence of supersymmetry and anomaly cancellation, the scale $\mathcal{M}$ at which $SU(2)_L \otimes SU(2)_R$ invariance holds can be significantly higher than the electroweak scale. In particular, we have found that scales $\mathcal{M}$ well above 100 TeV and triplet contributions to EWSB as large as 15% can easily be accommodated with ρ within the T-parameter constrains, this is shown in the left pannel of Fig. 5.3. At the same time we have checked that the 'realistic' SCTM can also give large tree-level and one-loop contributions to the Higgs mass as it does in the fully custodial picture. This allows to reproduce the measured Higgs mass even with small trilinear terms and top squarks with masses below 1 TeV.

As a byproduct of this analysis we have found a way to reconcile the Higgs mass measurement with low-scale supersymmetry breaking in the context of gauge mediation. We have proposed a particular model of general gauge mediation characterized by three species of messengers transforming as non-exotic representations under the SM gauge group, Eq. (5.21), with supersymmetric masses and Yukawa couplings to the spurion field breaking supersymmetry in the hidden sector, Eq. (5.22). In particular we have studied two benchmark scenarios consistent with all present experimental bounds, with the lightest neutralino (Bino-like) (Fig. 5.9) and right-handed stau (Fig. 5.10) as NLSP, respectively. For both scenarios the decay of the NLSP is prompt (inside the detector but with no displaced vertex).

We now enumerate a number of characteristic features of the 'realistic' SCTM, some of them particular to the SCTM embedded in gauge mediation:

- The first distinct feature is of course (as we already mentioned) that we can reproduce the Higgs mass with light stops (~ 1 TeV) while in the MSSM or in particular, minimal gauge mediation, values of the stops mass $\gtrsim 5$ TeV are required (Chapter 3).

- There is an extended fermiophobic triplet Higgs sector, absent from the usual supersymmetric extensions of the Standard Model, whose neutral components can acquire a sizeable VEV v_Δ (Fig. 4.1).

- The triplet VEV's can contribute with a non negligible amount to the mechanism of electroweak breaking. There is a direct relation between a sizable v_Δ and light triplet-like states (Fig. 4.4), in agreement with the upper bounds derived in [128]. This is a very interesting fact that will be explored by LHC13, as well as the next generation of colliders.

- There is a rich phenomenology by new singly ($H^\pm$) and doubly charged ($H^{\pm\pm}$) scalars which, if light enough, can contribute sizeably in loops to $r_{\gamma\gamma}$ (Table 5.3 and Figure 5.12). The couplings $H^\pm W^\mp Z$ and $H^{\pm\pm} W^\mp W^\mp$ are proportional to v_Δ and can thus provide unique signatures for models with extended Higgs sectors contributing to EWSB.

- From looking at the spectrums of Figures 5.9 and 5.10 we can see that, although exact custodial ordering is lost due to the RGE running, there is some remnant degeneracy. In particular the $SU(2)_V$ fiveplet F_S, Eq. (4.37), will be responsible for the appearance of a neutral, a singly and a doubly charged state close in mass as the lightest scalars in the spectrum (just above the light Higgs). Also, the lightest pseudoscalar and the next to lightest singly charged state will correspond to the triplet A, Eq. (4.33).

- One can measure the amount of custodial breaking by the departure of the universality parameter $\lambda_{WZ} \equiv r_{WW}/r_{ZZ}$ from its custodial value $\lambda_{WZ} = 1$ (Figure 5.6 and Table 5.3).

- The typical pattern for the values of M_a/α_a is strongly spoiled with respect to minimal gauge mediation. Also the sfermion spectrum is completely different from that of typical MGM, Eq. (5.26).

Let us end this chapter by making the remark that although we have constructed generic scenarios consistent with all experimental bounds, the constructions are by no means unique. Any of those scenarios should be contrasted with future experimental data, in order to find exclusion regions or some positive signatures which could unveil the true nature of the SCTM.

6

DM phenomenology with custodial triplets

As explained in the Section 2.6 of Chapter 2, supersymmetry also provides a nice solution to the dark matter problem. If R parity is assumed the lightest supersymmetric particle is stable and, provided that it is neutral, it may behave as a good DM candidate. However, not all dark matter candidates yield the correct relic abundance, only specific regions of the parameter space will allow the lightest neutralino to freeze out to the observed relic abundance and in the MSSM these regions are getting heavily constrained by experimental searches for DM. In this chapter we focus on the dark matter properties of the neutralino sector of the SCTM which, besides the interesting features described in the previous chapters, is able to generate neutralino phenomenology worth being studied. Moreover, a (nearly) custodial potential is interesting from a direct detection standpoint: The coupling of the Z to the neutralinos vanishes at tree level in the custodial limit of the MSSM ($\tan\beta = 1$), leading to blind spots in the spin-dependent dark matter searches [129], a property that will be maintained by a custodially symmetric extended Higgs sector.

We start the Chapter by summarizing the status of neutralino dark matter as of today (Sec. 6.1). We then explore the DM properties of the SCTM by means of a phenomenological approach that parametrizes the custodial breaking while retaining some of the calculability of the $SU(2)_V$ invariant situation (Sec. 6.2). From our study we find that there are large regions of parameter space where dark matter annihilation in the early Universe occurs through the new triplet states, we discuss these results and the consequences for direct and indirect detection in detail in Section 6.3. We end up making a summary in Section 6.4.

6.1 The status of neutralino DM

If the mass parameters of the electroweakinos are well separated, mixing can be neglected and the LSP can be a pure interaction eigenstate. If that is the case the pure bino does not annihilate enough in the early Universe, while both the wino and higgsino annihilate easily and need a mass near or above a TeV in order to freeze out with the correct relic abundance. If their masses are lighter than this, the pure wino or higgsino leave too little dark matter [1] and as $SU(2)_L$ triplets, the tripletinos should behave similarly to the wino in this regard.

To have neutralino dark matter lighter than a TeV and freeze out to the observed relic abundance, the LSP must have a large bino component, and there must be a process which helps

[1] Actually, the pure wino may already be excluded by astrophysical gamma ray searches and after constraints from LEP, the LHC, and astrophysics are applied, the only pure state that can generate the observed relic abundance is the higgsino [130–132].

the LSP to annihilate efficiently in the early universe. There are a few options to increase the rate at which the bino annihilates:

- Mixing: If the composition of the LSP contains a substantial amount of wino, higgsino or tripletino, the mixing can allow for efficient annihilations.
- Coannihilation: Having another supersymmetric particle slightly above the mass of the LSP opens the possibility of t-channel annihilations, which can greatly increase the annihilation cross section. For there to be enough of the heavier particle around as the universe expands and cools down, the mass must not be more than $\sim 10\%$ larger than the mass of the dark matter candidate.
- Funnel/Resonance: If the mass of the LSP is approximately half the mass of another state, the s-channel propagator becomes very large. There is a peak in the annihilation cross section, and a corresponding dip in the relic abundance after freeze-out.

If the LSP is coannihilating with squarks or sleptons, there are strong limits on the model from LHC searches. This is due to the production rate of squarks and the relatively clean signals for sleptons. In this case, one would expect to find the squark or slepton before the DM candidate.

In the literature, both mixing and coannihilation among electroweakinos are referred to as well tempering, [133]. Well tempering implies that there are multiple states around that can be produced, which is good for the production cross section of beyond-the-Standard-Model states. However, achieving the correct relic abundance requires the splitting to be small, which makes detection difficult. There have recently been studies on detecting electroweakinos with small splittings at colliders [134–142].

The resonant/funnel annihilations of the LSP do not need extra particles at the same mass, but instead at nearly twice the mass of the DM particle. In the MSSM, the funnel particle can be either of CP-even (H_1^0, H_2^0) or CP-odd (A^0) nature [143–149]. Since the dark matter particle itself cannot be detected at colliders, the way to look for such a model is through the heavier states, however, as exemplified by the long search for the Higgs, searches for neutral scalars are difficult. As will be shown later, in the SCTM, the triplet scalars provide a resonant channel over much of the parameter space. Moreover, because of the degeneracy of states in the custodial situation (Chapter 4), there are charged states near the neutral funnel that could aid in discovery.

6.2 Phenomenological approach to the SCTM

We know from Chapter 5 that a totally custodial situation at the EW scale is not realistic from a theoretical point of view and deviations from $SU(2)_V$ are to be taken into account when performing studies of the SCTM properties. For this study, we take a middle ground between the calculable (but unrealistic) fully custodial model of Chapter 4, and Chapter 5, where we perform a detailed analysis of the custodial breaking generated by the RGE running. In the latter, phenomenological studies which need parameter scans are challenging as every point in the parameter space is calculated in a non trivial way. In this chapter we assume a Higgs sector with a potential allowing for a non custodial vacuum, provided that it only comes from the ratio of the doublet VEV's, parameterized by $\tan\beta$. We do this in agreement with what is found performing the RGE analysis, i.e. because of the influence of the top quark Yukawa coupling,

the running differentiates the two soft doublet masses from each other much more than the three triplet ones among themselves (Figs. 5.2 and 5.8), resulting in a much bigger vacuum misalignment in the doublet sector. This misalignement in the doublet sector translates into a departure from $\tan\beta = 1$ and as the ρ parameter is affected only by the difference in the triplet VEV's, one can consider a breaking generated by $\tan\beta$ without worrying too much about ρ parameter constrains.

Let us now present this approach in detail as something similar will be also used in Chapter 7. The $SU(2)_L \otimes SU(2)_R$ invariant superpotential is defined as

$$W = \lambda \bar{H} \cdot \bar{\Delta} \bar{H} + \frac{\lambda_3}{3} \text{tr } \bar{\Delta}^3 + \frac{\mu}{2} \bar{H} \cdot \bar{H} + \frac{\mu_\Delta}{2} \text{tr } \bar{\Delta}^2 \,, \tag{6.1}$$

and again, the total potential

$$V = V_F + V_D + V_{\text{soft}} \,, \tag{6.2}$$

where the F and D terms are defined as in Chapters 4 and 5. The soft part of the potential in this approach is

$$\begin{aligned} V_{\text{soft}} &= m_{H_1}^2 |H_1|^2 + m_{H_2}^2 |H_2|^2 + m_{\Sigma_1}^2 \text{tr } |\Sigma_1|^2 + m_{\Sigma_{-1}}^2 \text{tr } |\Sigma_{-1}|^2 + m_{\Sigma_0}^2 \text{tr } |\Sigma_0|^2 \\ &+ \left\{ \frac{1}{2} m_3^2 \bar{H} \cdot \bar{H} + \frac{1}{2} B_\Delta \text{tr } \bar{\Delta}^2 + A_\lambda \bar{H} \cdot \bar{\Delta} \bar{H} + \frac{1}{3} A_{\lambda_3} \text{tr } \bar{\Delta}^3 + h.c. \right\} \end{aligned} \tag{6.3}$$

Note that the potential we just wrote is the same as that of Chapter 4 but with non custodial soft masses that will be used to satisfy the EOM's.

The $SU(2)_V$ breaking vacuum is parametrized as

$$v_1 = \sqrt{2} \cos\beta \, v_H, \quad v_2 = \sqrt{2} \sin\beta \, v_H \quad \text{and} \quad v_\psi = v_\chi = v_\phi \equiv v_\Delta, \tag{6.4}$$

where the custodial symmetry is only broken in the vacuum by $\tan\beta$. As in the previous chapter, the vacuum will preserve the relation (4.10) regardless of the $\tan\beta$ value, fixing a v_H for every v_Δ. From close inspection of Eq. (5.8), we can determine that the ρ parameter is not affected if custodial symmetry is broken in this way, however, only from the consideration of $\tan\beta \neq 1$ we already loose the degeneracy of minimization conditions present in the custodial situation. The five EOM's for this choice of vacuum are listed in Appendix C.1, where we can see that the degeneracy is recovered when $\tan\beta \to 1$. For the rest of the chapter we will refer to $\tan\beta = 1$ as the custodial case and $\tan\beta \neq 1$ as the non custodial case.

Benchmark parameters

To begin a study of the dark matter properties of the model, we first choose a set of benchmark values, given by

$$\begin{aligned} \lambda_3 &= 0.35, \\ m_3 &= 500 \text{ GeV}, \\ B_\Delta &= -(500 \text{ GeV})^2, \\ A_\lambda &= A_{\lambda_3} = A_t = A_b = A_\tau = 0, \\ m_{\tilde{Q}_3} &= 800 \text{ GeV}, \quad \text{and} \quad m_{\tilde{u}_3^c} = 700 \text{ GeV}, \end{aligned} \tag{6.5}$$

where other scalar soft masses have been decoupled and the ones corresponding to Higgs multiplets are determined by the minimization conditions. The SCTM triplet F terms yield a large tree-level Higgs mass, so smaller one-loop corrections are needed. This is the reason for our choice of

relatively light stops albeit above the current experimental limits. The value of λ_3 will not have much of an effect. We are considering the case $m_3^2 = |B_\Delta|$ for simplicity. Values of m_3 and B_Δ in the ballpark of those in Eq. (6.5) should provide similar results while larger values will decouple the heavy scalars more, and in addition will affect on how large v_Δ can be in the minimization of the potential. Similarly, we choose to examine the case in which all of the trilinear terms are zero to help ensure that the EW vacuum is the deepest one. This leaves μ, μ_Δ, λ, and v_Δ as the remaining free parameters to study.

Scalar spectrum

As noted in the previous chapter, there is a total of five *CP*-even, five *CP*-odd, six singly charged, and two doubly charged Higgs scalar fields in the SCTM. Since we will be examining both the custodial and the non custodial setups of the model, we will not use the notation in terms of $SU(2)_V$ multiplets, instead, we will work with mass eigenstates. After removing the Goldstone bosons, they will be denoted as $H^0_{1,\dots 5}$, $A^0_{1,\dots 4}$, $H^\pm_{1,\dots 5}$, and $T^{\pm\pm}_{1,2}$.

To study the dark matter annihilation in the model, we are only interested in the spectrum of the lightest neutral scalars rather than the charged components. Annihilating the neutralino through a resonance of the Higgs or the heavy Higgs has been shown before in the MSSM. As a new feature of this model, there are substantial regions of parameter space in the SCTM where the annihilation can proceed through a triplet-like resonance. To do this, the soft masses of the triplets must not be too large. Upon close examination of the minimization conditions for $m^2_{\Sigma_0}$, $m^2_{\Sigma_1}$, and $m^2_{\Sigma_{-1}}$ written in Appendix C.1, we see that there is a piece that scales as v_H^2/v_Δ for each soft mass. Smaller values for v_Δ yield large soft masses for the triplets, decreasing the chance of annihilating through the triplet funnel.

The Higgs mass

The results for the Higgs mass are pretty similar to what is presented in previous chapters. For $\tan\beta = 1$, there is no tree-level contribution to the mass of the Higgs from the MSSM sector of the model. Instead, the mass at tree level in the decoupling limit comes only from the triplet F terms, and is given (at leading order in v_Δ) by

$$m_h^2\big|_{\tan\beta=1} = 6\lambda^2 v_H^2. \tag{6.6}$$

We also examine the model in which $\tan\beta \neq 1$ (but is still small [2]) and the tree-level Higgs mass can no longer be written in a simple form. However, we comment that there are now MSSM contributions to the mass, and the triplet F terms contribute as $\lambda^2\left(4\cos^4\beta + 4\sin^4\beta + \sin^2 2\beta\right)$. Again, the SCTM allows for large tree-level contributions to the Higgs mass with no need of large one-loop corrections, and thus no need for heavy stops.

The dominant radiative corrections to the Higgs mass depend on the top Yukawa coupling which is defined as in Eq. (5.14). In the SCTM, increasing v_Δ increases the top Yukawa, which increases radiative corrections to the Higgs mass. In our study, we take the dominant one-loop corrections found in Ref. [44], [3] we use 700 GeV for the right-handed soft mass and 800 GeV

[2] In agreement with the $\tan\beta$ values found in Chapter 5.

[3] We will neglect radiative corrections proportional to λ^2 as the parameter λ affects the Higgs mass at the tree level and thus the corresponding radiative corrections are constrained to be small by perturbativity.

for the left-handed soft mass. These were chosen to be slightly above the current experimental bounds, regardless of the mass of the lightest neutralino. Raising the masses of the stops will not affect our dark matter results, only worsen the fine-tuning of the model. Note that even though the stop masses and A_t are fixed in the study, changing μ and $\tan\beta$ affects the mixing and thus the one-loop contributions to the Higgs mass. Therefore, by fixing the mass of the stops, the only way to alter the mass of the Higgs is through the remaining parameters, μ, μ_Δ, λ, and v_Δ. To study the effect of the triplet-like states on dark matter, we examine the case in which either the doublet- or the triplet-like fermions are lighter. We fix $\mu_\Delta = 250$ GeV and scan over the values of μ.

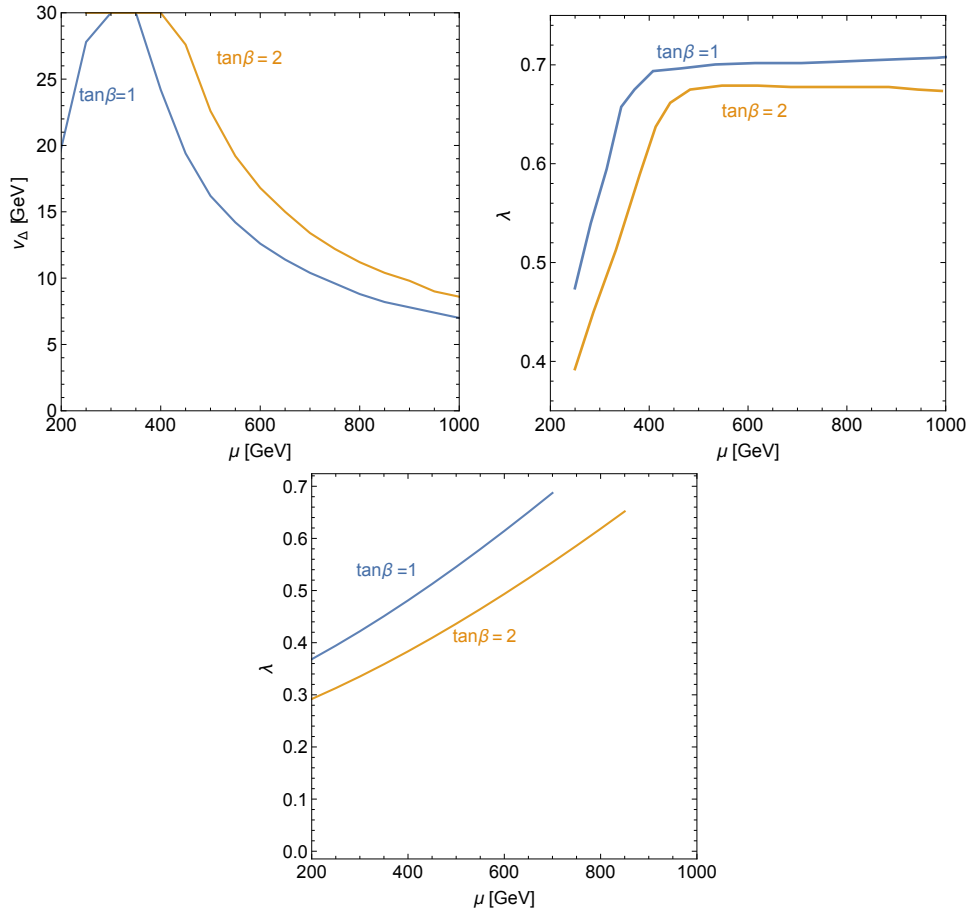

Figure 6.1: *Top row: Maximal values of* $\sqrt{2}\,v_\Delta$ *that allow* λ *to set the Higgs mass to* 125 *GeV and yield a minimized potential as a function of* μ. *Bottom: Value of* λ *needed to attain the observed Higgs mass for* $v_\Delta = 10/\sqrt{2}$ *GeV. The triplet supersymmetric mass is set to* $\mu_\Delta = 250$ *GeV, and the other values are as in Eq.* (6.5).

Recall that in order to achieve a minimum of the potential from the minimization conditions (see Appendix C.1) rather than a saddle point, there exist constraints on the relationship between μ and μ_Δ beyond Eq. (4.39), which forces the origin to be a saddle point. However, the latter equation might give us some intuition on which μ and μ_Δ values we can take since a saddle point at the origin forces the potential to have a minimum. When $\tan\beta = 1$ and $A_\lambda = 0$ the equation

simplifies to $2\mu > \mu_\Delta$ and we see that we cannot look at regions where μ_Δ is significantly heavier than μ and still minimize the potential [4]. Once μ and μ_Δ are fixed, we have to chose λ and v_Δ. We do this in two different ways:

- Maximizing v_Δ: We start with $v_\Delta = 30/\sqrt{2}$ GeV [5], which we take as the upper limit as suggested by the analysis of Chapter 5. We then scan over λ to set the Higgs mass (including radiative corrections). Once the lightest CP-even Higgs has a mass of 125 GeV, we examine the rest of the spectrum. If other scalars have gone tachyonic, or the value of λ needed is greater than 0.75, this value of v_Δ is excluded. We then lower v_Δ and repeat the process until a 125 GeV Higgs is obtained and the vacuum minimized. The resulting values of v_Δ and λ are plotted in the top row of Fig. 6.1 over a range of μ.
- Keep the value of v_Δ constant as we scan across μ. The region of μ that can yield the correct Higgs mass and successfully minimize the potential is smaller for large values of v_Δ. Because of this, we set $v_\Delta = 10/\sqrt{2}$ GeV for our study of this method. The lower panel of Fig. 6.1 displays the values of λ needed for both $\tan\beta = 1$ and $\tan\beta = 2$. Note that $\tan\beta = 2$ needs smaller values of λ because there are tree-level MSSM contributions to the Higgs mass, this allows for a larger range of μ than the $\tan\beta = 1$ case.

Rest of the scalar spectrum

The spectrum of the light neutral scalars is plotted in Fig. 6.2 for $v_\Delta = 10/\sqrt{2}$ GeV and v_Δ maximized in the left and right panels respectively. When $\tan\beta = 1$, shown in the upper panels, the scalars H_2^0, A_1^0, and H_3^0 have similar masses, which increase as a function of μ. The lightest that these scalars can be is ~ 300 GeV. The other neutral scalars all have masses greater than 600 GeV and therefore are not shown in the plots. In the lower panels, the same spectra is shown for $\tan\beta = 2$. In this case, both H_2^0 and A_1^0 are nearly degenerate in mass, and much lower in mass than when $\tan\beta = 1$. This partially comes from the smaller value of λ needed to raise the Higgs mass for $\tan\beta = 2$. Conversely, the mass of H_3^0 does not change much between the two choices of $\tan\beta$. If the maximum v_Δ is chosen instead of using the constant $v_\Delta = 10/\sqrt{2}$ GeV, the masses of H_2^0, A_1^0, and H_3^0 will drop. The separation of the states will also depend on v_Δ so increasing it helps to remove the degeneracy of the scalars.

We do not perform any collider constraints on searches for these extra possible scalars. However, we see that the model allows for some to be very light (Sec. 5.4). A dedicated search could therefore exclude large regions of parameter space in a quicker and more conclusive way than either Higgs precision measurements or direct detection experiments (see Chapter 8).

[4] Of course, this does not mean that triplets cannot be decoupled supersymmetrically. The limit $\mu_\Delta \to \infty$ yields the MSSM, in which case Eq. (4.39) does not apply.

[5] Because of computational issues, the paper in which this chaper is based, Ref. [7], had to be written using the normalization where $\phi = (v + \phi_R + i\,\phi_I)/\sqrt{2}$ and $v = 246$ GeV. To keep the text as cohesive as possible we change it here to the one that we use in the rest of the thesis, $\phi = v + (\phi_R + i\,\phi_I)/\sqrt{2}$ and $v = 174$ GeV; therefore some of the numbers and figures in this chapter will show values of v_Δ weighted by a factor $1/\sqrt{2}$.

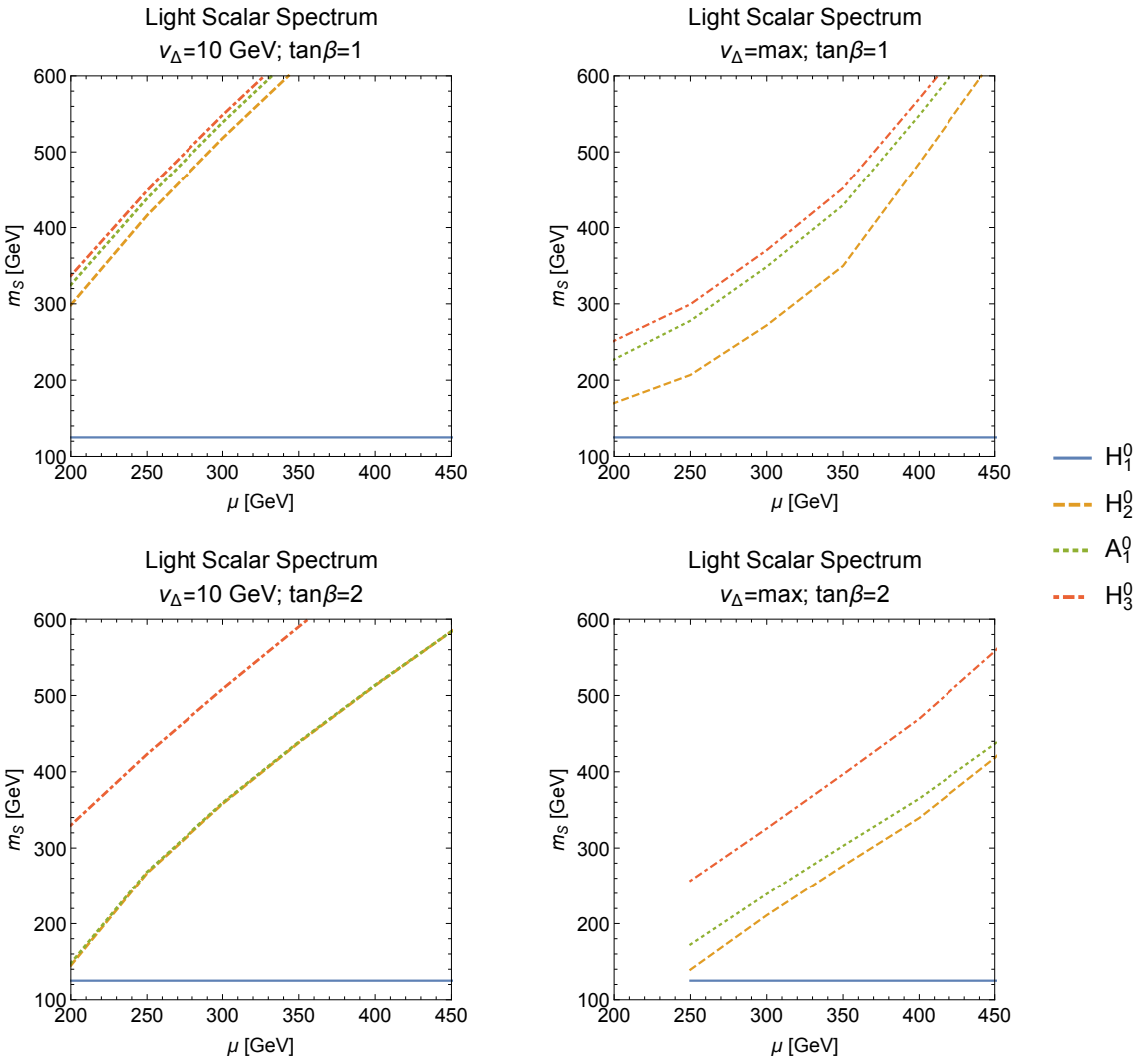

Figure 6.2: *Left panels: Spectrum of the neutral light scalars when* $v_\Delta = 10/\sqrt{2}$ *GeV and* λ *is changed to set the Higgs mass. Right panels: Spectrum of the neutral light scalars when we use the maximum allowed value for* v_Δ *for each* μ *value. The upper (lower) panels contain* $\tan\beta = 1$ *(*$\tan\beta = 2$*). Changing* $\tan\beta$ *greatly affects the masses of* H_2^0 *and* A_2^0*, but* H_3^0*'s mass is similar for both choices.*

Neutralino spectrum and mixings

The SCTM adds three neutralinos to the four MSSM ones; the bino, wino, and the two higgsinos. There are also two new charginos on top of the charged wino and higgsino, and finally a doubly charged triplet fermion. In the following, we will collectively refer to the fermion components of all of the triplet fields as tripletinos and to the combination of the neutralinos, charginos, and doubly charged tripletinos as electroweakinos.

The mass Lagrangian in the basis $\psi^0 = \left(\tilde{B}^0, \tilde{W}^3, \tilde{H}_1^0, \tilde{H}_2^0, \tilde{\phi}^0, \tilde{\chi}^0, \tilde{\psi}^0\right)$ is

$$\mathcal{L}_{1/2}^0 = -\frac{1}{2}(\psi^0)^T \mathcal{M}_{1/2}^0 \psi^0 + h.c.\,, \tag{6.7}$$

where $\mathcal{M}_{1/2}^0$ is written in Appendix C.1. Overall, the masses are controlled by M_1, M_2, μ, and μ_Δ for the bino, wino, higgsinos, and tripletinos respectively, but there are also additional contributions to the masses and mixings scaling with either v_H or v_Δ. To provide a good dark matter candidate, we want the LSP to be the lightest neutralino; its composition will then determine the annihilation and direct detection cross sections.

The composition of the LSP in terms of the gauge eigenstates is shown in Fig. 6.3 for the case in which the VEV of the triplets is constant (10 GeV) and $\tan\beta = 1(2)$ in the top (bottom) row. The left panels have the higgsino-like states lighter than the tripletino ones, using $\mu = 200$ GeV and $\mu_\Delta = 250$ GeV. The middle panel has both the higgsino and tripletino masses set to $\mu = \mu_\Delta = 250$ GeV. Finally, the right panel examines when the triplet states are lighter than the higgsino, with $\mu = 400$ GeV and μ_Δ still at 250 GeV. To simplify the situation as much as possible, we decouple the wino by setting $M_2 = 1$ TeV.

In the custodial situation, the doublet components of the LSP are equal and the triplet components are separately equal over most of the parameter space. The $\tan\beta = 2$ case has each higgsino and tripletino contributing differently to the LSP. Despite the complexity of the plots, there are a few overarching trends.

In Sec. 6.1, we argued that the bino component of the LSP must dominate in order to achieve the correct relic abundance of dark matter. The interesting regions to examine in the compositions plots are then $M_1 < \mu, \mu_\Delta$. In this region, even when $\mu > \mu_\Delta$, the second-largest component of the LSP is higgsino rather than tripletino which is true even for quite large values of the higgsino mass. This is due to the mixing of the bino with the higgsinos or tripletinos, which comes from off-diagonal terms in the neutralino mass matrix (C.4) weighted with v_H or v_Δ, respectively. Because of Eq. (4.10), $v_H \gg v_\Delta$ and the higgsino mass needs to be much larger than the tripletino mass in order for the triplet contribution to the LSP to be larger than the higgsino component. So even though the mass of the higgsino can be larger than the tripletino mass, the mixing of the bino with the higgsino can be what causes the correct annihilation rate. As μ is further increased, the amount of higgsino in the LSP drops past the point where mixing alone can yield the correct relic abundance. Looking only at regions where $M_1 < \mu_\Delta$, we see that the triplet states do not contribute much to the LSP. By removing the higgsino, the LSP is made more pure bino, rather than increasing the triplet amount. The only possibility of well tempering for this will then require coannihilations of the bino-like LSP with a triplet-like state.

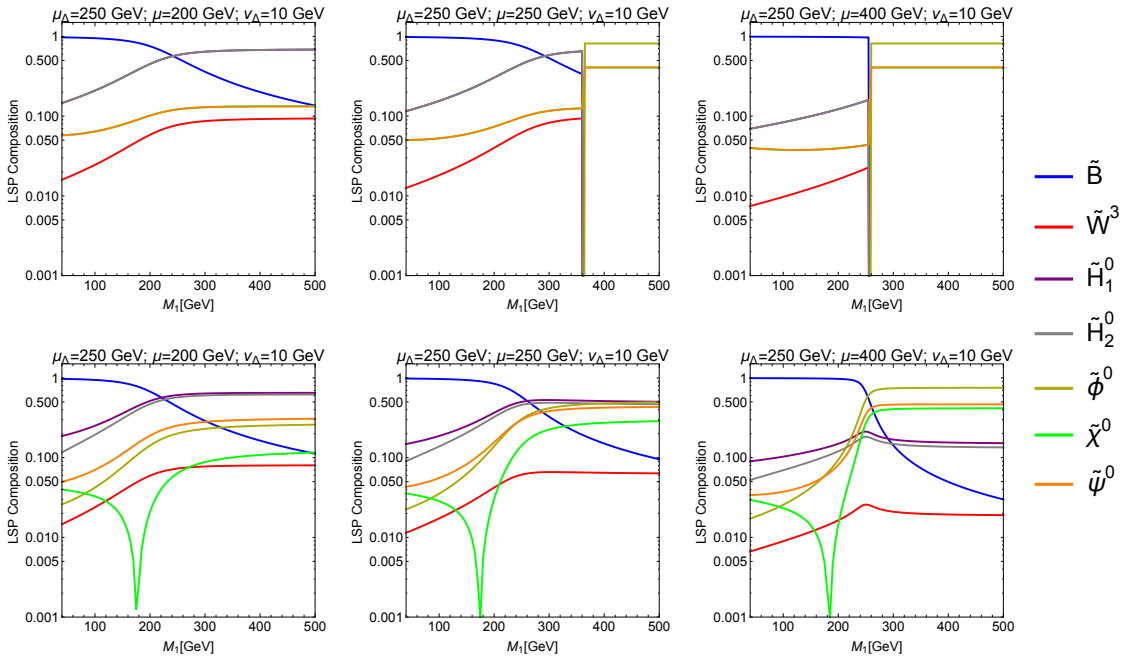

Figure 6.3: *Composition of the LSP in terms of gauge eigenstates. The top row shows* $\tan\beta = 1$ *and the bottom shows* $\tan\beta = 2$*. The columns correspond to* $\mu = (200, 250, 400)$ *GeV, respectively, while the tripletino mass is set to* $\mu_\Delta = 250$ *GeV and* $v_\Delta = 10/\sqrt{2}$ *GeV. The wino has been decoupled with* $M_2 = 1$ *TeV. Note in the top middle and top right plots the presence of a triplet-like eigenvalue, which is totally decoupled from the rest of the neutralino mass matrix, made out of only* $\tilde{\psi}, \tilde{\phi}$*, and* $\tilde{\chi}$*. It corresponds to an* $SU(2)_V$ *fiveplet in the custodial basis.*

6.3 Dark matter phenomenology

To examine the dark matter phenomenology of the SCTM the model was implemented into SARAH [150–154]. With this, a code was generated for SPheno [155,156] and CalcHep [157]. The SPheno code calculates the spectrum, outputting a parameter card that can be read by MicrOMEGAs 3 [158]. The program MicrOMEGAs 3 uses the CalcHep code to calculate the dark matter properties.

Thermal relic density

For each of the choices of $\tan\beta$ and the method of picking v_Δ, we scan over the possible μ values for $\mu_\Delta = 250$ GeV, using 50 GeV step sizes. At each point in μ, we then scan over M_1 to find the bino masses that yield the correct relic abundance of dark matter. We start with $M_1 = 40$ GeV and take 1 GeV steps until $M_1 > 100$ GeV, at which point a 5 GeV step is used to save on computing time.

Figure 6.4 shows an example of the relic abundance calculated at each M_1 value for the point $\mu = 200$ GeV, $v_\Delta = 10/\sqrt{2}$, and $\tan\beta = 1$. The gray line marks $\Omega h^2 = 0.1187$, the observed relic abundance in the Universe [159]. The scalar masses do not depend on the M_1 value and are

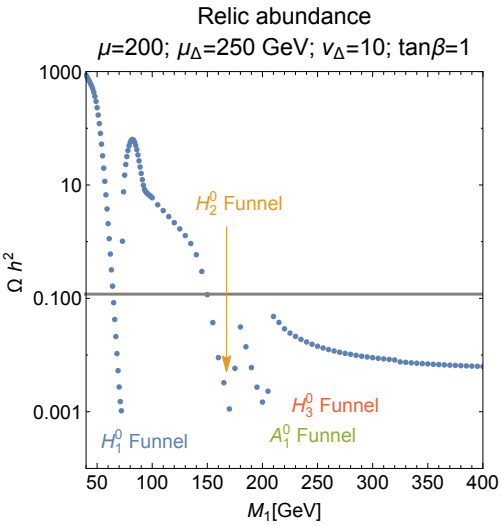

Figure 6.4: *Relic abundance for the model with $\mu = 200$ GeV, $\mu_\Delta = 250$ GeV, $v_\Delta = 10/\sqrt{2}$ GeV, and $\tan\beta = 1$. The gray line marks the observed relic abundance in the Universe today. As the mass of the LSP crosses over half the mass of one of the scalars in the model, the annihilation cross section greatly increases, leading to lower relic abundances. When the LSP mass gets close to the mass of the higgsino, the mixing and coannihilations take over and the relic abundance stays below the observed value.*

given by

$$\begin{aligned} m_{H_1^0} &= 125 \text{ GeV}, \quad m_{H_2^0} = 299 \text{ GeV}, \\ m_{A_1^0} &= 325 \text{ GeV}, \quad m_{H_3^0} = 337 \text{ GeV}, \quad \text{and others} > 700 \text{ GeV}. \end{aligned} \tag{6.8}$$

Three dips in the relic abundance are seen in the plot. These correspond to the H_1^0 funnel, the H_2^0 funnel, and one for the nearly degenerate A_1^0 and H_3^0 states occurring when the bino mass is roughly half the scalar mass. There are three M_1 values of this model point that yield the correct relic abundance. The first two correspond to going into and out of the lightest Higgs funnel, and the third one is at the start of the H_2^0 funnel. However, the next funnels corresponding to A_1^0 and H_3^0 are close together, so the effect of having multiple nearly resonant s-channel annihilations keeps the relic abundance below the observed value. Then M_1 runs into the region where $M_1 > \mu$ and the higgsino becomes the LSP, leaving not enough dark matter in the current Universe.

Determination of the mechanism responsible for $\Omega h^2_{\text{theory}} = \Omega h^2_{\text{observed}}$

For each μ value in our model scans, we do the same process. Whenever the relic abundance at one M_1 value crosses from one side of the observed value to the other at the next M_1 step, we do a more dedicated scan to find the M_1 value to a higher degree of accuracy. We then classify the point according to the process that is driving the annihilations by comparing the LSP mass to half the mass of the scalars or 10% higher than the LSP mass with that of the next to lightest electroweakino. The piece giving the minimum of

$$\min\left(\left|m_{\tilde{\chi}_1^0} - \frac{m_{H_1^0}}{2}\right|, \left|m_{\tilde{\chi}_1^0} - \frac{m_{H_2^0}}{2}\right|, \left|m_{\tilde{\chi}_1^0} - \frac{m_{A_1^0}}{2}\right|, \left|m_{\tilde{\chi}_1^0} - \frac{m_{H_3^0}}{2}\right|, \left|m_{\tilde{\chi}^{0(\pm)}_{\text{NLSP}}} - 1.1 \times m_{\tilde{\chi}_1^0}\right|\right) \tag{6.9}$$

yields a classification of the given scalar funnel or well tempering. This classification is only an approximation of what is actually causing the annihilations. In the nonrelativistic limit, annihilations through scalars occur through the p-wave, while pseudoscalars occur through the s-wave. Thus, when A_1^0 is close in mass to either H_2^0 or H_3^0, the classification scheme could point to the scalar instead of the pseudoscalar, even though the pseudoscalar contribution is larger. In addition, when the funnels are close to the well tempered region both process can be responsible for the annihilation.

Results

The results of the classifications are plotted in Fig. 6.5 for the different model choices in the $m_{\tilde{\chi}_1^0}$ vs. μ plane. The LSP is mostly bino, so $M_1 \sim m_{\tilde{\chi}_1^0}$. The triplet scalars can be very light for $\tan\beta = 2$ or if $\tan\beta = 1$ when the VEV of the triplets takes on the maximum value allowed. Recall that Fig. 6.2 shows that these masses increase as a function of μ. As such, the funnels for the triplet-like H_2^0, A_1^0, and H_3^0, scalars smoothly transition up to the point where well tempering happens at a lighter mass than needed for a triplet funnel.

For every model choice examined, there is an M_1 value that will yield the correct relic abundance either through a triplet-like scalar or well tempering. When μ is large enough and the triplet scalars funnels are not possible, the higgsinos are heavy enough that the well tempering is not caused by bino-higgsino mixing but instead by coannihilations with the triplet fermions. Thus, each model point examined is capable of setting the correct relic abundance using particles beyond the MSSM content.

The large VEV of the triplets allows for the triplet scalars to be light. The lightness of these scalars is what allows the model points examined to always be able to set the relic abundance using either the triplet scalar funnels or the triplet fermions. However, lowering the triplet VEV v_Δ, raising the triplet supersymmetric mass μ_Δ, or lowering the wino mass M_2, can disturb the possibility of achieving the correct relic abundance through a triplet state. The MSSM limit of the model takes the VEV of the triplets to zero. In this case, the triplet scalar soft masses go to infinity and do not contribute to the annihilations [6]. The higgsino alone satisfies the correct relic abundance if its mass is ~ 1.1 TeV. As such, if μ_Δ is much larger than that, the triplet fermions cannot play a role in well tempering. Such a large value of μ would also keep the triplet scalars heavy, so such a case would have no way of using the triplet superfield to set the relic abundance. Finally, the wino has been raised above the mass of the higgsinos and tripletinos for this study. bino-wino well tempering can also be done if $M_1 \simeq M_2 < \mu, \mu_\Delta$. In this case the relic abundance could be set before the triplets have a chance to affect things.

Direct detection

There have been many experimental searches for the direct detection of dark matter. For the mass ranges considered here, the Particle Data Group [159] shows that the best limits are currently coming from the LUX Collaboration [161] for spin-independent searches and the COUPP Collaboration [162, 163] for spin-dependent measurements. Super-Kamiokande [164] and IceCube [165, 166] have better spin-dependent exclusions, but are indirect constraints that rely on the annihilation of dark matter in the current Universe and depend on the byproducts of the

[6] This also happens in triplet models in which the ρ parameter is not protected by a custodial symmetry, as the triplet extension of the MSSM [160], and v_Δ is strongly constrained by electroweak precision observables.

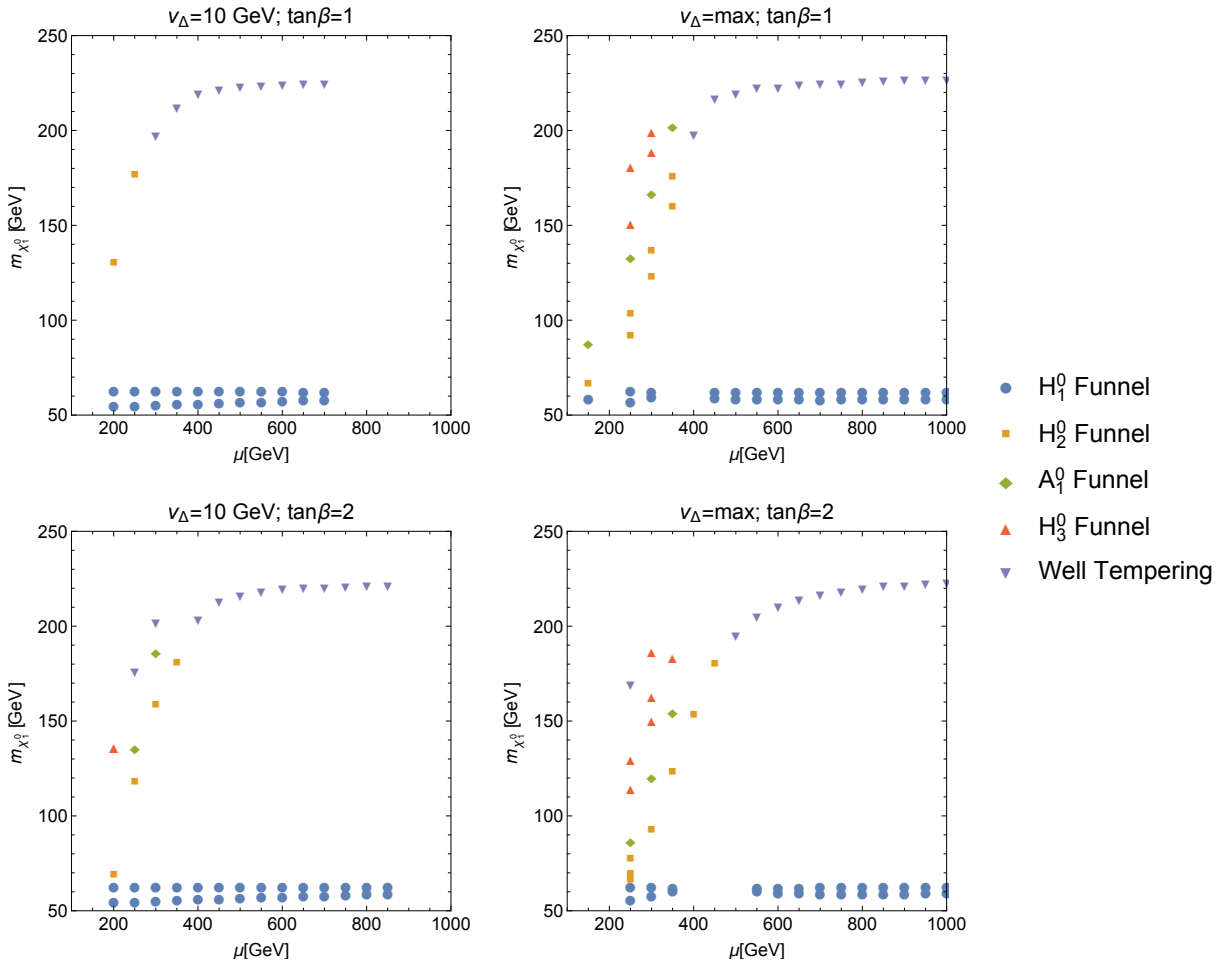

Figure 6.5: *Points that yield the correct relic abundance of dark matter. The upper row is for the custodial case, while the lower has* $\tan\beta = 2$. *The left panels keep* $v_\Delta = 10/\sqrt{2}$ *GeV constant, and the right panels use the maximum allowed value for* v_Δ *for each* μ *value. The points are labelled corresponding to which annihilation channel dominates in the early Universe.*

annihilation that change as the LSP composition changes. We then only compare our results with the LUX and COUPP constraints.

The spin-independent cross sections for the points satisfying the correct relic abundance are shown in Fig. 6.6. The MICROMEGAs 3 output provides both the cross section of the dark matter with a proton and a neutron; we take the maximum of these. The points are marked in the same fashion as Fig. 6.5 to show how the relic abundance is being achieved. The upper (lower) panels show $\tan\beta = 1\,(2)$ while the left and right panels display $v_\Delta = 10/\sqrt{2}$ GeV and when v_Δ is maximized at each point, respectively. The shaded blue region is excluded by the LUX bound, and the dashed blue line is the projected sensitivity of LUX.

The spin-independent cross section is mediated by the doublet scalars. There is not much difference between the $\tan\beta = 1$ and $\tan\beta = 2$ models in terms of the cross sections. For $v_\Delta = 10/\sqrt{2}$ GeV, both have a region where the dark matter mass is between 100 and 200 GeV which can be excluded by LUX. The points are achieved through a triplet funnel, and to get masses in this range for the LSP, the values of μ are low. Referring back to Fig. 6.3, low values

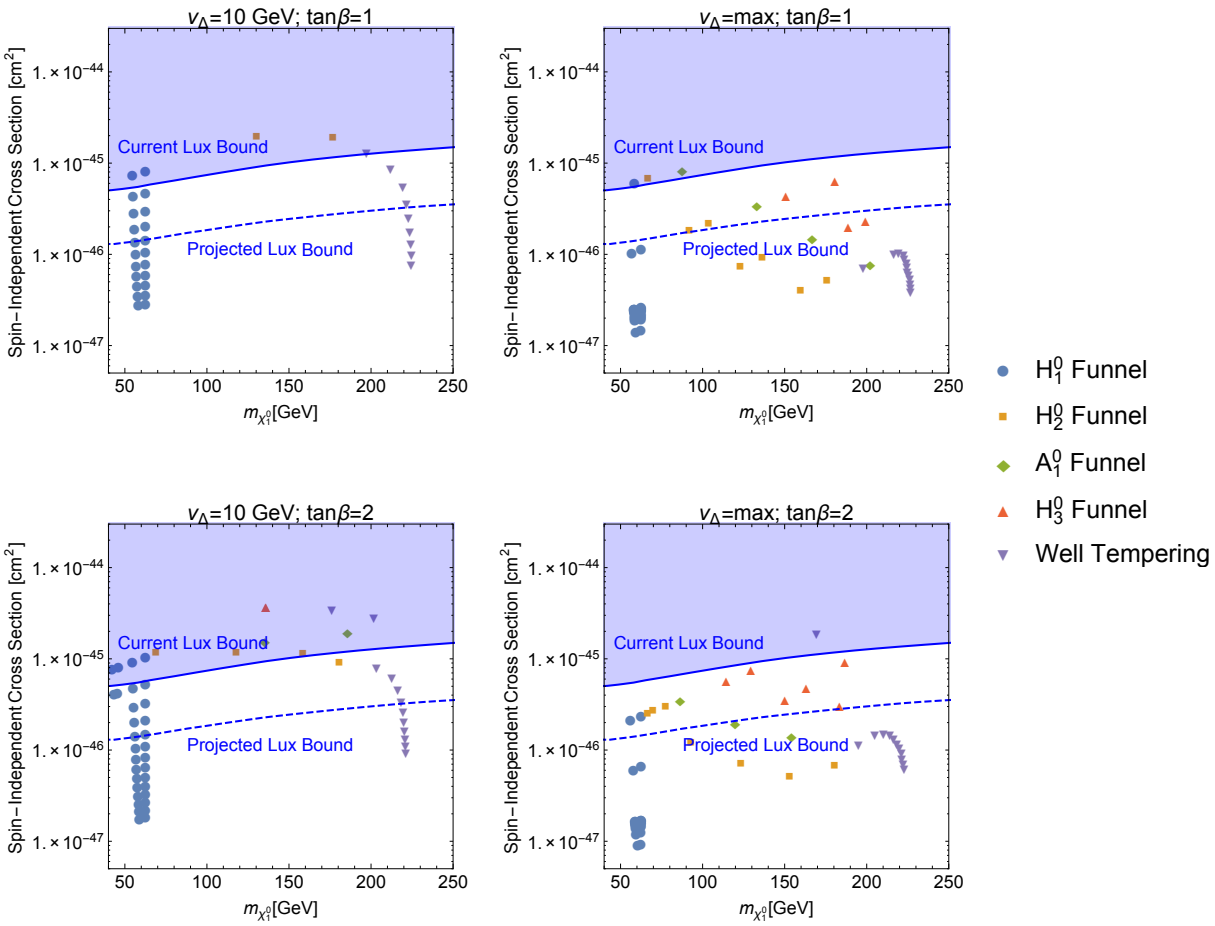

Figure 6.6: *Spin-independent dark matter nucleon cross sections. Each point meets the correct relic abundance with the annihilation mode marked. Points with smaller higgsino components have a lower spin-independent cross section. Left (right) column features* $v_\Delta = 10/\sqrt{2}$ *GeV (maximum allowed* v_Δ*) while top (bottom) row* $\tan\beta = 1$ $(\tan\beta = 2)$*.*

for μ and M_1 give the LSP a moderate higgsino component. This higgsino component is what drives the nuclear cross sections to be so large. The cross sections are lower when the maximum value of v_Δ is used. In this case, there are few points that are currently excluded by LUX. The larger value of v_Δ lowers the masses of the triplet-like scalars. This pushes the triplet funnels and the well-tempering regions to larger values of μ, further decreasing the higgsino component and the spin-independent cross section. Fortunately, there are still many points that can be probed by LUX in the future. However, the points which are well tempered through bino-tripletino coannihilations remain under the projected bound, due to the minimal higgsino component of the LSP.

The spin-dependent interactions are mediated by the Z boson and the cross sections are shown in Fig. 6.7. The panels use the same labelling as Figs. 6.5 and 6.6. In the custodial case, with $\tan\beta = 1$, the mass eigenstates of both the fermions and the scalars of the Higgs doublet and triplet superfields form representations of $SU(2)_V$. The parity-violating Z coupling therefore

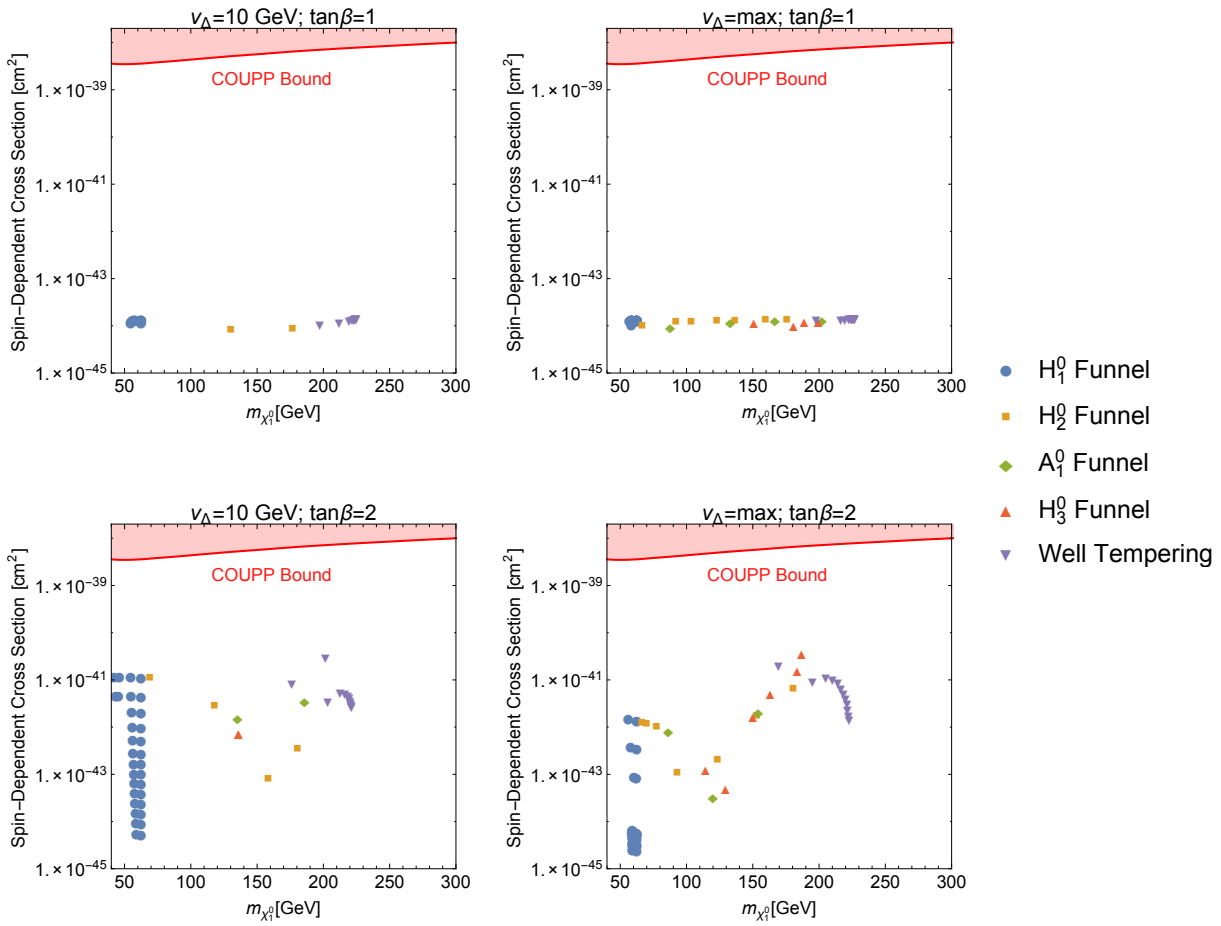

Figure 6.7: *Spin-dependent dark matter nucleon cross sections. Each point meets the correct relic abundance with the annihilation mode marked. The parity-violating Z couplings vanish in the custodial case. Left (right) column features $v_\Delta = 10/\sqrt{2}$ GeV (maximum allowed v_Δ) while top (bottom) row* $\tan\beta = 1$ *(*$\tan\beta = 2$*)*

vanishes in this case. And while this is also true in the MSSM for $\tan\beta = 1$, the SCTM provides motivation for this choice of $\tan\beta$, whereas this situation is excluded in the former. The model points examined for $\tan\beta = 2$ no longer have vanishing Z couplings with the LSP. The cross sections are much larger in this case, particularly for the well-tempered points, which have low spin-independent cross sections. However, even these large cross sections are still ~ 2 orders of magnitude below the COUPP bound.

Indirect detection

The direct detection experiments rely on dark matter interacting with detectors on Earth. It is also possible to observe astrophysical objects containing large dark matter densities. In these regions of space, the LSP can still annihilate. The annihilation does not occur through a diphoton process, which would lead to a monochromatic signal. Instead, experiments must search for

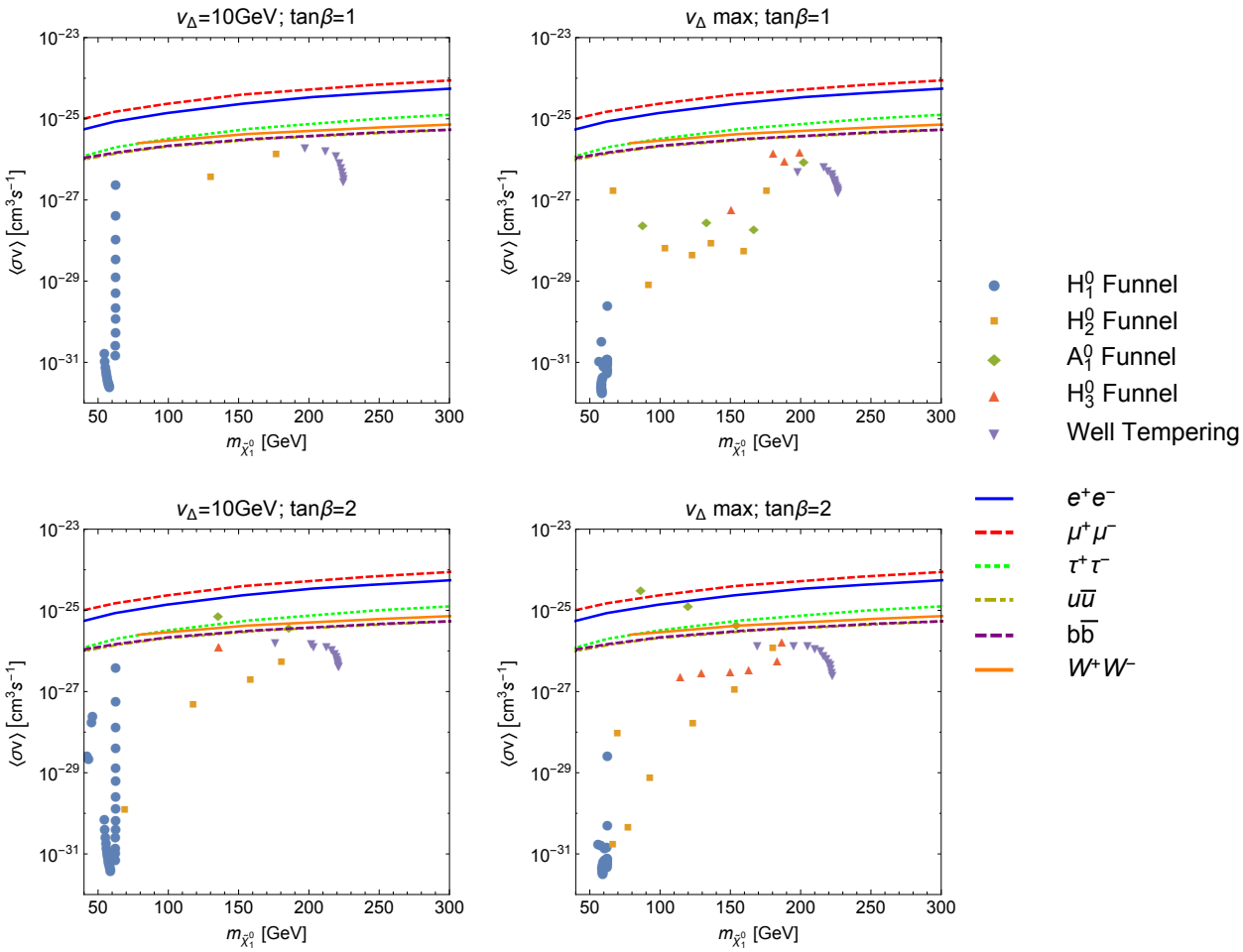

Figure 6.8: *Annihilation cross section times velocity of dark matter in the Galaxy in the current Universe. Each point meets the correct relic abundance with the annihilation mode in the early Universe marked. The lines mark the limits assuming the annihilation occurs* 100% *of the time through the given channel, each resulting in different spectra of photons measured here on Earth.*

photons coming from the byproducts of the annihilation.

The annihilation cross section in the current Universe can be much different than in the early Universe. Scalar funnels (not pseudo) are velocity suppressed in the nonrelativistic limit. As the temperature has cooled since freeze-out, the annihilations proceeding through scalars should be significantly smaller than the $\sim 3 \times 10^{-26}\text{cm}^3/\text{sec}$ needed at freeze-out. For the well tempering through coannihilations, the coannihilating particle is no longer around in the current Universe, so we expect the annihilation cross section to be lower now as well.

The Fermi-LAT Collaboration [167, 168] has placed limits on the annihilation cross section of dark matter from the observation of satellite galaxies. The limits are framed in the context of the annihilations proceeding 100% of the time through either the e^+e^-, $\mu^+\mu^-$, $\tau^+\tau^-$, $u\bar{u}$, $b\bar{b}$, or W^+W^- channel. In Fig. 6.8, the resulting limits are plotted with our model points yielding the correct relic abundance. The upper (lower) panels show $\tan\beta = 1$ (2), while the left and right panels display $v_\Delta = 10/\sqrt{2}$ GeV and when v_Δ is maximized at each point, respectively. A few

points for the $\tan\beta = 2$ case are possibly excluded by these searches. However, these each have the largest annihilation channel being $\tilde{\chi}_1^0\tilde{\chi}_1^0 \to H_1^0 Z$. The spectrum of photons coming from the decays of the H_1^0 and Z will not map directly onto any of the Fermi-LAT limits. The fact that the SCTM has more neutral Higgs funnels opens the possibility of having different annihilation modes. A more detailed study would therefore be needed in order to conclusively exclude points from the SCTM due to indirect constraints.

We also note that some of the points marked as annihilating through the pseudoscalar A_1^0 have particularly large annihilations in the current Universe. These interesting points have A_1^0 very close in mass to either H_2^0 or H_3^0, and there are interference effects in the early universe keeping the annihilation cross section small enough. In the current Universe, when the scalars do not play as much of a role, the annihilations proceed with less interference. Similarly, many points marked as H_3^0 funnels seem to have annihilation rates larger than expected in the current Universe. If the rates are scaled up by the larger velocity at freeze-out, the annihilation rate would seem to be too large. However, these points lie close to the well-tempered region, so it is likely that a simple classification does not work well for points where both processes are important.

6.4 Discussion

In this chapter, we studied the case where the lightest supersymmetric particle of the SCTM is a neutralino. In order for the dark matter candidate to yield the correct relic abundance, it must have a large bino component to not annihilate too quickly in the early Universe. Well tempering mixes the bino with either the higgsino, wino or, in the SCTM case tripletino, in just the right amount to give the observed relic abundance. If the bino component is too large, dark matter does not annihilate quickly enough in the early universe, unless the mass of the dark matter particle is about half the mass of a boson and there is a funnel (Section 6.1).

The SCTM offers new methods to annihilate dark matter in the early universe through triplet fermion co-annihilations or triplet scalar portals. We studied the annihilation of dark matter in the early universe over a large range of values for the higgsino mass parameter μ (Section 6.3). We compared the model points giving the correct relic abundance (Fig. 6.5) with the current best direct detection limits (Figures 6.6 and 6.7). The points with low μ values have at least a moderate higgsino component and have either been excluded already, or can be discovered in future results. At large values of μ the light triplet states still provide an efficient means of annihilating the dark matter, but hope of a direct detection is lost. This is an extra motivation for a detailed study of the LHC phenomenology of the SCTM. Actually, for the study of dark matter, we were only concerned with the neutral triplet states. However as we know from Chapters 4 and 5, the triplets contain charged states. In fact, the second lightest *CP*-even Higgs, H_2^0, is close in mass to both the lightest charged and doubly charged scalars. In addition, the mixing of the triplet like fermions leaves charged and doubly charged states very near in mass to the lightest neutral one. If the relic abundance of dark matter relies on these light states, they should be accessible at the LHC. Thus a dedicated study of methods for searching for doubly charged fermions and scalars could offer valuable constraints on models such as these with exotic particle content (Chapter 8).

7

Properties of the EW phase transition

Electroweak Baryogenesis is an interesting mechanism that could explain the observed asymmetry between matter and antimatter in the universe [169] (for reviews see [170–175]). It ties together cosmology and physics at the electroweak scale, specifically the process of electroweak symmetry breaking. For this scenario to work, the Electroweak Phase Transition (EWPT) needs to be a strong first order one, i.e. it should proceed through bubble nucleation and sphaleron transitions should be sufficiently suppressed in the broken phase. The latter point prevents the asymmetry generated in the bubble walls to not be washed out once the broken phase fills up the universe. With a 125 GeV Higgs the Standard Model potential does not feature a barrier between unbroken and broken phases at zero temperature, although this barrier could in principle be produced by temperature dependent contributions to the potential via cubic terms. However, the SM degrees of freedom are not sufficient to generate a large enough barrier [176] and one needs to add light degrees of freedom beyond the SM ones to radiatively generate the barrier, heavy degrees of freedom decouple from the thermal bath and only light states provide a non negligible contribution to the effective potential. Moreover the Sakharov conditions for successful baryogenesis require a much larger amount of CP violation than the one present in the SM, one thus expects extra sources from BSM physics. Supersymmetric extensions of the SM can be responsible for both, the extra amount of CP violation and a strong enough first order EWPT.

In principle, the MSSM is able to generate a first order EWPT by the introduction of light stops which can generate large cubic terms at finite temperature. The problem in this case is that stops are required to be really light (below ~ 150 GeV [177]) and, unless one goes to very contrived models, this mass range for stops is excluded by experimental searches. Moreover such light degrees of freedom modify the Higgs couplings and we would have seen these modifications by now [178–180]. This problem can actually be generalized to any BSM proposal that tries to generate a first order EWPT radiatively: new light degrees of freedom below experimental bounds are commonly required and it often becomes difficult to accommodate a strong enough first order EWPT with collider searches.

An interesting way out to the MSSM difficulties is to modify the tree level potential and try to generate a barrier already at $T = 0$. This can be done by extending the Higgs sector of the MSSM, for instance by adding a gauge singlet field, the NMSSM [181]. As we previously pointed out, the NMSSM can run into problems with tadpole generation and/or domain walls [65, 66]. Therefore, it is interesting to consider different extensions of the MSSM such as the SCTM and study the properties of their electroweak phase transition. The SCTM is able to generate a barrier between the origin and the EW minimum already at tree level. In this chapter we explore this fact and analyze the behavior of its EWPT for the purpose of being able to generate successful EWBG in supersymmetric extensions of the SM.

The chapter is organized as follows. In Section 7.1 we study the finite temperature potential of the model and then show the results for the strength of the phase transition in Section 7.2. We then study the process of thermal tunneling (Sec. 7.3) and the possible Gravitational Waves that could be generated as a result of the phase transition (Sec. 7.4). We discuss our results and their connection to the collider phenomenology of the SCTM in Section 7.5.

7.1 The SCTM phase transition

For this study we take a similar approach to that of the previous chapter: We will parametrize the possible custodial breaking of the vacuum by allowing for $\tan\beta \neq 1$ to deal with it. As we already argued, the full RGE analysis of Chapter 5 is too rigid as a framework to perform dedicated studies of non trivial features of the model such as the nature of the electroweak phase transition (or the DM phenomenology). This approach will capture the main properties of the custodial breaking without the need to perform a thorough study from a UV complete model.

Scalar potential at zero temperature and the vacuum

We will consider the $SU(2)_L \otimes SU(2)_R$ invariant superpotential of Eq. 6.1. As always, the total potential is given by

$$V_{\rm tree} = V_F + V_D + V_{\rm soft}\,, \tag{7.1}$$

where the F- and D-terms are defined as usual and the soft terms are

$$\begin{aligned} V_{\rm soft} &= m_{H_1}^2|H_1|^2 + m_{H_2}^2|H_2|^2 + m_{\Sigma_1}^2\ {\rm tr}\ |\Sigma_1|^2 + m_{\Sigma_{-1}}^2\ {\rm tr}\ |\Sigma_{-1}|^2 + m_{\Sigma_0}^2\ {\rm tr}\ |\Sigma_0|^2 \\ &+ \left\{\frac{1}{2}m_3^2\bar{H}\cdot\bar{H} + \frac{1}{2}B_\Delta\ {\rm tr}\ \bar{\Delta}^2 + A_\lambda\bar{H}\cdot\bar{\Delta}\bar{H} + \frac{1}{3}A_{\lambda_3}\ {\rm tr}\ \bar{\Delta}^3 + h.c.\right\}. \end{aligned} \tag{7.2}$$

Note that the equation above is the same as that of Chapter 6. The custodial breaking of the soft masses that explicitly spoils the $SU(2)_L \otimes SU(2)_R$ invariant structure is accounted for in the minimization process next described.

In order to explore the potential in detail, to the tree level piece one has to add the Coleman-Weinberg contribution for the one-loop radiative corrections at $T = 0$, which will depend on the considered background scalar fields: H_1^0, H_2^0 from the usual MSSM $SU(2)_L$ doublets, and ψ^0, ϕ^0, χ^0, corresponding to the new triplet sector. We will work for simplicity in the $\overline{MS}$ renormalization scheme for which

$$\Delta V_1^{T=0}(\phi_k) = \sum_i \frac{n_i}{64\pi^2} m_i^4(\phi_k)\left(\log\frac{m_i^2(\phi_k)}{Q^2} - C_i\right), \tag{7.3}$$

where $C_i = 5/6$ for gauge bosons and $C_i = 3/2$ for the rest of states, and n_i is the number of degrees of freedom for each particle ($n_W = 6$, $n_Z = 3$, $n_t = -12$, $n_{\tilde{t}_1} = 6$, $n_{\tilde{t}_2} = 6$, ...). We also write $\phi_k \equiv H_1^0, H_2^0, \psi^0, \phi^0, \chi^0$ for simplicity. In the $\overline{MS}$ (as in any mass independent renormalization scheme) decoupling of heavy particles is not automatically implemented, but has to be done by hand at a scale of the order of their mass where they are integrated out, eventually leaving some threshold corrections (the run-and-match procedure) in the low energy effective theory. The run-and-match procedure guarantees the absence of large logarithms in the effective potential (for useful examples of this procedure in the MSSM see Refs. [182, 183]). On the other

hand the $\overline{MS}$ renormalization scheme changes the location of the tree-level potential minimum as well as the value of the (running) Higgs masses. In other words the tree-level potential must be minimized after inclusion of radiative corrections, as we will do next.

The total background-dependent one-loop zero temperature potential is then

$$V_1(\phi_k) = V_{\rm tree}(\phi_k) + \Delta V_1^{T=0}(\phi_k) \tag{7.4}$$

and the EWSB vacuum is derived by solving the five minimization conditions

$$\left.\frac{\partial V_1(\phi_k)}{\partial H_1^0}\right|_{\phi_k=v_k} = \left.\frac{\partial V_1(\phi_k)}{\partial H_2^0}\right|_{\phi_k=v_k} = \left.\frac{\partial V_1(\phi_k)}{\partial \psi^0}\right|_{\phi_k=v_k} = \left.\frac{\partial V_1(\phi_k)}{\partial \phi^0}\right|_{\phi_k=v_k} = \left.\frac{\partial V_1(\phi_k)}{\partial \chi^0}\right|_{\phi_k=v_k} = 0\,, \tag{7.5}$$

where we impose the EW vacuum to be at

$$v_1 = \sqrt{2}\cos\beta\, v_H, \quad v_2 = \sqrt{2}\sin\beta\, v_H \quad \text{and} \quad v_\psi = v_\chi = v_\phi \equiv v_\Delta. \tag{7.6}$$

So that we allow breaking of custodial invariance only in the doublet sector, which, as we know, is a very good approximation as that breaking is triggered in the running mainly by the top Yukawa coupling (Figs. 5.2 and 5.8). The Higgs mass is computed numerically from the scalar mass matrix that is derived from the above potential, and we have checked that it is very well approximated by the analytical expressions from Refs. [44, 184], although the plots are based on the numerical calculation. Note that we are only including dominant contributions to the Higgs mass. From Chapters 4 and 5 we know that because we have introduced three extra $SU(2)_L$ triplets, the scalar sector of the model is enhanced with respect to the MSSM by a new set of states, however, these carry a large triplet component and couple very weakly to the Higgs, thus making their contributions to the Higgs mass unimportant.

To set the Z mass, we use the relation (4.10) that will fix v_H once we choose v_Δ. Finally, in order to solve the five minimization conditions we need to fix five parameters. We will choose for them the soft scalar masses m_{H_1}, m_{H_2} and $m_{\Sigma_1}, m_{\Sigma_{-1}}, m_{\Sigma_0}$ as we did in the previous chapter.

Finite temperature scalar potential

The finite temperature potential at one-loop is

$$V_1(\phi_k, T) = V_{\rm tree}(\phi_k) + \Delta V_1^{T=0}(\phi_k) + \Delta V_1(\phi_k, T) + \Delta V_{\rm daisy}(\phi_k, T) \tag{7.7}$$

with the finite temperature part

$$\Delta V_1(\phi_k, T) = \frac{T^4}{2\pi^2}\left(\sum_i n_i J_i\left[\frac{m_i^2(\phi_k)}{T^2}\right]\right), \tag{7.8}$$

where the thermal integrals are [1]

$$J_\pm(y) \equiv \int_0^\infty dx\, x^2 \log\left(1 \mp e^{-\sqrt{x^2+y}}\right). \tag{7.9}$$

[1] These integrals can also be written in terms of an infinite sum of Bessel functions [176]

$$J_\pm(y) \equiv -\sum_{n=1}^{\infty} \frac{(\pm 1)^n}{n^2}\, y^2 K_2(ny)\ .$$

By truncating the sum to a large enough order, one can obtain a more calculable situation which still represents a good approximation to the thermal integrals written above. We will not use any high (low) temperature expansion in this work since our interesting parameter space does not qualify for any of the two regimes.

Here $J_i = J_+(J_-)$ if the i^{th} particle is a boson (fermion). The Daisy piece is given by

$$\Delta V_{\text{daisy}}(\phi_k, T) = -\frac{T}{12\pi} \sum_{i=\text{bosons}} n_i \left[\mathcal{M}_i^3(\phi_k, T) - m(\phi_k)^3\right] , \tag{7.10}$$

where

$$\mathcal{M}_i^2 = m_i^2(\phi_k) + \Pi_i(\phi_k, T) . \tag{7.11}$$

Since the thermal corrections to the (un-resummed) one-loop potential potential automatically decouple heavy degrees of freedom we will only Daisy resum the longitudinal components of light gauge bosons W_L, Z_L and γ_L just as in the SM [172]. In the one-loop approximation

$$\begin{aligned} &\Pi_{W_T}(\phi_k, T) = \Pi_{Z_T}(\phi_k, T) = \Pi_{\gamma_T}(\phi_k, T) = 0 , \\ &\Pi_{W_L}(\phi_k, T) = \frac{11}{6} g^2 T^2 \end{aligned} \tag{7.12}$$

and the SM Debye masses $\mathcal{M}_i^2$ for Z_L, γ_L are given by

$$\begin{aligned} \mathcal{M}_{Z_L}^2 &= \frac{1}{2}\left(m_Z^2(\phi_k) + \frac{11}{6}\frac{g^2}{\cos^2\theta_W} T^2 + \Delta(\phi_k, T)\right) , \\ \mathcal{M}_{\gamma_L}^2 &= \frac{1}{2}\left(m_Z^2(\phi_k) + \frac{11}{6}\frac{g^2}{\cos^2\theta_W} T^2 - \Delta(\phi_k, T)\right) . \end{aligned} \tag{7.13}$$

Where

$$\Delta^2(\phi_k, T) = m_Z^4(\phi_k) + \frac{11}{3}\frac{g^2\cos^2 2\theta_W}{\cos^2\theta_W}\left(m_Z^2(\phi_k) + \frac{11}{12}\frac{g^2}{\cos^2\theta_W} T^2\right) T^2 . \tag{7.14}$$

7.2 Strength of the phase transition

We have found that μ and μ_Δ are the parameters to which the potential shows more sensitivity for creating a barrier between the origin and the EW minimum already at $T = 0$, they are therefore critical to the study of the phase transition. To simplify the study we will make contour plots of different quantities on the (μ, μ_Δ) plane while holding other parameters fixed. To start doing numerical computations we first choose a set of benchmark values given by

$$\begin{aligned} A_\lambda = A_{\lambda_3} = A_t = 0, \quad \lambda_3 = 0.35, \\ m_3 = 750 \text{ GeV}, \quad B_\Delta = -(750 \text{ GeV})^2, \\ m_{\tilde{Q}_3} = 800 \text{ GeV}, \quad \text{and} \quad m_{\tilde{u}_3^c} = 800 \text{ GeV}. \end{aligned} \tag{7.15}$$

In the left panel of Fig. 5.9 we plot regions in the (v_Δ, μ_Δ) plane, for $\mu = 750$ GeV and different values of $\tan\beta$, where the origin is a false minimum at zero temperature and therefore there is a barrier separating the origin from the true EW minimum. These regions are then eligible to generate, at finite temperature, a strong enough EWPT as that exhibited in the right panel of Fig. 5.9. One can realize from the plot in the left panel of Fig. 5.9 that this region only appears, and becomes important, when v_Δ is non negligible. By means of the needed sizeable values of v_Δ, the plot shows how critical is for the appearance of the barrier to have a non negligible contribution of the triplet sector to EWSB.

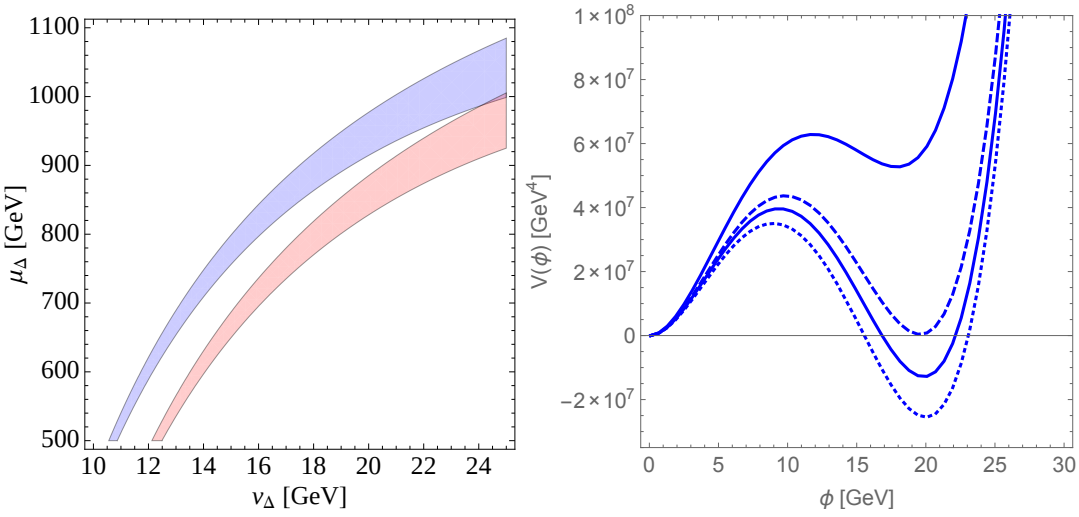

Figure 7.1: *Left: For* $\lambda = 0.7$, $\mu = 750$ *GeV, and* $\tan\beta = 1$ *(blue),* $\tan\beta = 1.5$ *(red), regions in the* (v_Δ, μ_Δ) *plane where the zero temperature tree level potential shows a false minimum at the origin. Right: For* $\tan\beta = 1$, $v_\Delta = 20$, *GeV* $\mu = 650$ *GeV and* $\mu_\Delta = 415$ *GeV sections of the five-dimensional potential at different temperatures along the direction that joins the false and true vacuums by a straight line,* $T = 0$ *and* $T = T_c$ *are depicted with dotted and dashed lines respectively.*

For any fixed value of $\tan\beta$ and points outside the corresponding band the zero temperature potential does not fulfil our required conditions for having a strong enough EWPT at finite temperature. In particular for points below the corresponding band the EW vacuum is a false minimum (or even it does not exist) and thus no transition from the origin to the EW minimum is possible at any temperature. This is exhibited at a particular point below the band, for the zero temperature potential along the direction where the slope of the barrier is minimized, in the left panel of Fig. 7.2 (solid line) where we can see that the EW minimum is not the true minimum. For points inside the corresponding band the EW minimum is the true minimum and the EWPT can proceed through a strong enough first order phase transition. The zero temperature potential for a point inside the band is exhibited in the left panel of Fig. 7.2 (dashed line). Finally for points above the corresponding band, the origin of the zero temperature potential becomes a saddle point as shown in the left panel of Fig. 7.2 (dotted line). Therefore in this region the barrier between the origin and the EWSB minimum can only be generated by thermal corrections, and the EWPT is too weak (or not even first order) as it happens in the SM or in the MSSM. At each point the value of the parameter λ is adjusted such that the value of the Higgs mass reproduces the experimental result $m_h = 125$ GeV. The needed values of λ are provided in the right panel of Fig. 7.2 where we show, for $v_\Delta = 20$ GeV, in the (μ, μ_Δ) plane contour lines of constant values of λ inside the bands for $\tan\beta = 1$ (blue) and $\tan\beta = 1.5$ (red).

Once identified the region in the parameter space where our potential is able to generate a first order EWPT we will study its temperature dependence. We will search for points where the phase transition is strong enough as to avoid any washout of the generated baryon asymmetry due to sphaleron transitions. This condition translates into the following bound for the Standard

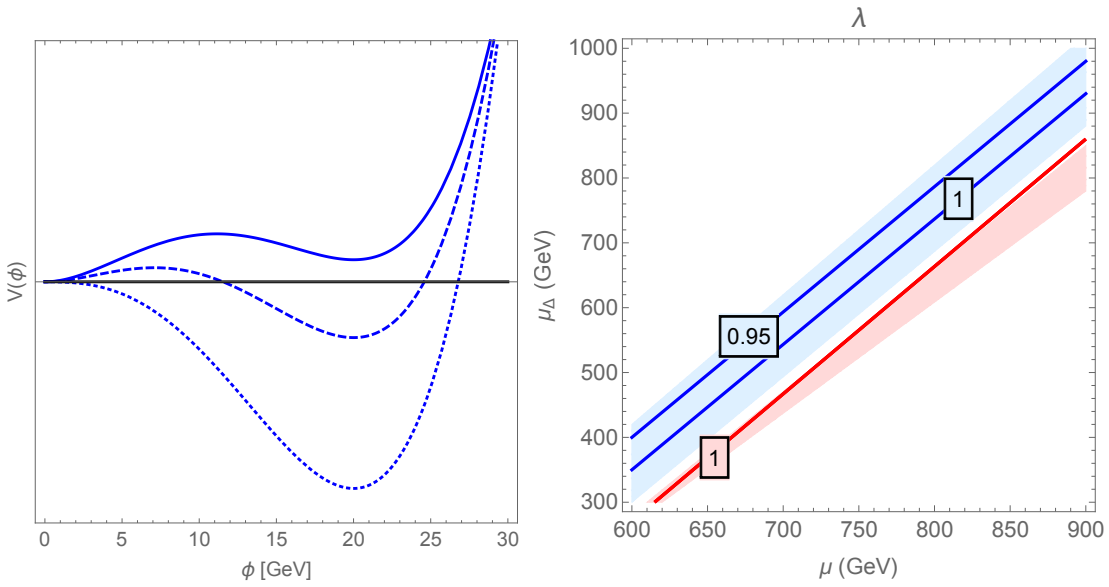

Figure 7.2: *Left: Sections of the potential at zero temperature in the direction of minimum slope for values of μ and μ_Δ above (dotted), inside (dashed) and below (solid) the bands where a first order phase transition is realized. Right: For $v_\Delta = 20$ GeV, values of λ that are needed to get the correct Higgs mass in the (μ, μ_Δ) plane for $\tan\beta = 1$ (blue) and $\tan\beta = 1.5$ (red).*

Model [185],

$$\frac{v(T_n)}{T_n} \gtrsim 1 \tag{7.16}$$

where $v(T_n)$ is the VEV of the Higgs field at the nucleation temperature (the temperature at which bubbles of the true vacuum start to nucleate and expand). We do not expect this bound to be very different in the present model, since the sphaleron energy is dominated by the contributions from the gauge field configurations excited in the sphaleron rather than the scalar ones [186].

The condition $v(T_c)/T_c \lesssim v(T_n)/T_n$, where $v(T_c)$ is the Higgs VEV at the critical temperature (the temperature at which both minima are degenerate) and is defined by

$$v(T_c) = \sqrt{H_1^0(T_c)^2 + H_2^0(T_c)^2 + 2\psi^0(T_c)^2 + 4\phi^0(T_c)^2 + 2\chi^0(T_c)^2}\,, \tag{7.17}$$

is generically satisfied, as we will see later on in this paper. Therefore, it is sufficient to consider the EWPT strong enough when the condition $v(T_c) \gtrsim T_c$ is fulfilled. In fact, this sufficient condition is much simpler to analyze than (7.16) as it can (and will) be easily done in the full five-dimensional Higgs potential.

In Figure 7.3 we present results for the critical temperature (left panel) and the order parameter of the phase transition at the critical temperature (right panel) in the (μ, μ_Δ) plane. Our results for the EWPT are even stronger than what it is shown in the left and right panels of Fig. 7.3, since the true order parameter of the EWPT (the order parameter at the nucleation temperature) will be bigger than the one at the critical temperature, as it was already observed. We only show points where the strong phase transition is generated by the zero temperature potential exhibiting a false minimum at the origin, the blue (for $\tan\beta = 1$) and red (for $\tan\beta = 1.5$)

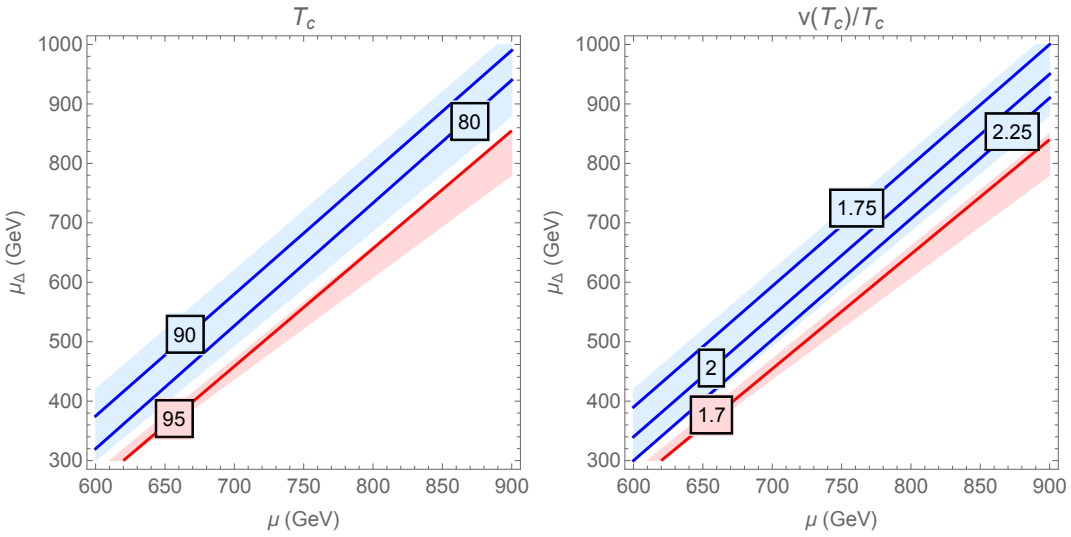

Figure 7.3: *Critical temperature in GeV (left panel) and order parameter of the phase transition (right panel) in the* (μ, μ_Δ) *plane for* $v_\Delta = 20$ *GeV and* $\tan\beta = 1$ *(blue),* $\tan\beta = 1.5$ *(red). In both plots we have shown the band where there is a barrier between the origin and the global EW minimum in the zero temperature effective potential for* $\tan\beta = 1$ *(blue) and* $\tan\beta = 1.5$ *(red). At each point* λ *is adjusted such that the Higgs mass reproduces the experimentally observed value.*

bands. We can see in the right panel of Fig. 7.3 that the strength of the phase transition increases as we approach the lower boundary of the corresponding band, as we will see in section 7.4, this region will be favored for the detection of the gravitational waves emitted during the EWPT.

7.3 Thermal tunnelling and nucleation temperature

Once we have computed the strength of the phase transition at the critical temperature, the next step is to compute the tunneling temperature to make sure that bubble nucleation does happen. Of course this is ensured if the phase transition is generated radiatively since there is no barrier at zero temperature and, as the universe cools down, we will always cross a point where the tunneling probability is $\mathcal{O}(1)$. However, in the region we are interested in, this is not guaranteed as there is a barrier at zero temperature and it could be too strong for the field to tunnel from the symmetric to the broken phase at any temperature.

The computation of the thermal tunneling in the five-field case presents computational challenges that are out of the scope of this work, hence, we will use an approximation to strip down our five field configuration to a one-dimensional field space. We will first consider the following,

$$H_1^0 \to \frac{v_1(T)}{v_2(T)} H_2^0 \quad \text{and} \quad \psi^0 \to \frac{v_\psi(T)}{v_\phi(T)}\phi^0,\ \chi^0 \to \frac{v_\chi(T)}{v_\phi(T)}\phi^0. \tag{7.18}$$

For the doublet sector this approximation is expected to be a very good one near the decoupling limit, where all scalar masses are much heavier than the SM Higgs mass, which is nearby the

spectrum we are considering in this paper [2], for the dependence of $\tan\beta$ on the temperature is a mild one [187]. Also, the smallness of v_Δ with respect to v_H will ensure that the triplet sector is well approximated by Eq. (7.18). Moreover, as pointed out in Ref. [188], the tunneling path is the one where the barrier is minimized and any approximation will only overestimate the size of it. In other words, if one finds that tunneling happens within the approximation, it is certain that it will also happen in the full five-dimensional field space.

In order to go from the two field configuration (H_2^0, ϕ^0) to one direction we will further reduce our field space by considering the smooth direction that joins the origin and the electroweak minimum passing through the saddle point, as can be seen in Fig. 7.4. We have chosen this direction by considering an ellipse in the (H_2^0, ϕ^0) plane,

$$H_2^0 \to f(\phi^0) = \left(1 - a + \sqrt{a^2 + (a-1)^2 - \left(\frac{\phi^0}{v_\phi} - a\right)^2}\right) v_2(T) \tag{7.19}$$

where the parameter a is the eccentricity of the ellipse. By tuning a we can get the right path and ensure that we connect smoothly the origin, the saddle point and the EW minimum at any temperature.

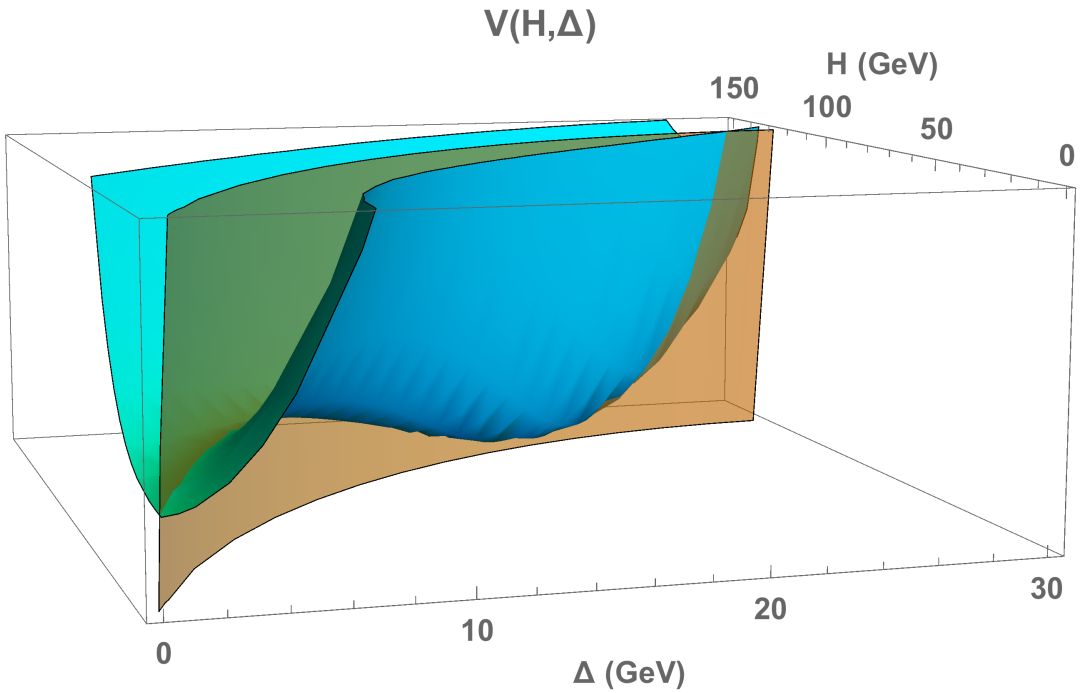

Figure 7.4: *Two dimensional projection of the tree level potential in a point which exhibits a first order phase transition between the origin and the EW minimum (which for the considered point is located at $v_\Delta = 20$ GeV and $v_H = 116.35$ GeV). The orange plane that intersects the potential corresponds to the ellipsoidal direction that joins the origin and the EW minimum.*

[2] For a light spectrum our calculation of the approximated nucleation temperature might require strong corrections.

The tunneling probability per unit time and unit volume from the false (symmetric) to the real (broken) minimum in a thermal bath is given by [189],

$$\frac{\Gamma}{\nu} \sim A(T) \exp\left[-B(T)\right], \quad B(T) \equiv \frac{S_3(T)}{T} \tag{7.20}$$

where the prefactor is $A(T) \simeq T^4$ and S_3 is the three-dimensional effective action. At very high temperature the bounce solution has $O(3)$ symmetry and the euclidean action is simplified to

$$S_3 = 4\pi \int_0^\infty r^2 dr \left[\sum_k \frac{1}{2}\left(\frac{d\phi_k}{dr}\right)^2 + V(\phi_k, T)\right], \tag{7.21}$$

where $r^2 = \vec{x}^{\,2}$. Using (7.18) and (7.19) we can rewrite it as,

$$S_3 = 4\pi \int_0^\infty r^2 dr \left[\frac{1}{2}F(\phi^0)\left(\frac{d\phi^0}{dr}\right)^2 + V(\phi^0, T)\right], \tag{7.22}$$

where

$$F(\phi^0) = \left(1 + \frac{v_1(T)^2}{v_2(T)^2}\right) f'(\phi^0) + \left(1 + \frac{v_\psi(T)^2}{v_\phi(T)^2} + \frac{v_\chi(T)^2}{v_\phi(T)^2}\right). \tag{7.23}$$

The bounce will be the solution to the euclidean equations of motion which yield the following equation

$$F(\phi^0)\left[\frac{d^2\phi^0}{dr^2} + \frac{2}{r}\frac{d\phi^0}{dr}\right] + \frac{1}{2}F'(\phi^0)\left(\frac{d\phi^0}{dr}\right)^2 = V'(\phi^0, T), \tag{7.24}$$

with the boundary conditions

$$\lim_{r\to\infty} \phi(r) = 0 \quad \text{and} \quad d\phi/dr|_{r=0} = 0. \tag{7.25}$$

The nucleation temperature T_n is defined as the temperature at which the probability for a bubble to be nucleated inside a horizon volume is of order one, in our case it turns out to happen when $S_3(T_n)/T_n \sim 135$.

In Figure 7.5 we plot the effective action over the temperature for two points of the (μ, μ_Δ) plane. These plots show how the nucleation temperature depends on the strength of the phase transition. If the phase transition is not very strong then there is no large gap between the T_n and T_c (right plot). When the phase transition is very strong, a supercooling phenomenon happens and the nucleation temperature is quite smaller than T_c (left plot in the figure). Of course if we move in the parameter space to points where $\phi(T_c)/T_c$ is even larger, we will eventually find a situation where S_3/T never reaches the correct value and bubble nucleation does not happen as the universe cools down. These points correspond to a thin band that is located at the bottom of the blue and red bands that we plot in Fig. 7.3.

7.4 Gravitational waves from the phase transition

It is known that a strong enough first order phase transition can generate sizable gravitational waves (GW's). Since we are able to generate such a strong phase transition, due to the tree level nature of the barrier, we analyze in this section the possible spectrum of GW's. The spectrum

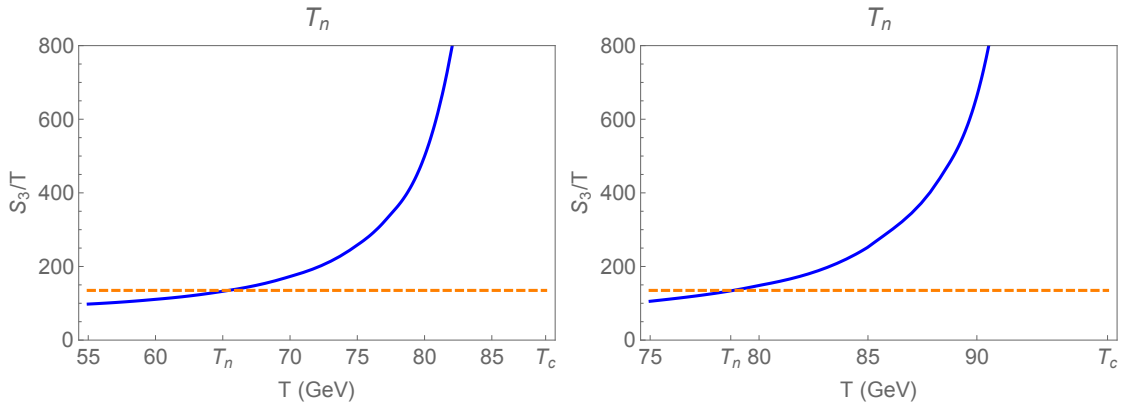

Figure 7.5: *Left: Plot of the effective action over the temperature for* $\mu = 650$ *GeV,* $\mu_\Delta = 475$ *GeV,* $v_\Delta = 20$ *GeV and* $\tan\beta = 1$. *The order parameter at the critical temperature is* $\phi(T_c)/T_c = 1.82$ *and* $T_c = 89$ *GeV. The dashed line corresponds to* $S_3(T)/T \sim 135$ *and the crossing point with the thick blue line happens at the nucleation temperature* $T_n = 65$ *GeV. Right: The same for* $\mu = 650$ *GeV,* $\mu_\Delta = 375$ *GeV,* $v_\Delta = 20$ *GeV and* $\tan\beta = 1.5$, *where* $\phi(T_c)/T_c = 1.65$, $T_c = 96$ *GeV and* $T_n = 79$ *GeV.*

can be characterized by only two parameters: the duration of the phase transition $1/\beta$, which is given by

$$\frac{\beta}{H} = T\frac{d}{dT}\left(\frac{S_3}{T}\right) , \tag{7.26}$$

and the latent heat

$$\epsilon = \Delta V(T_n) - T_n \frac{d\,\Delta V(T)}{dT}\Big|_{T_n} , \tag{7.27}$$

where

$$\Delta V(T) = V(0,T) - V(\langle\phi(T)\rangle, T) . \tag{7.28}$$

The latent heat is usually normalized to the energy density of the radiation in the plasma, through the dimensionless parameter α,

$$\alpha = \frac{\epsilon}{\frac{\pi^2}{30} g_* T_n^4} \tag{7.29}$$

where g_* is the effective number of degrees of freedom at the temperature T_n.

In Figure 7.6 we show results for the computation of the α (left panel) and β/H (right panel) parameters along a vertical straight line of the band in Fig. 7.3 which corresponds to a fixed $\mu = 650$ GeV value. In Figure 7.7 we also show the values of the nucleation temperature (right panel) and the order parameter at that temperature (left panel). Note that for stronger values of the phase transition, α gets bigger and β/H smaller. This means that the energy gap between the false and the true vacuum is big at the nucleation temperature and that the phase transition happens fast, which is precisely what one needs to get observable gravitational waves.

The above described parameters, which only depend on the finite temperature effective potential, are the only input coming from the particle physics model. Once we determine these two, we have to plug them into the cosmological picture. First we will treat the expanding bubbles, and the fluid they drag with, as if the bubbles where the only existing object. The collisions of these

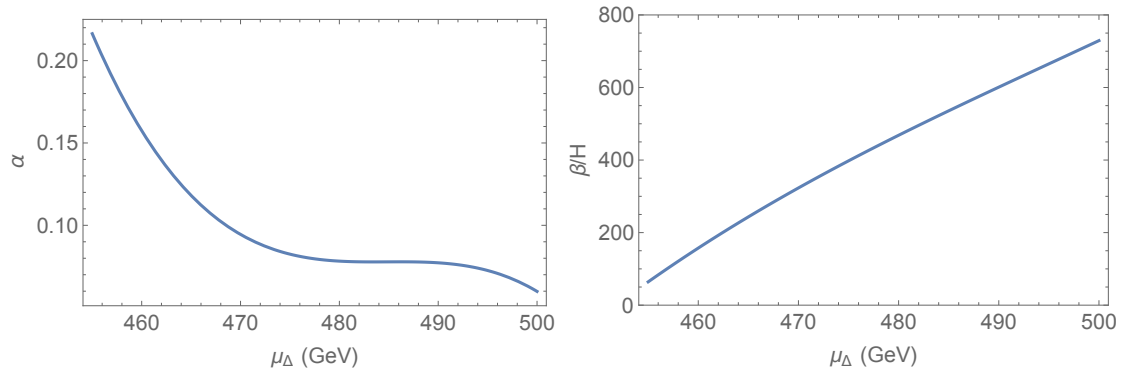

Figure 7.6: *Left: Values of the α parameter for $v_\Delta = 20$ GeV, $\mu = 650$ GeV and $\tan\beta = 1$. The number of effective degrees of freedom at the time of nucleation is $g_* = 115.75$. Right: Values of the β/H parameter for the same values of the model parameters.*

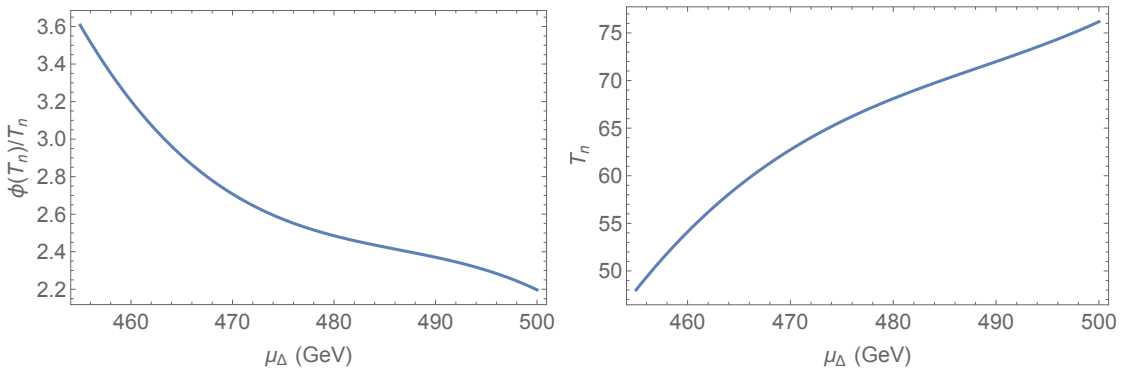

Figure 7.7: *Left: Values of the order parameter at the nucleation temperature as a function of μ_Δ for $v_\Delta = 20$ GeV, $\mu = 650$ GeV and $\tan\beta = 1$. Right: Nucleation temperature T_n for the same values of the parameters.*

vacuum bubbles will then generate a GW spectrum [190]. In the second part we will consider calculations that model the fluid in a more detailed manner, in this case the phase transition leads to the creation of sound waves which in turn will produce gravitational waves [191]. The formulas corresponding to each case are detailed in Appendix C.2.

Results for the spectrum of GW's

As we said in the previous section, when the phase transition is not radiatively generated, there can be points in the parameter space where the barrier is so large that no nucleation is possible. It is precisely close to these regions, but still inside the region where the nucleation still happens, where the characteristics of the phase transition will be optimized for the detection of its GW spectrum. In particular the parameter β/H, will be minimized close to the region where S_3/T never reaches the value ~ 135 and $\beta/H \sim 0$. As can be seen in Fig. 7.6, approaching this region we have found points where $\beta/H \sim 50$ and $\alpha \sim 0.22$. A spectrum coming from a point of these characteristics is shown in Fig. 7.8 and may be probed by eLISA [192, 193] and BBO [194, 195].

In the case of eLISA, the chances for detecting GWs improve with the design. Design 3, which features three 5 Gm arms and 5 years of data taking, is the one that could probe both GW's coming from bubble collisions, in the envelope approximation, and GW's coming from sound waves. We also see that the latter could be detected by eLISA, even with design 1.

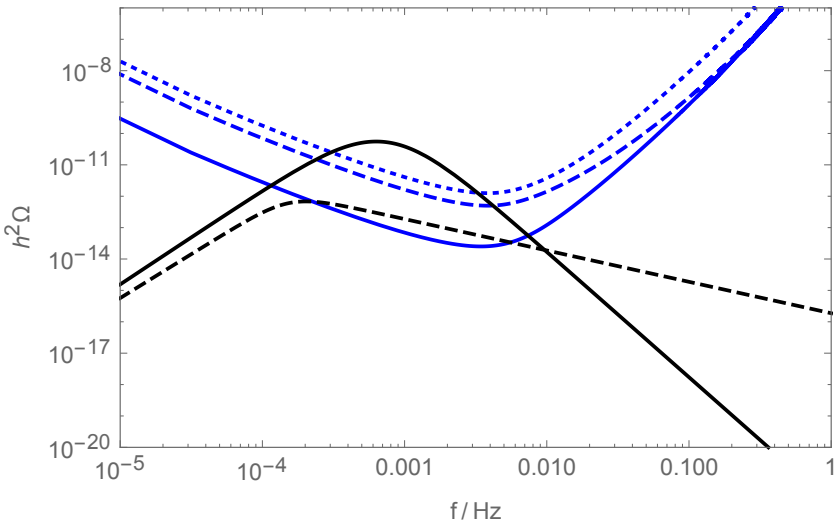

Figure 7.8: *Spectrum of the stochastic gravitational wave background coming from bubble collisions (dashed) and sound waves (solid) for a point where* $\alpha \sim 0.22$ *and* $\beta/H \sim 57$*, which corresponds to* $\mu = 650$ *GeV and* $\mu_\Delta = 455$ *GeV. The sensitivity curves of the eLISA designs are displayed in blue; design 1 (dotted), design 2 (dashed) and design 3 (solid).*

7.5 Discussion

During this chapter we have explored the nature of the EWPT in the SCTM. We have shown that, thanks to a tree level effect by which there is a barrier separating the minimum at the origin and the EWSB minimum, an important part of the parameter space of the model exhibits a phase transition whose order parameter is strong enough, both for the purpose of EWBG and for the detection of gravitational waves. We have decided not to focus on the regions where no barrier is generated at tree level (above the bands in Figs. 7.3 and 7.2), as analyzing the phase transition in this region would involve the consideration of higher order loop corrections in the thermal effective potential, which goes beyond the scope of our study.

In Sec. 7.2 we have discussed how the appearance of the barrier is directly linked to a non negligible contribution of the triplet sector to EWSB (Fig. 7.1). Moreover, as large v_Δ is tied to the presence of light triplet-like states, we can establish a relation between a strong EWPT and collider searches. One therefore expects these new states to be there in the regions where a barrier is generated at tree level, however, their detection is challenging due to their triplet like nature. In Chapter 5, we already studied the consequences for collider phenomenology of a scenario where EWSB is driven by doublets, but also features some triplet impurities. Modified Higgs coupling rates ($h \to \gamma\gamma$) or some signals such as $W^\pm W^\pm$ or $W^\pm Z$, which are specific of Higgs sectors with triplet representations, could act as smoking gun signals of the model and therefore probe the

nature of the phase transition at high temperature. A dedicated search of the lightest neutral triplet-like state could also be of great help in constraining this scenario (Chapter 8).

We also have checked that nucleation does happen in most parts of the parameter space where the order parameter is larger than one. The potential of the model features a five-dimensional field space due to the introduction of three new triplet chiral superfields, on top of the two usual MSSM doublets. To simplify the calculation of the nucleation temperature, we have minimized the euclidean action functional in the multi-field configuration space by using a smooth path going from the minimum at the origin to the EWSB minimum at finite temperature through the saddle point. Because of the character of our parameter space we are confident enough that the approximation works properly up to small corrections. In the last section it is shown how future interferometers such as eLISA could observe gravitational waves generated during the phase transition for some parts of the parameter space.

8

$SU(2)_V$ fiveplets at the LHC

As it can be seen for instance in the Figures 5.9 and 5.12 of Chapter 5, the SCTM scalar spectrum features a doublet MSSM-like spectrum that is difficult to probe, it is superheavy and out of the reach of LHC. However, there is also a set of light triplet-like states which is well within LHC reach and could thus provide a promising avenue to test the model, moreover, in Fig. 4.4 (Chapter 4) and Section 5.4 (Chapter 5), it is shown that the mass of the triplet-like states is tied to the value of v_Δ. Therefore searching for these scalars is also testing the nature of EWSB and probing the interesting properties that the SCTM has shown to feature when v_Δ is sizable (both in particle physics and cosmology). It is then of great importance to perform a collider study searching for these triplet-like states. In particular to search for the $SU(2)_V$ custodial fiveplet (H_5) [1] that features a neutral CP-even (H_5^0), singly ($H_5^\pm$), and doubly ($H_5^{\pm\pm}$) charged components and that, for reasonable values of v_Δ, is always going to be in the ballpark of $\mathcal{O}(150-400)$ GeV masses.

As the fiveplet does not couple to quarks (it is fermiophobic), production via gluon fusion is not available. Furthermore, if the VEV of the fermiophobic Higgs is small (as compared to the SM-like Higgs doublet VEV), vector boson fusion (VBF) and associated Higgs vector boson production (VH) quickly become highly suppressed. Since these are the dominant production mechanisms in the SM, they have been assumed as the production mechanisms in almost all Higgs-like boson searches regardless of if they are fermiophobic or not. On the other hand since LHC measurements of the 125 GeV Higgs boson couplings seem to indicate a SM-like Higgs boson, this implies a small VEV for any additional exotic Higgs boson. As these measurements increase in precision without observing a deviation from the SM prediction, previous collider searches for fermiophobic Higgs bosons, which assumed SM-like production mechanisms, become increasingly obsolete.

However, Drell-Yan (DY) Higgs pair production of the fiveplets is sizable even in the limit of small exotic Higgs VEV. Furthermore, since there is no $b\bar{b}$ decay to compete with, custodial fiveplets can have large branching ratios to vector boson pairs and in particular photons. This can be combined with DY pair production to place stringent constraints on the fiveplet Higgs bosons using multiphoton final states. Actually, the W boson mediated $H_5^\pm H_5^0$ production channel (see Figure 8.1), followed by $H_5^\pm \to W^\pm H_5^0$ and $H_5^0 \to \gamma\gamma$ decays, leads to a $4\gamma + X$ final state, which has been proposed as a probe [196, 197] of fermiophobic Higgs bosons at high energy colliders. However, the $H^\pm \to W^\pm H_F^0$ decay requires a mass splitting between the charged and neutral Higgs. In custodial Higgs triplet models such as the SCTM or the GM model, the neutral and charged Higgs scalars are predicted to be degenerate, thus the CDF $4\gamma + X$ search

[1] Since the collider analysis performed in this chapter can be extended to the non-supersymmetric GM model (where only one $SU(2)_V$ fiveplet is present in the scalar spectrum) we change the notation here and denote the fiveplet as H_5 instead of F_S.

of Ref. [198] cannot be applied to this case [2]. We show for the first time that when the W boson loop dominates the effective couplings to photons, a custodial fiveplet scalar below ~ 110 GeV is ruled out by 8 TeV LHC diphoton searches independently of the Higgs triplet VEV's. Larger masses possibly up to ~ 150 GeV can also be ruled out if charged scalar loops produce large constructive contributions to the effective photon couplings. We also find that diboson searches, and in particular ZZ searches, may be useful for higher masses allowing us to potentially obtain limits again for custodial fiveplet masses up to ~ 250 GeV independently of the Higgs triplet VEV's.

8.1 Pair production of H_5^0

The main focus of this study will be the $pp \to W^\pm \to H_5^0 H_5^\pm$ production channel shown in Fig. 8.1. The relevant vertex for this Drell-Yan pair production reads

$$V_{W H_5 H_5} \equiv ig\frac{\sqrt{3}}{2}(p_1 - p_2)^\mu \,, \tag{8.1}$$

where we can see the coupling does not depend on the triplet VEV's and therefore DY is not suppressed even in the case when the triplet VEV's are small. We show in Figure 8.2 the cross section (solid blue) as a function of H_5^0 for the $H_5^0 H_5^\pm$ channel. We see that it can be $\sim \mathcal{O}(100)$ fb all the way up to ~ 200 GeV at 8 TeV (dashed blue curve) while at 13 TeV (solid blue curve) it will be increased by roughly a factor of ~ 2. If the fiveplet is instead produced in pair with a custodial triplet which is 100 GeV heavier (dotted blue) the cross section is considerably reduced. Note that there are also NLO contributions which may generate $\sim \mathcal{O}(1)$ K-factors for Higgs pair production [199–201], but we do not explore this issue here as it does not qualitatively affect the discussion. Our leading order results for the $pp \to W^\pm \to H_5^\pm H_5^0$ production cross sections are obtained from Madgraph [202] using a modified version of the GM model implementation of Ref. [203], which, since the light triplet-like scalar spectrums of the GM model and the SCTM are identical, provides a good description of the fiveplet dynamics.

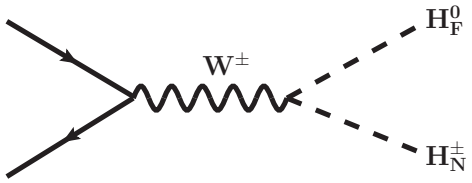

Figure 8.1: *The dominant contribution to custodial fiveplet scalar pair production.*

To demonstrate the utility of the DY Higgs pair production mechanism we show for comparison results for VBF single H_5^0 production. We see clearly that once the measurements of the

[2] Throughout this chapter we assume that the $SU(2)_V$ custodial ordering holds and the fiveplet is degenerate in mass. We consider this to be a good approximation since the mass splitting generated in the RGE improved SCTM between the neutral and singly charged components (which is critical for DY pair production, see Fig. 8.1) is not going to be larger than ~ 15 GeV (see Chapter 5, in particular Figs. 5.9 and 5.10). Furthermore, the CDF search was not able to rule out fermiophobic Higgs masses when $m_{H^0} > m_{H^\pm}$, which is precisely the situation that we encounter in realistic SCTM scenarios.

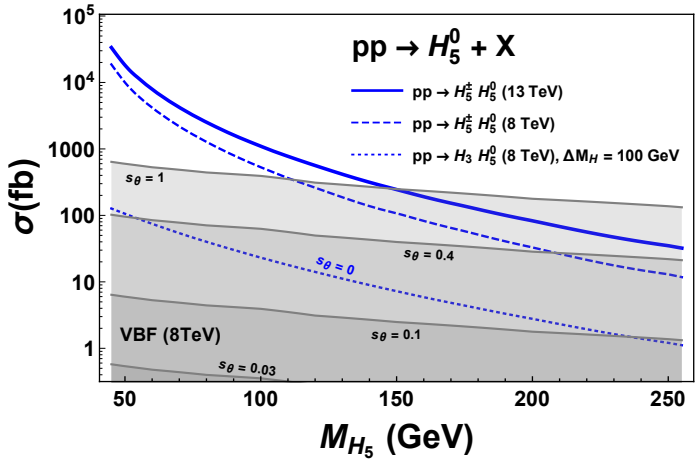

Figure 8.2: *Drell-Yan Higgs pair production cross sections for a custodial fiveplet scalar at the LHC with $\sqrt{s} = 8$ TeV (dashed blue curve) and $\sqrt{s} = 13$ TeV (thick blue solid curve). We also show the case where the fiveplet is produced along with a custodial triplet (blue dotted) which is 100 GeV more massive (see text for more information).*

Higgs boson at 125 GeV constrain $s_\theta \ll 1$ [3], the VBF production channel quickly becomes highly suppressed relative to the DY Higgs pair production. Similar behavior can be seen for the VH production channels which are typically smaller than the VBF cross sections except at very low masses [204–206].

To summarize, we see that $\sim \mathcal{O}(100)$ fb cross sections are obtained for the $pp \to H_5^0 H_5^\pm$ Higgs pair production channel in the mass range $45 - 250$ GeV. Crucially this production mechanism is independent of the Higgs triplet VEV's unlike VBF and VH production. As we will see, diphoton and diboson searches at the 8 TeV are sensitive to $\sim \mathcal{O}(100)$ fb cross section times branching ratios. Thus if the branching ratios to dibosons are large, searches at the LHC for pairs of photons or Z and W bosons should be able to probe the fiveplet in this mass range.

8.2 Decay of H_5^0

In addition to the WH_5H_5 vertex of Eq. (8.1), H_5^0 will have tree level couplings to WW and ZZ pairs which are generated during EWSB and which will be proportional to the triplet Higgs VEV's. These can be parametrized as

$$\mathcal{L} \supset s_\theta \frac{H_5^0}{v}\left(g_Z m_Z^2 Z^\mu Z_\mu + 2 g_W m_W^2 W^{\mu+} W_\mu^-\right), \tag{8.2}$$

where $g_Z = 4/\sqrt{3}$ and $g_W = -2/\sqrt{3}$. The ratio $\lambda_{WZ} = g_Z/g_W$ is fixed by custodial symmetry to be $\lambda_{WZ} = -1/2$ while for a custodial singlet such as the Higgs one has $\lambda_{WZ} = 1$ [207]. At one loop the couplings in Eq. (8.2) will also generate effective couplings to $\gamma\gamma$ and $Z\gamma$ pairs via the W boson loops shown in Fig. 8.3. We can parametrize these couplings with the effective operators

$$\mathcal{L} \supset \frac{H_5^0}{v}\left(\frac{c_{\gamma\gamma}}{4} F^{\mu\nu} F_{\mu\nu} + \frac{c_{Z\gamma}}{2} Z^{\mu\nu} F_{\mu\nu}\right), \tag{8.3}$$

[3] θ is the angle that mixes the doublet and triplet sectors (see Eq. (4.32)).

where $V_{\mu\nu} = \partial_\mu V_\nu - \partial_\nu V_\mu$. We again define similar ratios,

$$\lambda_{V\gamma} = c_{V\gamma}/g_Z \,, \tag{8.4}$$

where $V = Z, \gamma$ and we have implicitly absorbed a factor of s_θ into $c_{V\gamma}$. There are also contributions to the effective couplings in Eq. (8.3) from the additional charged Higgs bosons which are necessarily present in the GM model and the SCTM. These contributions can be large or small depending on the model and parameter choice. They can in principle lead to large enhancements [208] when there is constructive interference with the W boson loop, or suppressions if there are cancellations between the different contributions [209, 210] leading to small $c_{V\gamma}$ effective couplings.

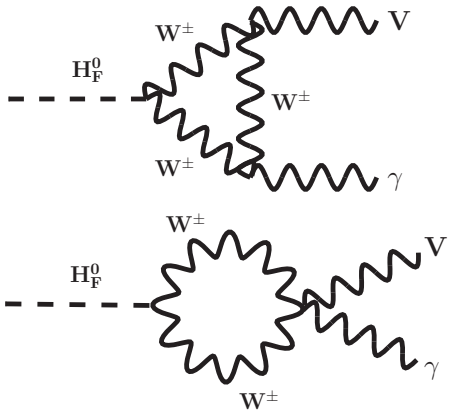

Figure 8.3: *One loop contributions from W boson loops to the $H_5^0 \to V\gamma$ decays ($V = Z, \gamma$).*

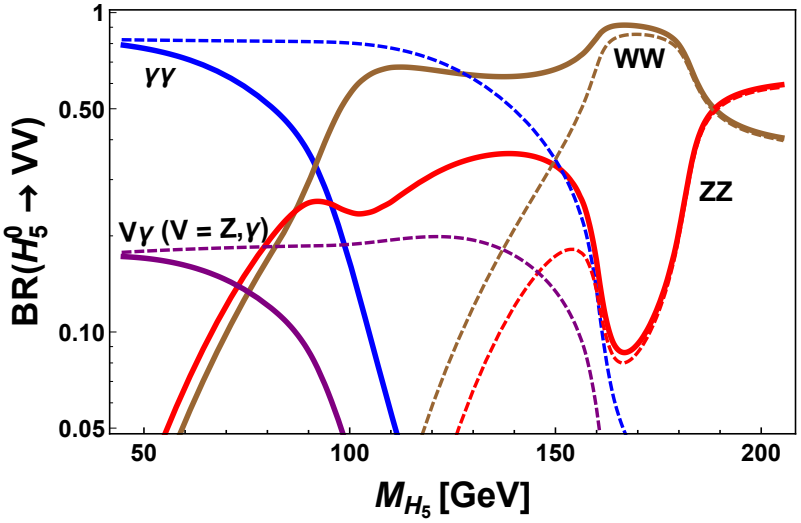

Figure 8.4: *Branching ratios for H_5^0 as a function of its mass.*

We show the Branching Ratios of H_5^0 in Figure 8.4. To obtain the three and four body decays we have integrated the analytic expressions for the $H_5^0 \to V\gamma \to 2\ell\gamma$ and $H_5^0 \to VV \to 4\ell$ fully

differential decay widths computed and validated in [97,211,212]. For the explicit W loop functions which contribute to the effective couplings we use the parametrization and implementation found in [213]. The branching ratios will only depend on the ratios λ_{WZ} and $\lambda_{V\gamma}$, and in some cases only on λ_{WZ} if the W loop (see Fig. 8.3) dominates the $H_5^0 V\gamma$ effective couplings (solid curves). In this case any s_θ dependence in $\lambda_{V\gamma}$ cancels explicitly. At low masses, below $\sim$ 100 GeV, the branching ratio into pairs of photons starts to become significant and quickly dominant below the W mass, or at higher masses if the couplings to photons are enhanced (dashed lines). We note that these branching ratios include the $\gamma^*\gamma$ contribution which, as shown in Fig. 8.4, can be sizeable at low masses. At larger masses the three and four body decays involving W and Z bosons become relevant and eventually completely dominant above the WW and ZZ thresholds.

8.3 Bounds on the H_5^0

In Figure 8.5 we show the $pp \to W^\pm \to H_5^\pm H_5^0$ production cross section times branching ratio for a custodial fiveplet decay into photon (blue), WW (brown), and ZZ (red) pairs at 8 TeV (top) and 13 TeV (bottom). We also show the limits (dashed lines) coming from ATLAS diphoton searches at 8 TeV [214] (blue) as well as CMS 7+8 TeV searches [215] for decays to WW (brown) and ZZ (red). To estimate the limits at 13 TeV we have simply rescaled the 8 TeV limits by a factor of 2 which is roughly the increase in Higgs pair production cross section. Our leading order results for the $pp \to W^\pm \to H_5^\pm H_5^0$ production cross sections are calculated using the Madgraph/GM model implementation from [202, 203]. The branching ratios are obtained from the partial widths into $\gamma\gamma, V^*\gamma$ $(V = Z, \gamma), WW$, and ZZ which are computed for the mass range $45 - 250$ GeV.

We focus on the regime where the effective couplings of the fiveplet to $\gamma\gamma$ and $Z\gamma$ are dominated by the W loop contribution shown in Fig. 8.3. The effects of the charged scalar sector could in principle be large leading to enhanced or suppressed effective couplings to photons. As discussed above, this can affect the upper limit of masses which can be ruled out and could in principle allow for masses up to the WW threshold to be ruled out by diphoton searches. Since these effects are more model dependent we do not consider them here.

We see in the top of Fig. 8.5 that by exploiting the $H_5^0 H_5^\pm$ Higgs pair production mechanism, custodial fiveplet scalars with masses $\sim$ 107 GeV can be ruled out by 8 TeV diphoton searches, independently of the Higgs triplet VEV's. These are the first such limits on custodial fiveplet scalars and in particular, since the charged and neutral components are degenerate, limits from Tevatron $4\gamma + X$ searches do not apply. This is because for cases like the custodial fiveplet where the masses are degenerate, the $H_5^\pm \to H_5^0 W^\pm$ decay is not available. In this case the one loop $H_5^\pm \to W^\pm\gamma$ decay can become dominant leading instead to a $3\gamma + W$ signal. Examining this decay as well should improve the sensitivity relative to LHC diphoton searches, but we do not explore that here.

To emphasize the utility of the DY pair production mechanism, we also show in the top of Fig. 8.5 the cross section times branching ratio assuming the VBF production (gray shaded region) mechanism at 8 TeV. We have fixed $s_\theta = 0.4$ for the doublet-triplet VEV mixing angle. The value $s_\theta = 0.4$ is towards the upper limit of values still allowed by electroweak precision and 125 GeV Higgs data ($s_\theta = 0.4$ corresponds roughly to $v_\Delta \sim 25$ GeV), but we can see in Fig. 8.5 this already renders diphoton searches for custodial fiveplet scalars based on VBF (and similarly for VH) production irrelevant.

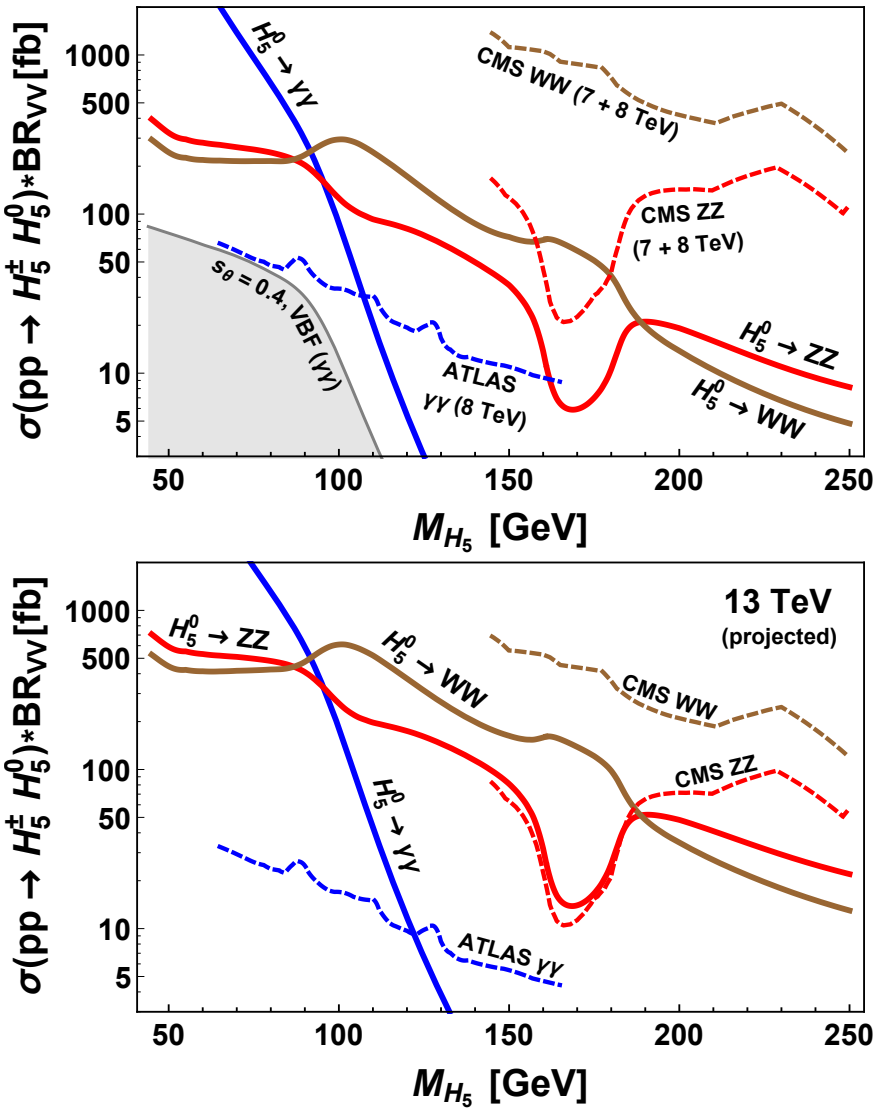

Figure 8.5: *Top: Drell-Yan $H_5^0 H_5^\pm$ production cross sections times branching ratio at 8 TeV (solid curves) into $\gamma\gamma$ (blue), ZZ (red), and WW (brown) for the fermiophobic fiveplet found in custodial Higgs triplet models. The 95% exclusion limits (dashed curves) from diphoton 8 TeV ATLAS [214] and 7+8 TeV CMS WW and ZZ searches [215] are also shown for each channel. In the gray shaded region we show for comparison the $s_\theta = 0.4$ contour for single H_5^0 VBF production (see text). Bottom: Similar to top, but for 13 TeV. For the 13 TeV limits we have simply rescaled 8 TeV limits by a factor of 2.*

We also emphasize that ruling out a custodial fiveplet below ~ 110 GeV independently of the VEV allows us to unambiguously close the fiveplet 'window' at masses below ~ 100 GeV [216] which is still allowed by electroweak precisions data [100] and essentially unconstrained by other LEP, Tevatron, and LHC direct searches. Thus we are able to rule out an interesting region of parameter space of custodial Higgs triplet models which would otherwise be difficult to constrain directly. We estimate in the bottom of Fig. 8.5 that 13 TeV diphoton searches will be sensitive to scalar masses up to ~ 125 GeV in the regime of dominant W boson loop, though NLO Higgs pair production effects [201] may allow this to be extended further. The diphoton search discussed here may of course be useful for other scalars which are found in custodial Higgs triplet models, but we do not explore this here.

Finally, we also see in Fig. 8.5 that WW and ZZ searches may be useful for probing custodial fiveplet scalars independently of the Higgs triplet VEV's as well. Though 8 TeV searches are not quite sensitive, larger Higgs pair production cross sections at 13 TeV (see Figure 8.1) should allow for fiveplet masses well above diphoton limits to be probed and possibly as high as ~ 250 GeV. In particular, as we can see in the bottom of Fig. 8.5, the ZZ channel should become sensitive with early 13 TeV data for masses around the ZZ threshold. These also serves as a useful compliment to W^+W^+ searches for the doubly charged component of the custodial fiveplet [217].

8.4 Discussion

As a way of probing the model, in this chapter we examined the collider properties of the SCTM scalar fiveplet. By using the Drell Yan pair production mechanism that opens up for representations larger than the doublet, we where able to derive bounds on the mass of the fiveplet. As v_Δ scales with the masses of the triplet-like states, these lower bounds on the fiveplet mass can be translated to upper bounds on v_Δ which will give us valuable information about features of the SCTM difficult to probe otherwise (see Chapters 6 and 7).

Let us emphasize that this study is valid both for the SCTM and the GM model. In particular, this is the first time that a custodial fiveplet scalar below ~ 110 GeV is ruled out by 8 TeV diphoton searches and possibly up to higher masses if charged scalar loops produce large constructive contributions to the effective photon couplings. Since these limits are largely independent of the Higgs triplet VEV's, they robustly close the 'fiveplet window' at masses below ~ 110 GeV still allowed by electroweak precision and 125 GeV Higgs boson data. We also find that 13 TeV diboson searches, and in particular ZZ searches, may be useful for larger fiveplet masses, allowing us to potentially obtain limits up to ~ 250 GeV, also independently of the VEV. Note that above ~ 200 GeV, these limits can become really interesting as they will start to probe the realistic realizations of the SCTM that we introduced in Chapter 5 and put upper bounds on triplet VEV's below $v_\Delta \sim 25$ GeV.

Along with direct searches, precision studies of the Higgs are important to test the value of v_Δ. Loop induced couplings like $h\gamma\gamma$ can get severely modified in the presence of light charged states. Since the fiveplet has charged and doubly charged components, it will also reveal its presence in deviations from $r_{h\gamma\gamma} = 1$ (the ratio of the coupling with respect to the SM value). For instance, for $v_\Delta \sim 20$ GeV we have $m_{H_5} \sim 250$ GeV and then $r_{h\gamma\gamma} \sim 1.2$ (see Figures 5.9 and 5.10, and Table 5.3) which, translated to signal strengths for different production mechanisms, can be close to the precision available at LHC. This deviation gets softened for smaller triplet VEV's, in particular for $v_\Delta \sim 10$ GeV, $m_{H_5} \sim 500$ GeV and $r_{h\gamma\gamma} \sim 1.05$ (Fig. 5.12).

Final remarks

The way in which progress in theoretical physics is carried out is twofold:

- Sometimes theory needs to adapt to new experimental results which cannot be explained by current theories. For instance, the formulation of quantum mechanics was triggered by experiments at the beggining of the XX$^{\text{th}}$ century who disagreed with the predictions of classical mechanics.

- The opposite is also possible, reductionism and the search for theoretical consistency can often lead to the construction of mathematical frameworks that are then vindicated by experiment. General relativity was formulated by Einstein in a single paper appeared in 1915, it follows from seeking to incorporate gravity to his 1905 special theory of relativity. Since 1915, GR has been able to pass a number experimental tests with tremendous success, the most recent just this year, the direct discovery of gravitational waves [218].

I think that the work presented in this thesis is a an example of the former approach. The 2012 discovery of the Higgs boson not only represents the experimental closure of the Standard Model but also the first direct probe of the mechanism by which the electroweak symmetry is broken and, since EWSB is universal, a new window to physics beyond the SM. It is therefore mandatory to use it as a tool to put to test the plethora of BSM proposals that have been appearing steadily for decades now. This is what we did with supersymmetry and in particular with the MSSM in Chapter 3. By using a run and match procedure we analyzed the consequences of a 125 GeV Higgs for minimal versions of supersymmetry. From this analysis we concluded that it is difficult to construct natural versions of SUSY using only the minimal picture and tried to solve this by giving up on minimality.

It is not the intention of these final remarks to be a thorough summary of the thesis, we refer the reader to the discussion section of each of the chapters for details. However, let us list a few generalities of the SCTM that we consider worth mentioning.

In Chapters 4 and 5 we introduced the SCTM. The main goal of the SCTM is to fit the observed Higgs mass in a more natural way without having to rely on large radiative corrections (e.g. superheavy stops). In addition we found many interesting features that alleviate some of the shortcomings of the MSSM when applied to cosmology (Chapters 6 and 7), or when embedded in a SUSY breaking mechanism such as gauge mediation (Section 5.3 of Chapter 5).

The SCTM is very non minimal, three extra $SU(2)_L$ triplet χ_{SF}'s translate into a lot of new DOF's to cope with. However, beyond the singlet, it is the most minimal extension of the MSSM that can feature the custodial pattern (1.22) when breaking the EW symmetry [207]. Because of this pattern, after EWSB the mass eigenstates get ordered under the $SU(2)_V$ remnant symmetry of the vacuum (Chap. 4). We consider this to be one of the most appealing features of the model, it allows to keep track of the plethora of new states that are introduced and most importantly, it holds to very good degree after quantum corrections (in the form of RGE's) are introduced and consistently considered. The latter point is one of the strengths of the SCTM with respect to its non-supersymmetric counterpart. Besides worsening the hierarchy problem of the SM by introducing new scalar masses, the GM model shows no theoretical consistency when carefully analyzed (see Sec. 4.1); this is due to the custodial breaking that loop corrections introduce in the theory and for which it lacks a reasonable explanation. In Chapter 5 we showed how these problems are overcome in the supersymmetric picture and demonstrated that realistic scenarios of the SCTM where the custodial breaking is taken into account can be easily derived.

During the course of our studies one thing became evident, besides the Higgs, sizable values of v_Δ are tied to the presence of light states in the spectrum of the model, in particular to triplet-like states which couple very weakly. Since a sizable value of v_Δ is responsible for a lot of the interesting features of the model, collider searches for these states can act as a probe. This is why we performed a detailed collider analysis to constrain these new states in Chapter 8. Although with 8 TeV data one is not able to derive sufficiently large upper bounds on the mass of these states, at 13 TeV LHC could start to probe larger masses that would translate into meaningful upper bounds on v_Δ, thus constraining the SCTM at a broader level than just its collider phenomenology. It is also worth mentioning that this collider study generated very interesting results that apply to more general situations than just the SCTM (or GM model) (see the original Ref. [9]). This is proof that sometimes studying non minimal situations presents non standard challenges which can lead to insights in directions that are not always expected.

In addition, for the SCTM the interplay between direct searches and precision measurements of the Higgs properties, in particular of loop induced couplings such as $h\gamma\gamma$, is of great importance. Some of the light triplet-like states mentioned above are charged and can modify loop induced couplings in a non negligible manner (see Chapters 4 and 5), for which LHC13 or next generation colliders could be sensitive.

Let us end these remarks by mentioning that although the SCTM does fit the Higgs mass in a more natural way, it does not solve the problem of not finding the superpartners responsible for canceling dangerous loop corrections to the Higgs mass. Because this model softens the Higgs sensitivity to UV physics in the same way as the MSSM, the final test to its naturalness will be given by the bounds on stops and gluinos. Just as for the MSSM, the more severe these bounds are, the more pressing is the need for an explanation of the hierarchy between $\mathcal{Q}_{EW}$ and $\mathcal{Q}_{Exp}$. At some point, the bounds can get to a point where both minimality and naturalness are lost and less baroque realizations of SUSY will be favored. It is in the hands of LHC13-14 and next generation colliders to tell us whether our strategy of continuing to work on non minimal model building is right, or wrong (Fig. 2).

Appendices

A

Tree level SCTM

A.1 The SCTM and the custodial $SU(2)_V$

In this appendix we present the transformation properties of the doublets (bidoublets) and triplets (bitriplets) under $SU(2)_L \otimes SU(2)_R$ and discuss how the $SU(2)_V$ custodial symmetry of the vacuum protects the ρ parameter. We also comment on fine-tuning considerations about the determination of the custodial vacuum at tree level.

$SU(N)$ groups

Let us start by making a summary of the few properties of $SU(N)$ groups that are relevant to this work.

Any representation $\mathbf{n}$ of an $SU(N)$ group is specified by a set of generators that obey,

$$[T^a_{\mathbf{n}}, T^b_{\mathbf{n}}] = i f^{abc} T^c_{\mathbf{n}} \,. \tag{A.1}$$

We can build the complex conjugate $\bar{\mathbf{n}}$ of that representation by taking

$$T^a_{\bar{\mathbf{n}}} = \bar{T}^a = -(T^a_{\mathbf{n}})^* = -(T^a_{\mathbf{n}})^t \,, \tag{A.2}$$

where we used the fact that the matrices associated to these generators are hermitian. When defining a finite $SU(N)$ transformation we have to take into account whether we are acting on a multiplet with components ξ_b, or in his complex conjugate ($\bar{\xi}^b$):

$$\mathcal{U}\xi = (\exp\{i\theta^c T_c\})^{ab}\, \xi_b \,, \tag{A.3}$$

$$\bar{\mathcal{U}}\bar{\xi} = (\exp\{i\theta^c \bar{T}_c\})_{ab}\, \bar{\xi}^b \,. \tag{A.4}$$

Note that by changing the representation from $\mathbf{n}$ to $\bar{\mathbf{n}}$ we also raise the group index of the multiplet, this is important as, for instance, the scalar (dot) product of $SU(2)$ changes sign when raising and lowering indices, $\epsilon_{ij} = -\epsilon^{ij}$. We can make the $\bar{\mathcal{U}}$ transformation act on the right by transposing the whole thing,

$$[\bar{\mathcal{U}}\bar{\xi}]^T = [(\exp\{i\theta^c \bar{T}_c\})_{ab}\bar{\xi}^b]^T = \bar{\xi}^b(\exp\{i\theta^c \bar{T}_c\})_{ba} = \bar{\xi}^T \mathcal{U}^\dagger \,, \tag{A.5}$$

and thus recover the way of writing transformations under $SU(2)_R$ that is generally used in the literature of custodial triplet models.

$SU(2)_L \otimes SU(2)_R$ representations

A finite $SU(2)_L \otimes SU(2)_R$ transformation acting on the Higgs bidoublet $(\mathbf{2_L}, \bar{\mathbf{2}}_\mathbf{R})$,

$$\bar{H} \to \mathcal{U}_L \otimes \bar{\mathcal{U}}_R \; \bar{H}\,, \tag{A.6}$$

leads to the usual transformation

$$\bar{H}^T \to \mathcal{U}_L \bar{H}^T \mathcal{U}_R^\dagger\,. \tag{A.7}$$

In detail,

$$\begin{pmatrix} H_1^0 & H_1^- \\ H_2^+ & H_2^0 \end{pmatrix} \to \exp\{i\theta_L^a \sigma_a/2\} \begin{pmatrix} H_1^0 & H_1^- \\ H_2^+ & H_2^0 \end{pmatrix} \exp\{-i\theta_R^a \sigma_a/2\}\,, \tag{A.8}$$

where $\mathcal{U}_L$ will act on the rows of the matrix and $\mathcal{U}_R$ on the columns. σ_a are the pauli matrices and $\theta_{L,R}$ the parameters of the transformation.

For this multiplet to break $SU(2)_L \otimes SU(2)_R$ to $SU(2)_V$ the relation $\langle \bar{H}^T \rangle = \mathcal{U}_L \langle \bar{H}^T \rangle \mathcal{U}_R^\dagger$ needs to hold. In matrix form, this relation is written as

$$\begin{pmatrix} v_1 & 0 \\ 0 & v_2 \end{pmatrix} = \exp\{i\theta_L^a \sigma_a/2\} \begin{pmatrix} v_1 & 0 \\ 0 & v_2 \end{pmatrix} \exp\{-i\theta_R^a \sigma_a/2\}\,. \tag{A.9}$$

If we make $\theta_L = \theta_R$ and $v_1 = v_2 \equiv v_H$ the vacuum leaves unbroken the vectorial subgroup $SU(2)_{L+R} \equiv SU(2)_V$, i.e. the custodial symmetry.

Let us now do the same with the bitriplet $(\mathbf{3_L}, \bar{\mathbf{3}}_\mathbf{R})$. If we use the vector representation, $\bar{\Delta}^T = (\Sigma_{-1}, \Sigma_0, \Sigma_1)$, an $SU(2)_L \otimes SU(2)_R$ transformation reads

$$\bar{\Delta}^T \to \mathcal{U}_L \bar{\Delta}^T \mathcal{U}_R^\dagger\,, \tag{A.10}$$

which in matrix form

$$\begin{pmatrix} \chi^0 & \phi^+ & \psi^{++} \\ \chi^- & \phi^0 & \psi^+ \\ \chi^{--} & \phi^- & \psi^0 \end{pmatrix} \to \exp\{i\theta_L^a t_a\} \begin{pmatrix} \chi^0 & \phi^+ & \psi^{++} \\ \chi^- & \phi^0 & \psi^+ \\ \chi^{--} & \phi^- & \psi^0 \end{pmatrix} \exp\{-i\theta_R^a t_a\}\,. \tag{A.11}$$

t_a are the generators of $SU(2)$ in 3 dimensions [1]. The custodial condition for EW breaking in the case of triplets is

$$\langle \bar{\Delta}^T \rangle = \mathcal{U}_L \langle \bar{\Delta}^T \rangle \mathcal{U}_R^\dagger\,, \tag{A.13}$$

in detail

$$\begin{pmatrix} v_\chi & 0 & 0 \\ 0 & v_\phi & 0 \\ 0 & 0 & v_\psi \end{pmatrix} = \exp\{i\theta_L^a t_a\} \begin{pmatrix} v_\chi & 0 & 0 \\ 0 & v_\phi & 0 \\ 0 & 0 & v_\psi \end{pmatrix} \exp\{-i\theta_R^a t_a\}\,. \tag{A.14}$$

This relation is preserved (the unbroken subgroup is the vectorial one) if $v_\chi = v_\psi = v_\phi \equiv v_\Delta$ and $\theta_L = \theta_R$.

[1]
$$t_a = \{t_1, t_2, t_3\} = \left\{ \frac{1}{\sqrt{2}} \begin{pmatrix} 0 & 1 & 0 \\ 1 & 0 & 1 \\ 0 & 1 & 0 \end{pmatrix}, \frac{1}{\sqrt{2}} \begin{pmatrix} 0 & -i & 0 \\ i & 0 & -i \\ 0 & i & 0 \end{pmatrix}, \begin{pmatrix} 1 & 0 & 0 \\ 0 & 0 & 0 \\ 0 & 0 & -1 \end{pmatrix} \right\}. \tag{A.12}$$

As it more useful in order to work along doublet representations, we can consider the 2 dimensional basis for triplets which uses the pauli matrices to contract the DOF's, $\Sigma_{2\times2} = \xi_a\sigma^a$. An $SU(2)$ transformation in this basis has the following form

$$\xi_a\sigma^a \to U\,(\xi_a\sigma^a)\,U^\dagger\,, \tag{A.15}$$

$$\bar{\xi}^a\bar{\sigma}_a \to \bar{U}\,(\bar{\xi}^a\bar{\sigma}_a)\,\bar{U}^\dagger\,. \tag{A.16}$$

Similarly to (A.5), using $T^a_{\mathbf{\bar{n}}} = -(T^a_{\mathbf{n}})^T$ we can see that $\bar{U}^T = U^\dagger$ and $(\bar{U}^\dagger)^T = U$, so by taking the transpose of the expressions above we can go from one to another [2]. In this basis the $SU(2)_L$ triplets and the bitriplet $(\mathbf{3_L}, \mathbf{\bar{3}_R})$ of the model are defined in Eqs. (4.4) and (4.5), also, an $SU(2)_L \otimes SU(2)_R$ transformation acting on the bitriplet reads

$$\bar{\Delta}_{2\times2} \to \bar{U}_R \otimes U_L\,\bar{\Delta}_{2\times2}\,U_L^\dagger \otimes \bar{U}_R^\dagger\,, \tag{A.17}$$

where $U_L = \exp\{i\theta^a_L\sigma_a/2\}$ and $\bar{U}_R = \exp\{i\theta^a_R\bar{\sigma}_a/2\}$. The condition to get an $SU(2)_V$ invariant vacuum,

$$\langle\bar{\Delta}\rangle = \bar{U}_R \begin{pmatrix} -U_L\frac{1}{\sqrt{2}}\langle\Sigma_0\rangle U_L^\dagger & -U_L\langle\Sigma_{-1}\rangle U_L^\dagger \\ -U_L\langle\Sigma_1\rangle U_L^\dagger & U_L\frac{1}{\sqrt{2}}\langle\Sigma_0\rangle U_L^\dagger \end{pmatrix} \bar{U}_R^\dagger\,, \tag{A.18}$$

is only preserved when $v_\chi = v_\psi = v_\phi \equiv v_\Delta$ and $\theta_L = \theta_R$, just as it happens with the vectorial ordering of DOF's. Note that we have dropped the 2×2 subindex on $\bar{\Delta}$ and Σ_i as this basis is the one which will be most used in this work, otherwise, we consider that context will allow the reader to distinguish between both bases.

From what is presented above, one would naively consider that the triplet is a complex representation of $SU(2)$ since none of the two bases seem to be real, however, the triplet is the adjoint of $SU(2)$ and there should be a basis where its nature as a real representation is manifest. The real basis for the adjoint representation of any $SU(N)$ group is given by $(T^a_A)^{bc} = -if^{abc}$.

ρ parameter at tree level

We now compute the tree-level contributions to the ρ parameter coming from the triplet sector. The triplet contribution to the $W^\pm$ and Z masses is derived from the kinetic term,

$$\frac{1}{2}\mathrm{tr}_{SU(2)_R,SU(2)_L}[(D_\mu\bar{\Delta})^\dagger(D^\mu\bar{\Delta})]\,, \tag{A.19}$$

which is the same thing as writing,

$$\frac{1}{2}\mathrm{tr}_{SU(2)_L}[(D_\mu\Sigma_{-1})^\dagger(D^\mu\Sigma_{-1})] + \frac{1}{2}\mathrm{tr}_{SU(2)_L}[(D_\mu\Sigma_0)^\dagger(D^\mu\Sigma_0)] + \frac{1}{2}\mathrm{tr}_{SU(2)_L}[(D_\mu\Sigma_1)^\dagger(D^\mu\Sigma_1)]\,. \tag{A.20}$$

The covariant derivatives in the spin-1 vector representation of the triplet and bitriplet

$$D_\mu\Sigma_Y = \partial_\mu\Sigma_Y - ig\,t_aW^a_\mu\Sigma_Y - ig'\,B_\mu Y\Sigma_Y\,, \tag{A.21}$$

$$D_\mu\bar{\Delta} = \partial_\mu\bar{\Delta} + ig\,t_aW^a_\mu\bar{\Delta} - ig'\,t_3B_\mu\bar{\Delta}\,. \tag{A.22}$$

[2] In the triplet case, we use the notation $\mathcal{U}$ and U to differentiate between transformations acting on 2×2 matrices or vectors, $U = \exp\{i\theta^a\sigma_a/2\}$ and $\mathcal{U} = \exp\{i\theta^at_a\}$ respectively. Note that for doublets $\mathcal{U} = U$.

Note that the definition of the covariant derivative for $\bar{\Delta}$ is different since we identify $Y = T_{3R} = -t_3$. In the 2×2 basis the covariant derivatives read

$$D_\mu \Sigma_Y = \partial_\mu \Sigma_Y - ig \left[\frac{\sigma^a}{2}, W_\mu^a \right] \Sigma_Y - ig' B_\mu Y \Sigma_Y \,, \tag{A.23}$$

$$D_\mu \bar{\Delta} = \partial_\mu \bar{\Delta} + ig \left[\frac{\sigma^a}{2}, W_\mu^a \right] \bar{\Delta} - ig' \left[\frac{\sigma^3}{2}, B_\mu \right] \bar{\Delta} \,. \tag{A.24}$$

Where the identification is now $Y = T_{3R} = -\sigma_3/2$.

The final result does not depend on the basis and the contributions to the $W^\pm$ and Z masses coming from $\bar{\Delta}$ are given by

$$\begin{aligned} \frac{1}{2} \mathrm{tr}_{SU(2)_R, SU(2)_L} [(D_\mu \bar{\Delta})^\dagger (D^\mu \bar{\Delta})] \supset g^2 \Bigg(& v_\chi^2 \, W_\mu^+ W^{\mu -} + \frac{v_\chi^2}{\cos^2 \theta_W} Z_\mu Z^\mu + v_\phi^2 \, W_\mu^+ W^{\mu -} \\ & + v_\phi^2 \, W_\mu^- W^{\mu +} + v_\psi^2 \, W_\mu^- W^{\mu +} + \frac{v_\psi^2}{\cos^2 \theta_W} Z_\mu Z^\mu \Bigg) \,, \end{aligned} \tag{A.25}$$

which together with the usual contributions coming from the doublets allow us to the compute deviation from $\rho = 1$ that is generated by the triplet sector

$$\rho - 1 \equiv \Delta\rho = \frac{2(2v_\phi^2 - v_\psi^2 - v_\chi^2)}{v_1^2 + v_2^2 + 4(v_\chi^2 + v_\psi^2)} \,. \tag{A.26}$$

From above we see that, if $v_1 = v_2$ and $v_\phi = v_\psi = v_\chi$ (which corresponds to the custodial $SU(2)_V$ invariant vacuum), then $\Delta\rho = 0$. However, unlike in the GM model, custodial symmetry is no longer a necessary (although certainly sufficient) condition for $\rho = 1$ at tree level. $\Delta\rho = 0$ is also satisfied along the more general non-custodial direction

$$2v_\phi^2 = v_\psi^2 + v_\chi^2 \,. \tag{A.27}$$

This 'extra direction' for the VEV's is a consequence of supersymmetry, where the $Y = 1$ and $Y = -1$ triplets are separate fields with distinct VEV's. in contrast to the GM model where they make up one complex field with hypercharge $Y = 1$. As we explain in Chapter 5, this additional direction allows us to have the scale $\mathcal{M}$ at which the $SU(2)_L \otimes SU(2)_R$ symmetry is imposed to be much higher than the electroweak scale.

The custodial vacuum at tree level

A five dimensional neutral scalar potential such as the one that the SCTM features is certainly a difficult function to scan for possible minima. Therefore, it is reasonable to ask if, beyond the custodial minimum, there are extra minima to which we could tunnel from the custodial one. Basically, how likely is the custodial minimum? If indeed the SCTM is realized in nature, is a fine-tuning required to break the EW symmetry by means of a custodial vacuum or does it come from the structure of the potential? Or in other words, is $\rho = 1$ an automatic prediction and therefore a consequence of the model? Since one of the main motivations to build the SCTM was to solve fine-tuning problems of the MSSM, it is important to study the potential and see if indeed, $\rho = 1$ is a consequence of the structure of the model or a tuning imposed by hand.

For the sake of clarity, let us review the approaches to this matter in the non supersymmetric GM model where the literature is extense and, at tree level, the situation is very similar to the SCTM. In the original paper by Georgi and Machacek, Ref. [67], an $SU(2)$ symmetry of the vacuum was first proposed as a way of keeping $\rho = 1$ at tree level in the presence of $SU(2)_L$ triplets. In that paper, Georgi and Machacek did not claim that small ρ was a consequence of their model but rather that it could be tuned so. However, the original GM paper is very brief and the structure of the potential which could generate EWSB and give rise to the $SU(2)$ invariant vacuum is not discussed. Of course, without a precise knowledge of the potential, any comments about the determination of the vacuum are meaningless and one cannot consider the $SU(2)$ symmetry as something arising from the structure of the theory. However this point is clarified by Golden and Chanowitz in Ref. [68], one of the first papers where the GM model is discussed in depth. They propose an $SU(2)_L \otimes SU(2)_R$ invariant potential for which the only possible vacuum is the $SU(2)_V$ invariant one. If the potential is given and it is such that only a custodially preserving VEV configuration solves the EOM's, we can consider that $\rho = 1$ at tree level is an automatic consequence of the structure of the model and no fine-tuning is needed to set it small.

At tree level, the SCTM features a scalar potential that is $SU(2)_L \otimes SU(2)_R$ invariant (see Appendix A.2). The criticality conditions of this potential are five (one for each scalar field subject to get a VEV, 2 coming from the doublets $v_{1,2}$ and 3 from the triplets v_ψ, v_ϕ, v_χ). Given the $SU(2)_L \otimes SU(2)_R$ invariant structure of the potential only two solutions are found: (i), the custodial one ($v_1 = v_2 \equiv v_H$ and $v_\psi = v_\phi = v_\chi \equiv v_\Delta$) where the 5 criticality conditions degenerate into only 2 (see Eq. (4.12)), and (ii), a more general one ($v_1 = v_2 \equiv v_H$, $v_\psi = v_\chi \equiv v_\Delta$ and v_ϕ) where the 5 conditions degenerate into 3. Upon close numerical inspection of (ii) we find that there is always a custodial minimum that goes along and that, for most parts of the parameter space, the configuration (ii) is a saddle point rather than a minimum of the potential. However, beyond this subtlety the important point is the following: No other VEV configurations are subject to solve the 5 criticality conditions if the parameters of the potential are such that the $SU(2)_L \otimes SU(2)_R$ invariance is maintained, moreover, (i) and (ii) are the only configurations which make the D-term part of the potential vanish, thus minimizing the energy. This behavior is similar to the simpler case of the MSSM where the conditions of $SU(2)_L \otimes SU(2)_R$ invariance, i.e. $m_1 = m_2$, lead to the minimum condition $\tan\beta = 1$, i.e. $v_1 = v_2$. Therefore we conclude that, in the SCTM, the $SU(2)_V$ custodial invariance of the vacuum is an automatic consequence of the structure of our model and $\rho = 1$ at tree level is a prediction.

This discussion applies to the tree level case of the SCTM presented in Chapter 4. In the RGE improved scenario of Chapter 5, the vacuum which provides $\rho = 1$ is not exactly the custodial one but rather the direction (A.27) for which the fine-tuning discussion is more subtle (see 'ρ parameter vs. custodially breaking vacuum' in Section 5.2).

A.2 Full $SU(2)_V$ invariant scalar potential

The superpotential of Eq. (6.1) in component fields is given by

$$\begin{aligned}
W_0 = \lambda \Big\{ & H_1^0\phi^0 H_2^0 + H_2^0\chi^0 H_2^0 + H_1^0\psi^0 H_1^0 + H_1^-\phi^0 H_2^+ - H_2^+\chi^{--}H_2^+ - H_1^-\psi^{++}H_1^- \\
& + \sqrt{2}(H_1^- H_2^0\phi^+ + H_2^+ H_2^0\chi^- - H_1^- H_1^0\psi^+ - H_2^+ H_1^0\phi^-) \Big\} \\
& + \lambda_3\{-\phi^0\chi^0\psi^0 + \psi^{++}\phi^0\chi^{--} + \phi^+\psi^0\chi^- + \phi^-\chi^0\psi^+ - \phi^+\chi^{--}\psi^+ - \phi^-\psi^{++}\chi^-\} \\
& + \mu_\Delta\left\{\frac{1}{2}\phi^0\phi^0 + \psi^0\chi^0 + \phi^+\phi^- + \psi^+\chi^- + \psi^{++}\chi^{--}\right\} + \mu\{H_1^- H_2^+ - H_1^0 H_2^0\}\,,
\end{aligned} \tag{A.28}$$

and correspondingly the F-term potential

$$\begin{aligned}
V_F = & \left|\lambda\left(\phi^0 H_2^0 + 2H_1^0\psi^0 - \sqrt{2}H_1^-\psi^+ - \sqrt{2}H_2^+\phi^-\right) - \mu H_2^0\right|^2 \\
& + \left|\lambda\left(\phi^0 H_1^0 + 2H_2^0\chi^0 + \sqrt{2}H_1^-\phi^+ + \sqrt{2}H_2^+\chi^-\right) - \mu H_1^0\right|^2 \\
& + \left|\lambda(H_1^0 H_2^0 + H_1^- H_2^+) - \lambda_3(\chi^0\psi^0 - \psi^{++}\chi^{--}) + \mu_\Delta\phi^0\right|^2 \\
& + \left|\lambda H_1^0 H_1^0 - \lambda_3(\phi^0\chi^0 - \phi^+\chi^-) + \mu_\Delta\chi^0\right|^2 + \left|\lambda H_2^0 H_2^0 - \lambda_3(\phi^0\psi^0 - \phi^-\psi^+) + \mu_\Delta\psi^0\right|^2 \\
& + \left|\lambda(\phi^0 H_2^+ - 2\psi^{++}H_1^- + \sqrt{2}H_2^0\phi^+ - \sqrt{2}H_1^0\psi^+) + \mu H_2^+\right|^2 \\
& + \left|\lambda(\phi^0 H_1^- - 2\chi^{--}H_2^+ + \sqrt{2}H_2^0\chi^- - \sqrt{2}H_1^0\phi^-) + \mu H_1^-\right|^2 \\
& + \left|\sqrt{2}\lambda H_1^- H_2^0 + \lambda_3(\psi^0\chi^- - \chi^{--}\psi^+) + \mu_\Delta\phi^-\right|^2 + \left|-\sqrt{2}\lambda H_1^0 H_2^+ + \lambda_3(\chi^0\psi^+ - \psi^{++}\chi^-) + \mu_\Delta\phi^+\right|^2 \\
& + \left|-\sqrt{2}\lambda H_1^- H_1^0 + \lambda_3(\phi^-\chi^0 - \phi^+\chi^{--}) + \mu_\Delta\chi^-\right|^2 + \left|\sqrt{2}\lambda H_2^0 H_2^+ + \lambda_3(\phi^+\psi^0 - \phi^-\psi^{++}) + \mu_\Delta\psi^+\right|^2 \\
& + \left|-\lambda H_1^- H_1^- + \lambda_3(\phi^0\chi^{--} - \phi^-\chi^-) + \mu_\Delta\chi^{--}\right|^2 + \left|-\lambda H_2^+ H_2^+ + \lambda_3(\phi^0\psi^{++} - \phi^+\psi^+) + \mu_\Delta\psi^{++}\right|^2 .
\end{aligned} \tag{A.29}$$

The D-terms are

$$\begin{aligned}
D^1 - iD^2 &= -g\Big\{ H_1^{0*}H_1^- + H_2^{+*}H_2^0 \\
&\qquad + \sqrt{2}\left[\phi^{0*}\phi^- - \phi^0\phi^{+*} + \psi^{+*}\psi^0 - \psi^+\psi^{++*} + \chi^{-*}\chi^{--} - \chi^-\chi^{0*}\right]\Big\} \\
D^1 + iD^2 &= (D^1 - iD^2)^* \\
D^3 &= -\frac{g}{2}\Big\{|H_1^0|^2 - |H_2^0|^2 - |H_2^+|^2 - |H_1^-|^2 \\
&\qquad + 2\left[|\chi^0|^2 - |\psi^0|^2 + |\phi^+|^2 - |\phi^-|^2 + |\psi^{++}|^2 - |\chi^{--}|^2\right]\Big\} \\
D_Y &= -\frac{g'}{2}\Big\{|H_2^0|^2 - |H_1^0|^2 + |H_2^+|^2 - |H_1^-|^2 \\
&\qquad + 2\left[|\psi^0|^2 - |\chi^0|^2 + |\psi^{++}|^2 + |\psi^+|^2 - |\chi^{--}|^2 - |\chi^-|^2\right]\Big\}\,,
\end{aligned} \tag{A.30}$$

hence V_D,

$$\begin{aligned}
V_D = \frac{g^2}{8}\Big\{ & |H_1^0|^2 - |H_2^0|^2 + |H_2^+|^2 - |H_1^-|^2 + 2|\chi^0|^2 - 2|\psi^0|^2 \\
& + 2|\phi^+|^2 - 2|\phi^-|^2 + 2|\psi^{++}|^2 - 2|\chi^{--}|^2 \Big\}^2 \\
& + \frac{g^2}{2}\Big| H_1^0 H_1^{-\,*} + H_2^{0\,*} H_2^+ \\
& + \sqrt{2}\left[\phi^0\phi^{-*} - \phi^0\phi^+ + \psi^+\psi^{0*} - \psi^{+*}\psi^{++} + \chi^-\chi^{--*} - \chi^{-*}\chi^0\right]\Big|^2 \\
& + \frac{g'^2}{8}\Big\{ |H_2^0|^2 - |H_1^0|^2 + |H_2^+|^2 - |H_1^-|^2 + 2|\psi^0|^2 - 2|\chi^0|^2 \\
& + 2|\psi^+|^2 - 2|\chi^-|^2 + 2|\psi^{++}|^2 - 2|\chi^{--}|^2 \Big\}^2 .
\end{aligned} \tag{A.31}$$

Finally, the soft breaking potential (7.2) can be written as

$$\begin{aligned}
V_{\text{soft}} = {} & m_H^2\left(|H_1^0|^2 + |H_2^0|^2 + |H_1^-|^2 + |H_2^+|^2\right) \\
& + m_\Delta^2\left(|\phi^0|^2 + |\phi^-|^2 + |\phi^+|^2 + |\psi^0|^2 + |\psi^+|^2 + |\psi^{++}|^2 + |\chi^0|^2 + |\chi^-|^2 + |\chi^{--}|^2\right) \\
& + \Big\{ m_3^2(H_1^- H_2^+ - H_1^0 H_2^0) + B_\Delta(\phi^0\phi^0/2 + \psi^0\chi^0 + \phi^+\phi^- + \psi^+\chi^- + \psi^{++}\chi^{--}) \\
& + A_{\lambda_3}\left(-\phi^0\chi^0\psi^0 + \phi^0\psi^{++}\chi^{--} + \phi^+\psi^0\chi^- + \phi^-\chi^0\psi^+ - \phi^+\chi^{--}\psi^+ - \phi^-\psi^{++}\chi^-\right) \\
& + A_\lambda\Big(H_1^0\phi^0 H_2^0 + H_2^0\chi^0 H_2^0 + H_1^0\psi^0 H_1^0 + H_1^-\phi^0 H_2^+ - H_2^+\chi^{--}H_2^+ - H_1^-\psi^{++}H_1^- \\
& + \sqrt{2}\left[H_1^-\phi^+ H_2^0 - H_1^0\phi^- H_2^+ + H_2^0\chi^- H_2^+ - H_1^-\psi^+ H_1^0\right]\Big) + h.c.\Big\} .
\end{aligned} \tag{A.32}$$

By taking the neutral and real part of this potential, we get the five minimization conditions that degenerate into two for a custodial configuration of the VEV's, Eq. (4.12).

A.3 $g_{\mathcal{H}VV}$ couplings

These are the relevant couplings used to study the restoration of unitarity in the SCTM (Chap. 4) and the collider properties of F_S (Chap. 8) [3]:

$$
\begin{aligned}
g_{F_S^{++}W^-W^-} &= g_{F_S^{--}W^+W^+} = -\sqrt{2} g m_W \sin\theta \\
g_{S_1W^+W^-} &= g m_W \left(\cos\theta \cos\alpha_S - \frac{2\sqrt{6}}{3} \sin\theta \sin\alpha_S \right) \\
g_{S_2W^+W^-} &= g m_W \left(\cos\theta \sin\alpha_S + \frac{2\sqrt{6}}{3} \sin\theta \cos\alpha_S \right) \\
g_{F_S^0W^+W^-} &= -\frac{g m_W \sin\theta}{\sqrt{3}} \\
g_{S_1ZZ} &= \frac{g m_W}{\cos^2\theta_W} \left(\cos\theta \cos\alpha_S - \frac{2\sqrt{6}}{3} \sin\theta \sin\alpha_S \right) \\
g_{S_2ZZ} &= \frac{g m_W}{\cos^2\theta_W} \left(\cos\theta \sin\alpha_S + \frac{2\sqrt{6}}{3} \sin\theta \cos\alpha_S \right) \\
g_{F_S^0ZZ} &= \frac{2 g m_W \sin\theta}{\sqrt{3}\cos^2\theta_W} \\
g_{F_S^-W^+Z} &= g_{F_S^+W^-Z} = -\frac{g m_W \sin\theta}{\cos\theta_W} \\
g_{G^-W^+Z} &= g_{G^+W^-Z} = -g m_W \sin\theta_W \tan\theta_W
\end{aligned}
\tag{A.33}
$$

[3] We are missing intentionally a global factor $i\eta_{\mu\nu}$.

B

Loop level SCTM

B.1 Renormalization group equations

In this appendix we present the complete set of one loop renormalizaton group equations of the SCTM used in Chapter 5. Wity $dx/dt = (1/16\pi^2)\beta_x$ we first write tye beta functions for the gauge coupling constants [1]

$$\beta_{g_1} = \frac{102}{10} g_1^3, \quad \beta_{g_2} = 7 g_2^3, \quad \beta_{g_3} = -3 g_3^3. \tag{B.1}$$

Yukawa couplings

$$\beta_{y_t} = y_t \left(6y_t^2 + y_b^2 + 6\lambda_b^2 + 3\lambda_c^2 - \frac{16}{3} g_3^2 - 3g^2 - \frac{13}{9} g'^2 \right) \tag{B.2}$$

$$\beta_{y_b} = y_b \left(6y_b^2 + y_t^2 + 6\lambda_a^2 + 3\lambda_c^2 - \frac{16}{3} g_3^2 - 3g^2 - \frac{7}{9} g'^2 \right) \tag{B.3}$$

$$\beta_{\lambda_a} = \lambda_a \left(6\lambda_c^2 + 14\lambda_a^2 + 6y_b^2 + 2\lambda_3^2 - 7g^2 - 3g'^2 \right) \tag{B.4}$$

$$\beta_{\lambda_b} = \lambda_b \left(6\lambda_c^2 + 14\lambda_b^2 + 6y_t^2 + 2\lambda_3^2 - 7g^2 - 3g'^2 \right) \tag{B.5}$$

$$\beta_{\lambda_c} = \lambda_c \left(8\lambda_c^2 + 6\lambda_a^2 + 6\lambda_b^2 + 3y_t^2 + 3y_b^2 + 2\lambda_3^2 - 7g^2 - g'^2 \right) \tag{B.6}$$

$$\beta_{\lambda_3} = \lambda_3 \left(6\lambda_3^2 + 2\lambda_a^2 + 2\lambda_b^2 + 2\lambda_c^2 - 12g^2 - 4g'^2 \right) \tag{B.7}$$

$$\beta_{y_\tau} = y_\tau \left(4y_\tau^2 + 3y_b^2 + 6\lambda_a^2 + 3\lambda_c^2 - 3g_2^2 - \frac{9}{5} g_1^2 \right) . \tag{B.8}$$

Superpotential mass terms

$$\beta_\mu = \mu(3y_t^2 + 3y_b^2 + 6\lambda_a^2 + 6\lambda_b^2 + 6\lambda_c^2 - 3g^2 - g'^2) \tag{B.9}$$

$$\beta_{\mu_a} = 2\mu_a(2\lambda_c^2 + 2\lambda_3^2 - 4g^2) \tag{B.10}$$

$$\beta_{\mu_b} = \mu_b(2\lambda_a^2 + 2\lambda_b^2 + 4\lambda_3^2 - 8g^2 - 4g'^2) . \tag{B.11}$$

Gaugino masses

$$\beta_{M_1} = \frac{102}{5} g_1^2 M_1, \quad \beta_{M_2} = 14 g_2^2 M_2, \quad \beta_{M_3} = (-6) g_3^2 M_3. \tag{B.12}$$

[1] Note that we use g_1 by identifying it with g' through the GUT normalization $g_1 = \sqrt{5/3}\, g'$.

Soft scalar mass terms

$$\beta_{m_{y_1}^2} = 2m_{y_1}^2(3y_b^2 + 6\lambda_a^2 + 3\lambda_c^2) + 6y_b^2(m_{\widetilde{Q}}^2 + m_{\tilde{b}}^2) + 12\lambda_a^2(m_{y_1}^2 + m_{\Sigma_1}^2) + 6\lambda_c^2(m_{y_2}^2 + m_{\Sigma_0}^2) + 6a_b^2 + 12A_a^2 + 6A_c^2 - 6g_2^2M_2^2 - \frac{6}{5}g_1^2M_1^2 - \frac{3}{5}g_1^2S \tag{B.13}$$

$$\beta_{m_{y_2}^2} = 2m_{y_2}^2(3y_t^2 + 6\lambda_b^2 + 3\lambda_c^2) + 6y_t^2(m_{\widetilde{Q}}^2 + m_{\tilde{t}}^2) + 12\lambda_b^2(m_{y_2}^2 + m_{\Sigma_{-1}}^2) + 6\lambda_c^2(m_{y_1}^2 + m_{\Sigma_0}^2) + 6a_t^2 + 12A_b^2 + 6A_c^2 - 6g_2^2M_2^2 - \frac{6}{5}g_1^2M_1^2 + \frac{3}{5}g_1^2S \tag{B.14}$$

$$\beta_{m_{\Sigma_0}^2} = 2m_{\Sigma_0}^2(2\lambda_c^2 + 2\lambda_3^2) + 4\lambda_c^2(m_{y_1}^2 + m_{y_2}^2) + 4\lambda_3^2(m_{\Sigma_1}^2 + m_{\Sigma_{-1}}^2) + 4A_c^2 + 4A_3^2 - 16g_2^2M_2^2 \tag{B.15}$$

$$\beta_{m_{\Sigma_1}^2} = 2m_{\Sigma_1}^2(2\lambda_a^2 + 2\lambda_3^2) + 8\lambda_a^2m_{y_1}^2 + 4\lambda_3^2(m_{\Sigma_0}^2 + m_{\Sigma_{-1}}^2) + 4A_a^2 + 4A_3^2 - 16g_2^2M_2^2 - \frac{24}{5}g_1^2M_1^2 + \frac{6}{5}g_1^2S \tag{B.16}$$

$$\beta_{m_{\Sigma_{-1}}^2} = 2m_{\Sigma_{-1}}^2(2\lambda_b^2 + 2\lambda_3^2) + 8\lambda_b^2m_{y_2}^2 + 4\lambda_3^2(m_{\Sigma_0}^2 + m_{\Sigma_1}^2) + 4A_b^2 + 4A_3^2 - 16g_2^2M_2^2 - \frac{24}{5}g_1^2M_1^2 - \frac{6}{5}g_1^2S \tag{B.17}$$

$$\beta_{m_{\widetilde{Q}}^2} = 2m_{\widetilde{Q}}^2(y_t^2 + y_b^2) + 2y_t^2(m_{y_2}^2 + m_{\tilde{t}}^2) + 2y_b^2(m_{y_1}^2 + m_{\tilde{b}}^2) + 2a_t^2 + 2a_b^2 - 6g_2^2M_2^2 - \frac{32}{3}g_3^2M_3^2 - \frac{2}{15}g_1^2M_1^2 + \frac{1}{5}g_1^2S \tag{B.18}$$

$$\beta_{m_{\tilde{t}}^2} = 2m_{\tilde{t}}^2(2y_t^2) + 4y_t^2(m_{y_2}^2 + m_{\widetilde{Q}}^2) + 4a_t^2 - \frac{32}{3}g_3^2M_3^2 - \frac{32}{15}g_1^2M_1^2 - \frac{4}{5}g_1^2S \tag{B.19}$$

$$\beta_{m_{\tilde{b}}^2} = 2m_{\tilde{b}}^2(2y_b^2) + 4y_b^2(m_{y_1}^2 + m_{\widetilde{Q}}^2) + 4a_b^2 - \frac{32}{3}g_3^2M_3^2 - \frac{8}{15}g_1^2M_1^2 + \frac{2}{5}g_1^2S \tag{B.20}$$

$$\beta_{m_{\tilde{\tau}_L}^2} = 2y_\tau^2m_{y_d}^2 + 2a_\tau^2 + 2y_\tau^2m_{\tilde{\tau}_L}^2 + 2y_\tau^2m_{\tilde{\tau}_R}^2 - 6g_2^2M_2^2 - \frac{6}{5}g_1^2M_1^2 \tag{B.21}$$

$$\beta_{m_{\tilde{\tau}_R}^2} = 2(2y_\tau^2m_{y_u}^2 + 2a_\tau^2 + 2y_\tau^2m_{\tilde{\tau}_L}^2 + 2y_\tau^2m_{\tilde{\tau}_R}^2) - \frac{24}{5}g_1^2M_1^2\ . \tag{B.22}$$

Trilinear terms

$$\begin{aligned}\beta_{a_t} = {} & a_t(3y_t^2 + 6\lambda_b^2 + 3\lambda_c^2) + y_t(6y_ta_t + 12\lambda_bA_b + 6\lambda_cA_c) - \frac{3}{2}g_2^2(a_t - 2M_2y_t) \\ & + a_t(2y_t^2) + y_t(4y_ta_t) - \frac{8}{15}g_1^2(a_t - 2M_1y_t) - \frac{8}{3}g_3^2(a_t - 2M_3y_t) \\ & + a_t(y_t^2 + y_b^2) + y_t(2y_ta_t + 2y_ba_b) - \frac{1}{30}g_1^2(a_t - 2M_1y_t) - \frac{3}{2}g_2^2(a_t - 2M_2y_t) \\ & - \frac{8}{3}g_3^2(a_t - 2M_3y_t) - \frac{3}{10}g_1^2(a_t - 2M_1y_t)\end{aligned} \tag{B.23}$$

$$\begin{aligned}\beta_{a_b} &= (a_b(3y_b^2+6\lambda_a^2+3\lambda_c^2)+y_b(6y_ba_b+12\lambda_aA_a+6\lambda_cA_c)-\frac{3}{2}g_2^2(a_b-2M_2y_b)\\ &+a_b(2y_b^2)+y_b(4y_ba_b)-\frac{2}{15}g_1^2(a_b-2M_1y_b)-\frac{8}{3}g_3^2(a_b-2M_3y_b)\\ &+a_b(y_b^2+y_t^2)+y_b(2y_ba_b+2y_ta_t)-\frac{1}{30}g_1^2(a_b-2M_1y_b)-\frac{3}{2}g_2^2(a_b-2M_2y_b)\\ &-\frac{8}{3}g_3^2(a_b-2M_3y_b))-\frac{3}{10}g_1^2(a_b-2M_1y_b)\end{aligned} \tag{B.24}$$

$$\begin{aligned}\beta_{A_a} &= 2(A_a(3y_b^2+6\lambda_a^2+3\lambda_c^2)+\lambda_a(6y_ba_b+12\lambda_aA_a+6\lambda_cA_c)-\frac{3}{2}g_2^2(A_a-2M_2\lambda_a)\\ &-\frac{3}{10}g_1^2(A_a-2M_1\lambda_a))-\frac{6}{5}g_1^2(A_a-2M_1\lambda_a)\\ &+A_a(2\lambda_a^2+2\lambda_3^2)+\lambda_a(4A_a\lambda_a+4A_3\lambda_3)-4g_2^2(A_a-2M_2\lambda_a)\end{aligned} \tag{B.25}$$

$$\begin{aligned}\beta_{A_b} &= 2(A_b(3y_t^2+6\lambda_b^2+3\lambda_c^2)+\lambda_b(6y_ta_t+12\lambda_bA_b+6\lambda_cA_c)-\frac{3}{2}g_2^2(A_b-2M_2\lambda_b)\\ &-\frac{3}{10}g_1^2(A_b-2M_1\lambda_b))-\frac{6}{5}g_1^2(A_b-2M_1\lambda_b)\\ &+A_b(2\lambda_b^2+2\lambda_3^2)+\lambda_b(4A_b\lambda_b+4A_3\lambda_3)-4g_2^2(A_b-2M_2\lambda_b)-\frac{6}{5}g_1^2(A_b-2M_1\lambda_b)\end{aligned} \tag{B.26}$$

$$\begin{aligned}\beta_{A_c} &= A_c(3y_t^2+6\lambda_b^2+3\lambda_c^2)+\lambda_c(6y_ta_t+12\lambda_bA_b+6\lambda_cA_c)-\frac{3}{2}g_2^2(A_c-2M_2\lambda_c)\\ &+A_c(3y_b^2+6\lambda_a^2+3\lambda_c^2)+\lambda_c(6y_ba_b+12\lambda_aA_a+6\lambda_cA_c)-\frac{3}{2}g_2^2(A_c-2M_2\lambda_c)\\ &+A_c(2\lambda_c^2+2\lambda_3^2)+\lambda_c(4A_c\lambda_c+4A_3\lambda_3)-4g_2^2(A_c-2M_2\lambda_c)\\ &-\frac{3}{10}g_1^2(A_c-2M_1\lambda_c)\end{aligned} \tag{B.27}$$

$$\begin{aligned}\beta_{A_3} &= A_3(2\lambda_b^2+2\lambda_3^2)+\lambda_3(4\lambda_bA_b+4\lambda_3A_3)-\frac{6}{5}g_1^2(A_3-2M_1\lambda_3)-4g_2^2(A_3-2M_2\lambda_3)\\ &+A_3(2\lambda_a^2+2\lambda_3^2)+\lambda_3(4\lambda_aA_a+4\lambda_3A_3)-\frac{6}{5}g_1^2(A_3-2M_1\lambda_3)-4g_2^2(A_3-2M_2\lambda_3)\\ &+A_3(2\lambda_c^2+2\lambda_3^2)+\lambda_3(4\lambda_cA_c+4\lambda_3A_3)-4g_2^2(A_3-2M_2\lambda_3)\end{aligned} \tag{B.28}$$

$$\begin{aligned}\beta_{a_\tau} &= 9y_\tau^2a_\tau+6\lambda_a^2a_\tau+3\lambda_c^2a_\tau+3a_\tau y_b^2+a_\tau y_\tau^2-3g_2^2a_\tau-\frac{9}{5}g_1^2a_\tau\\ &+y_\tau(12\lambda_aA_a+2y_\tau a_\tau+6\lambda_cA_c+6g_2^2M_2+6y_ba_b+\frac{18}{5}g_1^2M_1)\end{aligned} \tag{B.29}$$

Soft bilinear terms

$$\begin{aligned}\beta_{m_3^2} &= m_3^2(3y_t^2+3y_b^2+6\lambda_a^2+6\lambda_b^2+6\lambda_c^2-3g_2^2-\frac{3}{5}g_1^2)\\ &+\frac{2}{5}\mu(15g_2^2M_2+3g_1^2M_1+30\lambda_cA_c+15y_ba_b+15y_ta_t+30\lambda_aA_a+30\lambda_bA_b)\end{aligned} \tag{B.30}$$

$$\beta_{B_a} = 4\mu_a(4g_2^2 M_2 + 2\lambda_c A_c + 2\lambda_3 A_3) + 2B_a(2\lambda_c^2 + 2\lambda_3^2 - 4g_2^2)) \tag{B.31}$$

$$\begin{aligned}\beta_{B_b} &= B_b(2\lambda_a^2 + 2\lambda_b^2 + 4\lambda_3^2 - 8g_2^2 - \frac{12}{5}g_1^2) \\ &+ \frac{2}{5}\mu_b(10\lambda_a A_a + 10\lambda_b A_b + 20\lambda_3 A_3 + 12g_1^2 M_1 + 40g_2^2 M_2)\end{aligned} \tag{B.32}$$

B.2 Minimization procedure after the RGE running

We will here make a systematic study of the minimum induced by radiative corrections at the electroweak scale starting from a theory at the scale $\mathcal{M}$ which is $SU(2)_L \otimes SU(2)_R$ invariant. For pedagogical reasons we will start with the case of the MSSM with custodial symmetry at $\mathcal{M}$.

Warming up with the MSSM

In the MSSM the Higgs potential is a function of two fields $V = V(H_1^0, H_2^0)$ the real parts of the neutral components of the Higgs doublets (H_1, H_2). These two degrees of freedom will make up the CP-even MSSM mass eigenstates (h, H). At the minimum the VEV's are defined as $v_2 = v\sin\beta$ and $v_1 = v\cos\beta$ where $v = 174$ GeV. The equations of minimum $\partial V/\partial H_{1,2}^0 = 0$ provide the equations

$$m_2^2 - m_3^2\cot\beta - \frac{m_Z^2}{2}\cos 2\beta = 0\,, \tag{B.33}$$

$$m_1^2 - m_3^2\tan\beta + \frac{m_Z^2}{2}\cos 2\beta = 0\,, \tag{B.34}$$

where $m_{1,2}^2 \equiv m_{H_{1,2}}^2 + |\mu|^2$. Now the linear combinations Eq. (B.33) $\pm$ Eq. (B.34) lead respectively to

$$m_3^2 = \frac{\tan\beta}{\tan^2\beta + 1}(m_1^2 + m_2^2)\,, \tag{B.35}$$

$$\tan^2\beta = \frac{m_1^2 + \frac{1}{2}m_Z^2}{m_2^2 + \frac{1}{2}m_Z^2}\,, \tag{B.36}$$

where we are assuming $m_1^2 \geq m_2^2$.

Now we can first assume that the Higgs sector has custodial symmetry and that therefore $m_1 = m_2$. In this case we see that Eq. (B.36) is identically satisfied for $\tan\beta = 1$, which is precisely the custodial symmetric minimum, while Eq. (B.35) yields $m_3^2 = (m_1^2 + m_2^2)/2$ which is the condition for EWSB.

Second, we will assume that the theory is $SU(2)_L \otimes SU(2)_R$ symmetric at the scale $\mathcal{M}$ where supersymmetry breaking is communicated to the observable sector. In this case, as there are couplings which do not respect the custodial symmetry (in particular g' and h_t), even if $m_1 = m_2$, at $Q = \mathcal{M}$ at the EW scale the latter equality will not hold. In this case at the EW scale a value $\tan\beta \neq 1$ will be generated and the value of m_3^2 will then be correspondingly obtained from Eq. (B.35).

The SCTM

We will now apply the previous procedure to the case of the SCTM. The Higgs sector is $SU(2)_L \otimes SU(2)_R$ invariant at the scale $\mathcal{M}$ but the RGE running will spoil the custodial symmetry mainly because the couplings (g', h_t) break it. So in principle (as the MSSM example above) we should write the most general potential for this theory (see Eqs. (5.1), (5.3) and (5.4)). The EOM are the solutions to the equations $\partial V/\partial H_1^0 = \partial V/\partial H_2^0 = \partial V/\partial \psi^0 = \partial V/\partial \phi^0 = \partial V/\partial \chi^0 = 0$ which are satisfied at the (real part of the) field VEV's $(H_1^0, H_2^0, \psi^0, \phi^0, \chi^0) = (v_1, v_2, v_\psi, v_\phi, v_\chi)$.

Doublet sector

The equation $(1/H_1^0)\partial V/\partial H_1^0 + (1/H_2^0)\partial V/\partial H_2^0 = 0$ allows to trade the parameter m_3^2 by the other supersymmetric parameters, as

$$\begin{aligned}
&\frac{1}{\sin 2\beta}\left[m_3^2 - A_c v_\phi - \lambda_c(\lambda_3 v_\chi v_\Psi + \lambda_c v_1 v_2 + \mu_a v_\phi) - 2(\lambda_c v_\phi - \mu)(\lambda_a v_\psi + \lambda_b v_\chi)\right] \\
&= \frac{1}{2}(m_{H_u}^2 + m_{H_d}^2) + A_a v_\psi + A_b v_\chi + (\lambda_3 v_\phi + \mu_b)(\lambda_b v_\psi + \lambda_a v_\chi) \\
&+ \lambda_a^2 v_1^2 + \lambda_b^2 v_2^2 + (\lambda_c v_\phi - \mu)^2 + 2\left[\lambda_a^2 v_\psi^2 + \lambda_b^2 v_\chi^2\right] ,
\end{aligned} \tag{B.37}$$

where $\tan\beta = v_2/v_1$. The value of m_3^2 from Eq. (B.37) is now replaced into the equation $(1/H_1^0)\partial V/\partial H_1^0 - (1/H_2^0)\partial V/\partial H_2^0 = 0$ which then becomes

$$\begin{aligned}
&\frac{g'^2 + g^2}{2}(v_2^2 - v_1^2 + 2v_\psi^2 - 2v_\chi^2) = 2\cos 2\beta(\lambda_c v_\phi - \mu)^2 \\
&+2\cos^2\beta\left\{m_{H_1}^2 + 2A_a v_\psi + 2\lambda_a(\lambda_3 v_\phi + \mu_b)v_\chi + 2\lambda_a^2(v_1^2 + 2v_\psi^2)\right\} \\
&-2\sin^2\beta\left\{m_{H_2}^2 + 2A_b v_\chi + 2\lambda_b(\lambda_3 v_\phi + \mu_b)v_\psi + 2\lambda_b^2(v_2^2 + 2v_\chi^2)\right\} ,
\end{aligned} \tag{B.38}$$

this equation is identically satisfied in the custodial limit.

Triplet sector

Likewise equation $(1/\psi^0)\partial V/\partial \psi^0 + (1/\chi^0)\partial V/\partial \chi^0$ yields the parameter B_b as a function of the other supersymmetric parameters as

$$\begin{aligned}
&\frac{v_\psi^2 + v_\chi^2}{v_\psi v_\chi}\left[-B_b - A_3 v_\phi - \lambda_3(\lambda_c v_1 v_2 + \mu_a v_\phi + \lambda_3 v_\psi v_\chi)\right] = \\
&m_{\Sigma_1}^2 + m_{\Sigma_{-1}}^2 + (\lambda_3 v_\phi + \mu_b)\left(\frac{\lambda_a v_1^2}{v_\chi} + \frac{\lambda_b v_2^2}{v_\psi}\right) + 2(\lambda_3 v_\phi + \mu_b)^2 + 4(\lambda_a^2 v_1^2 + \lambda_b^2 v_2^2) \\
&+\frac{A_a v_1^2 + 2\lambda_a v_1 v_2(\lambda_c v_\phi - \mu)}{v_\psi} + \frac{A_b v_2^2 + 2\lambda_b v_1 v_2(\lambda_c v_\phi - \mu)}{v_\chi} .
\end{aligned} \tag{B.39}$$

The value of B_b is then replaced into equation $(1/\psi^0)\partial V/\partial \psi^0 - (1/\chi^0)\partial V/\partial \chi^0$ which then becomes

$$\begin{aligned}
&(g'^2 + g^2)(v_2^2 - v_1^2 + 2v_\psi^2 - 2v_\chi^2) = -2\,\frac{v_\psi^2 - v_\chi^2}{v_\psi^2 + v_\chi^2}(\lambda_3 v_\phi + \mu_b)^2 \\
&-2\,\frac{v_\psi^2}{v_\psi^2 + v_\chi^2}\left\{m_{\Sigma_1}^2 + 4\lambda_a^2 v_1^2 + (\lambda_3 v_\phi + \mu_b)\frac{\lambda_b v_2^2}{v_\psi} + \frac{A_a v_1^2 + 2\lambda_a v_1 v_2(\lambda_c v_\phi - \mu)}{v_\psi}\right\} \\
&+2\,\frac{v_\chi^2}{v_\psi^2 + v_\chi^2}\left\{m_{\Sigma_{-1}}^2 + 4\lambda_b^2 v_2^2 + (\lambda_3 v_\phi + \mu_b)\frac{\lambda_a v_1^2}{v_\chi} + \frac{A_b v_2^2 + 2\lambda_b v_1 v_2(\lambda_c v_\phi - \mu)}{v_\chi}\right\} ,
\end{aligned} \tag{B.40}$$

again this equation is identically satisfied in the custodial limit. Finally the value of B_a is obtained from the equation $\partial V/\partial\phi^0 = 0$ as

$$\begin{aligned}
&-\left[B_a + \mu_a^2 + m_{\Sigma_0}^2\right] v_\phi = (A_c + \lambda_c\mu_a)v_1v_2 + (A_3 + \lambda_3\mu_a)v_\psi v_\chi \\
&+\lambda_c v_1(2\lambda_b v_2 v_\chi + \lambda_c v_1 v_\phi - v_1\mu) + \lambda_c v_2(2\lambda_a v_1 v_\psi + \lambda_c v_2 v_\phi - v_2\mu) \\
&+\lambda_3 v_\chi\left[\lambda_a v_1^2 + v_\chi(\lambda_3 v_\phi + \mu_b)\right] + \lambda_3 v_\psi\left[\lambda_b v_2^2 + v_\psi(\lambda_3 v_\phi + \mu_b)\right] .
\end{aligned} \tag{B.41}$$

If we define $B_\mp = B_a \mp B_b$ then the EoM for B_- is

$$\begin{aligned}
B_- =& A_3\left(v_\phi - \frac{v_\psi v_\chi}{v_\phi}\right) + \frac{1}{v_\psi^2 + v_\chi^2}\left[v_\psi v_\chi(m_{\Sigma_1}^2 + m_{\Sigma_{-1}}^2) - (v_\psi^2 + v_\chi^2)m_{\Sigma_0}^2\right] \\
&+\lambda_3\left[\lambda_c v_1 v_2 + \lambda_a v_1^2\left(\frac{v_\phi v_\psi}{v_\psi^2 + v_\chi^2} - \frac{v_\chi}{v_\phi}\right) + \lambda_b v_2^2\left(\frac{v_\phi v_\chi}{v_\psi^2 + v_\chi^2} - \frac{v_\psi}{v_\phi}\right)\right] \\
&+\lambda_3^2\left[v_\psi v_\chi\frac{2v_\phi^2 + v_\psi^2 + v_\chi^2}{v_\psi^2 + v_\chi^2} - (v_\psi^2 + v_\chi^2)\right] + \mu_b^2\frac{2v_\psi v_\chi}{v_\psi^2 + v_\chi^2} - \mu_a^2 \\
&+\lambda_3 v_\phi\left[\mu_a\left(1 - \frac{v_\psi v_\chi}{v_\phi^2}\right) + \mu_b\left(\frac{4v_\psi v_\chi}{v_\psi^2 + v_\chi^2} - \frac{v_\psi^2 + v_\chi^2}{v_\phi^2}\right)\right] \\
&+\frac{A_a v_1^2 v_\psi + A_b v_2^2 v_\chi}{v_\psi^2 + v_\chi^2} - A_c\frac{v_1 v_2}{v_\phi} + \mu_b\frac{\lambda_a v_1^2 v_\psi + \lambda_b v_2^2 v_\chi}{v_\psi^2 + v_\chi^2} - \mu_a\frac{\lambda_c v_1 v_2}{v_\phi} \\
&+(\lambda_c v_\phi - \mu)\left[2v_1 v_2\frac{\lambda_a v_\chi + \lambda_b v_\psi}{v_\psi^2 + v_\chi^2} - \lambda_c\frac{v_1^2 + v_2^2}{v_\phi}\right] \\
&+4(\lambda_a^2 v_1^2 + \lambda_b^2 v_2^2)\frac{v_\psi v_\chi}{v_\psi^2 + v_\chi^2} - 2\lambda_c v_1 v_2\frac{\lambda_a v_\psi + \lambda_b v_\chi}{v_\chi} ,
\end{aligned} \tag{B.42}$$

which is also identically satisfied in the custodial limit. In fact we have written the different lines of Eq. (B.42) in such a way that they cancel independently in the custodial limit. Finally the parameters m_3^2, and B_+ are given by Eqs. (B.37), and (B.39) and (B.41), respectively. Eqs. (B.38), (B.40), and (B.42), which are identically satisfied in the custodial limit, will be used to compute the departure from the custodial symmetry triggered by the RGE running.

Solving the equations, finding the correct vacuum

As Eqs. (B.38), (B.40), and (B.42) do not depend on the parameters m_3^2 and B_+, we will use these to compute the departure of the vacuum solution with respect to the custodial configuration by considering the general configuration (5.6) and (5.7). Using the field configuration of Eq. (5.6) we can write an explicit solution to Eq. (B.38) as

$$\tan^2\beta = \frac{P_a - P_b + \sqrt{(P_a - P_b)^2 + 4Q_aQ_b}}{2Q_b} , \tag{B.43}$$

where $P_{a,b}$ and $Q_{a,b}$ are given by

$$\begin{aligned}
P_a &= m_{H_1}^2 + 2A_a v_\psi + 2\lambda_a v_\chi(\lambda_3 v_\phi + \mu_b) + 4\lambda_a^2 v_\psi^2 + (\lambda_c v_\phi - \mu)^2 + \frac{g'^2 + g^2}{2}(v_H^2 + v_\chi^2 - v_\psi^2) , \\
P_b &= m_{H_2}^2 + 2A_b v_\chi + 2\lambda_b v_\psi(\lambda_3 v_\phi + \mu_b) + 4\lambda_b^2 v_\chi^2 + (\lambda_c v_\phi - \mu)^2 + \frac{g'^2 + g^2}{2}(v_H^2 + v_\psi^2 - v_\chi^2) , \\
Q_a &= P_a + 4v_H^2\lambda_a^2, \quad Q_b = P_b + 4v_H^2\lambda_b^2 .
\end{aligned} \tag{B.44}$$

and where $v_{\phi,\psi}$ depend on $\theta_{0,1}$ through Eq. (5.6). In the custodial limit Eq. (B.43) yields $\tan\beta = 1$. Notice that Eq. (B.43) is a straightforward generalization of the similar one for the MSSM, Eq. (B.36).

Now on general grounds Eqs. (B.38), (B.40), and (B.42) should be solved numerically, after running the RGE, to get the correct values of $\tan\beta$, $\tan\theta_0$ and $\tan\theta_1$. Eq. (B.37) will determine the value of $m_3^2(\mathcal{Q}_{EW})$ and the equation for B_+ (a linear combination of Eqs. (B.41) and (B.39)) will fix the custodial value B_Δ at the high scale $\mathcal{M}$. Finally, notice that the RGE's for the parameters involved in (B.38) and (B.40) are decoupled from m_3^2, B_b and B_a so that this procedure for finding the vacuum solution is fully consistent with the RGE running of the theory.

C

Cosmology in the SCTM

C.1 EOM's and neutralino mass matrix in the DM study

Equations of minimum

The minimization conditions are

$$\left.\frac{\partial V}{\partial H_1^0}\right|_{v_1} = \left.\frac{\partial V}{\partial H_2^0}\right|_{v_2} = \left.\frac{\partial V}{\partial \phi^0}\right|_{v_\phi} = \left.\frac{\partial V}{\partial \psi^0}\right|_{v_\psi} = \left.\frac{\partial V}{\partial \chi^0}\right|_{v_\chi} = 0\,. \tag{C.1}$$

With the parametrization of custodial breaking given in Eq. (7.6) we get for the doublet soft masses

$$\begin{aligned}
m_1^2 \equiv m_{H_1}^2 + \mu^2 &= 2v_\Delta(\lambda\mu - A - \lambda\mu_\Delta) - v_\Delta^2(2\lambda_3\lambda + 5\lambda^2) \\
&+ t_\beta\left\{m_3^2 + v_\Delta(4\lambda\mu - A - \lambda\mu_\Delta) - v_\Delta^2(\lambda_3\lambda + 4\lambda^2)\right\} - \frac{g'^2+g^2}{2}v_H^2 c_{2\beta} - 2v_H^2\lambda^2(c_\beta^2+1)\,, \\
m_2^2 \equiv m_{H_2}^2 + \mu^2 &= 2v_\Delta(\lambda\mu - A - \lambda\mu_\Delta) - v_\Delta^2\left(2\lambda_3\lambda + 5\lambda^2\right) \\
&+ \frac{1}{t_\beta}\left\{m_3^2 + v_\Delta(4\lambda\mu - A - \lambda\mu_\Delta) - v_\Delta^2(\lambda_3\lambda + 4\lambda^2)\right\} - \frac{g'^2+g^2}{2}v_H^2 c_{2\beta} - 2v_H^2\lambda^2(s_\beta^2+1)\,,
\end{aligned} \tag{C.2}$$

and for the triplet masses

$$\begin{aligned}
m_{\Sigma_1}^2 &= -\Big\{B_\Delta + \mu_\Delta^2 + v_\Delta\left(A_3 + 3\lambda_3\mu_\Delta\right) + \frac{v_H^2}{v_\Delta}\left(2Ac_\beta^2 + 2\lambda\mu_\Delta s_\beta^2 - 4c_\beta s_\beta\lambda\mu\right) \\
&\quad + v_H^2\left(-(g'^2+g^2)c_{2\beta} + 2c_\beta s_\beta(\lambda_3\lambda + 2\lambda^2) + 2s_\beta^2\lambda_3\lambda + 8c_\beta^2\lambda^2\right) + 2v_\Delta^2\lambda_3^2\Big\}\,, \\
m_{\Sigma_{-1}}^2 &= -\Big\{B_\Delta + \mu_\Delta^2 + v_\Delta\left(A_3 + 3\lambda_3\mu_\Delta\right) + \frac{v_H^2}{v_\Delta}\left(2As_\beta^2 + 2\lambda\mu_\Delta c_\beta^2 - 4c_\beta s_\beta\lambda\mu\right) \\
&\quad + v_H^2\left(-(g'^2+g^2)c_{2\beta} + 2c_\beta s_\beta(\lambda_3\lambda + 2\lambda^2) + 2c_\beta^2\lambda_3\lambda + 8s_\beta^2\lambda^2\right) + 2v_\Delta^2\lambda_3^2\Big\}\,, \\
m_{\Sigma_0}^2 &= -\Big\{B_\Delta + \mu_\Delta^2 + v_\Delta\left(A_3 + 3\lambda_3\mu_\Delta\right) \\
&\quad + \frac{v_H^2}{v_\Delta}\left(2c_\beta s_\beta(A + \lambda\mu_\Delta) - 2\lambda\mu\right) + v_H^2\left(c_\beta s_\beta 8\lambda^2 + (2\lambda_3\lambda + 2\lambda^2)\right) + 2v_\Delta^2\lambda_3^2\Big\}\,.
\end{aligned} \tag{C.3}$$

By making $\tan\beta \to 1$ we recover the custodial limit where the five minimization conditions degenerate into only two, Eq. (4.12).

Neutralino mass matrix

Now we write the full neutralino mass matrix. The matrix $\mathcal{M}^0_{1/2}$ of eq. (6.7) is

$$\begin{pmatrix} M_1 & 0 & -g'c_\beta v_H & g's_\beta v_H & 0 & -\sqrt{2}g'v_\Delta & \sqrt{2}g'v_\Delta \\ 0 & M_2 & gc_\beta v_H & -gs_\beta v_H & 0 & \sqrt{2}gv_\Delta & -\sqrt{2}gv_\Delta \\ -g'c_\beta v_H & gc_\beta v_H & 2\lambda v_\Delta & \lambda v_\Delta - \mu & \sqrt{2}\lambda s_\beta v_H & 0 & 2\sqrt{2}\lambda c_\beta v_H \\ g's_\beta v_H & -gs_\beta v_H & \lambda v_\Delta - \mu & 2\lambda v_\Delta & \sqrt{2}\lambda c_\beta v_H & 2\sqrt{2}\lambda s_\beta v_H & 0 \\ 0 & 0 & \sqrt{2}\lambda s_\beta v_H & \sqrt{2}\lambda c_\beta v_H & \mu_\Delta & -\lambda_3 v_\Delta & -\lambda_3 v_\Delta \\ -\sqrt{2}g'v_\Delta & \sqrt{2}gv_\Delta & 0 & 2\sqrt{2}\lambda s_\beta v_H & -\lambda_3 v_\Delta & 0 & \mu_\Delta - \lambda_3 v_\Delta \\ \sqrt{2}g'v_\Delta & -\sqrt{2}gv_\Delta & 2\sqrt{2}\lambda c_\beta v_H & 0 & -\lambda_3 v_\Delta & \mu_\Delta - \lambda_3 v_\Delta & 0 \end{pmatrix} \tag{C.4}$$

where s_β and c_β are shorthand for the sine and cosine of β respectively. Note that when $\tan\beta \to 1$ we recover the matrix (4.41).

C.2 Formulae for the spectrum of gravitational waves

We present here the set of formulas used to calculate the spectrum presented in Figure 7.8.

Gravitational waves from bubble collisions

In the case we use the envelope approximation to model bubble collisions the peak frequency is [190]

$$\tilde{f}_{env} = 16.5\,\mu\text{Hz}\left(\frac{f}{\beta}\right)\left(\frac{\beta}{H}\right)\left(\frac{T_n}{100\,\text{GeV}}\right)\left(\frac{g_*}{100}\right)^{1/6} \tag{C.5}$$

and the energy density

$$h^2\tilde{\Omega}_{env} = 1.84\times 10^{-6}\kappa^2\left(\frac{v_b^3}{0.42+v_b^2}\right)\left(\frac{H}{\beta}\right)^2\left(\frac{\alpha}{\alpha+1}\right)^2\left(\frac{100}{g_*}\right)^{1/3}. \tag{C.6}$$

The efficiency factor κ is

$$\kappa = \frac{1}{1+0.715\alpha}\left(0.715\alpha + \frac{4}{27}\sqrt{\frac{3\alpha}{2}}\right) \tag{C.7}$$

the bubble wall velocity v_b is

$$v_b = \frac{\sqrt{1/3}+\sqrt{\alpha^2+2\alpha/3}}{1+\alpha}, \tag{C.8}$$

and

$$\frac{f}{\beta} = \frac{0.62}{1.8-0.1v_b+v_b^2}. \tag{C.9}$$

The spectrum then has the following shape

$$\Omega_{env}(f) = \tilde{\Omega}_{env}\frac{3.8(f/\tilde{f}_{env})^{2.8}}{2.8+(f/\tilde{f}_{env})^{3.8}}. \tag{C.10}$$

Gravitational waves from sound waves

The peak amplitude of GW radiation from sound waves is given by [191, 219]

$$h^2\tilde{\Omega}_{sw} = 2.65 \cdot 10^{-6}\, v_b\, \kappa^2 \left(\frac{H}{\beta}\right) \left(\frac{\alpha}{\alpha+1}\right)^2 \left(\frac{g_*}{100}\right)^{-1/3}, \tag{C.11}$$

which is larger than the result one gets from the envelope approximation by a factor β/H. The peak frequency is

$$\tilde{f}_{sw} = 19\,\mu\text{Hz}\, \frac{1}{v_b} \left(\frac{\beta}{H}\right) \left(\frac{T_n}{100\,\text{GeV}}\right) \left(\frac{g_*}{100}\right)^{1/6} \tag{C.12}$$

and the fit to the numerical spectrum is given by

$$\Omega_{sw}(f) = \tilde{\Omega}_{sw} \left(\frac{7}{4+3(f/\tilde{f}_{sw})^2}\right)^{7/2} (f/\tilde{f}_{sw})^3\,. \tag{C.13}$$

Bibliography

Bibliography

[1] **ATLAS Collaboration** Collaboration, G. Aad *et. al.*, *Observation of a new particle in the search for the Standard Model Higgs boson with the ATLAS detector at the LHC*, *Phys.Lett.* **B716** (2012) 1–29, [1207.7214].

[2] **CMS Collaboration** Collaboration, S. Chatrchyan *et. al.*, *Observation of a new boson at a mass of 125 GeV with the CMS experiment at the LHC*, *Phys.Lett.* **B716** (2012) 30–61, [1207.7235].

[3] A. Delgado, M. Garcia, and M. Quiros, *Electroweak and supersymmetry breaking from the Higgs discovery*, *Phys.Rev.* **D90** (2014) 015016, [1312.3235].

[4] L. Cort, M. Garcia, and M. Quiros, *Supersymmetric Custodial Triplets*, *Phys.Rev.* **D88** (2013) 075010, [1308.4025].

[5] M. Garcia-Pepin, S. Gori, M. Quiros, R. Vega, R. Vega-Morales, and T.-T. Yu, *Supersymmetric Custodial Higgs Triplets and the Breaking of Universality*, *Phys. Rev.* **D91** (2015), no. 1 015016, [1409.5737].

[6] A. Delgado, M. Garcia-Pepin, and M. Quiros, *GMSB with Light Stops*, *JHEP* **08** (2015) 159, [1505.07469].

[7] A. Delgado, M. Garcia-Pepin, B. Ostdiek, and M. Quiros, *Dark Matter from the Supersymmetric Custodial Triplet Model*, *Phys. Rev.* **D92** (2015), no. 1 015011, [1504.02486].

[8] M. Garcia-Pepin and M. Quiros, *Strong electroweak phase transition from Supersymmetric Custodial Triplets*, 1602.01351.

[9] A. Delgado, M. Garcia-Pepin, M. Quiros, J. Santiago, and R. Vega-Morales, *Diphoton and Diboson Probes of Fermiophobic Higgs Bosons at the LHC*, 1603.00962.

[10] M. Srednicki, *Quantum field theory*. Cambridge University Press, 2007.

[11] M. E. Peskin and D. V. Schroeder, *An Introduction to quantum field theory*. 1995.

[12] J. Elias-Miro, J. R. Espinosa, E. Masso, and A. Pomarol, *Higgs windows to new physics through d=6 operators: constraints and one-loop anomalous dimensions*, *JHEP* **11** (2013) 066, [1308.1879].

[13] S. Sachdev, *What can gauge-gravity duality teach us about condensed matter physics?*, *Ann. Rev. Condensed Matter Phys.* **3** (2012) 9–33, [1108.1197].

[14] R. Contino, *The Higgs as a Composite Nambu-Goldstone Boson*, in *Physics of the large and the small, TASI 09, proceedings of the Theoretical Advanced Study Institute in Elementary Particle Physics, Boulder, Colorado, USA, 1-26 June 2009*, pp. 235–306, 2011. 1005.4269.

[15] G. Degrassi, S. Di Vita, J. Elias-Miro, J. R. Espinosa, G. F. Giudice, G. Isidori, and A. Strumia, *Higgs mass and vacuum stability in the Standard Model at NNLO*, *JHEP* **08** (2012) 098, [1205.6497].

[16] M. E. Peskin and T. Takeuchi, *Estimation of oblique electroweak corrections*, *Phys. Rev.* **D46** (1992) 381–409.

[17] J. L. F. Barbon and J. R. Espinosa, *On the Naturalness of Higgs Inflation*, *Phys. Rev.* **D79** (2009) 081302, [0903.0355].

[18] S. Weinberg, *Anthropic Bound on the Cosmological Constant*, *Phys. Rev. Lett.* **59** (1987) 2607.

[19] M. Shaposhnikov, *Is there a new physics between electroweak and Planck scales?*, in *Astroparticle Physics: Current Issues, 2007 (APCI07) Budapest, Hungary, June 21-23, 2007*, 2007. 0708.3550.

[20] G. 't Hooft, *Naturalness, chiral symmetry, and spontaneous chiral symmetry breaking*, *NATO Sci. Ser. B* **59** (1980) 135.

[21] G. F. Giudice, *Naturally Speaking: The Naturalness Criterion and Physics at the LHC*, 0801.2562.

[22] D. B. Kaplan and H. Georgi, *SU(2) x U(1) Breaking by Vacuum Misalignment*, *Phys. Lett.* **B136** (1984) 183.

[23] P. W. Graham, D. E. Kaplan, and S. Rajendran, *Cosmological Relaxation of the Electroweak Scale*, *Phys. Rev. Lett.* **115** (2015), no. 22 221801, [1504.07551].

[24] A. N. Schellekens, *Life at the Interface of Particle Physics and String Theory*, *Rev. Mod. Phys.* **85** (2013), no. 4 1491–1540, [1306.5083].

[25] Z. Chacko, H.-S. Goh, and R. Harnik, *The Twin Higgs: Natural electroweak breaking from mirror symmetry*, *Phys. Rev. Lett.* **96** (2006) 231802, [hep-ph/0506256].

[26] S. P. Martin, *A Supersymmetry primer*, hep-ph/9709356. [Adv. Ser. Direct. High Energy Phys.18,1(1998)].

[27] F. Quevedo, S. Krippendorf, and O. Schlotterer, *Cambridge Lectures on Supersymmetry and Extra Dimensions*, 1011.1491.

[28] M. Bertolini, *Lectures on Supersymmetry*, http://people.sissa.it/bertmat/teaching.htm.

[29] G. Giudice and R. Rattazzi, *Theories with gauge mediated supersymmetry breaking*, *Phys.Rept.* **322** (1999) 419–499, [hep-ph/9801271].

[30] R. Haag, J. T. Lopuszanski, and M. Sohnius, *All Possible Generators of Supersymmetries of the s Matrix*, *Nucl. Phys.* **B88** (1975) 257.

[31] S. R. Coleman and J. Mandula, *All Possible Symmetries of the S Matrix*, *Phys. Rev.* **159** (1967) 1251–1256.

[32] A. Pomarol and M. Quiros, *The Standard model from extra dimensions*, *Phys. Lett.* **B438** (1998) 255–260, [hep-ph/9806263].

[33] A. Delgado, A. Pomarol, and M. Quiros, *Supersymmetry and electroweak breaking from extra dimensions at the TeV scale*, *Phys. Rev.* **D60** (1999) 095008, [hep-ph/9812489].

[34] G. F. Giudice and A. Masiero, *A Natural Solution to the mu Problem in Supergravity Theories*, *Phys. Lett.* **B206** (1988) 480–484.

[35] I. Antoniadis, K. Benakli, and M. Quiros, *Sequestered gravity in gauge mediation*, 1512.00029.

[36] G. Dvali, G. Giudice, and A. Pomarol, *The Mu problem in theories with gauge mediated supersymmetry breaking*, *Nucl.Phys.* **B478** (1996) 31–45, [hep-ph/9603238].

[37] M. J. G. Veltman, *The Infrared - Ultraviolet Connection*, *Acta Phys. Polon.* **B12** (1981) 437.

[38] J. A. Casas, J. R. Espinosa, and J. M. Moreno, *The 750 GeV Diphoton Excess as a First Light on Supersymmetry Breaking*, 1512.07895.

[39] M. Fabbrichesi and A. Urbano, *The breaking of the $SU(2)_L \times U(1)_Y$ symmetry: The 750 GeV resonance at the LHC and perturbative unitarity*, 1601.02447.

[40] N. Arkani-Hamed and S. Dimopoulos, *Supersymmetric unification without low energy supersymmetry and signatures for fine-tuning at the LHC*, *JHEP* **06** (2005) 073, [hep-th/0405159].

[41] L. E. Ibanez and G. G. Ross, *SU(2)-L x U(1) Symmetry Breaking as a Radiative Effect of Supersymmetry Breaking in Guts*, *Phys. Lett.* **B110** (1982) 215–220.

[42] L. E. Ibanez and A. M. Uranga, *String theory and particle physics: An introduction to string phenomenology*. Cambridge University Press, 2012.

[43] M. Koratzinos, A. P. Blondel, R. Aleksan, P. Janot, F. Zimmermann, J. R. Ellis, and M. Zanetti, *TLEP, first step in a long-term vision for HEP*, in *Snowmass 2013: Lepton Collider Workshop Cambridge, MA, USA, April 10-11, 2013*, 2013. 1306.5981.

[44] M. Carena, J. R. Espinosa, M. Quiros, and C. E. M. Wagner, *Analytical expressions for radiatively corrected Higgs masses and couplings in the MSSM*, *Phys. Lett.* **B355** (1995) 209–221, [hep-ph/9504316].

[45] L. E. Ibanez and I. Valenzuela, *The Higgs Mass as a Signature of Heavy SUSY*, *JHEP* **05** (2013) 064, [1301.5167].

[46] L. J. Hall and Y. Nomura, *Grand Unification and Intermediate Scale Supersymmetry*, *JHEP* **02** (2014) 129, [1312.6695].

[47] P. Draper, G. Lee, and C. E. M. Wagner, *Precise Estimates of the Higgs Mass in Heavy SUSY*, *Phys.Rev.* **D89** (2014) 055023, [1312.5743].

[48] G. F. Giudice and R. Rattazzi, *Living Dangerously with Low-Energy Supersymmetry*, *Nucl. Phys.* **B757** (2006) 19–46, [hep-ph/0606105].

[49] M. E. Cabrera, J. A. Casas, and A. Delgado, *Upper Bounds on Superpartner Masses from Upper Bounds on the Higgs Boson Mass*, *Phys. Rev. Lett.* **108** (2012) 021802, [1108.3867].

[50] G. F. Giudice and A. Strumia, *Probing High-Scale and Split Supersymmetry with Higgs Mass Measurements*, *Nucl. Phys.* **B858** (2012) 63–83, [1108.6077].

[51] H. Arason, D. J. Castano, B. Keszthelyi, S. Mikaelian, E. J. Piard, P. Ramond, and B. D. Wright, *Renormalization group study of the standard model and its extensions. 1. The Standard model*, *Phys. Rev.* **D46** (1992) 3945–3965.

[52] J. A. Casas, J. R. Espinosa, M. Quiros, and A. Riotto, *The Lightest Higgs boson mass in the minimal supersymmetric standard model*, *Nucl. Phys.* **B436** (1995) 3–29, [hep-ph/9407389]. [Erratum: Nucl. Phys.B439,466(1995)].

[53] S. Alekhin, A. Djouadi, and S. Moch, *The top quark and Higgs boson masses and the stability of the electroweak vacuum*, *Phys. Lett.* **B716** (2012) 214–219, [1207.0980].

[54] I. Masina, *Higgs boson and top quark masses as tests of electroweak vacuum stability*, *Phys. Rev.* **D87** (2013), no. 5 053001, [1209.0393].

[55] D. Buttazzo, G. Degrassi, P. P. Giardino, G. F. Giudice, F. Sala, A. Salvio, and A. Strumia, *Investigating the near-criticality of the Higgs boson*, *JHEP* **12** (2013) 089, [1307.3536].

[56] I. Masina and M. Quiros, *On the Veltman Condition, the Hierarchy Problem and High-Scale Supersymmetry*, *Phys. Rev.* **D88** (2013) 093003, [1308.1242].

[57] S. P. Martin and M. T. Vaughn, *Two loop renormalization group equations for soft supersymmetry breaking couplings*, *Phys. Rev.* **D50** (1994) 2282, [hep-ph/9311340]. [Erratum: Phys. Rev.D78,039903(2008)].

[58] L. J. Hall and Y. Nomura, *A Finely-Predicted Higgs Boson Mass from A Finely-Tuned Weak Scale*, *JHEP* **03** (2010) 076, [0910.2235].

[59] A. Hebecker, A. K. Knochel, and T. Weigand, *The Higgs mass from a String-Theoretic Perspective*, *Nucl. Phys.* **B874** (2013) 1–35, [1304.2767].

[60] A. Nelson, P. Tanedo, and D. Whiteson, *Limiting SUSY compressed spectra scenarios*, 1509.08485.

[61] G. D. Kribs and A. Martin, *Supersoft Supersymmetry is Super-Safe*, *Phys. Rev.* **D85** (2012) 115014, [1203.4821].

[62] J. Espinosa and M. Quiros, *Higgs triplets in the supersymmetric standard model*, *Nucl.Phys.* **B384** (1992) 113–146.

[63] A. Delgado, G. Nardini, and M. Quiros, *Large diphoton Higgs rates from supersymmetric triplets*, *Phys.Rev.* **D86** (2012) 115010, [1207.6596].

[64] P. Batra, A. Delgado, D. E. Kaplan, and T. M. P. Tait, *The Higgs mass bound in gauge extensions of the minimal supersymmetric standard model*, *JHEP* **02** (2004) 043, [hep-ph/0309149].

[65] J. Bagger, E. Poppitz, and L. Randall, *Destabilizing divergences in supergravity theories at two loops*, *Nucl. Phys.* **B455** (1995) 59–82, [hep-ph/9505244].

[66] S. A. Abel, S. Sarkar, and P. L. White, *On the cosmological domain wall problem for the minimally extended supersymmetric standard model*, *Nucl. Phys.* **B454** (1995) 663–684, [hep-ph/9506359].

[67] H. Georgi and M. Machacek, *DOUBLY CHARGED HIGGS BOSONS*, *Nucl.Phys.* **B262** (1985) 463.

[68] M. S. Chanowitz and M. Golden, *Higgs Boson Triplets With M (W) = M (Z) $\cos\theta\omega$*, *Phys.Lett.* **B165** (1985) 105.

[69] J. Gunion, R. Vega, and J. Wudka, *Higgs triplets in the standard model*, *Phys.Rev.* **D42** (1990) 1673–1691.

[70] J. Gunion, R. Vega, and J. Wudka, *Naturalness problems for rho = 1 and other large one loop effects for a standard model Higgs sector containing triplet fields*, *Phys.Rev.* **D43** (1991) 2322–2336.

[71] B. W. Lee, C. Quigg, and H. B. Thacker, *The Strength of Weak Interactions at Very High-Energies and the Higgs Boson Mass*, *Phys. Rev. Lett.* **38** (1977) 883–885.

[72] **ATLAS** Collaboration, *Combined coupling measurements of the Higgs-like boson with the ATLAS detector using up to 25 fb^{-1} of proton-proton collision data*, .

[73] M. A. Shifman, A. Vainshtein, M. Voloshin, and V. I. Zakharov, *Low-Energy Theorems for Higgs Boson Couplings to Photons*, *Sov.J.Nucl.Phys.* **30** (1979) 711–716.

[74] M. Carena, I. Low, and C. E. Wagner, *Implications of a Modified Higgs to Diphoton Decay Width*, *JHEP* **1208** (2012) 060, [1206.1082].

[75] P. Fileviez Perez and S. Spinner, *Higgs mass via type II seesaw mechanism*, *Phys.Rev.* **D87** (2013), no. 3 031702, [1211.1025].

[76] P. Fileviez Perez and S. Spinner, *On the Higgs Mass and Perturbativity*, *Phys.Lett.* **B723** (2013) 371–383, [1209.5769].

[77] **Particle Data Group** Collaboration, J. Beringer *et. al.*, *Review of Particle Physics (RPP)*, *Phys.Rev.* **D86** (2012) 010001.

[78] A. Delgado, G. Nardini, and M. Quiros, *A Light Supersymmetric Higgs Sector Hidden by a Standard Model-like Higgs*, *JHEP* **1307** (2013) 054, [1303.0800].

[79] P. Draper, P. Meade, M. Reece, and D. Shih, *Implications of a 125 GeV Higgs for the MSSM and Low-Scale SUSY Breaking*, *Phys.Rev.* **D85** (2012) 095007, [1112.3068].

[80] J. L. Feng, P. Kant, S. Profumo, and D. Sanford, *Three-Loop Corrections to the Higgs Boson Mass and Implications for Supersymmetry at the LHC*, *Phys.Rev.Lett.* **111** (2013) 131802, [1306.2318].

[81] K. Agashe, A. Azatov, A. Katz, and D. Kim, *Improving the tunings of the MSSM by adding triplets and singlet*, *Phys.Rev.* **D84** (2011) 115024, [1109.2842].

[82] H. E. Logan and M.-A. Roy, *Higgs couplings in a model with triplets*, *Phys.Rev.* **D82** (2010) 115011, [1008.4869].

[83] A. Falkowski, S. Rychkov, and A. Urbano, *What if the Higgs couplings to W and Z bosons are larger than in the Standard Model?*, *JHEP* **1204** (2012) 073, [1202.1532].

[84] *Precise determination of the mass of the Higgs boson and studies of the compatibility of its couplings with the standard model*, Tech. Rep. CMS-PAS-HIG-14-009, CMS Collaboration, Geneva, 2014.

[85] *Updated coupling measurements of the Higgs boson with the ATLAS detector using up to 25 fb^{-1} of proton-proton collision data*, Tech. Rep. ATLAS-CONF-2014-009, ATLAS Collaboration, Geneva, 2014.

[86] M. E. Peskin, *Estimation of LHC and ILC Capabilities for Precision Higgs Boson Coupling Measurements*, in *Community Summer Study 2013: Snowmass on the Mississippi (CSS2013) Minneapolis, MN, USA, July 29-August 6, 2013*, 2013. 1312.4974.

[87] **ATLAS** Collaboration, *Physics at a High-Luminosity LHC with ATLAS*, in *Community Summer Study 2013: Snowmass on the Mississippi (CSS2013) Minneapolis, MN, USA, July 29-August 6, 2013*, 2013. 1307.7292.

[88] **CMS** Collaboration, *Projected Performance of an Upgraded CMS Detector at the LHC and HL-LHC: Contribution to the Snowmass Process*, in *Community Summer Study 2013: Snowmass on the Mississippi (CSS2013) Minneapolis, MN, USA, July 29-August 6, 2013*, 2013. 1307.7135.

[89] R. Brock *et. al.*, *Planning the Future of U.S. Particle Physics (Snowmass 2013): Chapter 3: Energy Frontier*, in *Community Summer Study 2013: Snowmass on the Mississippi (CSS2013) Minneapolis, MN, USA, July 29-August 6, 2013*, 2014. 1401.6081.

[90] B. A. Dobrescu and J. D. Lykken, *Coupling spans of the Higgs-like boson*, *JHEP* **1302** (2013) 073, [1210.3342].

[91] G. Belanger, B. Dumont, U. Ellwanger, J. Gunion, and S. Kraml, *Global fit to Higgs signal strengths and couplings and implications for extended Higgs sectors*, *Phys.Rev.* **D88** (2013) 075008, [1306.2941].

[92] A. De Rujula, J. Lykken, M. Pierini, C. Rogan, and M. Spiropulu, *Higgs look-alikes at the LHC*, *Phys.Rev.* **D82** (2010) 013003, [1001.5300].

[93] N. D. Christensen, T. Han, and Y. Li, *Testing CP Violation in ZZH Interactions at the LHC*, *Phys.Lett.* **B693** (2010) 28–35, [1005.5393].

[94] I. Anderson, S. Bolognesi, F. Caola, Y. Gao, A. V. Gritsan, *et. al.*, *Constraining anomalous HVV interactions at proton and lepton colliders*, *Phys.Rev.* **D89** (2014) 035007, [1309.4819].

[95] J. S. Gainer, J. Lykken, K. T. Matchev, S. Mrenna, and M. Park, *Geolocating the Higgs Boson Candidate at the LHC*, *Phys.Rev.Lett.* **111** (2013) 041801, [1304.4936].

[96] Y. Chen, R. Harnik, and R. Vega-Morales, *Probing the Higgs Couplings to Photons in $h \to 4l$ at the LHC*, *Phys.Rev.Lett.* **113** (2014), no. 19 191801, [1404.1336].

[97] Y. Chen, A. Falkowski, I. Low, and R. Vega-Morales, *New Observables for CP Violation in Higgs Decays*, *Phys. Rev.* **D90** (2014), no. 11 113006, [1405.6723].

[98] A. Falkowski and R. Vega-Morales, *Exotic Higgs decays in the golden channel*, *JHEP* **12** (2014) 037, [1405.1095].

[99] S. Godfrey and K. Moats, *Exploring Higgs Triplet Models via Vector Boson Scattering at the LHC*, *Phys.Rev.* **D81** (2010) 075026, [1003.3033].

[100] C. Englert, E. Re, and M. Spannowsky, *Triplet Higgs boson collider phenomenology after the LHC*, *Phys.Rev.* **D87** (2013), no. 9 095014, [1302.6505].

[101] S. Kanemura, M. Kikuchi, K. Yagyu, and H. Yokoya, *Bounds on the mass of doubly-charged Higgs bosons in the same-sign diboson decay scenario*, *Phys.Rev.* **D90** (2014), no. 11 115018, [1407.6547].

[102] K. Nickel and F. Staub, *Precise determination of the Higgs mass in supersymmetric models with vectorlike tops and the impact on naturalness in minimal GMSB*, *JHEP* **07** (2015) 139, [1505.06077].

[103] N. Craig, S. Knapen, and D. Shih, *General Messenger Higgs Mediation*, *JHEP* **1308** (2013) 118, [1302.2642].

[104] J. A. Evans and D. Shih, *Surveying Extended GMSB Models with m_h=125 GeV*, *JHEP* **1308** (2013) 093, [1303.0228].

[105] J. A. Evans, D. Shih, and A. Thalapillil, *Chiral Flavor Violation from Extended Gauge Mediation*, *JHEP* **07** (2015) 040, [1504.00930].

[106] P. Byakti and T. S. Ray, *Burgeoning the Higgs mass to 125 GeV through messenger-matter interactions in GMSB models*, *JHEP* **1305** (2013) 055, [1301.7605].

[107] Z. Kang, T. Li, T. Liu, C. Tong, and J. M. Yang, *A Heavy SM-like Higgs and a Light Stop from Yukawa-Deflected Gauge Mediation*, *Phys.Rev.* **D86** (2012) 095020, [1203.2336].

[108] J. L. Evans, M. Ibe, and T. T. Yanagida, *Relatively Heavy Higgs Boson in More Generic Gauge Mediation*, *Phys.Lett.* **B705** (2011) 342–348, [1107.3006].

[109] L. Calibbi, P. Paradisi, and R. Ziegler, *Gauge Mediation beyond Minimal Flavor Violation*, *JHEP* **1306** (2013) 052, [1304.1453].

[110] L. Calibbi, P. Paradisi, and R. Ziegler, *Lepton Flavor Violation in Flavored Gauge Mediation*, *Eur.Phys.J.* **C74** (2014), no. 12 3211, [1408.0754].

[111] Z. Chacko and E. Ponton, *Yukawa deflected gauge mediation*, *Phys.Rev.* **D66** (2002) 095004, [hep-ph/0112190].

[112] Y. Shadmi and P. Z. Szabo, *Flavored Gauge-Mediation*, *JHEP* **1206** (2012) 124, [1103.0292].

[113] A. Delgado, G. Giudice, and P. Slavich, *Dynamical mu term in gauge mediation*, *Phys.Lett.* **B653** (2007) 424–433, [0706.3873].

[114] P. Meade, N. Seiberg, and D. Shih, *General Gauge Mediation*, *Prog.Theor.Phys.Suppl.* **177** (2009) 143–158, [0801.3278].

[115] T. Han, T. Yanagida, and R.-J. Zhang, *Adjoint messengers and perturbative unification at the string scale*, *Phys.Rev.* **D58** (1998) 095011, [hep-ph/9804228].

[116] S. Dimopoulos and G. Giudice, *Multimessenger theories of gauge mediated supersymmetry breaking*, *Phys.Lett.* **B393** (1997) 72–78, [hep-ph/9609344].

[117] S. Dimopoulos, G. Giudice, and A. Pomarol, *Dark matter in theories of gauge mediated supersymmetry breaking*, *Phys.Lett.* **B389** (1996) 37–42, [hep-ph/9607225].

[118] S. P. Martin, *Generalized messengers of supersymmetry breaking and the sparticle mass spectrum*, *Phys.Rev.* **D55** (1997) 3177–3187, [hep-ph/9608224].

[119] A. De Simone, R. Franceschini, G. F. Giudice, D. Pappadopulo, and R. Rattazzi, *Lopsided Gauge Mediation*, *JHEP* **05** (2011) 112, [1103.6033].

[120] **ATLAS** Collaboration, G. Aad *et. al.*, *Search for supersymmetry in events with large missing transverse momentum, jets, and at least one tau lepton in 20 fb^{-1} of $\sqrt{s} = 8$ TeV proton-proton collision data with the ATLAS detector*, *JHEP* **1409** (2014) 103, [1407.0603].

[121] M. Viel, J. Lesgourgues, M. G. Haehnelt, S. Matarrese, and A. Riotto, *Constraining warm dark matter candidates including sterile neutrinos and light gravitinos with WMAP and the Lyman-alpha forest*, *Phys.Rev.* **D71** (2005) 063534, [astro-ph/0501562].

[122] **ATLAS** Collaboration, G. Aad *et. al.*, *Search for direct production of charginos, neutralinos and sleptons in final states with two leptons and missing transverse momentum in pp collisions at $\sqrt{s} = 8$ TeV with the ATLAS detector*, *JHEP* **1405** (2014) 071, [1403.5294].

[123] **CMS** Collaboration, V. Khachatryan *et. al.*, *Searches for electroweak production of charginos, neutralinos, and sleptons decaying to leptons and W, Z, and Higgs bosons in pp collisions at 8 TeV*, *Eur.Phys.J.* **C74** (2014), no. 9 3036, [1405.7570].

[124] **CMS Collaboration** Collaboration, S. Chatrchyan *et. al.*, *Search for a fermiophobic Higgs boson in pp collisions at $\sqrt{s} = 7$ TeV*, *JHEP* **1209** (2012) 111, [1207.1130].

[125] **ATLAS** Collaboration, G. Aad *et. al.*, *Search for a Charged Higgs Boson Produced in the Vector-Boson Fusion Mode with Decay $H^{\pm} \to W^{\pm}Z$ using pp Collisions at $\sqrt{s} = 8$??TeV with the ATLAS Experiment*, *Phys. Rev. Lett.* **114** (2015), no. 23 231801, [1503.04233].

[126] O. Eberhardt, U. Nierste, and M. Wiebusch, *Status of the two-Higgs-doublet model of type II*, *JHEP* **1307** (2013) 118, [1305.1649].

[127] *Measurements of the Higgs boson production and decay rates and coupling strengths using pp collision data at $\sqrt{s} = 7$ and 8 TeV in the ATLAS experiment*, Tech. Rep. ATLAS-CONF-2015-007, CERN, Geneva, Mar, 2015.

[128] D. Comelli and J. R. Espinosa, *New limits on the mass of neutral Higgses in general models*, *Phys. Lett.* **B388** (1996) 793–802, [hep-ph/9607400].

[129] C. Cheung, L. J. Hall, D. Pinner, and J. T. Ruderman, *Prospects and Blind Spots for Neutralino Dark Matter*, *JHEP* **1305** (2013) 100, [1211.4873].

[130] **LEP2 SUSY Working Group** Collaboration, "LEPSUSYWG, ALEPH, DELPHI, L3 and OPAL experiments."

[131] T. Cohen, M. Lisanti, A. Pierce, and T. R. Slatyer, *Wino Dark Matter Under Siege*, *JCAP* **1310** (2013) 061, [1307.4082].

[132] J. Fan and M. Reece, *In Wino Veritas? Indirect Searches Shed Light on Neutralino Dark Matter*, *JHEP* **1310** (2013) 124, [1307.4400].

[133] N. Arkani-Hamed, A. Delgado, and G. Giudice, *The Well-tempered neutralino*, *Nucl.Phys.* **B741** (2006) 108–130, [hep-ph/0601041].

[134] H. Baer, E.-K. Park, and X. Tata, *Collider, direct and indirect detection of supersymmetric dark matter*, *New J.Phys.* **11** (2009) 105024, [0903.0555].

[135] P. Schwaller and J. Zurita, *Compressed electroweakino spectra at the LHC*, *JHEP* **1403** (2014) 060, [1312.7350].

[136] M. Low and L.-T. Wang, *Neutralino dark matter at 14 TeV and 100 TeV*, *JHEP* **1408** (2014) 161, [1404.0682].

[137] J. Bramante, A. Delgado, F. Elahi, A. Martin, and B. Ostdiek, *Catching sparks from well-forged neutralinos*, *Phys.Rev.* **D90** (2014), no. 9 095008, [1408.6530].

[138] L. Calibbi, J. M. Lindert, T. Ota, and Y. Takanishi, *LHC Tests of Light Neutralino Dark Matter without Light Sfermions*, *JHEP* **1411** (2014) 106, [1410.5730].

[139] C. Han, *Probing light bino and higgsinos at the LHC*, 1409.7000.

[140] J. Bramante, P. J. Fox, A. Martin, B. Ostdiek, T. Plehn, *et. al.*, *Relic neutralino surface at a 100 TeV collider*, *Phys.Rev.* **D91** (2015), no. 5 054015, [1412.4789].

[141] T. A. W. Martin and D. Morrissey, *Electroweakino constraints from LHC data*, *JHEP* **1412** (2014) 168, [1409.6322].

[142] C. Han, L. Wu, J. M. Yang, M. Zhang, and Y. Zhang, *New approach for detecting a compressed bino/wino at the LHC*, *Phys. Rev.* **D91** (2015) 055030, [1409.4533].

[143] J. Ellis and K. A. Olive, *Revisiting the Higgs Mass and Dark Matter in the CMSSM*, *Eur.Phys.J.* **C72** (2012) 2005, [1202.3262].

[144] A. Fowlie, M. Kazana, K. Kowalska, S. Munir, L. Roszkowski, *et. al.*, *The CMSSM Favoring New Territories: The Impact of New LHC Limits and a 125 GeV Higgs*, *Phys.Rev.* **D86** (2012) 075010, [1206.0264].

[145] T. Cohen and J. G. Wacker, *Here be Dragons: The Unexplored Continents of the CMSSM*, *JHEP* **1309** (2013) 061, [1305.2914].

[146] D. Hooper, C. Kelso, P. Sandick, and W. Xue, *Closing Supersymmetric Resonance Regions With Direct Detection Experiments*, *Phys.Rev.* **D88** (2013), no. 1 015010, [1304.2417].

[147] T. Han, Z. Liu, and A. Natarajan, *Dark matter and Higgs bosons in the MSSM*, *JHEP* **1311** (2013) 008, [1303.3040].

[148] S. Henrot-Versill, R. Lafaye, T. Plehn, M. Rauch, D. Zerwas, *et. al.*, *Constraining Supersymmetry using the relic density and the Higgs boson*, *Phys.Rev.* **D89** (2014), no. 5 055017, [1309.6958].

[149] A. Anandakrishnan, B. Shakya, and K. Sinha, *Dark matter at the pseudoscalar Higgs resonance in the phenomenological MSSM and SUSY GUTs*, *Phys.Rev.* **D91** (2015), no. 3 035029, [1410.0356].

[150] F. Staub, *SARAH*, 0806.0538.

[151] F. Staub, *From Superpotential to Model Files for FeynArts and CalcHep/CompHep*, *Comput.Phys.Commun.* **181** (2010) 1077–1086, [0909.2863].

[152] F. Staub, T. Ohl, W. Porod, and C. Speckner, *A Tool Box for Implementing Supersymmetric Models*, *Comput.Phys.Commun.* **183** (2012) 2165–2206, [1109.5147].

[153] F. Staub, *SARAH 4: A tool for (not only SUSY) model builders*, *Comput.Phys.Commun.* **185** (2014) 1773–1790, [1309.7223].

[154] F. Staub, *Exploring new models in all detail with SARAH*, *Adv. High Energy Phys.* **2015** (2015) 840780, [1503.04200].

[155] W. Porod, *SPheno, a program for calculating supersymmetric spectra, SUSY particle decays and SUSY particle production at e+ e- colliders*, *Comput.Phys.Commun.* **153** (2003) 275–315, [hep-ph/0301101].

[156] W. Porod and F. Staub, *SPheno 3.1: Extensions including flavour, CP-phases and models beyond the MSSM*, *Comput.Phys.Commun.* **183** (2012) 2458–2469, [1104.1573].

[157] A. Pukhov, E. Boos, M. Dubinin, V. Edneral, V. Ilyin, *et. al.*, *CompHEP: A Package for evaluation of Feynman diagrams and integration over multiparticle phase space*, hep-ph/9908288.

[158] G. Belanger, F. Boudjema, A. Pukhov, and A. Semenov, *micrOMEGAs_3: A program for calculating dark matter observables*, *Comput.Phys.Commun.* **185** (2014) 960–985, [1305.0237].

[159] **Particle Data Group** Collaboration, K. Olive *et. al.*, *Review of Particle Physics*, *Chin.Phys.* **C38** (2014) 090001.

[160] C. Arina, V. Martin-Lozano, and G. Nardini, *Dark matter versus $h \to \gamma\gamma$ and $h \to \gamma Z$ with supersymmetric triplets*, *JHEP* **1408** (2014) 015, [1403.6434].

[161] **LUX Collaboration** Collaboration, D. Akerib *et. al.*, *First results from the LUX dark matter experiment at the Sanford Underground Research Facility*, *Phys.Rev.Lett.* **112** (2014) 091303, [1310.8214].

[162] **COUPP Collaboration** Collaboration, E. Behnke *et. al.*, *Improved Spin-Dependent WIMP Limits from a Bubble Chamber*, *Science* **319** (2008) 933–936, [0804.2886].

[163] E. Behnke, J. Behnke, S. Brice, D. Broemmelsiek, J. Collar, *et. al.*, *Improved Limits on Spin-Dependent WIMP-Proton Interactions from a Two Liter CF_3I Bubble Chamber*, *Phys.Rev.Lett.* **106** (2011) 021303, [1008.3518].

[164] **Super-Kamiokande** Collaboration, T. Tanaka *et. al.*, *An Indirect Search for WIMPs in the Sun using 3109.6 days of upward-going muons in Super-Kamiokande*, *Astrophys.J.* **742** (2011) 78, [1108.3384].

[165] **IceCube** Collaboration, R. Abbasi *et. al.*, *Multi-year search for dark matter annihilations in the Sun with the AMANDA-II and IceCube detectors*, *Phys.Rev.* **D85** (2012) 042002, [1112.1840].

[166] **IceCube** Collaboration, M. Aartsen *et. al.*, *Search for dark matter annihilations in the Sun with the 79-string IceCube detector*, *Phys.Rev.Lett.* **110** (2013), no. 13 131302, [1212.4097].

[167] **Fermi-LAT** Collaboration, M. Ackermann *et. al.*, *Dark matter constraints from observations of 25 Milky Way satellite galaxies with the Fermi Large Area Telescope*, *Phys.Rev.* **D89** (2014) 042001, [1310.0828].

[168] **Fermi-LAT** Collaboration, M. Ackermann *et. al.*, *Searching for Dark Matter Annihilation from Milky Way Dwarf Spheroidal Galaxies with Six Years of Fermi Large Area Telescope Data*, *Phys. Rev. Lett.* **115** (2015), no. 23 231301, [1503.02641].

[169] A. D. Sakharov, *Violation of CP Invariance, c Asymmetry, and Baryon Asymmetry of the Universe*, *Pisma Zh. Eksp. Teor. Fiz.* **5** (1967) 32–35. [Usp. Fiz. Nauk161,61(1991)].

[170] A. G. Cohen, D. B. Kaplan, and A. E. Nelson, *Progress in electroweak baryogenesis*, *Ann. Rev. Nucl. Part. Sci.* **43** (1993) 27–70, [hep-ph/9302210].

[171] M. Quiros, *Field theory at finite temperature and phase transitions*, *Helv. Phys. Acta* **67** (1994) 451–583.

[172] M. Quiros, *Finite temperature field theory and phase transitions*, in *High energy physics and cosmology. Proceedings, Summer School, Trieste, Italy, June 29-July 17, 1998*, pp. 187–259, 1999. hep-ph/9901312.

[173] V. A. Rubakov and M. E. Shaposhnikov, *Electroweak baryon number nonconservation in the early universe and in high-energy collisions*, *Usp. Fiz. Nauk* **166** (1996) 493–537, [hep-ph/9603208]. [Phys. Usp.39,461(1996)].

[174] M. Carena and C. E. M. Wagner, *Electroweak baryogenesis and Higgs physics*, hep-ph/9704347.

[175] D. E. Morrissey and M. J. Ramsey-Musolf, *Electroweak baryogenesis*, *New J. Phys.* **14** (2012) 125003, [1206.2942].

[176] G. W. Anderson and L. J. Hall, *The Electroweak phase transition and baryogenesis*, *Phys. Rev.* **D45** (1992) 2685–2698.

[177] M. Carena, G. Nardini, M. Quiros, and C. E. M. Wagner, *The Baryogenesis Window in the MSSM*, *Nucl. Phys.* **B812** (2009) 243–263, [0809.3760].

[178] D. Curtin, P. Jaiswal, and P. Meade, *Excluding Electroweak Baryogenesis in the MSSM*, *JHEP* **08** (2012) 005, [1203.2932].

[179] M. Carena, G. Nardini, M. Quiros, and C. E. M. Wagner, *MSSM Electroweak Baryogenesis and LHC Data*, *JHEP* **02** (2013) 001, [1207.6330].

[180] A. Katz and M. Perelstein, *Higgs Couplings and Electroweak Phase Transition*, *JHEP* **07** (2014) 108, [1401.1827].

[181] M. Pietroni, *The Electroweak phase transition in a nonminimal supersymmetric model*, *Nucl. Phys.* **B402** (1993) 27–45, [hep-ph/9207227].

[182] M. Carena, G. Nardini, M. Quiros, and C. E. M. Wagner, *The Effective Theory of the Light Stop Scenario*, *JHEP* **10** (2008) 062, [0806.4297].

[183] I. Masina, G. Nardini, and M. Quiros, *Electroweak vacuum stability and finite quadratic radiative corrections*, *Phys. Rev.* **D92** (2015), no. 3 035003, [1502.06525].

[184] M. Carena, M. Quiros, and C. E. M. Wagner, *Effective potential methods and the Higgs mass spectrum in the MSSM*, *Nucl. Phys.* **B461** (1996) 407–436, [hep-ph/9508343].

[185] G. R. Farrar and M. E. Shaposhnikov, *Baryon asymmetry of the universe in the standard electroweak theory*, *Phys. Rev.* **D50** (1994) 774, [hep-ph/9305275].

[186] F. R. Klinkhamer and N. S. Manton, *A Saddle Point Solution in the Weinberg-Salam Theory*, *Phys. Rev.* **D30** (1984) 2212.

[187] J. M. Moreno, M. Quiros, and M. Seco, *Bubbles in the supersymmetric standard model*, *Nucl. Phys.* **B526** (1998) 489–500, [hep-ph/9801272].

[188] S. R. Coleman, *The Fate of the False Vacuum. 1. Semiclassical Theory*, *Phys. Rev.* **D15** (1977) 2929–2936. [Erratum: Phys. Rev.D16,1248(1977)].

[189] A. D. Linde, *Decay of the False Vacuum at Finite Temperature*, *Nucl. Phys.* **B216** (1983) 421. [Erratum: Nucl. Phys.B223,544(1983)].

[190] S. J. Huber and T. Konstandin, *Gravitational Wave Production by Collisions: More Bubbles*, *JCAP* **0809** (2008) 022, [0806.1828].

[191] M. Hindmarsh, S. J. Huber, K. Rummukainen, and D. J. Weir, *Gravitational waves from the sound of a first order phase transition*, *Phys. Rev. Lett.* **112** (2014) 041301, [1304.2433].

[192] C. Caprini *et. al.*, *Science with the space-based interferometer eLISA. II: Gravitational waves from cosmological phase transitions*, *JCAP* **1604** (2016), no. 04 001, [1512.06239].

[193] S. J. Huber, T. Konstandin, G. Nardini, and I. Rues, *Detectable Gravitational Waves from Very Strong Phase Transitions in the General NMSSM*, *JCAP* **1603** (2016), no. 03 036, [1512.06357].

[194] V. Corbin and N. J. Cornish, *Detecting the cosmic gravitational wave background with the big bang observer*, *Class. Quant. Grav.* **23** (2006) 2435–2446, [gr-qc/0512039].

[195] G. M. Harry, P. Fritschel, D. A. Shaddock, W. Folkner, and E. S. Phinney, *Laser interferometry for the big bang observer*, *Class. Quant. Grav.* **23** (2006) 4887–4894. [Erratum: Class. Quant. Grav.23,7361(2006)].

[196] A. G. Akeroyd, M. A. Diaz, and F. J. Pacheco, *Double fermiophobic Higgs boson production at the CERN LHC and LC*, *Phys. Rev.* **D70** (2004) 075002, [hep-ph/0312231].

[197] A. G. Akeroyd, A. Alves, M. A. Diaz, and O. J. P. Eboli, *Multi-photon signatures at the Fermilab Tevatron*, *Eur. Phys. J.* **C48** (2006) 147–157, [hep-ph/0512077].

[198] **CDF** Collaboration, T. A. Aaltonen *et. al.*, *Search for a Low-Mass Neutral Higgs Boson with Suppressed Couplings to Fermions Using Events with Multiphoton Final States*, 1601.00401.

[199] E. Eichten, I. Hinchliffe, K. D. Lane, and C. Quigg, *Super Collider Physics*, *Rev. Mod. Phys.* **56** (1984) 579–707. [Addendum: Rev. Mod. Phys.58,1065(1986)].

[200] S. Dawson, S. Dittmaier, and M. Spira, *Neutral Higgs boson pair production at hadron colliders: QCD corrections*, *Phys. Rev.* **D58** (1998) 115012, [hep-ph/9805244].

[201] C. Degrande, K. Hartling, H. E. Logan, A. D. Peterson, and M. Zaro, *Automatic predictions in the Georgi-Machacek model at next-to-leading order accuracy*, *Phys. Rev.* **D93** (2016), no. 3 035004, [1512.01243].

[202] J. Alwall, R. Frederix, S. Frixione, V. Hirschi, F. Maltoni, O. Mattelaer, H. S. Shao, T. Stelzer, P. Torrielli, and M. Zaro, *The automated computation of tree-level and next-to-leading order differential cross sections, and their matching to parton shower simulations*, *JHEP* **07** (2014) 079, [1405.0301].

[203] K. Hartling, K. Kumar, and H. E. Logan, *GMCALC: a calculator for the Georgi-Machacek model*, 1412.7387.

[204] LHC Higgs Cross Section Working Group, S. Dittmaier, C. Mariotti, G. Passarino, and R. Tanaka (Eds.), *Handbook of LHC Higgs Cross Sections: 1. Inclusive Observables*, *CERN-2011-002* (CERN, Geneva, 2011) [1101.0593].

[205] LHC Higgs Cross Section Working Group, S. Dittmaier, C. Mariotti, G. Passarino, and R. Tanaka (Eds.), *Handbook of LHC Higgs Cross Sections: 2. Differential Distributions*, *CERN-2012-002* (CERN, Geneva, 2012) [1201.3084].

[206] LHC Higgs Cross Section Working Group, S. Heinemeyer, C. Mariotti, G. Passarino, and R. Tanaka (Eds.), *Handbook of LHC Higgs Cross Sections: 3. Higgs Properties*, *CERN-2013-004* (CERN, Geneva, 2013) [1307.1347].

[207] I. Low and J. Lykken, *Revealing the electroweak properties of a new scalar resonance*, *JHEP* **1010** (2010) 053, [1005.0872].

[208] A. G. Akeroyd and S. Moretti, *Enhancement of H to gamma gamma from doubly charged scalars in the Higgs Triplet Model*, *Phys. Rev.* **D86** (2012) 035015, [1206.0535].

[209] A. Arhrib, R. Benbrik, M. Chabab, G. Moultaka, and L. Rahili, *Higgs boson decay into 2 photons in the type II Seesaw Model*, *JHEP* **04** (2012) 136, [1112.5453].

[210] S. Kanemura and K. Yagyu, *Radiative corrections to electroweak parameters in the Higgs triplet model and implication with the recent Higgs boson searches*, *Phys. Rev.* **D85** (2012) 115009, [1201.6287].

[211] Y. Chen, N. Tran, and R. Vega-Morales, *Scrutinizing the Higgs Signal and Background in the $2e2\mu$ Golden Channel*, *JHEP* **1301** (2013) 182, [1211.1959].

[212] Y. Chen and R. Vega-Morales, *Extracting Effective Higgs Couplings in the Golden Channel*, *JHEP* **1404** (2014) 057, [1310.2893].

[213] Y. Chen, D. Stolarski, and R. Vega-Morales, *Golden probe of the top Yukuwa coupling*, *Phys. Rev.* **D92** (2015), no. 5 053003, [1505.01168].

[214] **ATLAS** Collaboration, G. Aad *et. al.*, *Search for Scalar Diphoton Resonances in the Mass Range $65 - 600$ GeV with the ATLAS Detector in pp Collision Data at $\sqrt{s} = 8$ TeV*, *Phys. Rev. Lett.* **113** (2014), no. 17 171801, [1407.6583].

[215] **CMS** Collaboration, V. Khachatryan *et. al.*, *Search for a Higgs Boson in the Mass Range from 145 to 1000 GeV Decaying to a Pair of W or Z Bosons*, *JHEP* **10** (2015) 144, [1504.00936].

[216] H. E. Logan and V. Rentala, *All the generalized Georgi-Machacek models*, *Phys. Rev.* **D92** (2015) 075011, [1502.01275].

[217] C. Englert, E. Re, and M. Spannowsky, *Pinning down Higgs triplets at the LHC*, *Phys.Rev.* **D88** (2013) 035024, [1306.6228].

[218] **Virgo, LIGO Scientific** Collaboration, B. P. Abbott *et. al.*, *Observation of Gravitational Waves from a Binary Black Hole Merger*, *Phys. Rev. Lett.* **116** (2016), no. 6 061102, [1602.03837].

[219] M. Hindmarsh, S. J. Huber, K. Rummukainen, and D. J. Weir, *Numerical simulations of acoustically generated gravitational waves at a first order phase transition*, *Phys. Rev.* **D92** (2015), no. 12 123009, [1504.03291].